

**Regulation of adipogenesis and inflammation:  
role(s) of adipose microRNAs**

**Mashaël Aljaber**

Adipokines and Metabolism Research Group

Centre for Clinical Pharmacology

Division of Medicine

**UCL**

**A thesis submitted for the degree of Doctor of Philosophy in  
the Division of Medicine at University College London**

**Declaration**

No part of this thesis has been submitted in support of an application for any other degree or qualification at the University College London or any other university or institute. All the work presented is my own and all collaborations have been acknowledged.

**Signature:****Date:**

## **Abstract**

### **Background:**

Obesity is associated with elevated risk of premature death and a range of co-morbidities. It is multifactorial and heterogeneous in origin, and, stratification of this disease, depending on the range of associated pathogenicities could help identify mediators and in the design of targeted therapies. Recent research has focused on microRNA (miRs) as potential biomarkers of cardiovascular risk, as well as their role as causative agents in the obesity associated pathologies.

### **Aims of the project were to:**

- Stratify obese subjects depending on systemic biomarkers of insulin resistance and inflammation.
- Identify and validate specific miRs associated with these phenotypes.
- Confirm and validate, in the whole transcriptome, targets for the specific miRs to assign functionality.

### **Methods:**

Non-diabetic, morbidly obese subjects of Arab origin were studied. Blood and adipose tissue samples were obtained before and after weight loss, along with anthropometric data. Glucose and lipids levels were determined by conventional methods. Insulin and adipokine concentrations were assayed by commercially available 2-site ELISA (R & D Systems, Oxon, UK). The population was dichotomised according to their serum insulin levels: Metabolically Healthy Obese (MHO) insulin <6.5 miU/ml; Pathologically Obese (PO) insulin >7.0 miU/ml. Total RNA, including miR, was extracted from peripheral blood cells, whole adipose tissue, the stromal vascular fraction and adipocytes of the abdominal subcutaneous and omental adipose tissues. miR expression was assessed using an inflammatory

pathway specific array (Qiagen), and by small RNA sequencing (Ion Torrent).

mRNA expression was assessed by whole transcriptome analysis (Ion Proton) and validated by PCR based microarrays (SurePrint G3 Human Gene Expression).

### **Results:**

PO, matched for age and BMI, had significantly higher serum insulin levels and HOMA index of IR, compared to MHO. They also had higher leptin, a marker of fat mass and adipocyte hypertrophy, and lower adiponectin, an endogenous insulin sensitizer.

However, blood pressure, lipids and inflammatory markers, such as IL-6, MCP-1 and CRP were not significantly different between the groups.

Three miRs were significantly down-regulated in the PO; miR-29, miR-144 and miR-374, and associated with inflammation, along with miR-122, miR-302, miR-200, which were associated with hyperinsulinaemia and insulin resistance. Many of their targets, especially those of miR-29, showed elevated expression in the PO. Following surgical weight loss there was a significant reduction in insulin which correlated with an increase in the levels of expression of nine miRs; miR-9, miR-200c, miR-141, miR-124, miR-376c, miR-302, while one was downregulated, miR-26b.

Whole transcriptome analysis of mRNA in blood and adipose tissue revealed modulation of several genes in the cardiometabolic pathways in the PO compared to MHO, along with genes leading to increased fibrosis.

### **Conclusions:**

Significant differences in the expression of specific miR species occurred along with insulin resistance and inflammation in PO compared to MHO. The target genes of these miRs, especially miR-29, miR-144 and miR-122, suggested fibrosis, in the presence of IR and inflammation, as a major lesion in these patients. Functional studies to explore the role of these miRs in fibrosis may offer new insights on putative therapeutic targets

for this group of patients.

## **Acknowledgements**

I am indebted to numerous people who helped me throughout this project.

Firstly, I cannot thank Dr Mohammed Al-Maadheed and Dr Muhammed Al-Sayrafi enough for recognising the need for this programme and making it happen, further in selecting, trusting and giving me this chance to take the first step to being an independent scientist.

My supervisor, Dr.Vidya Mohamed-Ali for her unlimited help, support, patience and continuous guidance in the research field. She shared her expertise to help me develop an understanding and passion for science.

Dr Mohamed Al-Rayess and Dr Nelson Orie, for their advice and guidance in the ethics application, patient recruitment, who were always available for discussion and advice regarding hypotheses, experiments and results.

Mr Raj for his help in the transcriptome analysis and next generation sequencing.

My colleagues at ADLQ for their continuous help and patience in the lab. My colleagues at UCL for all their help.

Also, the surgeons at Al-Emadi, Dr Mohammed Al-Emadi and Dr.Moataz Bashah (HMC) for their help in patient recruitment and facilitating sample collection.

I'd like to thank my family especially my mum and my husband for encouraging me throughout the last three and half years and offering all their love and support to me.

The last but not least, I'd like to dedicate my work to my kids, especially the baby (Ahmed) who I was carrying and shared with me all what I learned during the last nine months.

## **TABLE OF CONTENTS**

<b>ABSTRACT.....</b>	<b>3</b>
<b>ACKNOWLEDGEMENTS .....</b>	<b>6</b>
<b>TABLE OF CONTENTS .....</b>	<b>7</b>
<b>ABBREVIATIONS.....</b>	<b>13</b>
<b>PUBLICATIONS FROM THIS PROJECT.....</b>	<b>15</b>
<b>CHAPTER 1.....</b>	<b>17</b>
<b>INTRODUCTION.....</b>	<b>17</b>
1.1 PREVELANCE AND DEFINITION OF OBESITY .....	18
1.2 PREVALENCE OF OBESITY IN THE ARABIAN GULF AND QATAR .....	19
FIGURE 1. OBESITY ASSOCIATED CO-MORBIDITIES .....	20
1.3 INSULIN RESISTANCE (IR) .....	21
1.3.1. Adipose tissue .....	22
1.3.2 White Adipose Tissue (WAT) derived factors .....	30
1.3.2.1 Free fatty acids (FFA).....	30
1.3.2.2 Adipokines .....	32
1.4 HETEROGENEITY OF OBESITY PATHOLOGY.....	37
1.4.1 METABOLICALLY HEALTHY (MHO) AND PATHOLOGICAL OBESITY (PO).....	40
1.4.2 Mediators of pathological heterogeneity .....	41
1.4.2.1 Specific biomarkers .....	41
1.4.2.2 Inhibition of Adipogenesis.....	44
1.4.2.3 Adipocyte cell size in obesity heterogeneity.....	45
1.4.2.4 Visceral Adipose Tissue and Insulin resistance.....	46
1.5 MEDIATORS OF ADIPOGENESIS AND IR .....	47
1.6 miR.....	44
1.6.1.1 Environmental mediators .....	49
1.6.1.2 Physiological/pathological regulation.....	50
1.6.1.3 Inflammation.....	50
1.6.1.4 Angiogenesis and Hypoxia response .....	50
1.7 ADIPOSE MICRO RNA .....	51
1.7.1 miR in obesity related diseases .....	52
1.7.1.1 The role of miRs in IR and endothelial dysfunction.....	55
1.7.2 Preventative miR therapies .....	58
1.8 OBESITY AND INSULIN SENSITIVITY IN ARABS .....	60
1.8.1 Cardiometabolic risk factors and their mediators in subjects of Arab origin .....	60
1.9 SUMMARY .....	61
1.10 THE AIMS OF THE PROJECT .....	63
<b>CHAPTER 2.....</b>	<b>64</b>
<b>MATERIALS AND METHODS.....</b>	<b>64</b>
2.1 MATERIALS AND METHODS .....	65
2.2 PATIENT RECRUITMENT .....	65
2.3 ANTHROPOMETRIC MEASUREMENTS .....	65
2.4 BLOOD AND ADIPOSE TISSUE SAMPLES .....	66
2.4.1 Biochemical analysis .....	66
2.4.2 Serum Adipokines levels .....	67
2.4.3 Preparation of adipocytes and stromal vascular fraction .....	67
2.4.4 Total RNA extraction.....	70
2.4.4.1 Adipose tissue RNA.....	70

2.4.4.2 Peripheral blood cell RNA and miR extraction .....	70
2.5 ASSESSMENT OF RNA QUALITY.....	71
2.5.1 Purity assessment using the Agilent Bioanalyser .....	71
2.5.2 Total RNA quality assessment.....	71
2.5.3 Small RNA quality assessment.....	71
2.6 CDNA SYNTHESIS .....	71
2.6.1 cDNA synthesis for RT-PCR.....	71
2.6.2 miR cDNA synthesis .....	74
2.6.3 cDNA Synthesis for target analysis .....	74
2.7 REAL-TIME PCR AND MISCRIPIT ARRAYS.....	74
2.7.1 RT-PCR .....	74
2.7.3 miR PCR Array .....	75
2.8 VALIDATION OF THE MIR ARRAY DATA .....	75
2.9 TARGET ARRAYS .....	77
2.9.1 Target array PCR .....	78
2.9.2 Validation of genes from the Target arrays .....	79
2.10 SMALL RNA SEQUENCING – PGM.....	79
2.10.1 Library preparation .....	79
2.10.2 Sample selection .....	79
2.10.3 Enrichment of RNA samples.....	79
2.10.4 Hybridization and ligation .....	82
2.10.5 PGM runs summary of the small miR samples.....	83
2.11 WHOLE TRANSCRIPTOME ANALYSIS .....	84
2.11.1 Sample selection .....	84
2.11.2 rRNA depletion.....	87
2.11.3 Fragmentation .....	88
2.11.4 The Hybridization-Ligation-cDNA.....	89
2.11.5 Assess the yield and size distribution of the amplified DNA .....	91
2.11.6 The Ion Touch version3 .....	94
2.12 VALIDATION OF THE NGS BY SUREPRINT G3 HUMAN GENE EXPRESSION MICROARRAYS .....	95
2.12.1 RNA Labelling, Amplification and Hybridization .....	97
2.12.2 Microarray Data Analysis.....	97
2.13 RUNS QC AND SUMMARY FOR NGS .....	100
2.14 DATA ANALYSIS .....	100
2.14.1 Analysis of RNA arrays .....	100
2.14.2 Analysis of small RNA Seq.....	101
2.14.3 Analysis of whole transcriptome data.....	101
2.14.4 Gene enrichment analysis .....	102
2.14.5 miR target analysis.....	102
<b>CHAPTER 3.....</b>	<b>103</b>
<b>CLINICAL STRATIFICATION OF MHO AND PO.....</b>	<b>103</b>
3.1 INTRODUCTION.....	104
3.2 GENDER.....	104
3.1.1 Adiponectin and leptin.....	105
3.2 ETHNICITY.....	106
3.3 SEDENTARY LIFESTYLE AND SURGICAL WEIGHT LOSS .....	108
3.4 DIAGNOSIS OF MES .....	108
3.5 AIMS OF THE STUDY WERE TO.....	109
3.6 METHODS .....	109
3.7 RESULTS.....	110
3.7.1 Gender differences in cardiometabolic risk in Arabs.....	111



3.7.2 Differences in cardiometabolic risk in Arab MHO and PO.....	111
3.7.3 Effect of ethnicity on cardiometabolic risk factors.....	111
3.7.3.1 Correlations.....	112
3.7.4 Comparison of effects of surgical weight loss in MHO and PO groups.....	118
3.8 DISCUSSION.....	121
<b>CHAPTER 4.....</b>	<b>123</b>
<b>SMALL RNA SIGNATURE FOR MHO.....</b>	<b>123</b>
4.1 INTRODUCTION.....	124
4.2 MiR IN INSULIN RESPONSIVE TISSUES.....	124
4.3 SPECIFIC AIMS OF THE STUDY.....	127
4.4 METHODS.....	128
4.5 RESULTS.....	129
4.5.1 Effect of IR on inflammatory miR expression in PBCs (analysed by SA Biosciences programme).....	130
4.5.1.1 Correlation of miR expression and systemic cardiometabolic risk factors.....	130
4.5.1.2 Inflammatory array data analysed by R-based in-house programme (QCRI).....	133
4.5.2 MiRs gene expression in OM adipose tissue (QCRI).....	134
4.5.3 MiRs gene expression in SC adipose tissue (QCRI).....	135
4.5.4 MiRs gene expression in Adipocytes (QCRI).....	136
4.5.5 Validation of the inflammatory miR array.....	137
4.5.5.1 Validation of circulating miRs.....	137
4.5.5.2 Validation of miRs in SVF samples.....	137
4.5.6 Small RNA sequencing of PBCs.....	140
4.5.6.1 The miRs expression profile in IR using NGS.....	143
4.5.7 The predicted target genes of miRs.....	145
4.5.7.1 The functional expression of miR-29 target genes.....	145
4.5.7.2 The functional expression of miR-144 target genes.....	147
4.5.7.3 The functional expression of miR-374a target genes.....	148
4.5.8 Experimental validation of miR-29 targets.....	149
4.5.9 Inflammatory miR profile associated with weight-loss.....	153
4.5.9.1 Effect of weight loss on inflammatory miRs using pathway specific arrays.....	153
4.5.9.2 The validation of selected miRs by qPCR after weight loss.....	154
4.6 DISCUSSION.....	156
4.6.1 Downregulation of miR expression in PBCs of PO compared to MHO.....	156
4.6.2 miR expression in AT of PO compared to MHO.....	161
4.6.3 miR NGS results.....	163
4.6.4 Changes in miR expression on weight loss.....	166
4.6.5 Conclusions.....	166
<b>CHAPTER 5.....</b>	<b>168</b>
<b>THE WHOLE TRANSCRIPTOME ANALYSIS.....</b>	<b>168</b>
5.1 INTRODUCTION.....	169
5.2 AIMS.....	170
5.3 NGS TARGET GENES IN THE BLOOD.....	171
5.3.1 Sample selection and data analysis.....	171
5.4 RESULTS.....	172
5.4.1 NGS of PBCs using Ion Proton platform.....	172
5.4.2 The dysregulation of the target genes in whole adipose tissues.....	174
5.4.3 The dysregulation of the target genes in the SVF and Adipocytes of PO.....	174
5.5 VALIDATION OF THE NGS SAMPLES USING THE SUREPRINT G3 HUMAN GENE EXPRESSION MICROARRAYS.....	176

5.5.1 The upregulation of pathways in PO.....	178
5.5.2 The upregulated mRNA in specific tissues.....	179
5.5.3 The role of certain target genes in signalling pathways.....	180
5.5.4. The down regulation of pathways in PO.....	180
5.5.5. The down regulation of genes in specific tissues.....	182
5.6 DISCUSSION.....	183
5.6.1 mRNA seq using the Ion Proton platform.....	183
5.6.2 The validation of Ion Proton mRNA seq by microarrays.....	183
<b>CHAPTER 6.....</b>	<b>185</b>
<b>DISCUSSION.....</b>	<b>185</b>
6.1 INTRODUCTION.....	186
6.2 CLINICAL PARAMETERS.....	186
6.2.1 Comparison of cardiometabolic risk factors by gender.....	186
6.2.2 Clinical parameters between MHO and PO groups.....	188
6.2.3 Effect of weight loss on the clinical parameters.....	190
6.3 MiR SIGNATURE IN OBESITY.....	191
6.4 EFFECT OF WEIGHT LOSS ON THE MiR GENE EXPRESSION.....	192
6.5 THE WHOLE TRANSCRIPTOME ANALYSIS.....	194
6.5.1 Two different technologies were used - RNAseq versus HTA.....	195
6.6 CONCLUSIONS.....	197
6.7 LIMITATIONS OF THE STUDY.....	199
6.8 LONG TERM FUTURE DIRECTION.....	199
6.9 FUTURE STUDIES.....	200
<b>APPENDIX.....</b>	<b>202</b>
APPENDIX 1.....	203
APPENDIX 2.....	203
APPENDIX 3.....	208
APPENDIX 4.....	208
APP.3.1.....	209
APP.3.2.....	210
APP.3.3.....	211
<b>CHAPTER 7.....</b>	<b>215</b>
<b>REFERENCES.....</b>	<b>215</b>

## **TABLE OF FIGURES**

Figure 1. Obesity associated co-morbidities .....	20
Figure 2. The Prevalence of Obesity in Qatar .....	21
Figure 3. Tracking Obesity to Its Source. ....	24
Figure 4. Adipose tissue hypertrophy and its local effects in obesity .....	29
Figure 5. The relationship between the oxidative stress and IR .....	29
Figure 6. The changes in abdominal adipose tissue to insulin resistance .....	35
Figure 7. Adipose tissue hypertrophy and its local effects in obesity .....	36
Figure 8. The relationship between the oxidative stress and IR .....	39
Figure 9. Clinical differences between MHO and PO subjects .....	43
Figure 10. The regulation of target genes by MicroRNAs during adipogenesis .....	54
Figure 11. The expression of select miRs with their observed functional role .....	57
Figure 12. Insulin levels increase with BMI .....	62
Figure 13. Preparation of adipocytes and stromal vascular fraction .....	69
Figure 14. Assessment of RNA quality .....	72
Figure 15. Size selection of small RNA species .....	73
Figure 16. Small RNA sequencing using the PGM .....	80
Figure 17. Quality control data of samples used for small RNA sequencing .....	81
Figure 18. First run summary report of the small RNA sequencing .....	85
Figure 19. Second run summary report of the small RNA sequencing .....	86
Figure 20. The size distribution of the fragmented and purified r-depleted RNA .....	90
Figure 21. The area of interest was selected in a region .....	93
Figure 22. Work flow of the sample preparation and array scan .....	99
Figure 23. The prevalence of obesity in the Arab countries .....	107
Figure 24. Glucose and insulin parameters after weight loss .....	120
Figure 25. Adipokines after weight loss .....	120
Figure 26. The role of different miRs in adipogenesis .....	126
Figure 27. Effect of insulin resistance on miRs expression (SA Biosciences) .....	131
Figure 28. Correlations between miRs and systemic biomarkers .....	132
Figure 29. Effect of insulin resistance on miRs expression (QCRI) .....	133
Figure 30. Effect of IR on miR expression in the OM adipose tissue .....	134
Figure 31. Effect of IR on miR expression in the SC Adipose tissue .....	135
Figure 32. Effect of IR on miR expression in the adipocytes .....	136
Figure 33. Validation of the miR array data by q-PCR in PBCs .....	139
Figure 34. Summary of miR expression in MHO, PO and T2DM .....	141
Figure 35. Summary of miR expression in MHO, PO and T2DM .....	142
Figure 36. Down regulation of miR by IR - identified by small RNA seq .....	143
Figure 37. Upregulation of miR by IR - identified by small RNA seq .....	144
Figure 38. The functional expression of miR-29 target genes .....	146
Figure 39. The functional expression of miR-144 target genes .....	147
Figure 40. The functional expression of miR-374a target genes .....	148
Figure 41. Effect of weight loss on expression of systemic miRs .....	153
Figure 42. The validation of the weight loss effects on miRs by qPCR .....	154
Figure 43. The role of miR-29 in insulin responsive tissues .....	159
Figure 44. Hepatic fibrosis associated with dysregulation of systemic miRs .....	160
Figure 45. The role of miR-181s in neural development .....	165
Figure 46. The cluster map showing variability in gene expression .....	177
Figure 47. The results showed the up-regulation in PO versus MHO .....	178

Figure 48. Up-regulation of mRNAs implicated in insulin signaling and inflammation .....	179
Figure 49. Down-regulation of key pathways of IR and inflammation.....	180
Figure 50. Tissue specific downregulation of genes .....	182
Figure 51. Effects of stress in developing IR, Fibrosis and Vascular dysfunction.....	188
Figure 52. miR-29 mediated changes in IR and inflammation.....	196
Figure 53. Schema of pathways involved in development of disorders in PO.....	198

## **LIST OF TABLES**

Table 1. Adipocyte size in MHO and PO omental adipose tissue.....	48
Table 2. miRNAs regulated by NRs .....	48
Table 3. Inflammation associated miR array.....	77
Table 4. miR-29 target genes .....	78
Table 5. Sample selection for miRNA sequencing.....	84
Table 6. The samples were used for validation after sequencing .....	96
Table 7A. Gender differences in cardiometabolic risk factors in the whole cohort .....	113
Table 7B. Gender differences in cardiometabolic risk factors- matched for glycemia .....	1137
Table 8. Characteristics of Arab MHO and PO subjects.....	115
Table 9. Characteristics of female Arab MHO and PO subjects.....	116
Table 10. Comparison of basic characteristics of the Arab and Caucasian cohorts .....	117
Table 11. MeS in Arabs and Caucasians.....	119
Table 12. Expression of collagen gene targets of miR-29b in PBCs by qPCR.....	150
Table 13. Expression of collagen gene targets of miR-29b in SVF by qPCR.....	150
Table 14. The summary of MiRs results from different tissues. ....	152
Table 15. Summary of the mRNAs (Targets of miRs) results from different tissues .....	152
Table 16. Validation of 5 miRs after weight loss.....	155
Table 17. Details of the samples used for sequencing studies.....	171
Table 18. PBCs target gene expression, miRs and affected function in PO.....	173
Table 19. NGS target genes in the AD of PO compared to MHO .....	174
Table 20. Depot specific downregulated genes in PO, SVF and AD .....	175
Table 21. mRNA target in the adipose tissue components compared to PBCs.....	175
Table 22. The summary of differentially regulated genes in PO compared to MHO.....	176
Table 23. The specific genes involved in diferent downregulated pathways .....	181

## Abbreviations

<b>BP</b>	Blood pressure
<b>CHD</b>	Coronary Heart Disease
<b>CVD</b>	Cardiovascular disorder
<b>C/EBP- <math>\alpha</math></b>	CCAAT/enhancer binding protein- $\alpha$
<b>HOMA</b>	Homeostasis model assessment
<b>IR</b>	Insulin Resistant
<b>IS</b>	Insulin Sensitive
<b>LDL</b>	Low Density Lipoprotein
<b>HDL</b>	High-Density Lipoprotein
<b>MCP-1</b>	Monocyte Chemoattractant Protein- 1
<b>IL-6</b>	Interleukin- 6
<b>MCP-1</b>	Monocyte Chemotactic Protein-1
<b>MHO</b>	Metabolically Healthy Obese
<b>PO</b>	Pathologically Obese
<b>mRNA</b>	messenger ribonucleic acid
<b>OGTT</b>	Oral Glucose Tolerance Test
<b>PCR</b>	Polymerase Chain Reaction
<b>RNA</b>	Ribonucleic acid
<b>MiR</b>	Micro ribonucleic acid
<b>WHO</b>	World Health Organization
<b>MAPK</b>	Mitogen Activated Protein Kinases

<b>BMI</b>	Body Mass Index
<b>FFA</b>	Free Fatty Acids
<b>FPG</b>	Fasting Plasma Glucose
<b>IGT</b>	Impaired Glucose Tolerance
<b>MeS</b>	Metabolic Syndrome
<b>NAFLD</b>	Non-Alcoholic Fatty Liver Disease
<b>NPY</b>	Neuropeptide Y
<b>OGTT</b>	Oral Glucose Tolerance Test
<b>OM</b>	Omental depot
<b>SC</b>	Subcutaneous depot
<b>TNF-<math>\alpha</math></b>	Tumor Necrosis Factor- alpha
<b>TGF- <math>\beta</math></b>	Transforming Growth Factor- $\beta$
<b>NF<math>\kappa</math>B</b>	Nuclear factor $\kappa$ B
<b>BMP</b>	Bone Morphogenetic Protein
<b>NF-KB</b>	Nuclear Factor B
<b>HIF-1<math>\alpha</math></b>	Hypoxia Inducing Factor
<b>FoxO</b>	Forkhead box O
<b>NOS</b>	Nitrous Oxide Synthase
<b>HTA</b>	Human Transcriptome Array.
<b>RFW</b>	RNAase Free Water
<b>PGM</b>	Personal Genome Machine
<b>PPAR- <math>\gamma</math></b>	Peroxisome Proliferator-Activated Receptor- $\gamma$
<b>SMCS</b>	Smooth Muscle Cells

### **Publications from this project.**

1. **Al-Jaber, M**, Casale, C, Bakhamis A.A, Lei, S, Orié N.N, ElRayess, M, Sufi, P, Marina, N, Rida, S, Al-Emadi, M, Alsayrafi, M, Mohamed-Ali, V. *Hyperinsulinaemia and hyperleptinaemia are BMI independent features of morbid obesity in a Qatari, compared to a Caucasian, population: Effect of surgical weight loss.* QF Annual Research Forum Proceedings, 2012.
2. Orié N.N, Bakhamis A.A, **Al-Jaber, M**, Rida, S, Al-Emadi, M, Mohamed-Ali, V, Alsayrafi, M. *Differential impact of obesity on endothelium-dependent relaxation of omental vs. subcutaneous adipose small vessels from young morbidly obese, female Qataris.* Obesity Soc. Annual Scientific Meeting, 2012.
3. Bakhamis A.A, Orié N.N, **Al-Jaber, M**, Rida, S, Al-Emadi, M, Mohamed-Ali, V, Alsayrafi, M. *Depot-specific differences in vascular noradrenergic sensitivity in morbidly obese Qataris.* QF Annual Research Forum Proceedings, 2012.
4. Orié N.N, Bakhamis A.A, **Al-Jaber, M**, Al-Emadi, M, Rida, S, Alsayrafi, M, Mohamed-Ali, V. *Endothelial dysfunction in morbidly obese young Qataris.* QF Annual Research Forum Proceedings, 2012.
5. **Al-Jaber, M**, ElRayess, M, Alsowaidi, S, Bakhamis A.A, Orié, N.N, Rida, S, Al-Emadi, M, Alsayrafi, M, Mohamed-Ali, V. *Role(s) of microRNAs as markers and mediators of insulin resistance.* QF Annual Research Forum Proceedings, 2013.
6. Bakhamis A.A, Orié N.N, **Al-Jaber, M**, Al-Emadi, M, Rida, S, Alsayrafi, M, and Mohamed-Ali V. *Insulin resistance alters noradrenergic sensitivity of omental vessels from morbidly obese Qataris.* Endocr Rev, 2013.
7. Orié, N.N, Bakhamis, A.A, **Al-Jaber, M**, Al-Emadi, M, Rida, S, Alsayrafi, M, Mohamed-Ali, V. *Insulin resistance as the major determinant of endothelial dysfunction in morbidly obese Qataris.* Endocr Rev, 2013.



8. ElRayess, M, **Al-Jaber, M**, Bakhamis A.A, Orie, N.N, Alsayrafi, M. *Characterization of insulin resistance and insulin sensitivity in a Qatari population*. Endocr Rev, 2013.
9. Orie, N.N, Bakhamis A.A, **Al-Jaber, M**, Al-Emadi, M, Rida, S, Alsayrafi, M, Mohamed-Ali, V. *Impact of metabolic health on microvascular endothelial function in morbidly obese Qataris*. QF Annual Research Forum Proceedings, 2013.
10. Elrayess, MA, **Al-Jaber, M**, Al-Sowaidi. S, Al-Muraikhy S, Bakhamis A.A, Orie, N.N, Al-Emadi, M, Rida, S, Alsayrafi, M, Mohamed-Ali, V. *let7 as a potential mediator of insulin resistance in normal weight subjects*. QF Annual Research Forum Proceedings, 2013.
11. **Al-Jaber M**, Elrayess MA, Al-Sowaidi S, Bakhamis A, Orie NN, Rida S, Al-Emadi M, Al-Sayrafi M, Mohamed-Ali V. *The role(s) of microRNAs in inflammation and Insulin resistance*. Obesity Soc. Annual Meeting, 2013.
12. Al-Jaber MY, **Al-Jaber M**, Orie, NN, Bakhamis A, Bashah M, AlEmadi M, AlNaemi H, AlSayrafi M, Sufi P, Gray R, Casale C, Shen L, Mohamed-Ali, V. *Early onset obesity is associated with insulin resistance and precedes endothelial dysfunction in non-diabetic Qataris*. QF Annual Research Forum Proceedings, 2014.
13. **Al-Jaber M**, Bakhamis A, Orie N N, Lei S, Casale C, Elrayess MA, Al-Sowaidi. S, Al-Emadi. M, Bashah M, Sufi P, Gray R, Al-Sayrafi M, Mohamed-Ali V. *Insulin resistance is exaggerated in early-onset obesity and accompanied by down-regulation of miRs that mediate inflammation and fibrosis*. European Congress for Obesity, 2015.

**Manuscript under review**

Al-Jaber M, Mohamed-Ali V. (2015). Adipose Tissue-Derived Factors. Frayn, K. N, Stanner, S, Foundation, B. N. (Eds.). In *Cardiovascular Disease: Diet, Nutrition and Emerging Risk Factors*. 2<sup>nd</sup> edition, Wiley-Blackwell.

# **Chapter 1**

## **Introduction**

## 1.1 Prevalence and definition of Obesity

It was reported by the World Health Organisation (WHO) in 2008 that around 200 million men and 300 million women were obese. Projections for 2015 suggest that these figures will have nearly doubled to 700 million obese adults. The rise in human obesity is mainly due to increased energy intake and decreased energy expenditure, resulting in a significant increase in adipose tissue, the inappropriate accumulation of which is generally harmful to health. This obesity epidemic reflects a lot of changes including social, economic and life-style (International Obesity Taskforce, 2005).

Obesity is defined predominantly as an increase of the total mass of adipose tissue, due to both hyperplasia and/or hypertrophy of adipocytes. It is associated with an elevated risk of premature death and a range of co-morbidities, including Type 2 diabetes mellitus (T2DM), cardiovascular disease and cancers (Hotamisligil, 2006). The effects of obesity on disease outcome are shown in Figure 1.

Obesity is multifactorial in origin. Environmental and genetic factors have major roles to play in the development of obesity, which determine not just obesity but also the distribution of the body fat tissue and its accumulation (Wajchenberg, et al, 2000). Obesity is not a homogenous pathological phenotype; it is heterogeneous in terms of its causes and metabolic complications. The regional body fat distribution appears to be an important correlate of the metabolic complications that have been associated with obesity. Abdominal fat accumulation increases the risk of metabolic complications to a greater extent in men, than in women. Several studies have suggested molecular mechanisms that link abdominal obesity, T2DM and cardiovascular disease. Both total body fatness and body fat distribution have a significant genetic correlation, perhaps explaining why some obese individuals are more susceptible to metabolic complications than others. Insulin resistance, a major precursor and risk factor for all the obesity associated diseases, has been shown to be more

related to abdominal adipose tissue accumulation, especially in the visceral depots (Ohlson et al, 1997).

## **1.2 Prevalence of Obesity in the Arabian Gulf and Qatar**

Since the discovery of oil in the Arabian Gulf region in the 1960s, the countries that make up the Gulf Cooperation Council including Qatar, Bahrain, Kuwait, Saudi Arabia,

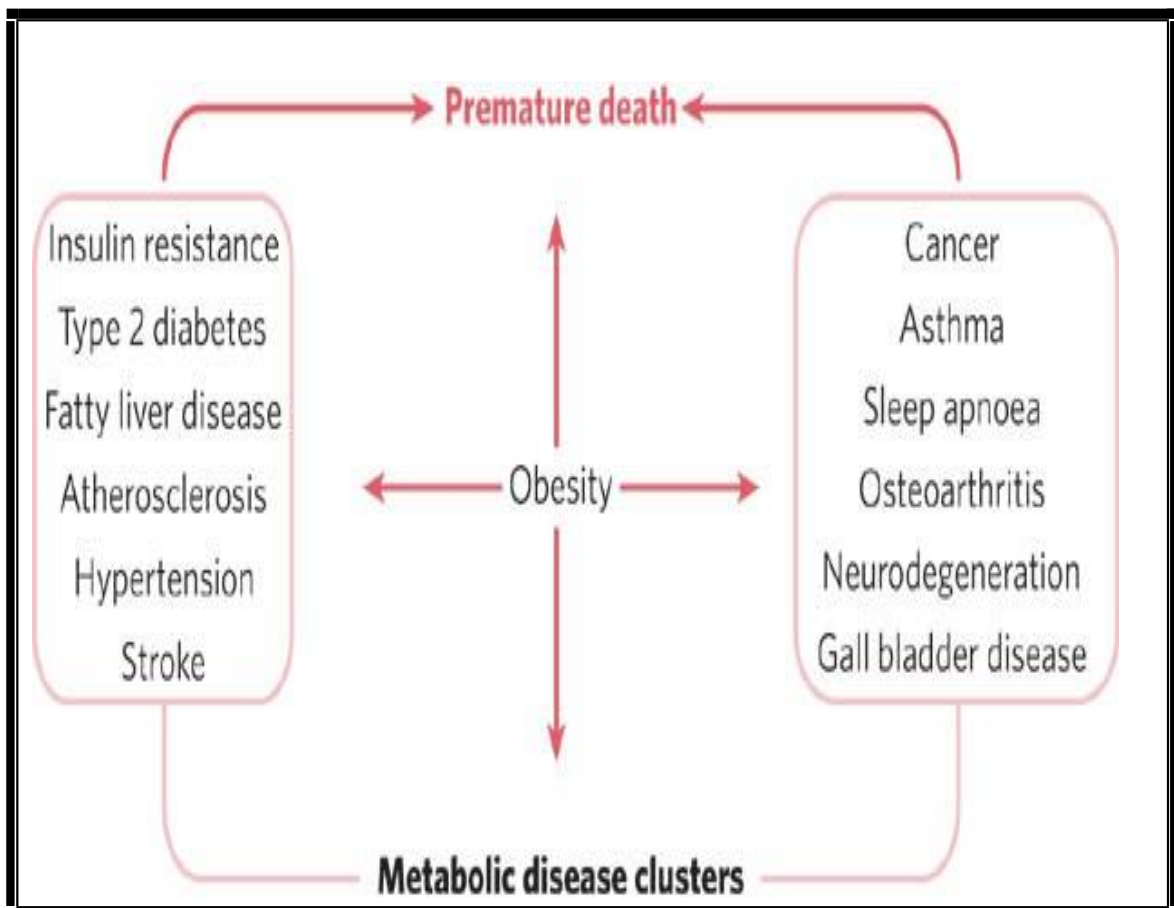


**Figure 1. Obesity associated co-morbidities**

(Hotamisligil, 2006).


United Arab Emirates and Oman have experienced continued growth in both population and wealth. There has been a concomitant increase in obesity, associated with nutritional health problems and related diseases. The Arabian Gulf has amongst the highest rates of hypertension and T2DM in the world. Alarming in Qatar it has increased by over 7 fold in just the last two decades, ranking sixth in terms of global obesity prevalence ([www.iaso.org](http://www.iaso.org)) as shown in Figure 2. According to a recent survey by the Public Health Department of the Supreme Council of Health (SCH) in Qatar, 70% of the Arab population were overweight, of whom 40% were obese with early onset of the disease, and especially so amongst women (55%).

Various factors have contributed to the world-wide obesity epidemic, including increased intake of food rich in carbohydrates and fat, in addition to a lifestyle characterised by diminished physical activity. Qatar is a clear example of such changes, as Arabs have altered their lifestyle from pearl hunters, living mostly on sea food into a fast-food consuming population with minimal physical activity as the country's economy has become almost completely dependent on gas and oil in the past 5 decades. The government has started to increase health awareness in the community and to encourage national programmes which help to support a healthy life-style, increase physical activities and choice of a balanced diet. However, a greater understanding of the effects of these changes in lifestyle to physiological and pathological outcomes still requires investigation.

### **1.3 Insulin Resistance (IR)**

IR may be described as the inability of a specified concentration of insulin to increase cellular glucose uptake and its utilization. This is a comparative measure, using as a reference a normal population. Insulin action is brought about by the binding of the hormone to its cell surface receptor followed by cellular signal transduction through a series of protein-protein interactions. Insulin plays a role in two major pathways, the first

involved in regulating intermediary metabolism and the other in controlling growth and mitoses. In T2DM the lesion appears to be in the first pathway regulating metabolism, 0 while its role in the mitogenic pathways is normal.



**% Global prevalence of adult obesity(BMI  $\geq$  30 kg/m<sup>2</sup>): country rankings 2012**  
 Ranking based on Females

	Country	Year of Data Collection	Males	Females
1	Tonga	1998-2000	46.6	70.3
2	Samoa	1995	32.9	63
3	Nauru	2004	55.7	60.5
4	Kuwait	2006	36.4	47.9
5	Niue	1987	15	46
6	Qatar	2003	34.6	45.3
7	French Polynesia	1995	36.3	44.3
8	Saudi Arabia	1995-2000	26.4	44
9	Palestine	n/a	23.9	42.5

**Figure 2. The Prevalence of Obesity in Qatar**

According to World Health Organisation statistics updated in 2010. (IASO website).



The mechanisms underlying the development of IR include genetic abnormalities of the insulin receptor and/or proteins of the insulin action cascade, fetal malnutrition, as well as increases in adiposity, especially in the visceral compartments. IR occurs as part of a cluster of cardiometabolic abnormalities referred to as the ‘Insulin Resistance Syndrome’ or ‘Metabolic Syndrome’ (MeS). Often this cluster of risk factors leads to the accelerated development of T2DM, atherosclerosis, hypertension or polycystic ovarian syndrome.

(Saltiel et al, 2001; Lumeng et al, 2011).

### **1.3.1. Adipose tissue**

There are three types of adipose tissue in humans, white (WAT), brown (BAT) and Brite/Beige adipose tissue. (Ishibashi and Seale, 2010). WAT is the predominant type of AT in humans and acts as a storage organ, storing energy as TAGs for utilization during periods of energy deficit. In addition its secretory signals mediate glucose homeostasis, immune and various other angiogenic and metabolic function (see section 1.3.2; Karastergiou and Mohamed-Ali, 2010). In contrast, BAT is a mainly thermogenic organ. It dissipates the chemical energy stored in TAGs as heat to preserve core temperature during hypothermia and, perhaps, to help maintain body weight (Rosen and Spiegelman, 2014). Recently another type of AT has been described with an intermediate phenotype known as ‘Biege’ or ‘Brite’ AT.

**BAT:** Brown adipocytes (BAT) is made up of multilocular adipocytes with a high density of mitochondria, as well as other cells such as endothelial and epithelial cells. It is highly vascularized, with elevated expression of uncoupling protein-1 (UCP-1) allowing for the uncoupling of fatty acid oxidation from ATP production to generate heat (Rosen and Spiegelman, 2014). In addition two other members of the UCP family, UCP2 and UCP3, have also been described in this tissue, the roles of which are still being investigated. In previous studies in rodents leptin was suggested to increase UCP-3 mRNA expression in

skeletal muscle, and increase UCP-2 mRNA expression in WAT. Pinkney and colleagues reported that UCP-2 gene expression in SC abdominal AT is inversely related to adiposity and its biochemical correlates which may offer a therapeutic target (Pinkney et al, 2000). Although BAT was initially considered to be present in humans only in infants and neonates, recent data has established that substantial depots of UCP-1 expressing BAT can be detected in the supraspinal, supraclavicular, pericardial, and neck regions of adult humans (Virtanen et al., 2009; see Figure 3).

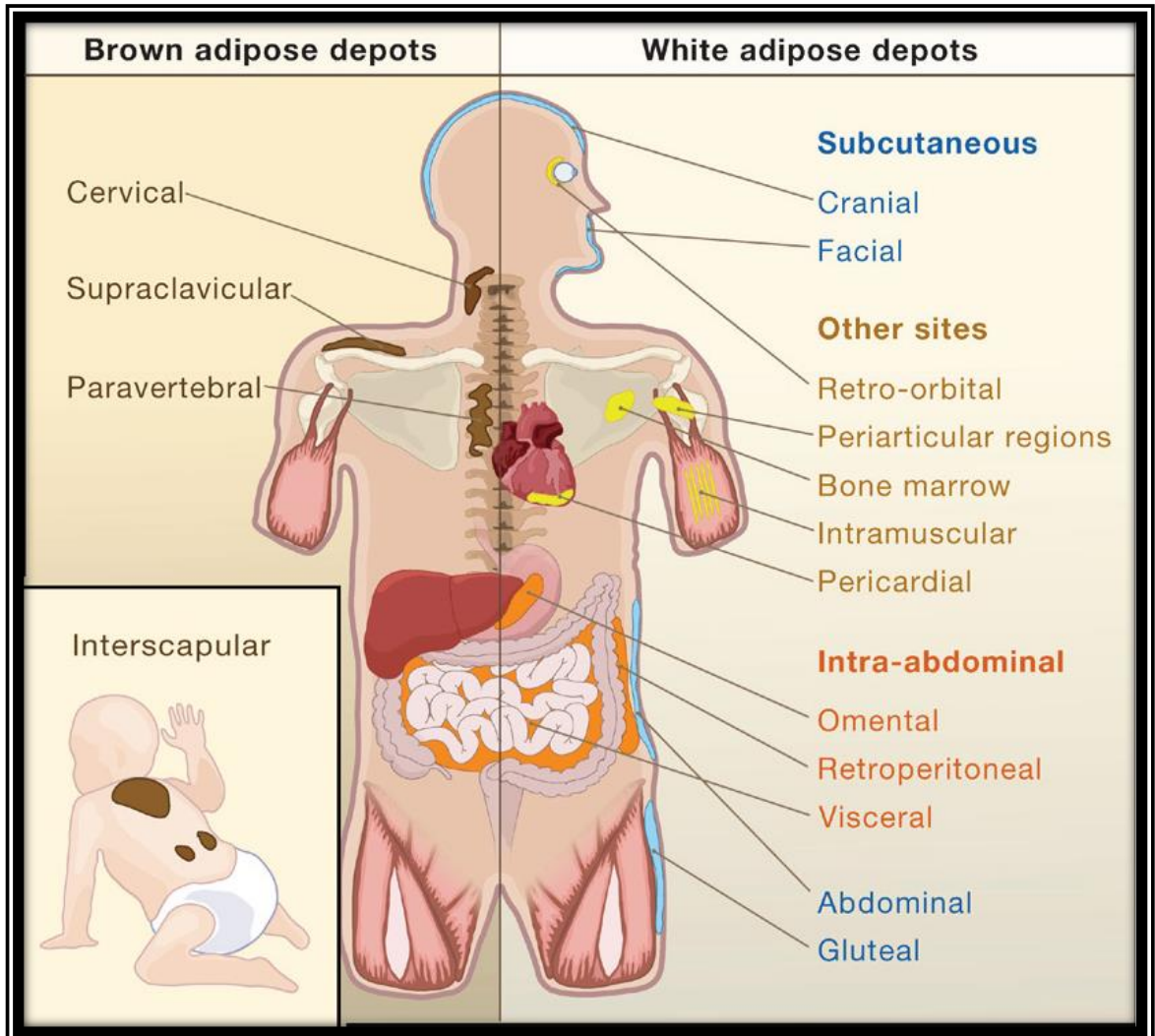


**Figure 3. Tracking Obesity to Its Source.**

Fat distribuion: Brown adipose tissue is abundant at birth and still present in adulthood but to a lesser extent (Biege AT). Gesta et al, 2007.

In rodents the thermogenic process in brown adipocytes can be mimicked by the addition of fatty acids (Nedergaard et al 1979). This fatty acid-induced thermogenesis is also completely UCP1 dependent. Therefore, the activation of lipolysis, recorded as glycerol or fatty acid release, is induced by norepinephrine, and a sufficient trigger for initiation of thermogenesis in brown adipocytes (Nedergaard et al 1979). An interscapular BAT depot was recently discovered in humans, where it is thought to maintain normal body temperature in newborns (Sanchez-Gurmaches et al, 2012). It is believed that this tissue is significantly reduced in adulthood or completely lost in obesity (Lee et al, 2014; Ouellet et al, 2011).

Most brown fat cells originate from precursor cells in the embryonic mesoderm that also give rise to skeletal muscle cells and a subpopulation of white adipocytes. These precursors transiently express *Myf5* and *Pax7*, two genes that were previously thought to selectively mark skeletal myogenic cells in the mesoderm (**Figure 4a**). Consistent with a developmental relationship between brown fat and muscle, brown fat precursor cells express a muscle-like gene signature, and brown fat and muscle have related mitochondrial proteomes. (Sanchez-Gurmaches et al, 2012).

The recent discovery that both brown and white adipocytes derive from vascular endothelial cells of the adipose organ brings strong new support to another origin for the brown adipocytes: the transdifferentiation theory (Tran et al, 2012; Gupta et al, 2012). This theory basically suggests that in special circumstances, such as chronic cold exposure, the white part of the organ might 'help' the brown part by forming new BAT like AT (Cinti, 2009a). Environmental factors play an important role in this transdifferentiation, including cold, exercise and diets high in fat.

**Beige adipose tissue.** The embryonic origin of beige adipocytes is even less clear. Beige and brown adipocytes may arise from distinct cell lineages, given that the former, at least

in the subcutaneous depot, do not consistently show *Myf5* expression (Seale et al, 2008). An important question is whether beige adipocytes arise from white adipocytes through transdifferentiation or through the *de novo* differentiation and maturation of precursors. Initial data suggested that most beige adipocytes arise from pre-existing, nondividing cells that were presumed to be mature adipocytes (Himms-Hagen, 2000). However, more recent evidence from Cinti and others have provided substantial evidence in support of the idea that large unilocular white adipocytes transform into beige adipocytes in response to cold or  $\beta$ 3-adrenergic agonists (Cinti, 2009a). These data suggest that cold, mediated by  $\beta$ -adrenergic agonists, triggers the differentiation of Cd137+Tmem26+ (transmembrane protein 26) precursor cells into UCP1+ beige adipocytes and that these beige cells require constant stimulation to maintain their thermogenic programming (**Figure 5**). In the basal state beige adipocytes are most abundant in the inguinal WAT, which is a major subcutaneous depot in rodents. However, UCP1-expressing adipocytes were evident in most WAT depots in response to cold exposure (Vitali et al, 2012). In perigonadal (visceral) fat of male mice, beige adipocytes develop from a population of precursors that also differentiates into white adipocytes (**Figure 4b**). These bipotent precursors express platelet-derived growth factor receptor- $\alpha$  (Pdgfr- $\alpha$ ) and are closely associated with blood vessels. After treatment of mice with  $\beta$ 3-adrenergic agonists, these precursor cells proliferate, lose Pdgfr- $\alpha$  expression and differentiate into UCP1+ adipocytes. Conversely, a high-fat diet stimulates the differentiation of Pdgfr- $\alpha$ + cells into white adipocytes (Lee et al 2012; **Figure 4b**).

Both the PET (positron-emission tomography)–CT studies and tissue biopsy specimens indicate that healthy, normal weight adult humans have brown adipose tissue. However it is still unclear whether the deposits of UCP1-expressing adipocytes identified by fluorodeoxyglucose (FDG) PET in adult humans are analogous to beige or brown fat.

Reports of supraclavicular tissue (Sharp et al, 2012), the largest FDG-PET–positive depot in humans, show expression of selective markers of beige fat cells. By contrast, Jespersen *et al.* found that tissue and *in vitro*–differentiated adipocytes from this depot express both brown- and beige-specific markers. Thus, brown and beige adipocytes appear to express distinct and distinguishing gene signatures (Wu et al 2013; Sharp et al, 2012; **Figure 5**). A striking difference between the two cell types is that brown adipocytes express high levels of *Ucp1* and other thermogenic genes under basal (unstimulated) conditions, whereas beige adipocytes express these genes only in response to activators such as agonists of the  $\beta$ -adrenergic receptor or peroxisome proliferator-activated receptor- $\gamma$  (Ppar- $\gamma$ ). (Petrovic et al 2010 and Wu et al 2013).

Several factors have been shown to regulate brown and beige adipocyte differentiation by modulating Prdm16 expression or activity, a key regulator of brown fat cell fate). In addition to the bone morphogenetic protein 7 (Bmp7), a signal that is essential for brown fat development, which increases the amounts of *Prdm16* mRNA in brown and white fat precursor cells. Additionally, thiazolidinediones (TZDs), which agonize Ppar- $\gamma$ , induce thermogenic gene expression in fat cells through effects on Prdm16 (Ohno et al, 2012). Interestingly, the muscle-enriched microRNA miR-133 directly targets and reduces the amounts of Prdm16 to block both brown and beige adipose development. Cold exposure suppresses miR-133 expression in fat cells, which leads to increased amounts of Prdm16 and increased expression of downstream thermogenic target genes. Reduction of miR-133 in regenerating muscle causes the ectopic development of brown adipocytes and an associated increase in energy expenditure. (Trajkovski et al, 2012).

Overall, low brown and brown-like fat activity in humans correlates with aging, obesity and reducing metabolic health (Ouellet et al., 2011), but the basis for the decline remain unclear. Functional marker genes or assays are needed to better categorize the different

human and mouse fat depots and cell types, with concomitant studies to determine the biology and therapeutic potential of both classic BAT and inducible beige fat. Understanding the molecular processes governing WAT browning is highly significant, as this may identify novel approaches for increasing energy expenditure and combating obesity and the metabolic syndrome. Efforts to date have focused primarily on the role of factors that act directly on beige preadipocytes, such as irisin and FGF21 (Bostrom et al., 2012; Figure 5). However, there is mounting evidence that the central nervous system (CNS) control of WAT browning may also be important (Cannon et al., 1986).

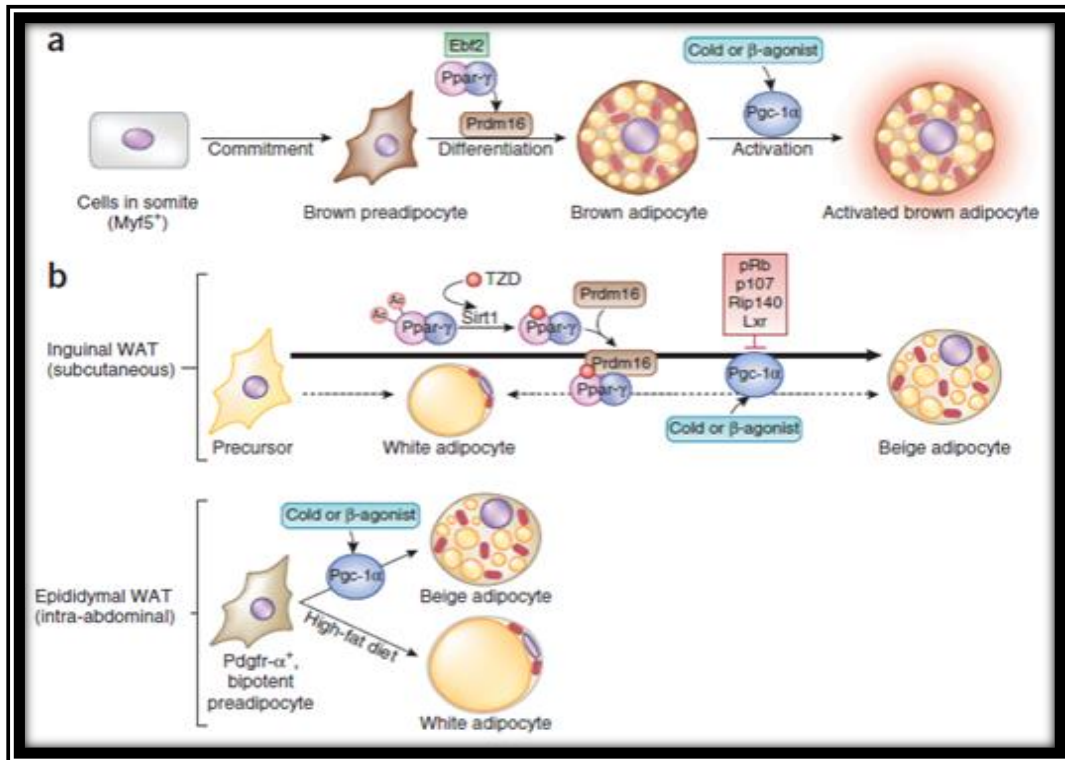


**Figure 4. Adipose tissue hypertrophy and its local effects in obesity**

**a.** The origin of BAT from Mycf5+ cells. And, **b.** the transformation of precursor cells in denovo to form Biege cells through regulation of Prdm 16. The upper line shows the bieging conversion from the SC precursor, while the lower one shows the intra-abdominal preadipocytes conversion to WAT under the HFD or Biege fat under cold or  $\beta$ -adrenergic activators.

	Immunohistochemistry with anti-Ucp1	Location in humans	Location in mice	Developmental origin in mice	Enriched markers	Key transcription factors	Activators
Brown		Neck Interscapular (newborns) (Perirenal?)	Interscapular Cervical Axillary Perirenal (Endocardial?)	Myf5 <sup>+</sup> cells (dermomyotome)	Zic1 Lhx8 Eva1 Pdk4 Epst1 miR-206, miR-133b	C/ebp $\beta$ Prdm16 Pgc-1 $\alpha$ Ppar- $\alpha$ Ebf2 TR	Cold Thiazolidinediones Natriuretic peptides Thyroid hormone Fgf21, Bmp7, Bmp8b Orexin
Beige		Supraclavicular (Paraspinal?)	Interspersed within WAT subcutaneous fat > visceral fat	Myf5 <sup>+</sup> cells Pdgfr- $\alpha$ <sup>+</sup> (perigonadal)	Cd137 Tbx1 Tmem26 Cited1 Shox2	C/ebp $\beta$ Prdm16 Pgc-1 $\alpha$ (Ppar- $\alpha$ ?)	Cold Thiazolidinediones Natriuretic peptides (Thyroid hormone?) Fgf21 Irisin

**Figure 5. The relationship between the oxidative stress and IR**

The comparison between Bat and Biege: In human compared to mice, the enriched markers, Key transcription factors and activators.



### **1.3.2 White Adipose Tissue (WAT) derived factors**

The close association of the MeS and obesity has led to it being postulated that adipose tissue-derived mediators act on various organs such as the endothelium, liver and skeletal muscle to produce detrimental effects. Initial research into the secretory connections between adipose tissue and MeS centered on free fatty acids (FFA) and more recently on other ‘hormones’ and cytokines such as leptin, TNF $\alpha$ , IL-6 and adiponectin (Mohamed-Ali et al, 1997; Van Gaal et al, 2006; Karastergiou and Mohamed-Ali, 2010).

#### **1.3.2.1 Free fatty acids (FFA)**

The altered balance of the cross talk between skeletal muscle, the liver and adipose tissue, with varying effects at the systemic level, leads to rising levels of FFA (also known as non-esterified fatty acids, NEFA) due to the lack of the lipolysis-inhibiting effect of insulin on adipose tissue, in addition to impaired control of gluconeogenesis and glucose uptake. This leads to release of glucose, amino and fatty acids into the circulation along with compensatory increases in insulin secretion by pancreatic  $\beta$ -cells to maintain euglycaemia (DeFronzo et al, 1991). This in turn predisposes to T2DM, as systemic glucose concentrations increase.

Regional distribution of adipose tissue has a significant impact on the correlation of obesity to disturbances in glucose and lipid metabolism (Kahn et al, 2006). Previous studies have shown that excess fat in the upper compartments (thoracic, cardiac and abdominal) of the body has a stronger correlation with increased mortality and higher risk for disorders such as T2DM, hypertension, hyperlipidaemia, and atherosclerosis, compared to that deposited in the lower parts (gluteal and femoral) (Brunzell, 1999; Phillips et al, 1996; Wajchenberg et al, 1994).

Additionally the visceral adipose tissue is related to IR to a greater extent than subcutaneous adipose tissue. Visceral adipose tissue shows high lipolytic activity,

releasing FFAs into the portal and systemic circulation. This elevation of FFA levels in the liver leads to decreased hepatic insulin extraction by inhibiting insulin binding and degradation (Svedberg et al, 1990). Increase in FFA levels results in increased esterification of FFAs and reduced hepatic degradation of apolipoprotein B and greater secretion of small VLDL particles (Brunzell et al, 1999). Furthermore, FFAs induce IR in obesity and T2DM by the initial inhibition of glucose transport. FFAs, and cytokines such as tumour necrosis factor (TNF- $\alpha$ ), all mainly derived from visceral adipose tissue, impair insulin action at target cells in liver and muscle, by causing a post-binding defect that blocks tyrosine kinase activity, uncoupling insulin signal transduction from cellular glucose uptake. In addition, the accumulation of triglyceride in muscle has been linked to impaired glucose disposal (Phillips et al, 1996). IR is followed by pancreatic  $\beta$ -cell compensation and hyperinsulinaemia, due to fuel and neurohormonal signals derived from fat, liver, intestine and brain (Cornier et al, 2008). Although some data suggests that the  $\beta$ -cell defect may come first, ie.the  $\beta$ -cells, perhaps due to a genetic lesion, releases increased and unwanted levels of insulin leading to the hyperinsulinaemia and this then causes IR as a way to protect the insulin responsive organs.

Thus, chronic exposure to very high levels of exogenous FFAs increases basal insulin levels and impairs glucose-stimulated insulin secretion. The outcome is that endogenous FFAs enhance insulin secretion in obesity/IR syndromes, which accumulates to toxic levels and contribute to cell failure and the development of T2DM (Dobbins, 1998). IR induced by cytokines (IL-6, TNF- $\alpha$ , CRP and low levels of adiponectin), FFA and retinol-binding protein 4 (RBP-4), may induce oxidative stress and subsequent endothelial dysfunction (Wajchenberg, 2000). Fat accumulation, IR, hepatic inflammation and dyslipidaemia may all lead to premature atherosclerosis (Figure 3).

### 1.3.2.2 Adipokines

Adipose tissue, in addition to adipocytes, that make up about 50% of its cellular composition, also contains the stromal vascular fraction (SVF) which includes preadipocytes, fibroblasts, vascular endothelial cells and a variety of immune cells. Obesity is mediated via increased fat mass through hypertrophy of adipocytes, and to a lesser degree their hyperplasia (see Figure 4; Karastergiou and Mohamed-Ali, 2010). While the main role of the adipose organ is to store energy in the form of triacylglycerols, the tissue also acts as an endocrine and immune organ secreting hormones and cytokines, including leptin, adiponectin, resistin, omentin, visfatin, IL-6 and TNF $\alpha$ . Through these factors the tissue can affect other organ systems of the body and lead to the development of obesity-associated MeS and IR. The various factors derived from adipose tissue have collectively been referred to as adipokines. Specially, hypertrophied adipocytes secrete pro-inflammatory adipokines, such as, leptin, IL-6, IL-8, and MCP-1, that exacerbate macrophage infiltration and secretion of IL-1 $\beta$  and TNF $\alpha$ , leading to reduced IRS-1 and GLUT4 expression and promoting insulin resistance (Gustafson et al., 2009). This is also associated with increased lipolysis and reduced adiponectin release (Karastergiou and Mohamed-Ali, 2010).

Adiponectin is defined as an anti-inflammatory and anti-diabetic adipokine, predominantly secreted by adipocytes, whose low levels in obesity appear to be related to the IR (Adiels et al, 2007, Arita et al, 1999). Elevated concentrations of circulating adiponectin have been associated with a lower incidence of T2DM (Trujillo et al, 2005, Zhu et al, 2010, Li et al, 2009). Adiponectin was detected in human plasma and shown to be expressed specifically in adipose tissue. There was a significant inverse correlation between BMI and plasma adiponectin. In obese subjects circulating concentrations of adiponectin are reduced, and subsequently, hypoadiponectinemia is associated with IR

(Zhu et al, 2010). Activation of adiponectin receptors stimulates AMPK, which increases fatty acid oxidation and glucose uptake in muscle. Adiponectin also increases PPAR $\alpha$  activity and reduces inflammation. Additionally, one mechanism by which adiponectin directly improves insulin sensitivity is that the globular C-terminal fragment reduces glucose levels by increasing fatty acid combustion in myocytes (Turer et al, 2012). Adiponectin exerts anti-atherogenic actions including a reduction in the expression of several adhesion molecules, increased endothelial nitric oxide production, which improves vasodilation, and reduced vascular smooth muscle proliferation (Kadowaki et al, 2005, Karastergiou et al, 2011). A very recent in vitro study identified a variety of factors overexpressed in obesity, which are potential mediators linking hypertrophic obesity to IR (Weyer et al, 2001). In turn, weight loss results in a hypercellular state with reduced adipocyte size and subsequent alterations in the secretory activity (Toledo et al, 2006). It was established that obesity results in elevations in circulating IL-6 (Mohamed-Ali et al, 1997, 2010, Khaodhiar et al, 2004, Vozarova et al, 2001). Leptin is a mainly fat cell derived factor, whose secretion is also dependent on fat cell size. There are sex differences in its release, whereby the circulating levels of leptin are higher in women than in men at all BMI values (Trayhurn et al, 1998), perhaps reflecting regulation by the sex steroids. (Mohamed-Ali et al, 1998). Obese individuals have elevated circulating levels of inflammatory markers, such as C-reactive protein, and of proinflammatory cytokines, like IL-6 and leptin. Leptin as a proinflammatory cytokine mediates several immune responses (Fain et al, 2000; Madani et al, 2009). Its expression and release has been shown to depend on adipocyte size in rodents and humans (Loffreda et al, 1998; Hamilton et al, 1995). There was a positive correlation between BMI and leptin secretion from subcutaneous and omental fat tissue. The subcutaneous fat depot is the major source of leptin, which starts to decline in the face of weight loss and starvation. TNF $\alpha$

positively modulates leptin secretion (Guo et al, 2004).

Recent studies have suggested that systemic oxidative stress has a strong correlation with BMI (Grundy et al, 2004; Keaney et al, 2003). It has been shown that inducers of oxidative stress could suppress mRNA expression and secretion of adiponectin, and increase levels of inflammatory adipokines (PAI-1, TNF- $\alpha$ , MCP-1). (Furukawa et al, 2004), suggested that the adipose tissue is a major source of the high plasma ROS level. Hypoxia occurs when oxygen availability does not match the demand of the surrounding tissue, resulting in decreased oxygen tension, which is shown to impair insulin secretion and glucose transport, as well as affecting the vascular walls, resulting in hypertension and atherosclerosis. (Rudich et al, 1998, Matsuoka et al, 1997, Keaney et al, 2003), Hypoxia-inducible factor-1 (HIF-1) is a transcription factor that accumulates during hypoxia and increases the mRNA expression of a wide variety of genes for erythropoiesis, angiogenesis, and glycolysis. (Semenza et al, 2000). Hypoxia results in the rapid accumulation of HIF-1 in the nucleus, where it homodimerizes and binds to the core DNA, leading to the transcriptional activation of VEGF and several other known target genes (Semenza et al, 2000).

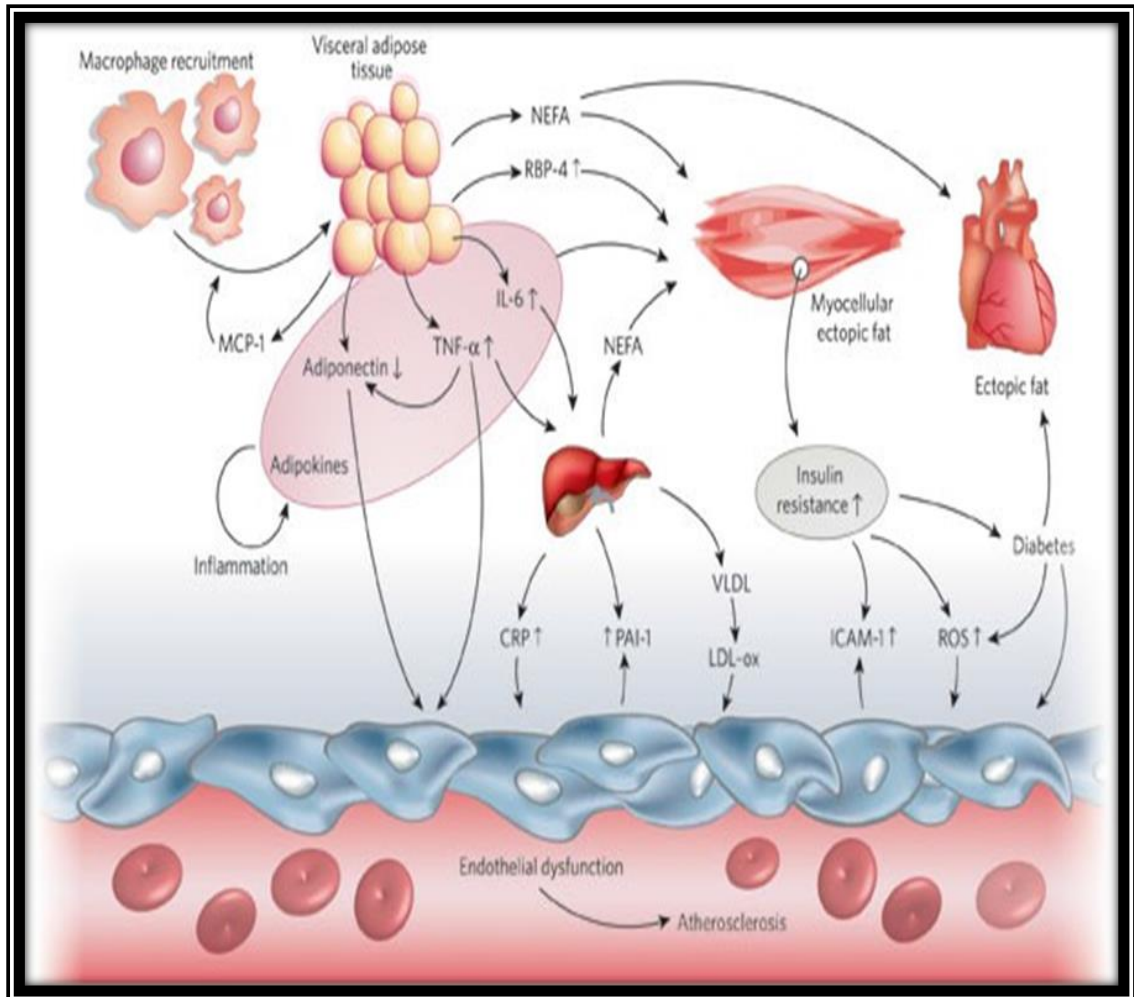


**Figure 6. The changes in abdominal adipose tissue to insulin resistance**

Fat accumulation, insulin resistance, liver-induced inflammation and dyslipidemia features may all lead to the premature atherosclerotic process. (Van Gaal et al, 2006).

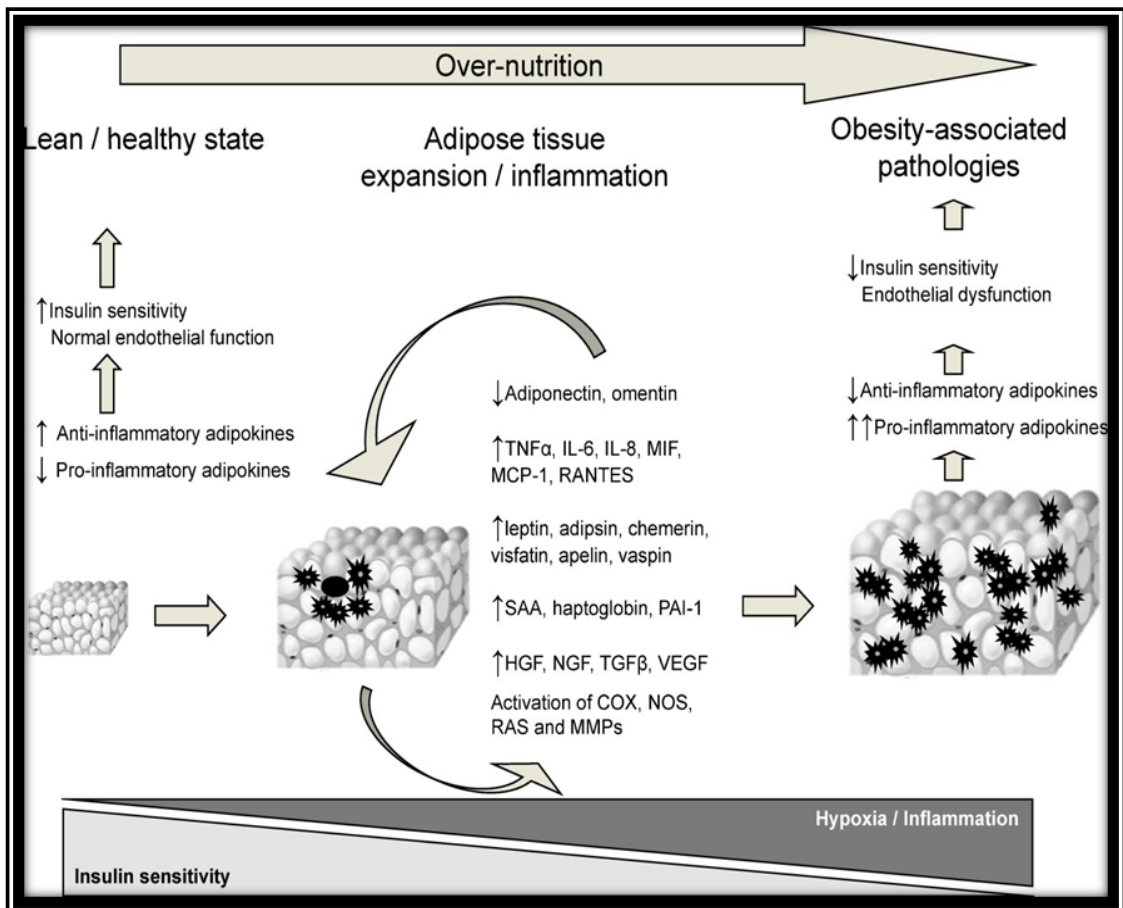


**Figure 7. Adipose tissue hypertrophy and its local effects in obesity**

(Karastergiou and Mohamed-Ali, 2010).

In addition, hypoxia reduces uptake of FFAs by the adipose tissue through inhibition of various transcription factors PPAR $\gamma$  and C/EBP. Therefore, hypoxia is associated with an increased expression of the inflammatory genes such as HIF-1, and decreased expression of adiponectin. This process initiates adipose tissue fibrosis, with an associated increase in local inflammation. Lysyl oxidase (LOX) is a transcriptional target of HIF-1 and acts by cross-linking collagen I and III to form the fibrillar collagen fibers which complicates the inflammation and ends with IR (Halberg et al, 2009, see Figure 8).

#### **1.4 Heterogeneity of obesity pathology**

MeS is a complex disorder which includes increased visceral obesity, hyperglycaemia, dyslipidaemia and hypertension. The major risk factors for the development of the MeS are obesity, regional body fat distribution, physical inactivity and food composition (Grundy et al 2004). It has been found in some studies that visceral abdominal adipose tissue (AT) and muscle-associated AT are related to IR in older subjects, especially in those who are of normal weight. Thus, normal-weight individuals may still be at risk for the MeS and its complications (Groop et al, 1989).

It is also equally apparent that some obese subjects appear to be free of MeS. The common definition used to identify the metabolically healthy obese (MHO) individuals is the absence of metabolic complications (e.g; inflammation, dys-lipidemia and hypertension) and/or preserved insulin sensitivity despite excessive body fatness. Several studies have identified MHO individuals based on insulin sensitivity using the gold-standard hyperinsulinemic–euglycemic clamp technique. However, this technique is invasive, expensive and time consuming. Therefore, other techniques like the HOMA index that has been combined with clinical criteria to identify MHO individuals (Stefan et al, 2008; Meigs et al, 2006; Wildman et al, 2008).

There are studies that show an increase in insulin sensitivity (IS) after weight loss in the



pathologically obese (PO) individuals, as opposed to a slight worsening of IR in the MHO population, suggesting that specific differences must be taken into account with respect to treatment for these individuals (Kantartzis et al , 2011). Other studies showed an improvement in inflammatory markers and lipid profiles of MHO women after weight loss, proving diet restrictions to be more effective in MHO than PO women (Kantartzis et al, 2006).

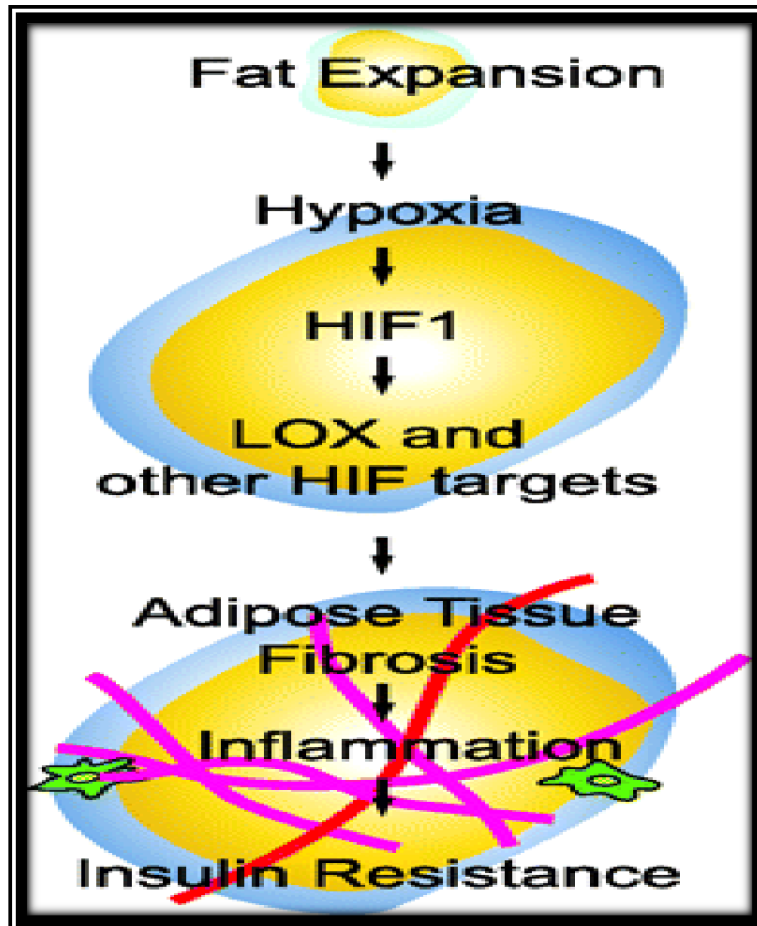


**Figure 8. The relationship between the oxidative stress and IR**

Adipose tissue expansion is accompanied by the production of adipokines increase the production of ROS both locally and from other tissues leading to fibrosis, inflammation and IR. (Halberg et al, 2009).

However, Karelis *et al.* showed that low calorie diet-induced weight loss in MHO women gave a more unfavourable IR profile than with PO individuals, who showed improvement after weight loss (Karelis et al, 2008). Bariatric surgery has become one of the most popular ways of managing sustained weight loss in obese patients in the developed world (Dent et al, 2010). The proof of its effectiveness at reducing T2DM incidence among morbidly obese populations is well known (Buchwald et al, 2009), as well as reducing overall obesity mortality in morbidly obese patients (Adams et al, 2007). However its effectiveness at improving an MHO metabolic profile is much less known. Healthy metabolic profiles, even in the morbidly obese, have less benefit to gain from bariatric surgery than IR. Although other studies showed that MHO subgroup of morbidly obese patients had significant weight loss and improvement in cardiometabolic risk markers compared to before gastric banding (Sesti et al, 2011).

Therefore, more research needs to be carried out in order to discern MHO from PO patients in a clinical context, and to decide on different therapeutic approaches for the two groups. Further studies are needed to investigate the molecular mechanisms that explain the increased protection that this interesting group of patients have to enable them to avoid developing metabolic abnormalities across various BMI and age ranges (Cummings et al, 2012).

#### **1.4.1 Metabolically healthy (MHO) and Pathological Obesity (PO)**

Several studies have shown that MHO individuals present a favourable blood lipid profile as evidenced by lower triglycerides (TGs) and elevated high density lipoprotein (HDL) cholesterol levels. Ferrannini and colleagues initially showed the need for characterisation of obese patients who were healthy (insulin sensitive) from the unhealthy insulin resistant, (Ferrannini et al, 1997). Ethnicity studies are also important given differences in the incidence of obesity complications in different populations. The

identification of the MHO individual in both the clinical and research set-up could have important implications for therapeutic decision making. Thus understanding the molecular differences that lead to the MHO and PO phenotypes is important (see Figure 6).

Impaired adipose tissue function may contribute to a proinflammatory, atherogenic and diabetogenic state, linked to the development of obesity-associated disorders (Karelis et al, 2008).

#### **1.4.2 Mediators of pathological heterogeneity**

##### **1.4.2.1 Specific biomarkers**

The differences in the secretory profile of adipose tissue with respect to its expansion could suggest an inherent difference in the levels of specific circulating adipokines, such as resistin (associated with increased insulin resistance), adiponectin (known to be an insulin sensitizer) and TNF- $\alpha$  (associated with insulin resistance), all of which have been seen to be altered in the presence of insulin resistance in humans (Hivert et al, 2008). Since these and other adipokines, like IL-6, which all also have autocrine and paracrine effects on glucose metabolism, lipolysis and insulin sensitivity (Karastergiou and Mohamed-Ali, 2010) could be different between MHO and PO in their levels and effects on IR, there could be a fundamental difference in secretion levels of these adipokines that could also be used as a biomarker for the onset of insulin resistance and MeS, which makes quantification of these adipokines and their metabolic effects important. Ratios of adiponectin to HOMA-IR index have already been used as a predictive tool for MeS in humans (De Luis et al, 2011), and inflammatory adipokine levels have been determined and shown to decrease during weight loss, while anti-inflammatory adipokines such as adiponectin increase after the weight loss (Blüher et al, 2012).

Small adipocytes have been linked to whole body insulin sensitivity especially with

increased abdominal adipocyte surface area being associated with an elevated risk of developing insulin resistance and T2DM (Weyer et al, 2000, Lundgren et al, 2007).

As yet unknown interactions of genetic and/or environmental factors may cause dysfunction of adipose tissue by a sequence of adipocyte hypertrophy, followed by tissue hypoxia, perhaps as a consequence of reduced capillary density, adipocyte cell death and initiation of inflammatory processes (Lundgren et al, 2007; Pasarica et al, 2009). Adipokines may underlie associations with insulin resistance and endothelial dysfunction (Karastergiou and Mohamed-Ali, 2010). Thus, in PO subjects elevated levels of proinflammatory adipokines may induce IR, and lead to suppression of

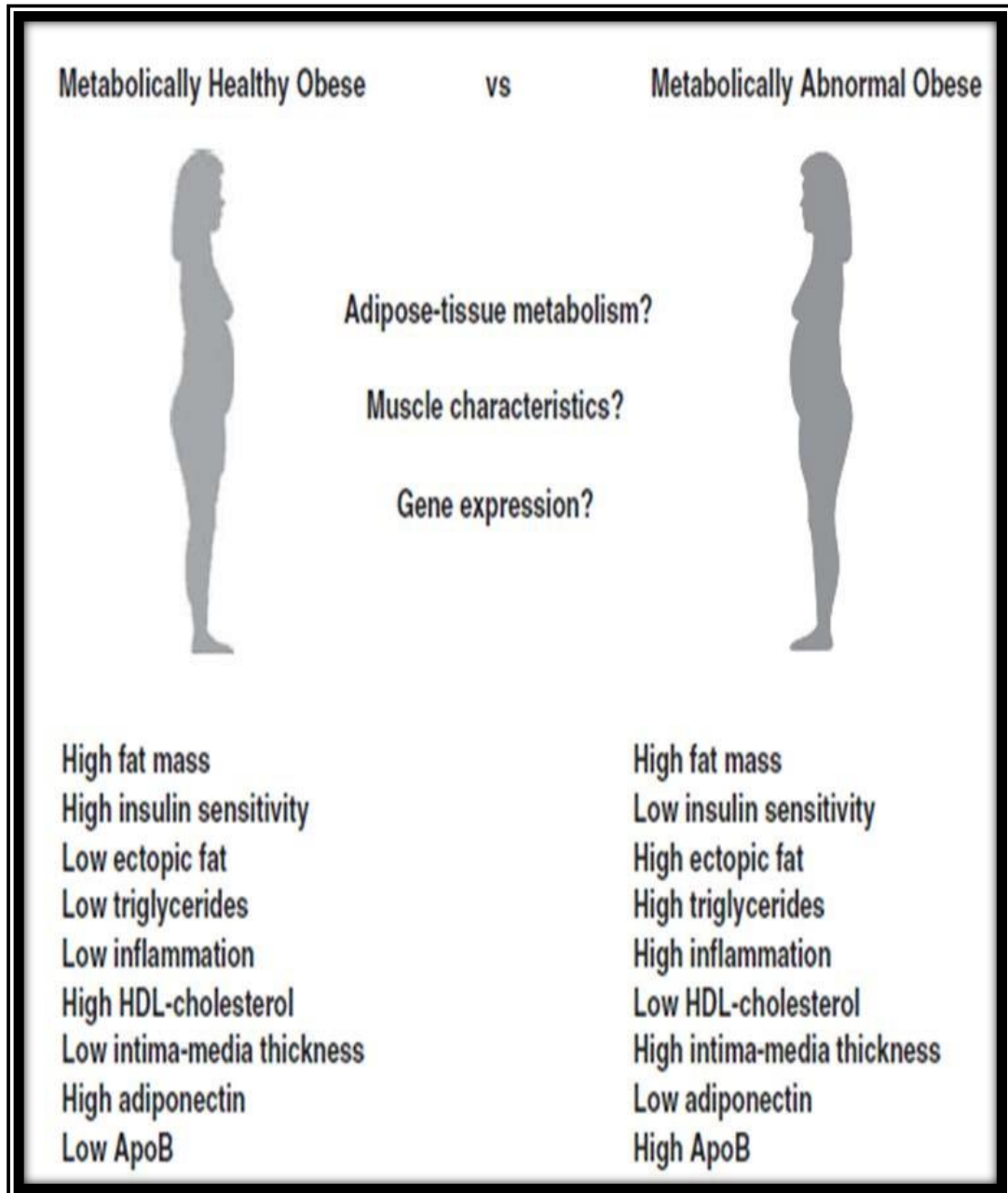


**Figure 9. Clinical differences between MHO and PO subjects**

The figure shows the documented differences in insulin sensitivity, fat mass, lipids, and inflammation in the two patient groups (Primeau et al, 2011).

adiponectin, an endogenous insulin sensitizer. MHO subjects fail to show these changes. This could account for their lower risk of developing obesity-associated diseases. However, data for this hypothesis is varied and detailed comparisons of the adipose tissue of MHO and PO subjects have yet to be done. Furthermore, there are uncertainties about the appropriateness of such costly, and potentially risky, procedures such as bariatric surgery for weight reduction, in patients who might best be treated otherwise. Therefore the molecular mechanisms that give rise to the different obesity phenotypes need to be elucidated.

#### **1.4.2.2 Inhibition of Adipogenesis**

Two independent prospective studies showed that adipose hypertrophy is an independent risk factor for developing T2DM (Olga et al, 2012). Large adipocytes may be a marker for impaired adipogenesis, or also increased deposition of fibrosis within the tissue which renders it less elastic. Lower levels of adipogenesis-inhibiting genes such as preadipocyte-factor1 (*pref-1*) in MHO patients may enable normal adipogenesis in these patients, while conversely increased (*pref-1*) may lead to inhibition of adipogenesis in PO adipose tissue (O'Connell et al, 2011). Other inhibitors of adipogenesis, such as Wnt signalling pathway, may also be candidates for further investigation. The hypothesis that MHO patients have smaller adipocytes had been confirmed in various depots of the adipose tissue and lower levels of (*pref-1*) (O'Connell et al, 2011). Also, an association between smaller adipocyte size and heightened local inflammation signalling has been observed (McLaughlin et al, 2007, McLaughlin et al, 2010). It was reported that omental adipose tissue has smaller adipocytes than the SC but conversely these small adipocytes are inflamed and insulin resistant.

The inflammation impairs differentiation and/or maturation of pre-adipocytes into mature adipose cells; and the small adipose cells demonstrate biological activity similar

to inflammatory cells due to the dysfunction of adipose cell differentiation caused by inflammation (McLaughlin et al, 2010).

In addition to the high capacity of the subcutaneous adipose tissue for adipocyte differentiation and lipid storage where hyperplasia is correlated with decreased the glucose and IR (Kursawe et al, 2010). On the other hand, visceral adipose tissue accumulates macrophages that release inflammatory cytokines, which can impair insulin sensitivity upon this depot expansion or hypertrophy.

Age may also be a determining factor, as recent data from Wildmann et al, demonstrated that the prevalence of metabolic normality decreases with age, as well as BMI (Wildmann et al, 2008). These differences may also reflect different criteria used to select patients for the two different groups, therefore making the need for a common definition of an MHO individual ever more important.

#### **1.4.2.3 Adipocyte cell size in obesity heterogeneity**

‘Benign obesity’ as reported by Stefan et al, demonstrated a higher degree of insulin sensitivity, lower levels of ectopic fat in liver and skeletal muscle, when compared with an insulin resistant obese group (Stefan et al, 2008). However, waist circumference and degree of visceral adiposity were similar between the two groups pointed at the importance of considering the ectopic liver fat more than the visceral fat (Stefan et al, 2008).

Adipocyte size was shown to vary inversely with adipocyte insulin sensitivity, where adipose tissue with enlarged cells, showed a diminished response to insulin. After weight loss and reduction in adipose cell size, insulin sensitivity of the adipose tissue of obese patients was restored to normal. (Salans et al, 1968). More recently, studies have shown functional differences in large and small adipocytes from the same subjects, including altered gene expression profiles (Hansen et al, 2010). Adipocyte size has been shown to



influence adipokine secretion, with increasing adipocyte Size (Skurk et al, 2007). It was shown that OM adipocytes of PO are larger in size than OM adipocytes in MHO where they are equal in size for SC in both groups (O'Connell et al, 2010). Suggesting the role of OM Adipocytes during inflammation where they become larger and release lots of adipokines, see Table 1.

#### **1.4.2.4 Visceral Adipose Tissue and Insulin resistance**

Insulin sensitivity in humans effectively decreases by 30-40% when body weight increases by >35-40% (DeFronzo et al, 1991) and the development of IR has been directly shown to occur in response to experimental overfeeding in normal weight individuals (Sims et al, 1987). Progressive exacerbation of insulin resistance to T2DM, following a prolonged state of hyperinsulinemia has also been reported (Kahn et al, 2006). The size of the visceral adipose depot and adipocyte size in humans is linked to systemic insulin resistance, as well as increased expression of chemokines and cytokines by immune cells in the tissue (Hardy et al, 2011).

A recent study also revealed a correlation between increased amounts of visceral fat, adipocyte hypertrophy, insulin resistance, and elevated expression of autophagy genes in human omental adipose tissue (Kovsan et al, 2011). Therefore, FFAs, cytokines, adipokines and ROS all secreted from visceral adipose tissue, impair insulin action in liver and muscle which leads to a blockage in tyrosine kinase activity interrupting the insulin signal transduction (Hardy et al, 2012). Therefore, the effects of insulin resistance results in the development of non-alcoholic fatty liver disease and dyslipidaemia (Abdul-Ghani et al, 2010).

The greater omental release of fatty acids which have been shown to increase insulin resistance are thought to act through the activation of inhibitory protein kinases such as JNK, and Protein Kinase C which inhibit IRS-1 function in the insulin signalling pathway

as it is shown in Figure (DeFronzo et al, 2010).

Furthermore, South Asians (Indian, Bangladeshi, and Pakistani) living in urban societies have a higher incidence of obesity complications, and greater abdominal fat deposition than other ethnic groups. Therefore, weight loss and maintenance are crucial in the prevention of non-insulin dependent diabetes mellitus (McKeigue, 1996).

### **1.5 Mediators of adipogenesis and IR**

Adipogenesis is the conversion of preadipocytes to lipid engorged fat cells. The majority of genes with altered expression encode proteins involved in cell proliferation, metabolism, immune response, signal transduction, and angiogenesis. A major regulator of adipogenesis is PPAR $\gamma$ . It is a nuclear receptor and is highly tissue selective, being abundant mostly in adipose tissue. It plays an important role as an adipogenic master switch and marker of terminal differentiation through suppressing pro-inflammatory adipokines by interfering with NF- $\kappa$ B and AP-1 or inducing transcription of anti-inflammatory genes. PPAR $\gamma$  activity associated with smaller adipocytes is related more to its metabolic effects.

<b>Adipocyte size</b>		<b>MHO</b>	<b>PO</b>
<b>Omental</b>	n=35	80.9	98.2
<b>Subcutaneous</b>	n=19	104.1	104.9

**Table 1. Adipocyte size in MHO and PO omental adipose tissue**

OM adipocytes of PO were larger in size than those of MHO, while adipocytes of the SC were similar in both groups. O’Connell et al, 2010.

The elevation of PPAR $\gamma$  promotes the differentiation of pre-adipocytes into mature adipocytes (McGregor and Choi, 2011).

Studies have suggested that preadipocytes account for most of the cytokines/chemokines secretion seen in the adipose tissue stromal cells (Isakson et al, 2009). Preadipocytes are morphologically indistinguishable from fibroblasts. Their transcriptional regulation is determined by a sequential activation of transcription factors, where induction of PPAR $\gamma$  and CCAAT/enhancer binding protein (C/EBP), C/EBP $\alpha$ , along with inhibition of Wnt signalling, are important regulatory steps in determining commitment to adipogenesis (Rosen et al, 2006). Four variants of the PPAR $\gamma$  mRNA are known, the PPAR $\gamma$ 1, PPAR $\gamma$ 2, PPAR $\gamma$ 3 and PPAR $\gamma$ 4. PPAR $\gamma$  can be activated naturally by fatty acid derivatives, these acids act as PPAR agonists that transcribe the genes involved in glucose and lipid homeostasis (Neschen et al, 2007). They include docosahexaenoic acid and eicosapentaenoic acid used in the prevention and treatment of cardiovascular and metabolic diseases (Bang et al, 1985). Also synthetic ligands such as thiazolidinediones (TZDs), for example rosiglitazone are widely used for the treatment of diabetes mellitus. The WNT signalling pathway has recently been the focus of much research in this area as an inhibitor of adipogenesis. Studies have shown that macrophage-induced TNF $\alpha$  can activate Wnt signalling during early stages of adipogenesis leading to inhibition of preadipocyte differentiation (Gustafson et al, 2006). Further studies have suggested that TNF $\alpha$  inhibits preadipocyte differentiation through MAPK activation with cross-talk with the Wnt signalling cascade.

PPAR $\gamma$  regulates the expression of various genes involved in adipocyte differentiation, glucose uptake and lipid metabolism (Rosen et al, 2006). Interestingly, this effect was

found to be long-lasting in cultured cells, even after several generations (Isakson et al, 2009). Multipotent mesenchymal stem cells can develop into lineage committed pre-adipocytes. PPAR and C/EBP transcription factors co-ordinate adipogenic gene expression during terminal differentiation into lipid storing mature adipocytes (McGregor and Choi, 2011).

Numerous other genes have been implicated in mediating some of the changes associated with the pathologies of obesity. Omental adipose tissue of obese humans, with its closer relationship to MeS, exhibits an up-regulation of lipolysis repressor genes and a down-regulation of genes involved in lipolysis activation (Gómez-Ambrosi et al, 2004). Another gene of interest is that of NPY, a neurotransmitter, whose central functions include regulation of food intake and body weight, and acts peripherally as a vasoconstrictor as well as an anti-lipolytic agent. The increase of its expression in adipose tissue of obese individuals has been linked to the increased inhibition of lipolysis.

## **1.6 miR**

MicroRNAs are small oligonucleotides, 21-25 in length that post-transcriptionally regulate gene expression by binding to the 3'-untranslated region (3'-UTR) of message encoding RNAs resulting in mRNA degradation or inhibition of translation (Esau et al, 2004). The primary miR transcript is cut by the RNaseIII enzyme known as DROSHA in the nucleus to yield a 70–100 nucleotide product that forms a hairpin structure which is exported to the cytosol by exportin (Zeng, and Cullen, 2004). In the cytosol, these hairpin structures are cut by the endonuclease DICER to a double stranded product of 20–25 bp. This double-stranded RNA is incorporated into the RNA-induced silencing complex (RISC) where the dominant miR is retained and used to direct RISC to the

target mRNA.

Identical pairing of the entire miR with its target results in target degradation, whereas imperfect pairing beyond the first 7–9 bases at the 5' end of the miR blocks translation of the targeted mRNA but does not destroy it (Novina, and Sharp, 2004). To date, 2,042 mature miRs have been identified in human cells (miRBase version 19; <http://miRbase.org/>), and each is predicted to regulate several target genes (Kozomara et al, 2011).

Novel findings suggest that miRs may be stable and functional mediators able to distinguish MHO from PO individuals. The discovery of microRNAs (miRs) by (Ambros et al, 1993) has introduced another level of intricacy in the regulation of the genome. A recent study by Laterza et al established the general principle that microRNAs may act as biomarkers of disease secreted into the systemic circulation upon tissue injury (Laterza et al, 2009). The team demonstrated how circulating miRs may serve as potential indicators of what is happening at the tissue level. Also, Kosaka et al reported how these circulatory miRs are released through secretory machinery and then transferred to the recipients where they can resume their functions (Kosaka et al, 2010). The origin of circulating miRs remains largely unknown, despite intense research. A number of studies have reported that miRs are actively secreted in microvesicles or exosomes from different cell types, which are a likely source of circulating miRs (Caby et al, 2005). In addition to microvesicles or exosomes, microparticles and lipoprotein complexes (such as high-density lipoprotein complexes) are other possible sources of circulating miRs (Olivieri et al, 2013). The exosomes are microvesicles that are present in biological fluids such as urine, saliva and blood (Michael et al, 2010). Within these exosomes are cellular gene products including miRs, mRNAs and proteins that can be transferred to recipient cells to carry out specific molecular functions (Mathivanan et al

2010). Such interactions allow exosomes to mediate cell-to-cell communication by facilitating the exchange of molecular components.

### **1.6.1 Regulation of miRNA expression**

MiRNA expression profiles represent a promising new category of disease biomarkers. However, several endogenous and exogenous factors regulate their expression and need to be borne in mind. These include genetics factors such as ethnicity, sex, nuclear receptors, diet and dietary components as well as exercise. These factors are discussed in the following section.

Population specific genetic variation can affect the prevalence and baseline expression of miRNAs in diverse populations. Consequently, miRNA genetic and expression level variation among ethnic groups may contribute, at least in part, to health disparities observed in multiple forms of cancer, specifically breast cancer, and may be an essential consideration when assessing the utility of miRNA as biomarkers in the clinic. Somatic mutations and dysregulation by miRNAs have been reported in cancer patients (Renata et al, 2014). Also common SNPs in the 3'UTR of GATA4 that alter miRNA gene regulation may be contributing to the pathogenesis of CHDs (Sabina et al 2013).

NRs are ligand activated transcription factors that regulate gene transcription by binding to the promoter region or by interacting with other transcription factors. NRs can regulate miRNA expression either at the transcriptional level or through posttranscriptional maturation by interacting with miRNA processing factors. Growing evidence suggests that miRNAs can be regulated extensively at the levels of promoter transcription, methylation, miRNA processing, RNA editing, and miRNA-target interactions (Breving et al, 2010). Transcriptional regulation by nuclear receptors is the primary level of control for miRNA expression (Table 2). As shown in the Table 2 as an example, miR-122 is regulated by a

nuclear receptor, HNF4 $\alpha$ , which binds to its promotor to regulate miR-122 target genes like Hfe, Hfv, CPEB, HCV, CAT-1, smarcd1/Baf60a. Another interesting miR is miR-29a which is regulated by FXR which binds to its promotor and is regulated by TGF-b, c-Myc, Hedgehog or NF-B to alter the expression of targets such as Ski, MCT1, PTEN and CDK6. The importance of gender has been highlighted in immunerelated diseases, many cancers, and coronary heart disease (CHD). Recent studies have begun identifying sex differences and specificity in miR responses to pathologic conditions, such as cerebral ischemia and radiation, and in cancers including hepatocellular and squamous cell carcinomas (Yeh et al, 2010; Ober et al, 2008; Voskuhl et al, 2011). A thorough analysis of the effects of sex steroid signaling on the transcriptome (Hah et al, 2011) identified 322 distinct pri-miRs, 37% regulated by oestradiol. A microarray analysis of uterine tissue samples from ovariectomized female mice treated with oestradiol identified 39 miRs that were suppressed, surprisingly none were induced (Yamagata et al., 2009).



miRNA name	NR	Endogenous ligands and 2 signals	miR target
Let 7 family	ER;PPAR;PR	Induced by estradiol; PPAR $\alpha$ and PR agonist regulate let-7c.	K-ras; HMGA2; caspase-3; c-Myc; PGRMC1
miR-17-92 cluster	ER	c-Myc, adiol, binds induced by estr to the miR-17-92 promoter; p53 and STAT3 bind to the miR-17-92 promoter.	Myc;E2F;HNF1;PTEN; B IM;ER;AIB1;cyclin D1
miR-21	ER;AR	STAT3, NF-B, CREB and CBP/p300, ER and AR bind to the miR-21 promoter.	Pdcd4;PTEN;PPAR $\alpha$ ;
miR-221/222	ER;AR	NF-B, c-JUN, ER and AR bind to the miR-221/222 promoter.	P27kip1;PTEN;ER $\alpha$ ;PU
miR-200 family	ER;AR;PR	Upregulated by estradiol, androgen and progesterone.	ZEB1; ZEB2; BMI1
miR-146a	ER;AR	Repressed by estradiol, androgen and LPS; LPS induces NF- $\kappa$ B binding to the miR-416a promoter.	ROCK1; TRAF6; IRAK1; CD40L;
miR-26a	ER;AR	Estradiol induces miR-26a, which reduces PR mRNA level	EZH2;MTDH
miR-101	AR	ARE identified in the miR-101 promoter	EZH2; MAGI-2; MKP-1; ATP5B; COX-2; MYCN
miR-125b	AR	AR loading to the 5' UTR region	MUC1; PIGF; IGF-II; PUMA;E2F3FGFR2;
miR-122	HNF4 $\alpha$	HNF4 $\alpha$ binds to the miR-122 promoter.	Hfe; Hjv; CPEB; HCV; CAT-1; Smarcd1/Baf60a
miR-29a	FXR	FXR-responsive element in the miR-29a promoter; regulated by TGF- $\beta$ , c-Myc, Hedgehog or NF-B.	Ski; MCT1; PTEN; CDK6
miR-210	RA R $\alpha$	RAR $\alpha$ /RXR $\alpha$ heterodimers bind to the miR-210 promoter.	FGFRL1; HOXA3; E2F3; RAD52
miR-23a/24-2	RA R $\alpha$	RAR $\alpha$ /RXR $\alpha$ heterodimers bind to the miR-23a/24-2 promoter.	Runx2; XIAP; IL6R
miR-9	TLX	TLX binds to the downstream of miR-9 and miR-9 targets TLX mRNA to form a feedback loop.	PDGFR- $\beta$ ; Nr2e1; FoxP1; Gsh2; NF-kB1
miR-34a	FXR;SH P	p53 binds to the miR-34a promoter; FXR interacts with p53 through SHP to regulate miR-34a	FoxP1; Bcl-2;CDK4;E2F3; N-
miR-433/127	SHP	SHP inhibits ERR $\gamma$ which binds to the miR-433/127 promoters	HDAC6;BCL6
miR-206	SHP	SHP represses ERR $\gamma$ leading to decreased YY1 which inhibits AP1	Notch3; HDAC4; KLF4; activation of the miR-206 promoter Pax7

**Table 2. miRNAs regulated by NRs**

### 1.6.1.1 Environmental mediators

Epigenetics, including miR regulation, has revolutionized our understanding of how genes are switched on and off. A single miR can regulate several biological processes, as well as a group of miRs affecting the expression of a single gene. In addition, miRs themselves are regulated by various molecules such as sex steroid hormones or insulin. In addition dietary components (e.g. PUFA, cholesterol, Vitamin A) have been shown to alter the level of the miRs gene expression, The regulation of adipogenic genes by miRNA can be influenced by dietary fatty acids (FA) in mice (Parra et al, 2010). Meale and colleagues examined the effect of DHA-Gold, an algal meal high in *n*-3 FA docosahexaenoic acid (DHA), on the expression of 15 miRNA, and found that the expression of miR-142 changed significantly when DHA-G was included in the diet (Meale et al, 2014). Previous reports (Jin et al., 2010; Romao et al., 2012), which examined a wide range of miRNA associated with adipogenesis also indicate that diet has a significant influence on the molecular regulation of adipogenesis. Furthermore, it has also been reported that many macro- and micronutrients, such as vitamins, amino acid, fatty acids, retinoic acid, and folate, can modulate miRNA expression (Drummond et al, 2009). As with diet, responses to exercise as a mediator of weight loss shows a high level of interindividual variability. Several studies have identified some circulating miRNAs associated with weight loss following dietary and physical activity interventions. MiRNAs showing differential expression after an acute bout of exercise also appear to differ from those that are altered as a result of long-term training.

In addition circulating miRNAs can differ in their cellular origin, as shown in studies that evaluated monocytes (Radom-Aizik et al, 2014), neutrophils (Radom-Aizik et al, 2010), and whole blood (Tonevitsky et al, 2013). Cellular origin was a determinant of miRs species expressed and involved in regulating different mRNAs and thus their associated

biological pathways.

### **1.6.1.2 Physiological/pathological regulation**

Changes in miR expression and activity have been reported in various pathological states. An overall decrease of miRNA expression has been observed in many types of cancer, though their functional significance remains largely unknown (Lu et al, 2005; Chen and Stallings, 2007; Ozen et al, 2008). In type 2 diabetes, CVD and MeS miRs may regulate the major mechanisms involved in these disorders, such as, inflammation, angiogenesis and hypoxia.

### **1.6.1.3 Inflammation**

Disruption of miRNA biogenesis has a major impact on the overall immune system. Emerging studies indicate that some miRNAs, especially miR-21, miR-146a/b and miR-155, play a key role in regulating inflammatory processes. Furthermore, the brain-specific miR-124 appears to abrogate inflammation by turning off activated microglial cells and macrophages (Ponomarev et al, 2010; Rink et al, Roy et al, 2010). Of relevance to tissue repair is the regulatory loop between cytokines and miRs: cytokines induced following injury are regulated by miRNAs and in turn regulate miRNA expression.

### **1.6.1.4 Angiogenesis and Hypoxia response**

The significance of miRNAs in the regulation of mammalian vascular biology came from experimental studies involved in arresting miRNA biogenesis to deplete the miRNA pools of vascular tissues and cells (Sen et al, 2009). Dicer-dependent biogenesis of miRNA is required for blood vessel development during embryogenesis. Mice with endothelial cell-specific deletion of Dicer, a key enzyme supporting biogenesis of miRNAs, display defective postnatal angiogenesis. Various aspects of angiogenesis, such as proliferation, migration, and morphogenesis of endothelial cells, appear to be regulated by specific

miRNAs in an endothelial specific manner. miRNA-126 is specific to endothelial cells and regulates vascular integrity and developmental angiogenesis. Manipulating angiomiRs in the setting of tissue repair may represent a new therapeutic approach that could be effective in promoting wound angiogenesis.

Tissue injury is often associated with disruption of vascular supply to the injury site. Thus, the injured tissue often suffers from insufficient oxygen supply or hypoxia. Hypoxia induces specific miRNAs, collectively referred to as hypoxamirs (Chan et al, 2010). miR-210 is a classical hypoxamir. Expression of hypoxia-inducible factor 1 (HIF-1) is also controlled by specific miRs. In turn, HIF-1 controls the expression of hypoxamirs that are induced in the injured tissue (Loscalzo et al, 2010). Hypoxamirs are also induced by HIF independent pathways. Although hypoxamirs generally favor angiogenesis their metabolic and cell cycle arrest functions need to be finely regulated, especially when considering tissue repair in an ischemia. Silencing specific hypoxamirs may therefore represent an approach to facilitate tissue repair.

### **1.7 Adipose micro RNA**

Over 2000 microRNAs have been identified. MiRs are abundant in adipocytes and adipose tissue and have been assigned various functions. In differentiated human adipocytes it has been shown that regulation of SirT1 by miR-132 leads to IL-8 and MCP-1 production through activation of NFkB (Strum et al, 2009). Recently using a global miR expression microarray in human subcutaneous fat samples from non-obese and obese women with and without type-2 diabetes (Ortega et al, 2010), it was shown that approximately 6% of miRs significantly differed between fat cells from lean and obese subjects, 9% were highly and significantly up- or down-regulated in mature adipocytes as compared to preadipocytes, while 2% of miRs were correlated with BMI, fasting glucose and triglycerides. They identified 1.4% of miRs significantly deregulated

in subcutaneous fat from obese subjects with and without T2DM and also many of the changes associated with miRs appeared to regulate adipocyte differentiation (Xie et al, 2009; see Figure 7). MicroRNAs may play regulatory roles in many biological processes including adipocyte differentiation (see Figure 8) and insulin resistance. Additionally, miRs may also regulate functions in other insulin responsive tissues such as the liver and the skeletal muscle (Rottiers et al, 2012).

The liver is where the triglycerides and cholesterols are synthesised and transported to the blood through the lipoproteins such as Very Low Density Lipoprotein (VLDL), Low Density Lipoprotein (LDL), and High Density Lipoprotein (HDL). The excess accumulation of triglycerides and FFAs has a strong correlation with insulin resistance and MeS (Cornier, et al 2008). The role of miR-122 in lowering circulating cholesterol has been described by some studies (Elmen et al, 2008). In addition, other studies highlighted the role of miR33a and miR33b and the SREBP gene regulators in controlling cholesterol and lipid homeostasis (Gerin et al, 2010). MiR-375 is highly expressed in the pancreatic alpha and beta cells, implicated in their maintenance in mice. It may also be required for glucose homeostasis (Poy et al, 2009). Therefore the dysregulation of miRs may contribute to metabolic abnormalities, and this opens up the possibility that miRs may serve as therapeutic targets for cardiometabolic disorders.

### **1.7.1 miR in obesity related diseases**

T2DM is characterized by a dysregulation of blood glucose levels and results from progressive peripheral insulin resistance in conjunction with pathologically altered pancreatic insulin secretion. Diabetes is diagnosed by repeated measurement of fasting glucose levels over 126 mg/dL (7 mmol/L), or over 200 mg/dL (11.1 mmol/L) following oral glucose challenge, and T2DM often presents in obese, inactive individuals. Men and

women with diabetes have an increased risk for cardiovascular disease (Kannel et al , 1979), and the frequent comorbidity of T2DM with other cardiovascular risk factors, such as hypertension, dyslipidemia, and obesity, significantly increases the risk of heart failure in these patients (He et al, 2001). Therefore, diabetes is one of the most important risk factors for the development of cardiovascular diseases, and miRs involved in diabetic-related cardiovascular disorders have received much attention, especially in trying to elucidate how cardiovascular risk factors might affect miR signalling. (Han et al 2012). Recently the miR-mediated regulation of the cardiomyocyte-relevant transcription factor GATA4 and pressure-induced cardiac hypertrophy was reported (Han et al 2012).

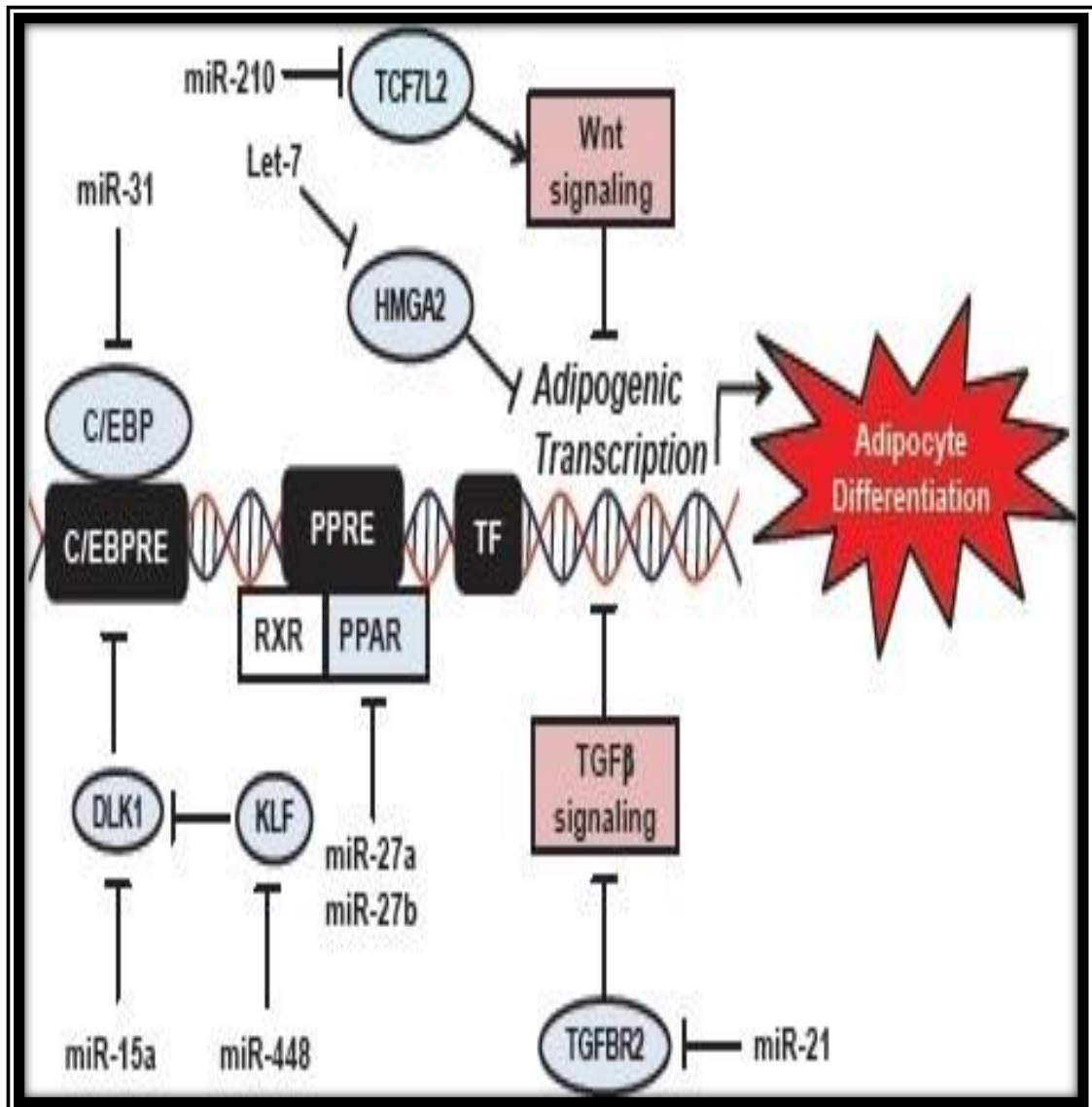


**Figure 10. The regulation of target genes by MicroRNAs during adipogenesis**

(McGregor & Choi, 2011).

### 1.7.1.1 The role of miRs in IR and endothelial dysfunction

Accumulated adiposity leads to increased oxidative stress in adipose tissue and increased production of ROS and inflammatory chemokines which then promotes insulin resistance. Collectively, these processes induce the progression of endothelial dysfunction (see Figure 8). Excess production of ROS and inflammatory adipokines eventually induce deregulation of inflammatory-associated miRs and vice versa in the endothelium. MiRs regulate insulin secretion and  $\beta$ -cell function and several miRs are differentially regulated in diabetes during endothelial dysfunction, diabetic heart disease, and diabetic retinopathy (Shantikumar et al, 2012). Another important aspect of miR function is the regulation of smooth muscle cells (SMCs). SMCs in the vessel wall contribute to vascular remodelling and activation of inflammatory cells. miRs involved in acute vascular injury and pulmonary vascular remodelling have recently been described (McDonald et al, 2012). The identification of key miRs in vascular SMCs may result in novel therapeutic strategies. For example, miR-214 appears to play a role in regulating angiogenesis and has been identified as a potentially important target for pro- or anti-angiogenic therapies (Van Mil et al, 2012).

The prolonged pathogenesis of atherosclerosis is marked by endothelial cell dysfunction, followed by infiltration of macrophages into the vessel wall and SMC proliferation, leading to occlusion of the arterial lumen. Hypertension and hyperlipidemia significantly contribute to the process of atherosclerotic plaque formation (Chobanian et al, 1996). Hypoxia results in the activation of miR-210 and miR-92a, which promote and inhibit angiogenesis, respectively. miR-126, an endothelial-cell-enriched miR encoded by an intron of the *Egfl7* gene, modulates atherosclerosis and angiogenesis by regulating MAPK and PI(3)K signalling. Angiogenesis is also regulated by miR-218, which is encoded by an intron of the *Slit* genes. miR-143 and miR-145 are expressed in SMCs and



control blood pressure and vascular tone, and contribute to vascular remodelling. Therefore, gain and loss of function of smooth muscle–enriched miR-143/145 in vivo results in reduced smooth muscle cell proliferation and consequently prevents neointima formation in surgical models of vascular injury, suggesting that closely titrated levels of miR-143/145 are required for the pathological proliferative response to injury (see Figure 8). MiR-21 is induced in SMCs after vascular injury, and promotes proliferation and

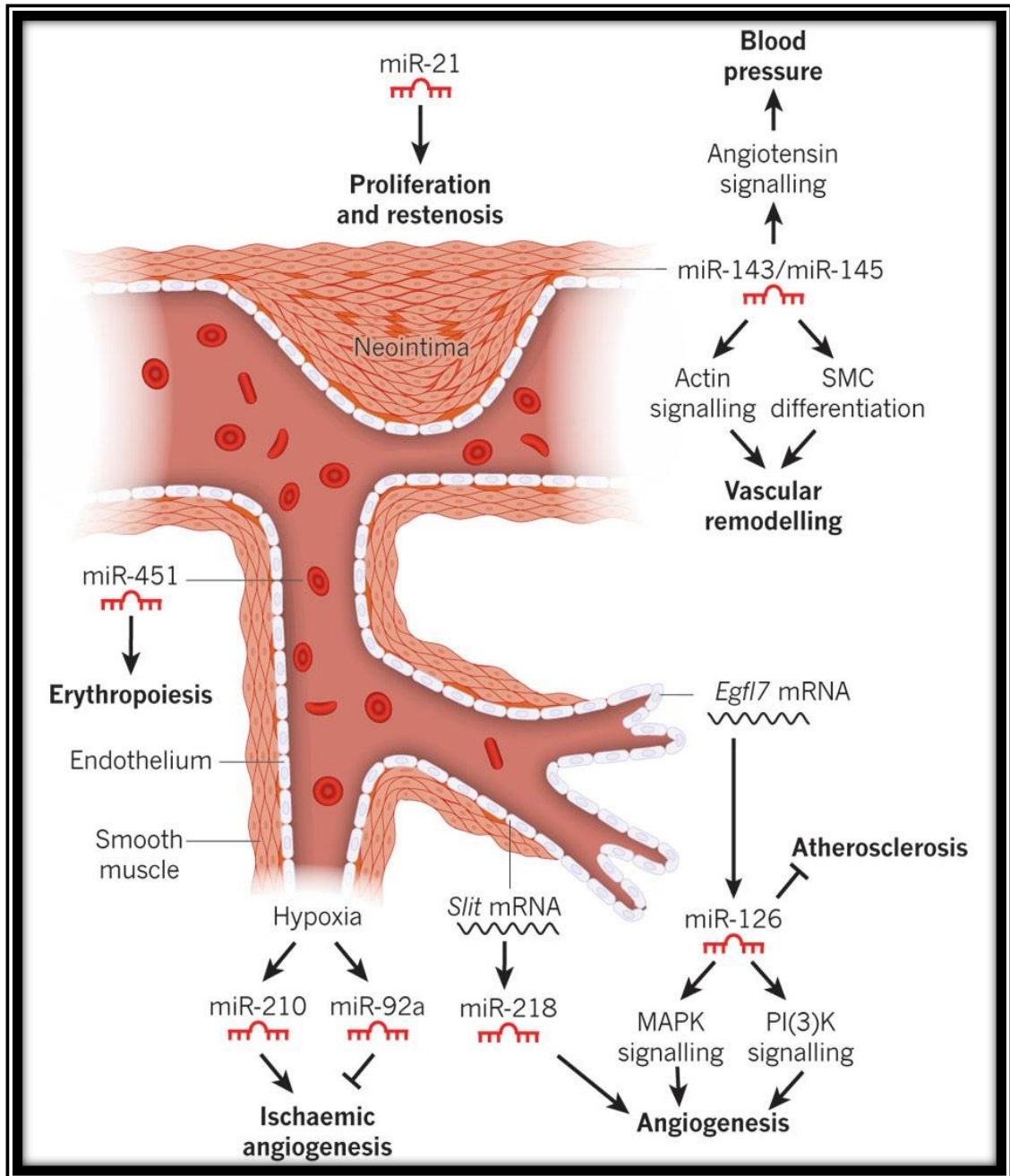


**Figure 11. The expression of select miRNAs with their observed functional role**

Blood vessel schematic showing the endothelial and smooth muscle layers, red blood cells and the proliferating SMCs of a neointimal lesion (Small and Olson, 2011).

neointima formation. miR-451 regulates the proliferation and differentiation of erythroid cells (Small and Olson, 2011).

Thus the discovery of circulating miRs has highlighted their potential as both endocrine signalling molecules and disease markers. Dysregulation of miRs may contribute to various vascular and metabolic abnormalities, further proof that miRs may potentially serve as therapeutic targets for ameliorating cardiometabolic disorders.

### **1.7.2 Preventative miR therapies**

Through the understanding of the role miRs play in normal physiology and pathological conditions, researchers will be able to unlock a new class of therapeutic targets with the potential to significantly alter multiple aspects of their respective conditions. The role of miRs in the pathogenesis of the cardiovascular risk factors suggests that they might be interesting candidate drug targets. However their pluripotency needs to be considered when considering administration of miR-targeted therapies for long-term risk modification as this may have several potential adverse effects. The potential use of anti-let-7 therapy to counteract the diabetic state should take into consideration the long-term risk of developing cancer. There is a need for targeting  $\beta$  cell-enriched miRs to increase insulin secretion which could aid in glycemic control in diabetic patients. But the role of miRs remains to be tested in vivo in disease models. Overexpressed miRs could be inhibited by introducing complementary anti-miR oligonucleotides (antagomiRs), while those miRs that are under-expressed could have their activity restored by synthetic miR mimics. The manipulation of miR expression comprises of two main approaches: miR inhibition therapy and miR replacement therapy. Numerous studies have reported various miRs which showed deregulated expression during the manifestation of metabolic disorders prior to clinical cardiovascular diseases (Hulsmans et al, 2013). Among these, reduced expression of miR-126 in particular, could be detected years before the

appearance of diabetes and symptoms of related vascular diseases. These findings not only feature miRs as good markers for early diagnosis of cardiovascular events but also prompted several clinicians and scientists to assess the predictive value of other miRs in diabetes-induced vascular dysfunction. Early identification of cardiovascular events in obese and diabetic individuals raises the possibility for pharmacotherapy to delay progression and prevent future vascular complications. In addition, several studies have also demonstrated different methods of modulating miR expression and activity to treat vascular complications in obese/diabetic study models. With capacity to control gene expression and regulate various biological pathways, miRs are definitely intriguing targets for novel therapeutic interventions, distinct from that of the classical single-drug-target strategy and analogous to strategies that advocated the use of nuclear receptors or transcription factors as drug targets.

Moreover, the existence of stable miRs in the circulation has made them easily accessible for detection and thus serves as an effective platform for prevention, early diagnosis and treatment.

Therapeutic replacement can be done by using miR antagonists, such as anti-miRs, locked-nucleic acids (LNA) or antagomiRs. These miR antagonists are oligonucleotides with sequences complementary to the endogenous miR. Several studies have reported on efficient antagonism of several miRs, using high-affinity 15 to 16 nucleotide LNA-modified DNA/PS oligonucleotides targeting the 5' region of the mature miR. The best example is therapeutic targeting of miR-122 for treatment of hepatitis C virus infection using a high-affinity 15-mer LNA-modified anti-miR-122. (Elmen et al, 2008, Hedtjarn et al, 2008).

However, a detailed understanding still is required of the molecular mechanisms regulated by the miRs of interest in the specific pathological condition, before

proceeding into clinical applications.

## **1.8 Obesity and Insulin sensitivity in Arabs**

Obesity constitutes a major health problem in Qatar. Increased obesity prevalence among Arabs has rendered a high proportion of this population IR. However, like in Caucasians, some obese individuals maintain IS. The characterization of IR and IS obesity may shed light on the mechanisms underlying the association between increased fat accumulation in obesity and impaired insulin sensitivity. Adipocytes play a central role in the development of obesity-associated MeS, mainly through promoting IR. Understanding the molecular mechanisms underlying the site-specific impaired adipogenesis associated with IR may offer novel ways to prevent the metabolic consequences of obesity and may constitute the basis for future treatment strategies.

Preliminary data showed that systemic insulin levels increased with BMI. Fasting insulin levels appear to be a good surrogate to differentiate between MHO and PO (see Figure16), and both obesity phenotypes were present at every BMI criteria.

### **1.8.1 Cardiometabolic risk factors and their mediators in subjects of Arab origin**

Lack of data on any of these parameters in non-caucasian subjects therefore need for studies: It is very recently that there is emerging data on the prevalence in Arab, gender, ethnicity and insulin differences. How the disease progress related to the diet and genetic predisposition are poorly reported. MIRs useful as mediators. Much of data suggested that Arabs have intermediate phenotypes in Arabs specific to this population between, South Asian and Caucasians. Mechanistic studies about the mediators that could be different from the previous reported studies in other ethnicities which required to be done in Arabs.

## **1.9 Summary**

Studies have shown that MHO have less fat accumulation in the liver, lower muscle fat infiltration and lower concentrations of hepatic enzymes compared to PO individuals (Diabetes care 2011). Their metabolic profiles are not significantly different from those of lean subjects, and longitudinal studies show them to have a lower incidence of T2DM and CHD, compared to PO subjects (Meigs et al, 2006). Furthermore, it was shown that all-cause mortality was higher in the PO subjects, but not MHO subjects, when compared with lean subjects. Therefore, recent interest has focused on trying to stratify obesity into groups with varying degrees of disease risk, understanding the mechanisms that underlie these differences and the most appropriate therapeutic strategies to adopt for treating these different phenotypes. It is not clear whether MHO individuals maintain IS throughout life or whether it only represents delayed onset of obesity-related IR. Little is also known about the effect of this heterogeneity in obesity on responsiveness to diet, exercise or surgery (Karelis et al, 2008).

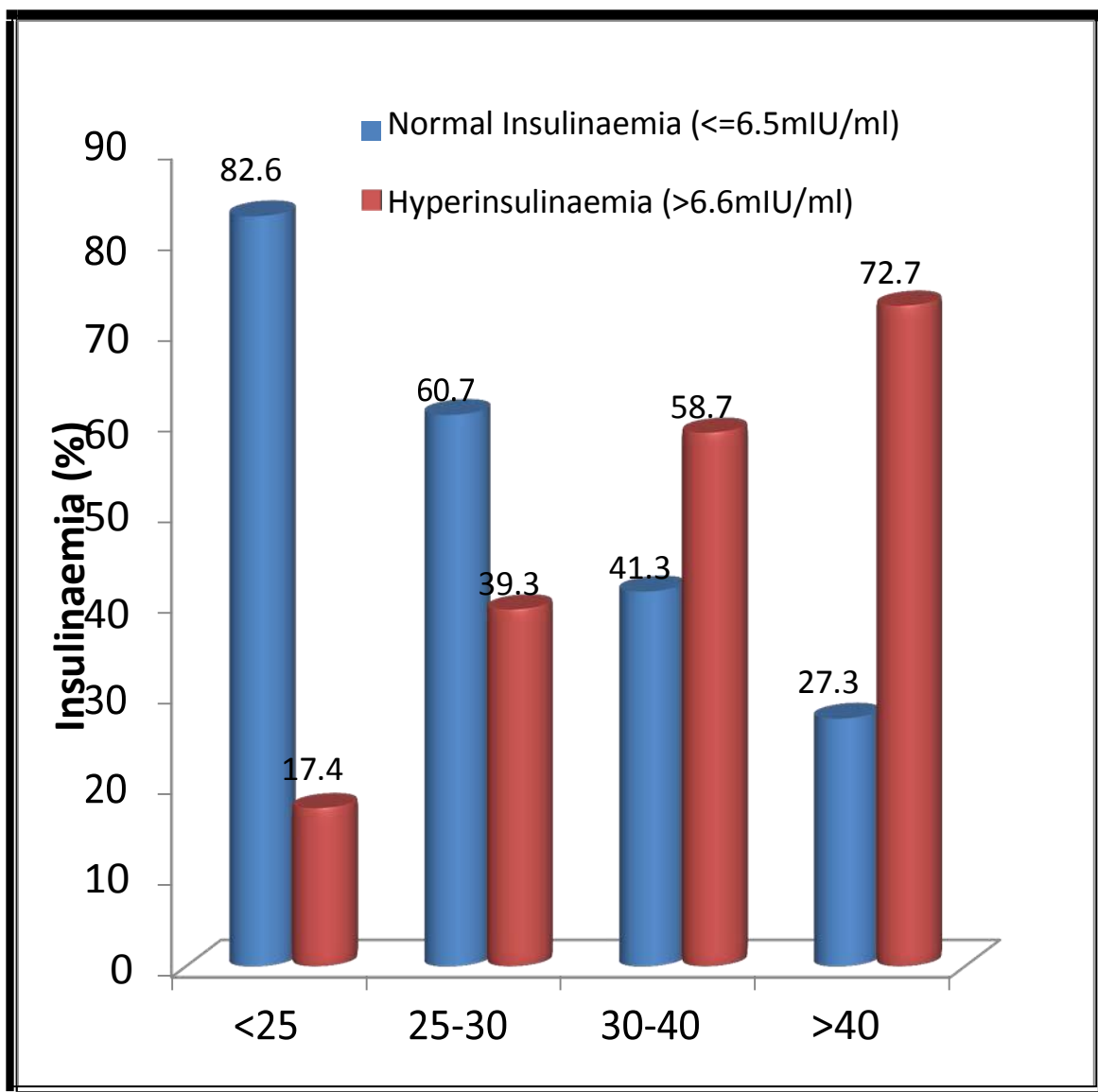


**Figure 12. Insulin levels increase with BMI**

In a pilot study carried out in 2009 in a non-diabetic Arab population (n=149), the prevalence of normoinsulinamia decreased with increasing obesity, while hyperinsulinaemia increased. However, even at normal BMI, hyperinsulinaemia was apparent in a subset, while conversely normoinsulinaemia prevailed in a subset of morbidly obese subjects. (Aspetar, unpublished, 2009). IS decreased when body weight increased past ideal levels by >35-40% leading to IR.

## **1.10 The Aims of the project**

**The aims of the project were, in subjects of Arab origin, to:**

1. Stratify obese subjects depending on systemic biomarkers of insulin sensitivity and inflammation.
2. Identify and validate specific miRs that might be associated with these phenotypes.
3. Confirm and validate, in the whole transcriptome, targets for the specific miRs and assign functionality.



# **Chapter 2**

## **Materials and Methods**

## **2.1 Materials and Methods**

### **2.2 Patient recruitment**

Morbidly obese patients, of Arab origin, undergoing laparoscopic bariatric surgery (gastric bypass, gastric sleeve, or gastric band) were recruited from the pre-operative clinic (Al-Emadi Hospital and Hamad Medical Corporation, Doha, Qatar). Morbid obesity was defined as BMI  $\geq 40 \text{ kg.m}^{-2}$  or BMI  $\geq 35 \text{ kg.m}^{-2}$  with significant co-morbidities. Patients with coronary artery disease, uncontrolled hypertension, malignancy or terminal illness, connective tissue disease or other inflammatory conditions likely to affect cytokine levels, immuno-compromised subjects and those with substance abuse or other causes for poor compliance were excluded. It was ensured that the duration of obesity in all patients was greater than 10 years.

Effect of surgical weight loss was explored using a sub-set of patients, 3-6 months post-surgery, from the Al-Emadi Hospital cohort.

Patients of Arab origin were compared to Caucasian patients recruited from an analogous clinic based at the Whittington Hospital (North London Obesity Surgery Service, Whittington Hospital, London, UK)

The studies were approved by the Ethics Committees of Al-Shafallah, of Hamad Medical Corporation (HMC), Doha, Qatar and National Ethics Committees (UK).

The studies included both males and females over the age of 18 years. Written informed consent was obtained from all participants.

### **2.3 Anthropometric measurements**

Weight (kg) and height (m) were measured in pre-clinic assessment and BMI was calculated ( $\text{kg.m}^{-2}$ ). Blood pressure was measured using digital monitor (Halma, India). Patient information including demographic data (date of birth, gender, ethnicity), surgery type

(gastric bypass, gastric band, gastric sleeve), co-morbidities, current medication, weight loss history, smoking habits and alcohol consumption were recorded from hospital notes.

## **2.4 Blood and Adipose tissue samples**

Blood samples (EDTA, NaF, no anti-coagulant, PAX RNA-later), following an overnight fast, were drawn from an ante-cubital vein on the day of the operation immediately after anaesthesia. Similar fasting samples were obtained in the sub-set cohort after surgical weight loss when attending routine post-surgery clinics.

Samples were centrifuged (3000 rpm, 15 minutes, 25°C), and the plasma or serum was collected and stored at -80 °C until analysis.

AT from the abdominal subcutaneous and intra-abdominal greater omental depots was obtained during the surgery (~5g each) and quickly transported in serum-free medium (Cellgro, Mediatech Manassas, VA) to the laboratory. Approximately 0.5g of the tissue were preserved in RNA-later solution (Life Technologies, Paisley UK) and stored at - 80°C for subsequent extraction. In addition 1-2 grams of tissue was digested by collagenase to separate the adipocytes from the stomal vascular fraction (SVF).

The tissue and the fractionated components were used for organ cultures (Appendix 1), histology (Appendix 1), mRNA and miR gene expression studies as described below.

### **2.4.1 Biochemical analysis**

Plasma glucose concentration was assayed with glucose oxidase reagent (Beckman, USA). Serum triglycerides, total, low density lipoprotein (LDL) and high density lipoprotein (HDL) cholesterol were assayed with commercial reagents (Roche Diagnostics, UK).

Serum insulin levels were determined by ELISA (Mercodia, Uppsala, Sweden).

Insulin resistance was calculated using the homeostatic model assessment where  $HOMA = (\text{glucose in mmol/L} \times \text{insulin in miU/ml})/22.5$ .

After determination of fasting insulin and glucose levels patients were classified as MHO

based on the presence of the following criteria:

- No metabolic disorders including T2DM, dyslipidaemia and hypertension
- Systolic blood pressure at < 140 mmHg, diastolic blood pressure at <85mmHg
- Absence of cardiovascular disease (diastolic blood pressure less than 85mmHg).
- Fasting plasma glucose of <6.8 mmol/l and insulin <6.5 miU/ml.
- 

#### **2.4.2 Serum Adipokines levels**

All circulating adipokines were tested in the serum (adiponectin) or plasma and measured by 2-site ELISA (R&D Systems (UK), according to manufacturer's instructions.

Briefly, standards and samples were pipetted into the 96 wells of microplates pre-coated with antibody against the target protein. After incubation, target protein was bound to the antibody pre-coated on the bottom of the well. The unbound substance was then washed away, followed by adding a detecting enzyme-linked antibody specific for the target protein. After washing, to remove the unbound antibody-enzyme reagent, the substrate was added and colour development in proportion to the amount of target protein bound was observed. Colour development was stopped at set times as per manufacturer's instructions and the intensity of the colour measured by the microplate reader (Tecan, U.S), as absorbance at 450 nm, with correction at 540 nm. All assays had inter- and intra-assay coefficients of variation (CVs) less than 10%.

#### **2.4.3 Preparation of adipocytes and stromal vascular fraction**

Adipose tissue biopsies (1-2g) were washed with warm PBS containing 1% antibiotic solution then minced into small pieces. Then digested using freshly made collagenase solution (0.1% collagenase I/1% BSA in PBS). Adipocytes were separated from SVF after centrifugation at 400g for 10 min and mature adipocytes are collected for further analysis

(see Figure 10). Erythrocytes were removed by resuspension of stromal vascular cell pellets in lysis buffer (2.06 mg/ml Tris base, pH 7.2, 7.49 mg/ml NH<sub>4</sub>Cl) for 10 min. After centrifugation, the pellets were resuspended in HBSS containing 2% fetal bovine serum (FBS) and filtered through a 70µM and 40µM sieves. RNA extraction procedure was performed using a trizol RNA extraction procedure (Section 2.3.4.1).

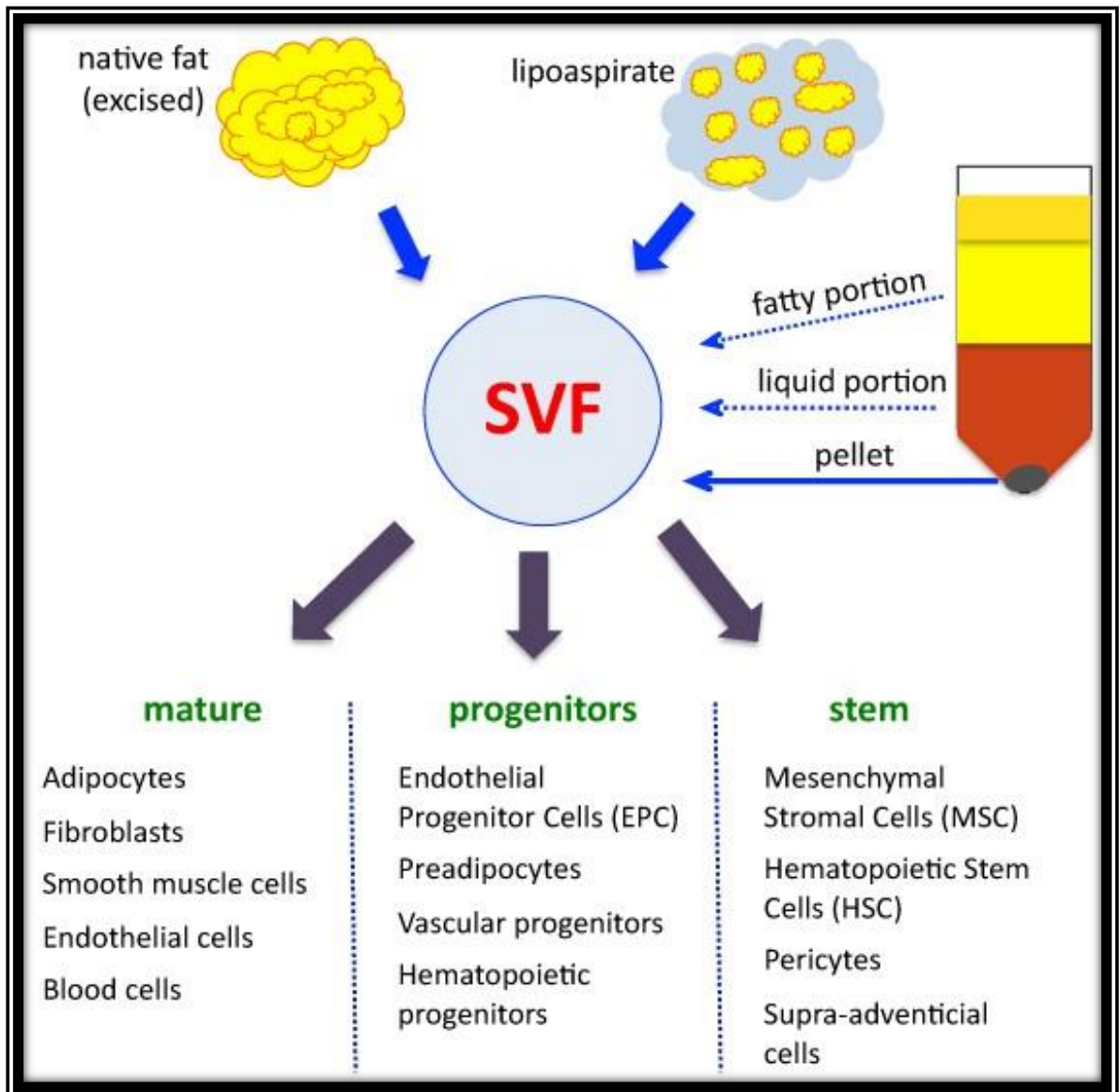


**Figure 13. Preparation of adipocytes and stromal vascular fraction**

The composition of stromal vascular fraction is described (*from google images Alexey Bersenev. Stem cell assay, 2013: <http://stemcellassays.com/2013/05/breaking-fat-svf/>*).

## **2.4.4 Total RNA extraction**

### **2.4.4.1 Adipose tissue RNA**

Approximately 0.15 g of AT was ground in liquid N<sub>2</sub> using a pestle and mortar. Tissue powder were collected and homogenized in TRIzol reagent (Invitrogen, Life Technologies, UK). Then chloroform was added and mixed thoroughly (0.2 ml chloroform per 1ml TRIzol). After centrifugation (3200 rpm, 15 minutes, 4 °C), the mixture was separated into a lower red phenol-chloroform phase, an interphase, and a colourless upper aqueous phase. The upper phase containing total RNA was transported into a new Eppendorf and an equal volume of 100% isopropanol was added and mixed gently. The sample was incubated at -20°C for 1.5 hour. After another round of centrifugation (3200 rpm, 15 minutes, 4°C), the RNA pellet was visible at the bottom of the eppendorf. The pellet was washed twice in 75% ethanol (molecule biology grade, Sigma-Aldrich, UK) and nuclease-free water (Invitrogen, Life Technologies, UK) and dissolved in 40 µl nuclease-free water. The purity and yield of total RNA were determined spectrophotometrically (NanoDrop- 1000 Spectrophotometer, Thermo Scientific, USA). The concentration of RNA was measured as absorbance at 260 nm. The purity was determined by the ratios between 260 nm and 280 nm (260/280) and between 260 nm and 230 nm (260/230). 260/280 and 260/230 ratios within 1.7-2.0 were accepted purity for RNA.

Further assessment of purity was carried out using the Agilent Bioanalyser (Section 2.5).

### **2.4.4.2 Peripheral blood cell RNA and miR extraction**

Total RNA and miR was extracted from peripheral blood cells (n= 58 samples) using two different commercially available kits (PAXgene Blood RNA and miR kits, Qiagen, UK. The extracted RNA species were assayed on the Agilent Bioanalyzer using the Pico 6000 and small RNA chip and ladder 50nt (Section 2.5).

## **2.5 Assessment of RNA quality**

### **2.5.1 Purity assessment using the Agilent Bioanalyser**

Further assessment of total RNA and miRNA quality and quantity was required for the comparison of the gene expression profile of total RNA by pathway specific arrays and validation of hits by next generation sequencing (NGS). For miR NGS, RNA exhibiting high yield and RNA integrity number (RIN) greater than 7 was used for miR enrichment and library preparation. The same samples were used for the pathway specific arrays.

### **2.5.2 Total RNA quality assessment**

Total RNA from the SC and OM adipose tissue was extracted from 48 patients, however, only seventeen samples were selected depending on their quality/purity ( $RIN \geq 7$ ), as assessed by the analyzer (Figure 11). These samples were used for sequencing and the miR pathway specific array (Qiagen, UK).

### **2.5.3 Small RNA quality assessment**

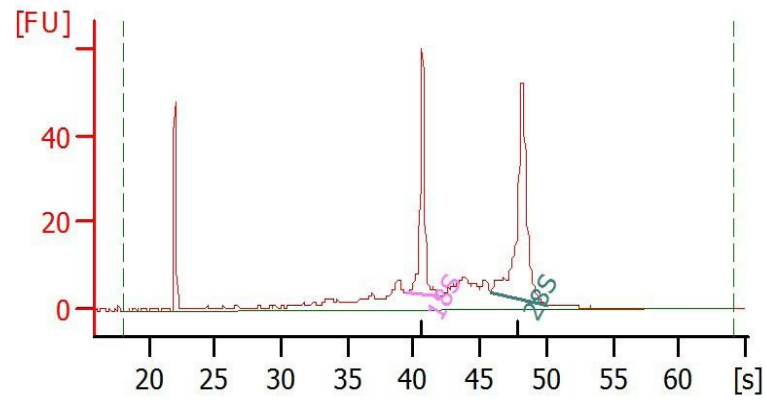
For small RNA sequencing the best samples (n=6 each of MHO and PO) were selected, enriched for miR and checked on the analyser (see Figure 12 and more figures showed the different concentration in the appendix 2).

## **2.6 cDNA synthesis**

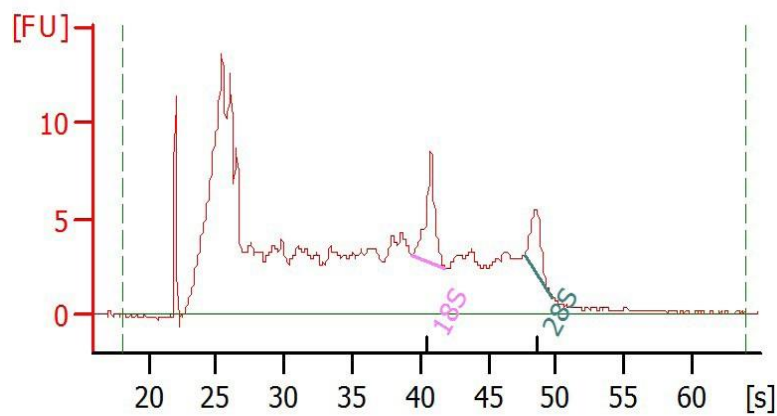
### **2.6.1 cDNA synthesis for RT-PCR**

For reverse transcription, 0.5 $\mu$ g of total RNA was incubated with recombinant Moloney Murine Leukaemia Virus Reverse Transcriptase (1.25 U/ $\mu$ L), deoxyNTP mixture (ATP, CTP, GTP, UTP at 500  $\mu$ M each), oligo d(T)16 (2.5  $\mu$ M), RNase inhibitor (0.4 U/ $\mu$ L), MgCl<sub>2</sub> (5.5 mM) and reaction buffer (all Applied Biosystems, Paisley, UK) at 42<sup>o</sup>C for 60 min.

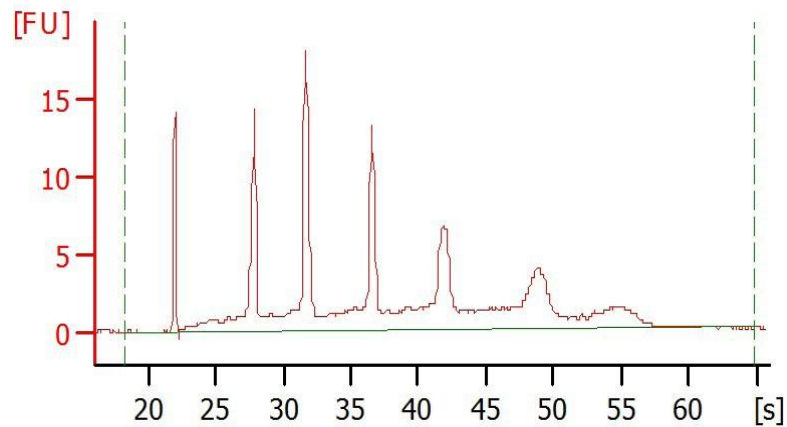




**A**



**B**



**C**

**Figure 14. Assessment of RNA quality**

The Agilent 2100 Bioanalyzer was used to check the quality of the different types of RNA: A: Intact total RNA. RIN=8.7 B: Partially degraded RNA. RIN=3.6. C: with the RNA

ladder (50-300bp).

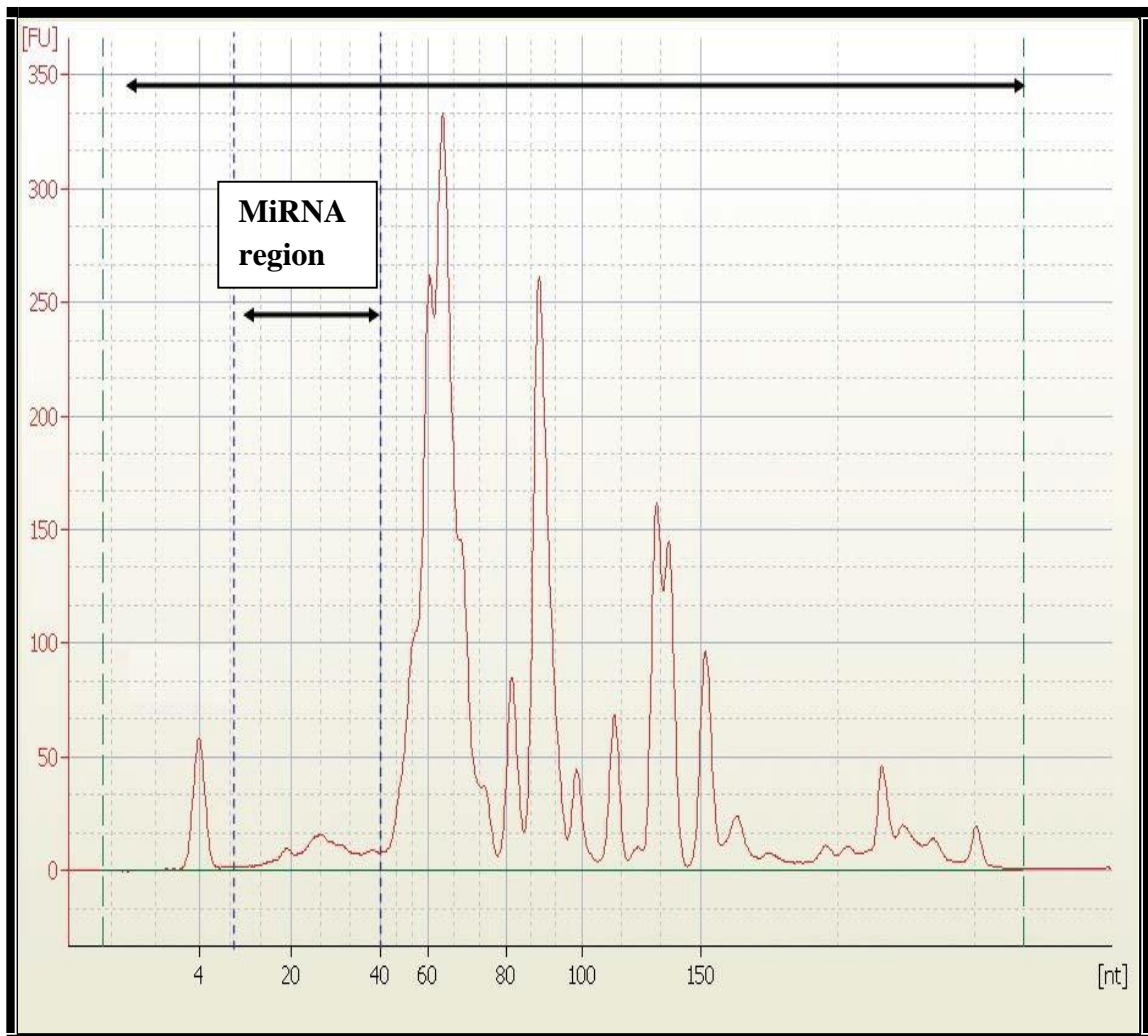


**Figure 15. Size selection of small RNA species**

The miR size required for further investigation was in the region of 10-40nt. Samples were selected depending on the percentage of miR within the small RNA fraction (sRNA).

### **2.6.2 miR cDNA synthesis**

miR cDNA synthesis (200ng per sample) was performed using the miScript Reverse Transcriptase Mix (Qiagen). cDNA samples were diluted with 200µl of RFW after the incubation (one hour at 36°C and 95°C for five minutes) and stored at -80°C.

### **2.6.3 cDNA Synthesis for target analysis**

Samples from patients (n=3; SC and OM adipose tissues and PBCs) were used for the target arrays analysis.  $\beta$ -actin was used as the house-keeping gene. Depot specific differences in the expression of the target genes were also investigated in SVF samples (SC/OM; n=6). For cDNA synthesis 1 µg of RNA, 2µl of gDNA Wipeout Buffer (7x), water to a volume of 14µl, along with 6µl of the PCR master mix that contained 1µl of Quantiscript Reverse Transcriptase, 4µl of Quantiscript RT Buffer (5x) and 1µl of RT primer mix. The mixture was incubated for 15 minutes at 42°C, followed by incubation for three minutes at 95°C.

## **2.7 Real-time PCR and Miscript Arrays**

### **2.7.1 RT-PCR**

Transcripts encoding various genes were measured by real-time PCR on an Applied Biosystems ABI7500 machine, using ABI SYBR Green master mix (Applied Biosystems, USA). This technique was used to analyze expression of target genes in peripheral blood samples and adipose tissues (subcutaneous and omenta) from PO and MHO samples. Specific primers were obtained from Qiagen (UK). PCR reaction conditions were 50°C for 2 minutes, 95°C for 15 minutes, followed by 40 cycles of 94°C for 15 seconds, 56°C for 30 seconds and 76°C for 30 seconds. The level of  $\beta$ -actin in each sample was used to normalize for the variability in RNA quantity or differences in the efficiency of the reverse transcriptase reaction. Data was presented as fold change ( $2^{-\Delta\Delta C_t}$ )

$\Delta\Delta\text{CT}$ ) after normalisation.

### **2.7.3 miR PCR Array**

100 $\mu\text{l}$  of the diluted cDNA samples was used to run the Pathway specific miScript miR PCR Array. This protocol enables real-time PCR profiling of mature miR using miScript miR PCR Arrays in combination with the miScript SYBR Green PCR Kit, which contains the miScript Universal Primer (reverse primer) and QuantiTect SYBR Green PCR Master Mix. 0.5–1 ng of cDNA was added per well of the plate. After the addition of the master mix, the plate was sealed, centrifuged and amplified. PCR reaction conditions were 95°C for 15 minutes, followed by 40 cycles of 94°C for 15 seconds, 55°C for 30 seconds and 70°C for 30 seconds (ViaVII, Applied Biosystems, USA).

Pathway specific PCR arrays (Qiagen) were used to assess the expression of 84 key miR genes involved in the metabolism, differentiation and maintenance of mature adipocytes using real time PCR (see Table 2). Endogenous reference RNA controls were used to normalize the amount of target miR which is known as relative quantification. Normalization corrects for factors that could otherwise lead to inaccurate quantification. These factors include variation in quantity of input RNA, possible RNA degradation or presence of inhibitors in the RNA samples, and differences in sample handling.

Normalization also allows results from different experiments and samples to be compared directly. MiScript PCR house-keeping genes used a panel as described in the array (SNORD61, SNORD68, SNORD72, SNORD95, SNORD96A, snRNA, RNU6B and RNU6-2). Results were analyzed as described in Section 2.16.

### **2.8 Validation of the miR Array data**

Specific miRs were selected for further validation by q-PCR as they gave significant results on comparison between MHO and PO, or before and after weight loss or by their

correlation with inflammation and IR. MiR from both peripheral blood and SVF were used for these validations. The following miR was chosen: miR-122, miR-29b, let7c, let7g, miR-124, miR-302a, miR-302-b, miR-302-c, miR-9a, miR-9b and miR-9. Housekeeping genes were included for normalization (see section 2.7.2). The protocol of the RT-PCR was described in section 2.7.1. Results were analyzed using the Qiagen on-line programme (see Section 2.16).

## 2.9 Target arrays

Commercially available target arrays for miR-29 (Qiagen, UK) were used to detect expression of 84 hsa-miR target genes (see Table 3). This panel of 84 genes includes currently known experimentally verified and bioinformatically predicted target genes regulated by hsa-miR.

hsa-miR-142-5p A01	hsa-miR-9-5p A02	hsa-miR-150-5p A03	hsa-miR-27b-3p A04	hsa-miR-101-3p A05	hsa-let-7d-5p A06	hsa-miR-103a-3p A07	hsa-miR-16-5p A08	hsa-miR-26a-5p A09	hsa-miR-32-5p A10	hsa-miR-26b-5p A11	hsa-let-7g-5p A12
hsa-miR-30c-5p B01	hsa-miR-96-5p B02	hsa-miR-185-5p B03	hsa-miR-142-3p B04	hsa-miR-24-3p B05	hsa-miR-155-5p B06	hsa-miR-146a-5p B07	hsa-miR-425-5p B08	hsa-miR-181b-5p B09	hsa-miR-302b-3p B10	hsa-miR-30b-5p B11	hsa-miR-21-5p B12
hsa-miR-30e-5p C01	hsa-miR-200c-3p C02	hsa-miR-15b-5p C03	hsa-miR-223-3p C04	hsa-miR-194-5p C05	hsa-miR-210-3p C06	hsa-miR-15a-5p C07	hsa-miR-181a-5p C08	hsa-miR-125b-5p C09	hsa-miR-99a-5p C10	hsa-miR-28-5p C11	hsa-miR-320a C12
hsa-miR-125a-5p D01	hsa-miR-29b-3p D02	hsa-miR-29a-3p D03	hsa-miR-141-3p D04	hsa-miR-19a-3p D05	hsa-miR-18a-5p D06	hsa-miR-374a-5p D07	hsa-miR-423-5p D08	hsa-let-7a-5p D09	hsa-miR-124-3p D10	hsa-miR-92a-3p D11	hsa-miR-23a-3p D12
hsa-miR-25-3p E01	hsa-let-7e-5p E02	hsa-miR-376c-3p E03	hsa-miR-126-3p E04	hsa-miR-144-3p E05	hsa-miR-424-5p E06	hsa-miR-30a-5p E07	hsa-miR-23b-3p E08	hsa-miR-151a-5p E09	hsa-miR-195-5p E10	hsa-miR-143-3p E11	hsa-miR-30d-5p E12
hsa-miR-191-5p F01	hsa-let-7i-5p F02	hsa-miR-302a-3p F03	hsa-miR-222-3p F04	hsa-let-7b-5p F05	hsa-miR-19b-3p F06	hsa-miR-17-5p F07	hsa-miR-93-5p F08	hsa-miR-186-5p F09	hsa-miR-196b-5p F10	hsa-miR-27a-3p F11	hsa-miR-22-3p F12
hsa-miR-130a-3p G01	hsa-let-7c-5p G02	hsa-miR-29c-3p G03	hsa-miR-140-3p G04	hsa-miR-128-3p G05	hsa-let-7f-5p G06	hsa-miR-122-5p G07	hsa-miR-20a-5p G08	hsa-miR-106b-5p G09	hsa-miR-7-5p G10	hsa-miR-100-5p G11	hsa-miR-302c-3p G12
cel-miR-39-3p H01	cel-miR-39-3p H02	SNORD6 1 H03	SNORD6 8 H04	SNORD7 2 H05	SNORD9 5 H06	SNORD9 6A H07	RNU6-2 H08	miRTC H09	miRTC H10	PPC H11	PPC H12

**Table 3. Inflammation associated miR array**

The array consisted of a panel of 84 inflammatory miRs.

This array also includes target genes regulated by other miRs that have the same seed sequence as hsa-miR-29a-3p, including hsa-miR-29b-3p and hsa-miR-29c-3p. A set of controls present on each array enables data analysis using the  $\Delta\Delta C_T$  method of relative quantification as well as assessment of reverse transcription performance, genomic DNA contamination, and PCR performance.

## 2.9.1 Target array PCR

102µl of cDNA (see section 2.5.3), 1350µl of 2X RT Syber Green mastermix and 1248µl RFW was added to each well of the miR-29 target plate (Table 4). The plate was sealed, centrifuged and amplified for 95°C for 10 minutes, followed by 40 cycles of 95°C for 15 seconds, and 60°C for 1 minute.

ACVR2A A01	ADAM12 A02	ADAMTS9 A03	AK3 A04	BACE1 A05	BAK1 A06	BBC3 A07	BCL2 A08	BCL2L11 A09	BMF A10	NREP A11	CD276 A12
CDC42 B01	CDK6 B02	COL15A1 B03	COL1A1 B04	COL1A2 B05	COL21A1 B06	COL2A1 B07	COL3A1 B08	COL4A1 B09	COL4A2 B10	COL5A2 B11	COL5A3 B12
COL7A1 C01	CTNBP1 C02	DGKD C03	DICER1 C04	DNAJB11 C05	DNMT1 C06	DNMT3A C07	DNMT3B C08	DUSP2 C09	ELF2 C10	ELN C11	EOMES C12
FBN1 D01	FEM1B D02	FGA D03	FGB D04	FGG D05	FOXJ2 D06	GLUL D07	GRN D08	HDAC4 D09	HRK D10	IFI30 D11	IREB2 D12
ITGA11 E01	LAMC1 E02	LPL E03	MBTD1 E04	MCL1 E05	MMP15 E06	MMP24 E07	MYCN E08	NAV3 E09	NID1 E10	PCDHA12 E11	PIK3R1 E12
PMP22 F01	PPM1D F02	PPP1R13B F03	PTEN F04	PXDN F05	RLF F06	S100B F07	SERPINB9 F08	SESTD1 F09	SFPQ F10	SP1 F11	SPARC F12
SPRY1 G01	SRSF10 G02	TBX21 G03	TCL1A G04	TDG G05	TET1 G06	TFAP2C G07	TGFB3 G08	TNFAIP3 G09	VEGFA G10	ZFP36 G11	ZFP36L1 G12
ACTB H01	B2M H02	GAPDH H03	HPRT1 H04	RPLP0 H05	HGDC H06	RTC H07	RTC H08	RTC H09	PPC H10	PPC H11	PPC H12

**Table 4. miR-29 target genes**

The array (Qiagen) detected 84 genes previously examined experimentally. See Appendix for full gene list.

## **2.9.2 Validation of genes from the Target arrays**

Three collagen genes that were seen in the miR 29 target arrays, and have also been reported both by predictive software and in functional studies of adipose tissue, were chosen for further validation studies: COL1A, COL3A and COL6A and  $\beta$ -actin (house keeping gene). cDNA synthesis and real time PCR were performed following the protocol as mentioned in section 2.6 and 2.7.

RNA samples of whole SC and OM adipose tissue (n=14; 2 MHO, 5 PO) were used.

## **2.10 Small RNA sequencing – PGM**

### **2.10.1 Library preparation**

Libraries were prepared to analyse miR, using magnetic bead-based clean up, for the detecting of transcripts and changes in miRNA gene expression (Ion Torrent, Life Technologies; see Figure 13).

### **2.10.2 Sample selection**

Samples that passed the QC checks were enriched for miRs. The miR (%) was calculated according to the formula:  $\% \text{ miR} = (\text{mass of miR} \div \text{mass of total RNA}) \times 100$ .

The RNA were enriched and assessed of quality using the bio analyzer, Figure 14.

### **2.10.3 Enrichment of RNA samples**

The Nucleic Acid Binding Beads were gently mixed and 7 $\mu$ L added to each well of the processing plate with 120 $\mu$ L of the Binding Solution Concentrate and the contents mixed (10 times). Total RNA (0.5–20)  $\mu$ g was resuspended in 75 $\mu$ L NFW and 75 $\mu$ L of each RNA sample (30 $\mu$ L of RNA+45 of NFW) transferred to the prepared processing plate. Absolute ethanol (105 $\mu$ L) was added to each well, mixed (X 10) and incubated for 5 minutes at room temperature off the magnetic stand. The supernatant was removed from



the beads without disturbing the beads and transferred to a new well in the plate. 30µL of NFW was added to the supernatant in a new sample well. 570µL of 100% ethanol was added to each well, 7µL Nucleic Acid Binding beads were added to the wells of the processing plate and mixed 10 times. The samples were incubated for 5 minutes at room temperature off the magnetic stand, and then the supernatant was aspirated and discarded. 150µL of Wash Solution Concentrate with ethanol were added to each sample, and the samples were incubated for 30 seconds, aspirated and discarded from the plate, followed by air drying and elution in 30µL of pre-warmed (80°C) NFW (one minute). 30µL of the eluate was collected and stored at -80°C. One µL of the purified and enriched small RNA sample was run on the Agilent 2100 Bioanalyzer using the Small RNA Kit chip to assess the quality and quantity.

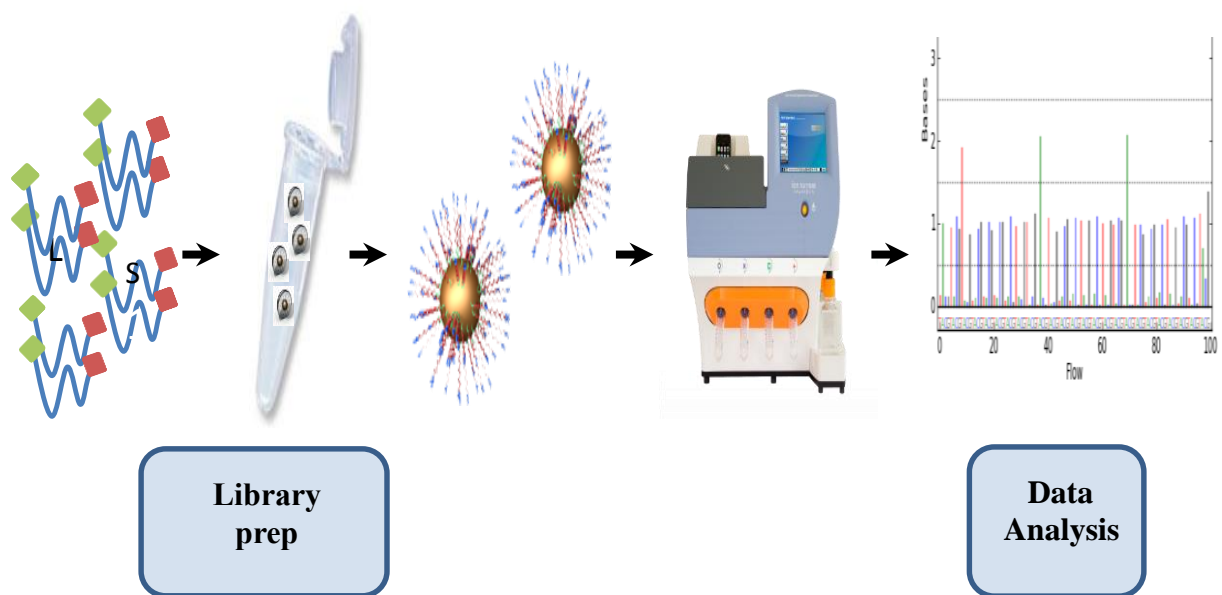


**Figure 16. Small RNA sequencing using the PGM.** Libraries were prepared using magnetic bead–based clean up for the detection of miRs expression.

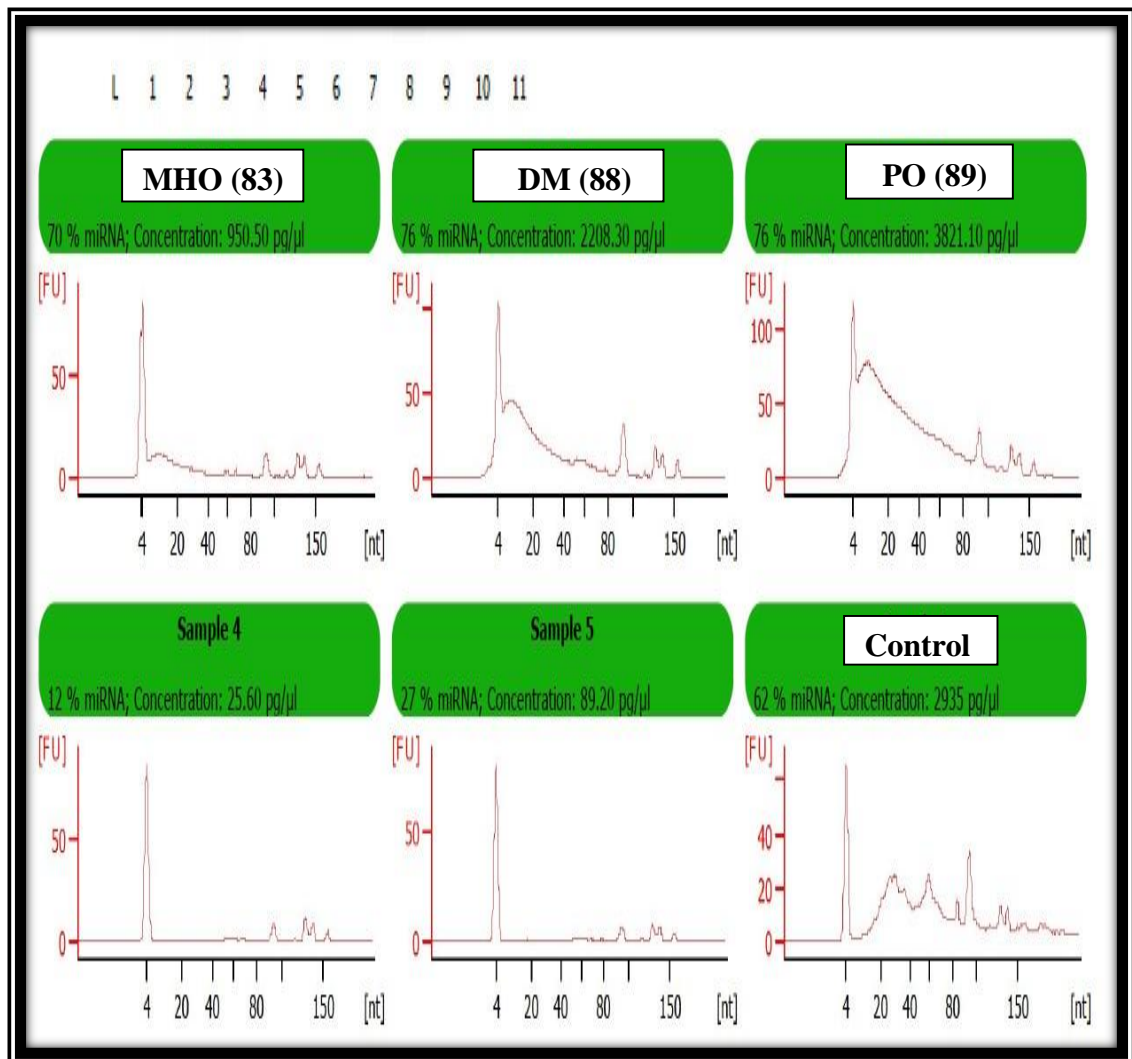


**Figure 17. Quality control data of samples used for small RNA sequencing.**

Three samples were selected, along with their controls, and used for NGS (shown in box).

#### **2.10.4 Hybridization and ligation**

The hybridization was performed by adding 5µl of hybridization master mix (2µL of Ion adaptor were mixed with 3µl of hybridization solution) to 3µL of the enriched miR (1-100ng) and incubating after mixing at 65°C for 10 minutes followed by 16°C for 5 minutes. Next 12µl of the ligation master mix (10µl of 2X ligation buffer and 2µl of ligation Enzyme mix) was added to each of the 8µl hybridization reactions. The mixture was centrifuged and incubated at 16°C for 2-16 hours (8 hours was the minimum time used). The cDNA was prepared by reverse transcriptase kit by adding 2µl of NFR with 4µl of 10X RT buffer, 2µl of 2.5 mM of NTP mix and 8µl of ion RT primer v2. The RT master mix and the ligation mix were pooled, vortexed gently and incubated for 10 minutes at 70°C and snap cooled on ice. 4µl of 10X Superscript III Enzyme mix was added to the ligated mix and left at 42°C for 30 minutes. The cDNA was purified using the magnetic beads clean up module. Seven µl of the beads was added to each well with 140µl of the binding solution concentrate, mixed well (10 X) and 40µl of the cDNA transferred into each well. 120µl of 100% ethanol was added to each well and mixed (10 X), incubated for five minutes at room temperature, followed by a another incubation on the magnetic stand for five minutes to separate the beads. The supernatant was transferred to a new well in the plate to which 72µl of NFW were added, mixed with 78µl of 100% ethanol and 7µl of beads. 150µl of wash solution concentrate with ethanol was added into each well on the magnetic stand for 5 minutes. The supernatant was discarded and the residual ethanol removed followed by air drying on the magnetic stand for 2 minutes. The cDNA was eluted on the stand by adding 12µl of pre-warmed RFW for 10 minutes at 37°C and snap cooled on ice and collected to be amplified. Six µl of cDNA, 45µl of PCR mix (45µl of platinum PCR Super Mix High Fidelity) and 1µl of barcode specific primer were mixed and incubated at 94°C for 2 min, two cycles at 94°C

for 30 sec, 50°C for 30 sec and 68°C 30 sec, followed by 14 cycles at 94°C for 30 sec, 62°C for 30 sec and 68°C for 30 sec. The final cycle was for 5 minutes at 68°C. The amplified cDNA was purified by the magnetic beads clean up module. The yield and size distribution was assessed by DNA High Sensitivity kit. The molar concentration (nM) of each of the barcoded cDNA libraries was measured and diluted, equal volume of each diluted samples in the library were mixed to prepare a pool of the barcoded libraries. The template dilution factor was determined by the use of the final molar concentration using the formula:

$$(\text{Library concentration in nM}) \times (5 \times 10^9 \text{ molecules}/\mu\text{l}) / (8.3 \text{ nM}) \times (20 \mu\text{l}) = (210 \times 10^6 \text{ molecules}).$$

It was recommended that the highest quality of libraries should not be less than 50% amplified DNA after selecting the region of interest of miR (10-40nt). The samples used here were close to this recommendation and found to be acceptable.

MiR conc (10-40nt) on Small RNA chip 1 uL) / Total RNA con from Nano Chip NG/UI (1 ul) \* 100.

Four samples were pooled together in an equal volume of each library to get a final concentration of 14pM of each diluted library. Three samples with their control were pooled and loaded in the PGM.

### **2.10.5 PGM runs summary of the small miR samples**

miR samples from 3 patients were sequenced, (1 MHO, 1 T2DM and 1 PO – Table 5).

The same samples were used as a replicate for the second run (83-001, 88-002, 89-003).

The report summaries are shown in Figures 15 and 16.

## 2.11 Whole transcriptome analysis

### 2.11.1 Sample selection

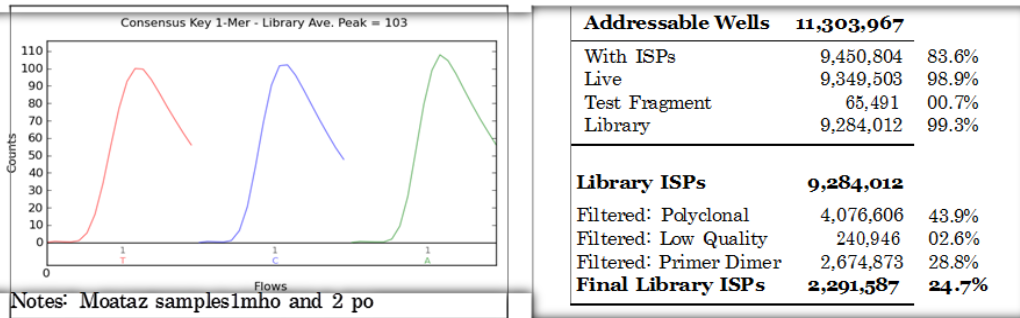
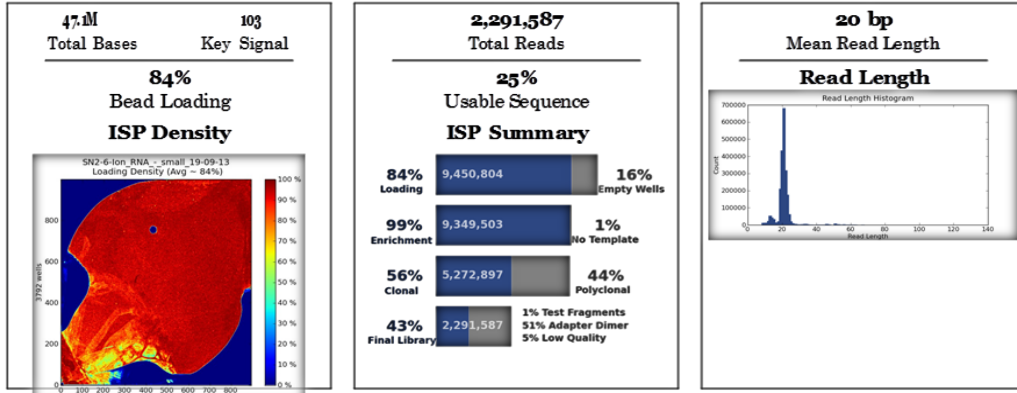
PBCs samples (n=100 patients) and adipose tissue samples (n=5 patients; two depots, SC and OM, from which the SVF and adipocytes were isolated; total n=20 samples) were checked for RNA quality/quantity. The final number of samples that fulfilled the necessary QC for sequencing were: 25 blood samples (7MHO, 15PO and 3Diabetics) and 16 tissue samples (2PO and 2MHO: 2 depots of SVF and adipocytes for each depot).

<b>Samples</b>	<b>Condition</b>	<b>Description</b>
001_R2	MHO	metabolically healthy obesity
002_R2	DM	diabetes mellitus
003_R2	PO	pathological obesity

**Table 5. Sample selection for miRNA sequencing.**

Three samples were used for the sequencing of miR gene expression.

### Run Summary



Barcode Name	Sample	Bases	≥Q20	Reads	Mean Read Length
No barcode	NOSM	30.8M	12.6M	1558773	19 bp
IonXpressRNA_001	AM83-MHO	4.1M	3.6M	118725	34 bp
IonXpressRNA_002	AM88-PO	7.6M	6.6M	397332	19 bp
IonXpressRNA_003	AM89-PO	2.5M	2.2M	133864	18 bp
IonXpressRNA_004	Control	2M	1.8M	82674	24 bp

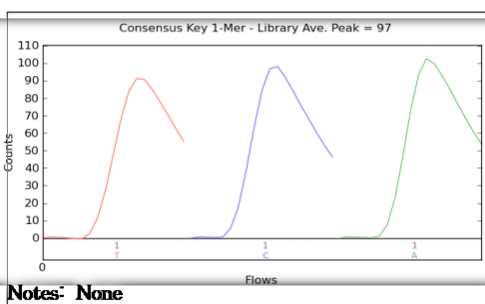
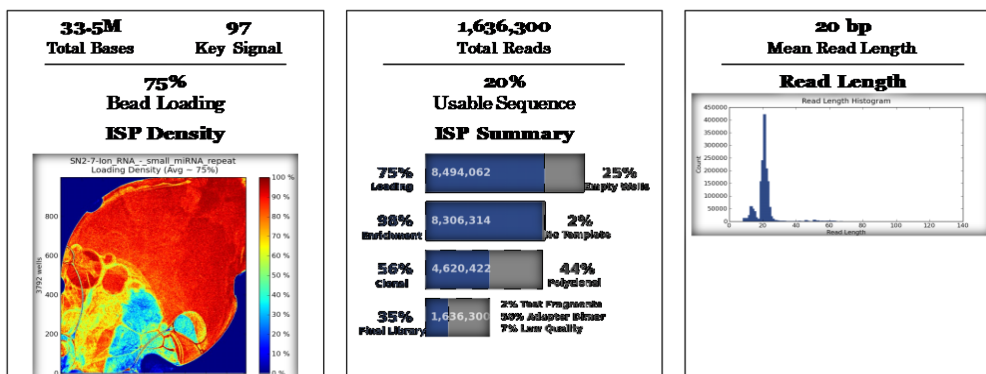
Test Fragment	Reads	Percent 50AQ17	Read Length Histogram
<b>TF D</b>	<b>29,954</b>	<b>95%</b>	
<b>TF A</b>	<b>31,910</b>	<b>93%</b>	

Figure 18. First run summary report of the small RNA sequencing

Three samples were used, barcoded: 001 MHO, 002 T2DM and 003 PO.

Run Report for Auto user SN2-7-Ion RNA - small miRNA repeat 7

**Run Summary**



<b>Addressable Wells</b>	<b>11,303,089</b>	
With ISPs	8,494,062	75.1%
Live	8,306,314	97.8%
Test Fragment	113,854	01.4%
Library	8,192,460	98.6%
<b>Library ISPs</b>	<b>8,192,460</b>	
Filtered: Polyclonal	3,685,892	45.0%
Filtered: Low Quality	281,244	03.4%
Filtered: Primer Dimer	2,589,024	31.6%
<b>Final Library ISPs</b>	<b>1,636,300</b>	<b>20.0%</b>

Barcode Name	Sample	Bases	=Q20	Reads	Mean Read Length
No barcode	NOSM	17.2M	8.2M	873674	19 bp
IonXpressRNA_001	83	3.5M	3.2M	101588	35 bp
IonXpressRNA_002	88	9.9M	8.7M	515380	19 bp
IonXpressRNA_003	89	2.7M	2.4M	145526	18 bp

Test Fragment	Reads	Percent 50AQ17	Read Length Histogram
<b>TF D</b>	<b>49,105</b>	<b>95%</b>	
<b>TF A</b>	<b>49,498</b>	<b>84%</b>	



Figure 19. Second run summary report of the small RNA sequencing

Three samples were used, barcoded: 001 MHO, 002 T2DM and 003 PO.

### 2.11.2 rRNA depletion

ERCC (external control) was added to each sample prior to the process of ribosomal RNA (rRNA) depletion. The efficiency of rRNA depletion in RiboMinus™ RNA, RNA degradation, and RNA concentration were analyzed using Agilent 2100 Bioanalyzer with the Agilent RNA 6000 Pico Kit. The RiboMinus™ Eukaryote Kit for RNA-Seq provides a novel and efficient method to isolate RNA molecules of the transcriptome devoid of large rRNA species from total RNA for transcriptome analysis. One µg of RNA was added gently to 100 µL of Hybridization Buffer and 10µL of RiboMinus™ Probe (15 pmol/µL), vortexed gently and incubated at 70–75°C for 5 minutes to denature the RNA. The tubes were transferred immediately to a 37°C water bath/heat block for 30 minutes to promote the sequence-specific hybridization. During the cooling step, the RiboMinus™ Magnetic Beads bottle was vortexed and 750µL of the beads were added to 1.5 ml tube and placed on a magnetic separator for 1 minute. The supernatant was aspirated and discarded. Then 750µL of sterile NFW was added to resuspend the beads and placed on a separator for another 1 minute. The supernatant was discarded and the last step was repeated once. The beads were resuspended in 750µL Hybridization Buffer and 250µL transferred to a new tube and kept at 37°C for a later stage. The remaining 500µL of the beads were placed on a magnetic separator for one minute where the supernatant was aspirated and discarded. The beads were resuspended in 200µL of Hybridization Buffer at 37°C. Briefly the tube of RNA/ RiboMinus™ Probe mixture (after cooling at 37°C) was centrifuged to collect the sample to the bottom of the tube. The sample was transferred to the prepared ribominus beads and mixed well by pipetting and incubated at 37°C for 15 minutes. The samples were centrifuged and separated on a magnetic separator to collect the supernatant, which contains the ribominus RNA. The smaller RNA (low input) was concentrated using the ribominus concentration module.



The ribonucleic acid (RNA) samples were transferred into clean tubes and concentrated using ethanol precipitation, to which 10  $\mu$ L of glycogen (20  $\mu$ g/ $\mu$ L) was added and mixed with 32  $\mu$ L of 3M sodium acetate and 800  $\mu$ L of 100% ethanol. The samples were incubated at -80°C for  $\geq$ 30 minutes. The tubes were centrifuged for 15 minutes at  $\geq$ 12,000  $\times$  g at 4°C. Carefully, the supernatant was discarded without disturbing the pellet, and 500  $\mu$ L of cold 70% ethanol was added twice with a centrifugation step in between for 5 minutes at  $\geq$ 12,000  $\times$  g at 4°C. Finally the supernatant was removed and the pellet was dried completely before adding 20  $\mu$ L of nuclease-free water.

### **2.11.3 Fragmentation**

Eight  $\mu$ L of depleted RNA (100-500ng) was mixed with 1  $\mu$ L of 10X RNase III Reaction Buffer and 1  $\mu$ L of RNase III and incubated at 37°C for 10 minutes. Immediately after the incubation, 20  $\mu$ L of NFR was added and stored on ice. The fragmented RNA was purified following the magnetic bead clean up module: Five  $\mu$ L of beads, 90  $\mu$ L of binding solution concentrate, 30  $\mu$ L of fragmented RNA and 150  $\mu$ L of 100% ethanol were mixed (10 X) and incubated for 5 minutes at room temperature, followed by another incubation on the magnetic stand for 5 minutes to separate the beads. The supernatant was discarded and 150  $\mu$ L of wash solution concentrate with ethanol was added into each well on the magnetic stand for 5 minutes. The supernatant was discarded and the residual ethanol removed and air dried on the magnetic stand for 2 minutes. The fragmented RNA was eluted on the stand by adding 12  $\mu$ L of pre-warmed RFW for 10 minutes at 70° C and snap cooled on ice. The fragmented RNA was then assessed for the concentration and size distribution using the 1000 PICO chip on the bioanalyser (see Figure 17). A final total concentration of 50-100 ng is optimal. The whole sample was vacuum dried, reconstituted in 3  $\mu$ L of RNF and stored on -80°C.

#### **2.11.4 The Hybridization-Ligation-cDNA**

The hybridisation was performed by adding 5µl of hybridization master mix, (2µl of Ion adaptor were mixed with 3µl of hybridization solution) with 3µl of the fragmented sample. The mixture was incubated at 65°C for 10 minutes and 30°C for five minutes. Then 12µl of the ligation master mix (10µl of 2X ligation buffer and 2µl of ligation Enzyme mix) was added to each 8µl of hybridization reactions. The 20µl of the ligation mix was incubated at 30° C for one hour. cDNA was synthesized by adding 2µl of RFW with 4µl of 10X RT buffer, 2µl of 2.5 mM of NTP mix and 8µl of ion RT primer v2. The RT master mix was incubated with the ligation mix and vortexed gently and incubated for 10 minutes at 70° C and snap cooled on ice. 4µl of 10X Superscript III Enzyme mix

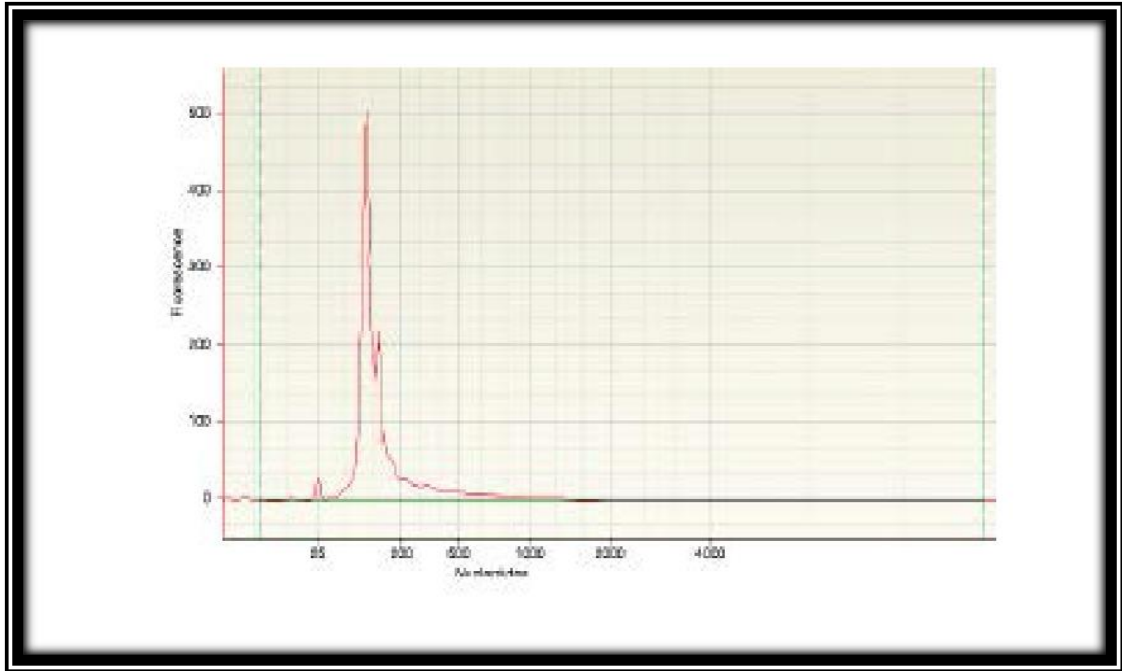


**Figure 20. The size distribution of the fragmented and purified r-depleted RNA**  
Average size (100-200).

was added to the ligated mix and incubated at 42°C for 30 minutes. The cDNA was purified using the magnetic beads clean up module. Five µl of beads and 72µl of the binding solution concentrate were added and mixed (10 X). 40µl of the RT mix and 56µl of 100% ethanol were added to each well, mixed (10 X) and incubated for five minutes at room temperature, followed by a another incubation on the magnetic stand for five minutes to separate the beads and the supernatant discarded. 150µl of wash solution concentrate with ethanol was added into each well on the magnetic stand for 5 minutes. The supernatant was discarded and the residual ethanol was removed followed by air drying on the magnetic stand for 2 minutes. cDNA was eluted on the stand by adding 12µl of pre-warmed RFW for 10 minutes at 70°C and snap cooled on ice and collected to be amplified. Six µl of cDNA, 47µl of the PCR mix (45µl of platinum PCR Super Mix High Fidelity, 1µl of Ion5 PCR Primer v2 and 1µl of Ion3 PCR Primer V2) and 1µl of barcode specific primer was added to the platinum master mix and incubated for 94°C for 2 min, two cycles at 94°C for 30 sec, 50°C for 30 sec, 68°C for 30 sec and held for 5 minutes at 68°C. The amplified cDNA was purified by the magnetic beads clean up module. The yield and size distribution was assessed by DNA High Sensitivity. The template dilution factor was determined by the use of the final molar concentration. The highest quality libraries was less than 50% amplified DNA, between 25-160bp.

#### **2.11.5 Assess the yield and size distribution of the amplified DNA**

The molar concentration (pM) was determined using the Agielent High Sensitivity DNA kit as in the Figure 18. The cDNA concentration in pM was used to calculate the final TDF required as per the protocol to get 11pM as a final concentration for each sample. TDF was used to calculate the direct dilution of the final library (2µl).

The dilution= (the final library\*TDF)-final library.

Three samples were pooled (after diluting each of them according to the formula) by

adding 33.3 $\mu$ l of each to make the total volume of three of them to 100 $\mu$ l, which was used in the Ion Touch version3.

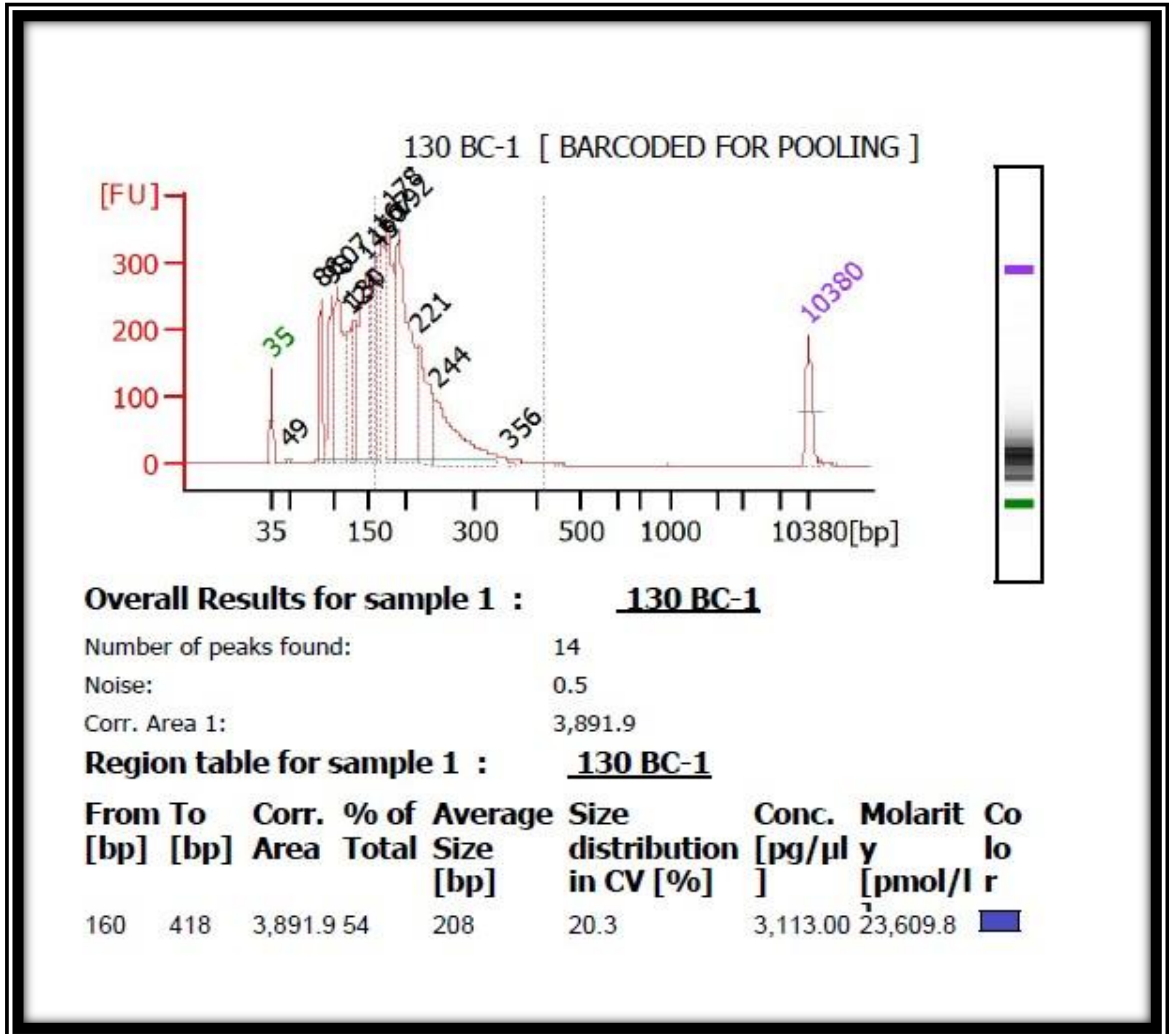


Figure 21. The area of interest was selected in a region

The region of interest in this sample was between 160-418bp which gave 23619pM.

### 2.11.6 The Ion Touch version3

The diluted library for each sample was prepared according to the calculation and equal volume of each sample was mixed together to reach upto 75µl final volume (25µl each of three samples were mixed together), vortexed, briefly centrifuged and stored on ice.

At room temperature 2.5ml reaction mix was prepared with the following reagents:

- 160µl of NFW
- 1200µl of Ion PI Reagent Mix TL
- 720µl of Ion PI PCR Reagent B
- 120µl of Ion PI Enzyme Mix TL
- 100µl of Ion PI ion sphere Particles V3
- 100µl of the diluted library.

The amplification solution (2400µl) was mixed at maximum speed for 5 seconds, centrifuged and 800µl inserted into the port of the reaction filter assembly three times then inverted to be inserted into the Ion one touch 2 instrument. The positive template (IPS) was recovered after the run and washed with NFW two times through centrifugation at 15500g for 8 minutes and resuspended in ISP resuspension solution. The IPS was enriched with the Ion one touch ES instrument for 30 minutes, where the 8 well strip was filled with IPS in the first well, 130µl of the Dynabeads in the second, the three wells with the wash solution and the 7th well with the melting off solution which was composed of 280µl of Tween solution (supplied) mixed with 40µl of 1 M NaOH (prepared). By the end of the run, The IPS was collected in a 0.2ml tube closed, centrifuged 15500xg for 5 minutes, washed and resuspended in NFW to be stored at 4°C for up to three days or proceed to sequencing.

The Ion PI control Ion sphere particles was vortexed and centrifuged before taking 5µl to be added directly to the IPS where it was mixed and centrifuged for 5 minutes at

15500xg. The supernatant was removed carefully leaving 10µl of liquid. 15µl of ion PI Annealing Buffer was added followed by 20µl of Ion PI sequencing Primer and making the final volume up to 45µl of adding the annealing buffer. It was incubated for 95°C for 2 minutes and 37°C for 2 minutes. After cycling, 10µl of Ion PI loading buffer was added, vortexed and centrifuged (ready for loading).

The run of the samples was set up following the protocol: (Ion PI sequencing 200 kit V3 on the Proton):

The Instrument was cleaned, and the process of initialization started when the reagent bottles were filled with required volume of all reagents supplied according to the protocol. All the bottles were attached including 3 bottles of wash buffer and 2 bottles for cleaning in addition to 4 dNTPs bottles. The chip was prepared and calibrated ready for loading the samples. Finally it was inserted into the proton and the run started.

## **2.12 Validation of the NGS by SurePrint G3 Human Gene Expression Microarrays**

With the new Human Gene Expression v2 Microarray, long intergenic non-coding RNA (lincRNA) probes designed to the human catalog of lincRNAs from the Broad Institute, along with an update of mRNA content, sourced from RefSeq, Ensembl, UniGene, and GenBank databases provides a full coverage of the human transcriptome.

Eight RNA samples from PBCs that were sequenced on the Proton were sent for the microarrays validation by Genotypic Technology Pvt. Ltd in India. All samples were checked for quality and quantity and the best four samples were used for scanning (See Table 6; 4 samples in duplicate and Figure 19 for workflow).



No.	ID	260/280	260/230	RNA Conc. (ng/μl)	Total yield (ng)	RIN	QC conc./yield
2	PO-122	2.1	0.6	88.9	1510.7	5.0	Optimal
3	MHO-102	2.0	0.6	107.6	3336.8	7.5	Optimal
4	MHO-128	2.0	0.9	152.4	2591.4	8.8	Optimal
6	PO-48	2.1	0.8	123.9	929.1	6.6	Optimal

**Table 6. The samples were used for validation after sequencing**

All samples were checked for quality and quantity and the best four samples were used for scanning (4 in duplicate).

### **2.12.1 RNA Labelling, Amplification and Hybridization**

The samples were labelled using Agilent Quick Amp Labeling Kit one color (Part number: 5190-0442). 500ng of total RNA was reverse transcribed using oligodT primer tagged to T7 promoter sequence. cDNA thus obtained was converted to double stranded cDNA in the same reaction. Further the cDNA was converted to cRNA in the in-vitro transcription step using T7 RNA polymerase enzyme and Cy3 dye was added into the reaction mix. During cRNA synthesis Cy3 dye was incorporated into the newly synthesized strands. cRNA obtained was cleaned up using RNeasy Mini Kit (Qiagen, Cat No: 74106). Concentration and amount of dye incorporated was determined using Nanodrop. Samples that pass the QC for specific activity were taken for hybridization. 600ng of labeled cRNA were hybridized on the array using the Hi-RPM large Hybridization Kit (Part No: 5190-0404; Agilent) in Sure hybridization Chambers (Agilent) at 65° C for 16 hours. Hybridized slides were washed using Agilent Gene Expression Wash Buffers Set (Part No: 5188-5327). The hybridized, washed microarray slides were then scanned on a G2600D scanner (Agilent Technologies) Feature Extraction. Data extraction from Images was done using Feature Extraction software Version 11.5 of Agilent.

### **2.12.2 Microarray Data Analysis**

Images were quantified using Feature Extraction Software (Version-11.5 Agilent). Feature extracted raw data was analyzed using GeneSpring GX Version 12.0 software from Agilent. Normalization of the data was done in GeneSpring GX using the 75th percentile shift (Percentile shift normalization is a global normalization, where the locations of all the spot intensities in an array are adjusted. [This normalization takes each column in an experiment independently, and computes the  $n^{th}$  percentile of the

expression values for this array, across all spots (where n has a range from 0-100 and n=75 is the median). It subtracts this value from the expression value of each entity) and fold expression values were obtained with respect to Specific control Samples]. Significant genes up and down regulated showing one fold (log base2) and above within the samples with respect to control sample were identified. Differential expression patterns were identified among the samples. Differentially regulated genes were clustered using hierarchical clustering based on Pearson coefficient correlation algorithm to identify significant gene expression patterns. Genes were classified based on functional category and pathways using GeneSpring GX and Genotypic Biointerpreter-Biological Analysis Software. (Biointerpreter is a user-friendly web-based Biological interpretation tool developed by Genotypic Technology Private Limited, Bangalore).

**The procedure was carried out as below:**

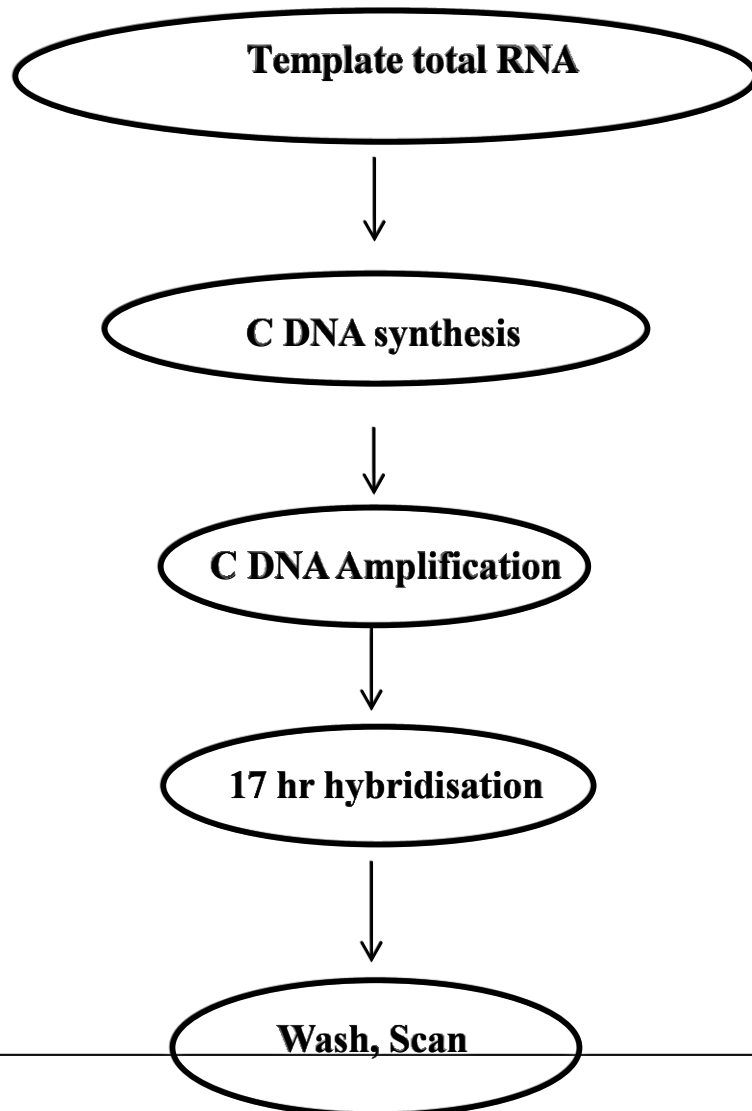


**Figure 22. Work flow of the sample preparation and array scan**

## 2.13 Runs QC and summary for NGS

See the appendix 2 for the summary reports.

## 2.14 Data analysis

Results were expressed as mean  $\pm$  SD or median (interquartile range), unless otherwise stated. Normally distributed data were compared by Student's paired or independent *t*-test or for skewed data by Wilcoxon or Mann-Whitney U test to describe statistical significance. Statistical significance was assumed at the level of *p* values  $<0.05$ . All data analyses were performed with the SPSS 14.0 software package.

### 2.14.1 Analysis of RNA arrays

RNA expression was calculated either as a ratio of the house-keeping gene threshold cycle value (Ct) or using the  $2^{-\Delta\Delta Ct}$  method (Livak and Schmittgen, 2001).

The microarray data were analysed by two separate methods:

First method: The expression of a target gene (TG) relative to the EC, the comparative Ct ( $\Delta\Delta Ct$ ) as per the following equation was calculated:

$$\Delta\Delta Ct = (Ct \text{ Target gene}) - (Ct \text{ EC}) - ((Ct \text{ Target gene}) - (Ct \text{ EC}))$$

The  $\Delta\Delta Ct$  values were converted to a linear form using the formula:  $E^{-\Delta\Delta Ct}$ . All results with a  $p < 0.05$  were considered statistically significant. To correct for variables, such as the amount of starting template and enzymatic efficiencies, RQ-PCR data is routinely normalised using endogenous control genes (house-keeping genes) which are highly and stably expressed across a sample set. The appropriate choice of endogenous control is critical to ensure validity and accuracy of the results generated. The data was exported into an excel sheet through the sabioscience website for the data analysis.

The analysis was carried out using the online program from Qiagen:

[http://www.sabiosciences.com/miRna\\_pcr\\_product/HTML/MIHS-001Z.html](http://www.sabiosciences.com/miRna_pcr_product/HTML/MIHS-001Z.html)).

Second method: The normalization of the data was performed against the housekeeping genes, obtaining  $\Delta Ct$  values, and the miR expression values were calculated as  $2^{(-\Delta Ct)}$ . For each miR Fold Change ( $\Delta\Delta Ct$ ) =  $2^{(-\Delta Ct)_{PO}} / 2^{(-\Delta Ct)_{MHO}}$ . P-value (Student's t-Test) was calculated. Selected significant PO vs. MHO differentially expressed miRs: absolute Fold Change  $\geq 2$  and p-value  $\leq 0.05$ .

#### **2.14.2 Analysis of small RNA Seq**

miR-seq data was processed using RandA tool (Isakov et al, 2012). Sequencing reads were trimmed to clip the adapter sequence and then mapped by Burrows-Wheeler alignment algorithm (Li and Durbin, 2009) against a database derived from Rfam (Burge et al, 2012). Differential expression was tested by a negative binomial distribution model for variance estimation, using the Bioconductor package DESeq (Anders and Huber et al, 2010).

#### **2.14.3 Analysis of whole transcriptome data**

Whole transcriptome sequencing data (RNA-seq) was analysed to find differentially expressed genes. Quality control of raw sequencing data, FASTQ files, was performed using FastQC tool (<http://www.bioinformatics.babraham.ac.uk/projects/fastqc/>). The short sequencing reads that pass the quality check were mapped to the Homo sapiens reference genome GRCh37/hg19 using the TopHat2 algorithm (Kim et al, 2013). The reads were either aligned or unaligned in this process. The unaligned reads were then mapped with the Bowtie2 algorithm (Langmead et al, 2012). The output BAM files from these two alignment processes were then merged to generate final aligned BAM for further downstream analysis. Mapped reads were counted using *countOverlaps* function of Bioconductor package, to measure how many reads in the sample overlap with each

specific gene. Gene expression was analysed through the Bioconductor package EdgeR (Robinson et al, 2010). Read counts were normalized for different library size and to account for sample-specific effects using EdgeR TMM method. Differential expression was determined by negative binomial exact test and significant genes were selected with corrected p-Value (FDR)  $\leq 0.05$  and absolute  $\log_2$  (Fold Change)  $\geq 1$ .

#### **2.14.4 Gene enrichment analysis**

Ingenuity Pathways Analysis (IPA, <http://www.ingenuity.com/>) was used to perform gene enrichment analysis. Gene expression data was mapped into relevant pathways based on their functional annotation and known molecular interactions. Statistical significance was evaluated with Fisher's exact test adjusted for multiple comparisons by the Benjamini-Hochberg method.

#### **2.14.5 miR target analysis**

Differentially expressed microRNAs were analysed to find their experimentally validated target genes, using the databases Ingenuity Knowledge Base (<http://www.ingenuity.com/>), miRecords (Xiao et al, 2009), TarBase (Vergoulis et al, 2012), and their predicted targets, using TargetScan (Benjamin et al, 2005). miR expression and gene expression results were integrated to verify if validated or predicted microRNA-targets were regulated coherently with the expression of their microRNA. For each regulated microRNA we selected those experimentally validated or predicted targets that resulted differentially expressed from RNAseq data.

# **Chapter 3**

## **Clinical**

### **Stratification**

#### **of MHO and**

##### **PO**



### **3.1 Introduction**

The prevalence of obesity has increased globally and as a consequence so has the associated comorbidities, such as T2DM and hypertension. These diseases pose a significant risk of morbidity and mortality (Hotamisligil, 2006). While 60-80% of obese subjects rapidly develop metabolic diseases a proportion still remain relatively healthy, either because the progression to disease is slower in these individuals or they have developed pathways that renders them immune (Stefan et al, 2008 ). Understanding the mediators and mechanisms for this apparent protection is imperative. Some of the heterogeneity in susceptibility includes gender, ethnicity and physical fitness; all of which have a significant impact on the early predictors of cardiometabolic disease, such as insulin resistance and inflammation (Stefan et al, 2008, Meigs et al, 2006; Wildman et al, 2008).

### **3.2 Gender**

Many studies have shown that there is a difference between males and females related not just to the incidence of obesity, but also to the pathological consequences of being obese. However, emerging data suggest that this gender difference disappears in the face of weight gain. There is a higher prevalence of obesity in females, implying that they carry more of its burden, including reduced life expectancy, greater risk of obesity-related disease, and increased medical costs. In pre-menopausal females sex hormones (e.g.oestrogen) are thought to provide protection from cardiometabolic diseases. But this protection disappears in obesity, making both males and females at least equally susceptible to comorbidities. Depending on ethnicities the heterogeneity between males and females in the prevalence of obesity can vary from 4 to 22% (Dobbs et al, 2014, Figure 20). The difference between males and females in a Qatari population is relatively small, and may be related to the ethnic admixture, compared to, for example Egypt,

which has a higher gender difference in the prevalence of obesity, perhaps reflecting homogeneity in ethnicity.

The reasons for these differences in predisposition to obesity associated pathologies are still under investigation. However, gender differences in body composition and regional fat deposition may be a factor. Women have a higher percentage of body fat and more often develop peripheral adiposity, whereas men accumulate abdominal fat. This male pattern of fat deposition is also seen in a proportion of overweight women. Also men, and post-menopausal women, tend towards more visceral fat which releases greater levels of FFAs and proinflammatory adipokines (Wajchenberg, 2000). It may be that these factors, via the portal circulation, reach the liver to induce hepatic IR and a more atherogenic lipid profile. Among patients with T2DM, 40% of men and up to 70% of women display abdominal obesity, perhaps pointing to a closer association between T2DM and central obesity in women than in men (Krotkiewski et al, 1983). Females also have higher systemic leptin and adiponectin, perhaps reflecting both greater body fat and regulation by the sex hormones.

### **3.1.1 Adiponectin and leptin**

Adiponectin is a hormone synthesized almost exclusively in adipose tissue and increases insulin sensitivity of the liver and skeletal muscle. Its synthesis is stimulated by insulin and PPAR $\gamma$  agonists, and inhibited by  $\beta$ -adrenergic stimulation, cytokines and androgens. Adiponectin levels decrease with IR and obesity, which may explain why they are higher in women as well in non-diabetic subjects. Low levels are a marker of IR, whereas high levels have been associated with reduced risk of T2DM and cardiovascular disease. Leptin is an adipokine that acts as a satiety factor and is involved in the regulation of food intake. Normal human obesity appears to be a 'leptin resistant' state, perhaps reflecting reduced signaling through leptin receptors. Leptin levels are higher in women

than in men, reflecting greater total percent fat mass. It is positively correlated with free estrogen in post-menopausal women, and with free testosterone in men. Increased leptin levels are associated with cardiovascular disease in men, while they may be protective in women.

### **3.2 Ethnicity**

Ethnicity may also be a cause for the heterogeneity in the consequence of obesity. Some ethnicities, such as South Asians and Arabs, appear especially susceptible to obesity

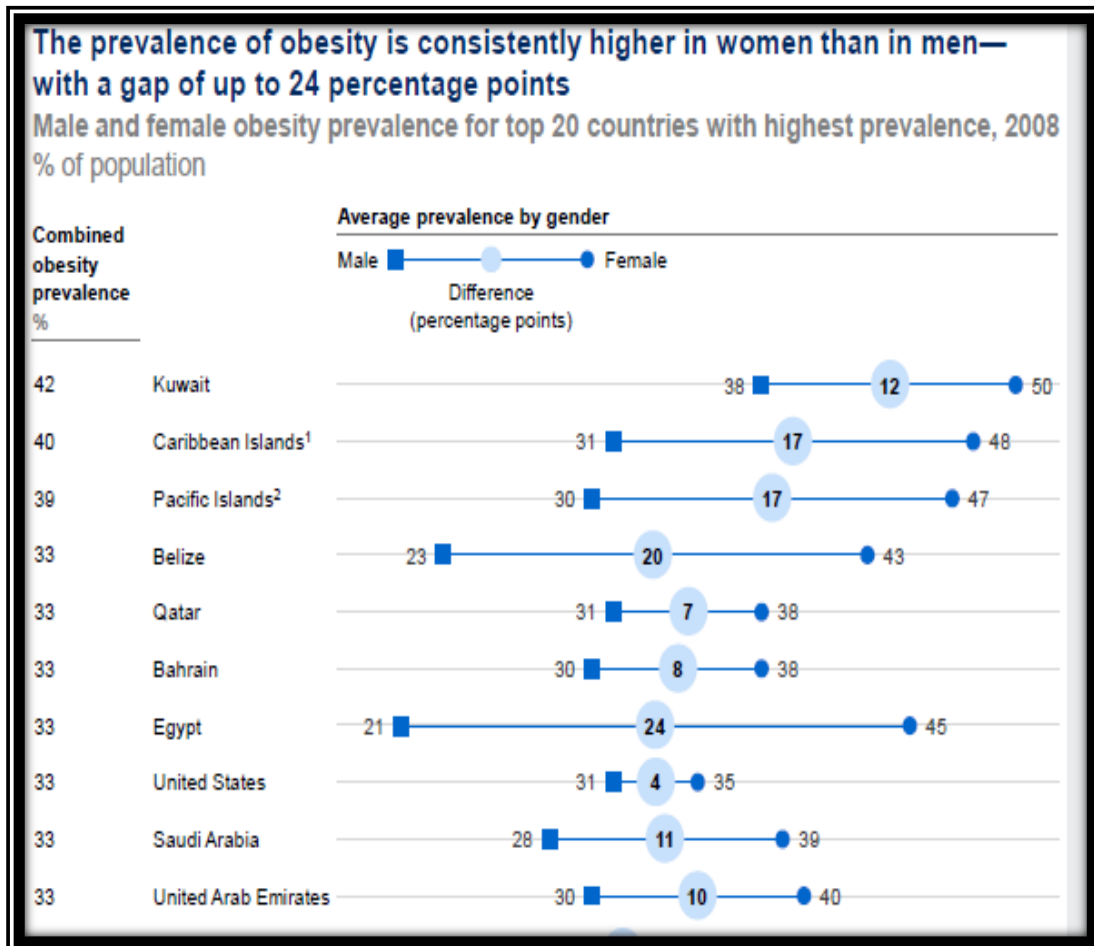


**Figure 23. The prevalence of obesity in the Arab countries**

While the prevalence was higher in women than men globally, the gender disparity varies significantly between countries. (Dobbs et al, 2014).

associated T2DM and the reasons for this warrant further study.

### **3.3 Sedentary lifestyle and surgical weight loss**

Sedentary lifestyle plays a critical role in the development of metabolic disease, leading to chronic inflammation and MeS. Few studies have compared the efficacy of exercise interventions, or the benefits of various types of exercise, in men versus women. It appears that intensive exercise appeared to prevent T2DM in both men and women; however weight loss retarded the development of T2DM more effectively in men. However, among patients with T2DM, women were found to be more successful at losing weight after initiation of glucose-lowering therapy. Thus, exercise is important to reduce morbidity and mortality in patients with T2DM regardless of sex.

Surgery results in greater sustained improvement in weight loss and weight associated comorbidities compared with non-surgical interventions, be it diet, exercise and/or pharmacotherapy. Some surgical procedures may result in greater weight loss and improvements in comorbidities than others, but outcomes were similar between RYGB and sleeve gastrectomy, and both of these procedures had better outcomes than adjustable gastric banding. These are the main procedures carried out in Qatar. However, adverse effects and reoperation rates were generally poorly reported and also the long-term effects of surgery yet unclear.

### **3.4 Diagnosis of MeS**

It is obvious that the MeS is a cluster of risk factors for T2DM and cardiovascular disease that occurs together to a greater extent than by chance alone. However, the description and definition of MeS for diagnosis varies somewhat depending on what criteria is used. WHO, in 1999, stipulated that MeS patients should have one of 3 of the following: T2DM, IGT or IR, as well as, at least 2 of these: hypertension, obesity, raised TG/low HDL or microalbuminuria. EGIR, also in 1999, stipulated that MeS should not

include IGT or T2DM but have IR and 2 of the following: central obesity, raised TG/low HDL, hypertension or fasting plasma glucose greater than 6.1 mmol/l. More recently, in 2001, ATP III defined MeS as having 3 or more of the following: Central obesity, raised TG, low HDL, hypertension and fasting plasma glucose greater than 6.1mmol/l.

All three classifications included obesity, suggesting that in obesity there can be those who were insulin sensitive and others insulin resistant. Both the WHO and EGIR need measures of IR but the problem is that there is no standard measurement for insulin. More recently hyperleptinemia and inflammation have also been included as additional measures of MeS, as they occur as part of the cluster of risk factors.

Also many of these measures have been mainly described in Caucasian populations and norms for all these measures in other ethnicities are still being generated. As both obesity and the associated diseases have a greater prevalence in non-Caucasian populations having robust biomarkers in these populations is important both for diagnosis and for treatment.

### **3.5 Aims of the study were to**

1. Stratify morbidly obese Arab subjects depending on systemic biomarkers of insulin sensitivity and inflammation.
2. Investigate the markers of insulin sensitivity and inflammation in obesity-matched Arabs and Caucasians, in the absence of type 2 diabetes.
3. Investigate the effect of the surgical weight loss in insulin sensitive and insulin resistant morbidly obese Arabs.

### **3.6 Methods**

The methods have been described in detail in section 2.3.1. Briefly, randomly selected morbidly obese patients awaiting bariatric surgery were recruited in Doha, Qatar (Hamad Hospital and al-Emadi hospitals) and London, UK (Whittington Hospital). The study was

approved by national ethics committees and all patients gave written informed consent.

Anthropometric measurements were recorded (age, weight, height systolic and diastolic blood pressure).

Fasting blood samples were used to determine glucose (hexokinase), lipids (Total Cholesterol, LDL and HDL: Roche) and insulin (ELISA, Mercodia). Adipokines (leptin, adiponectin, interleukin-6 and MCP1) were assayed by ELISA (R&D Systems, Oxon, UK).

Two separate calculations were to generate indices of insulin resistance:

HOMA1IR –  $\text{Insulin (mU/L)} * \text{FBG (mmol/L)} / 22.5$

HOMA2IR - HOMA calculator v2.2.3. This index was also used for obtaining measures of  $\beta$ -cell function and insulin sensitivity.

Criteria for MeS: HOMA1IR > 2.7 and HOMA2IR > 1.8.

Stratification criteria for MHO and PO.

Subjects were considered MHO if free of T2DM, dyslipidaemia, and cardiovascular disease, and exhibited systolic blood pressure less than 140 mmHg, diastolic blood pressure less than 85mmHg, fasting plasma glucose less than 6.8 mmol/l and insulin less than 6.5 miU/ml.

Based on these criteria, obese subjects were dichotomised into MHO and PO accordingly.

Data were entered in SPSS version 22.0 for statistical analysis. Parametric tests were used for normally distributed data and non-parametric analysis for skewed data.

### **3.7 Results**

### **3.7.1 Gender differences in cardiometabolic risk in Arabs**

The population was relatively young (Table 7A). Despite being BMI and age matched, the males had higher SBP and DBP, were relatively hyperglycaemic, with hyperinsulinaemia and insulin resistance, compared to females. The females had higher leptin that probably reflects greater fat mass, despite having similar BMI.

The data was reanalyzed after excluding those with fasting blood glucose greater than 6.1mmol/L (Table 7B). Despite being matched for BMI, age and glucose, both SBP and DBP was higher in males, along with slightly lower HDL-cholesterol. However the males also still remained hyperinsulinaemic and insulin resistant compared to females. Leptin still remained higher in the females.

### **3.7.2 Differences in cardiometabolic risk in Arab MHO and PO**

There were differences between PO and MHO after they were all matched for glycemia (glucose less than 6.1mmol/l; Table 8) and gender (Table 9). When males and females were analysed together (Table 8) the PO had higher TG, IL-6, glucose, insulin and HOMA-IR, compared to the MHO. However, leptin was lower in PO compared to MHO. In order to exclude gender as a confounding factor, the analysis repeated in females only, and this confirmed higher TG, insulin and HOMA-IR and a reduced leptin in PO subjects compared to MHO (Table 9).

### **3.7.3 Effect of ethnicity on cardiometabolic risk factors**

The objectives of the study were to investigate markers of insulin resistance and MeS in obesity-matched Arabs and Caucasians, in the absence of diabetes. Basic characteristics of the two populations were shown in Table 10. Despite the Arab cohort being significantly younger they were hyperglycemic and hyperinsulemic compared to the Caucasians. This population also had elevated  $\beta$ -cell function and insulin resistance,



while insulin sensitivity was lower. However there was no significant difference in blood pressure. Total-, LDL- and HDL-cholesterol were higher, but triglycerides lower, in Arabs. Leptin, a marker of adipose tissue mass, was elevated in Arabs. Furthermore the proinflammatory adipokines (MCP-1, IL-6) were higher and the anti-inflammatory adipokines (adiponectin) lower in this population (Table 10).

### **3.7.3.1 Correlations**

Fasting Blood Glucose (FBG) significantly correlated with age ( $p=0.02$ ), DBP ( $p=0.01$ ) and with HOMA-IR with  $p$ -value  $< 0.01$  among Arabs, while a negative correlation was found with %B (Betacell Function %) and %S (Insulin sensitivity %). TG also correlated with fasting blood sugar ( $p=0.04$ ) and with adipokines, leptin ( $p<0.001$ ).

On the other hand FBG among the Caucasian cohort correlated with insulin ( $p=0.06$ ), HOMA-IR ( $p=0.01$ ) and IL-6 ( $p=0.02$ ) and negatively with %B ( $p<0.001$ ), %S ( $p=0.01$ ) and MCP1 ( $p=0.03$ ). As expected, insulin correlated with HOMA, %B and IR ( $p<0.01$ ) and negatively correlated with %S ( $p<0.01$ ) in both cohorts. It also correlated with DBP among Arabs ( $p=0.017$ ) and with FBG ( $p=0.058$ ) among Caucasians.

<b>Characteristics</b>	<b>Males</b>	<b>Females</b>	<b><i>p</i>-value</b>
<b>N</b>	24	58	
<b>Age (years)</b>	32.0 ± 8.1	33.8 ± 9.6	0.40
<b>BMI (kg.m<sup>-2</sup>)</b>	45.5 ± 5.6	45.2 ± 14.3	0.90
<b>SBP (mmHg)</b>	132.0 ± 13.2	121.5 ± 14.1	0.001
<b>DBP (mmHg)</b>	78.1 ± 14.7	71.6 ± 9.8	0.05
<b>Cholesterol (mmol/L)</b>	4.6 ± 1.2	4.5 ± 1.0	0.96
<b>LDL (mmol/L)</b>	2.9 ± 0.9	2.9 ± 0.7	0.57
<b>HDLC (mmol/L)</b>	1.1 ± 0.3	1.3 ± 0.3	0.21
<b>Triglyceride (mmol/L)</b>	1.4 (0.9-1.8)	1.2 (0.8-1.5)	0.22
<b>Interleukin-6 (pg/ml)</b>	3.3 (1.9 – 6.0)	3.8 (2.2 - 5.7)	0.54
<b>MCP1 (pg/ml)</b>	216.63(122.9-301.5)	220.0 (179.0-297.0)	0.55
<b>Leptin (ng/ml)</b>	49.4 (33.7-70.5)	72.9 (52.0-96.5)	0.001
<b>Adiponectin (µg/ml)</b>	2.5 (2.4-3.9)	3.1 (2.4-4.8)	0.65
<b>Plasma Glucose (mmol/L)</b>	7.2 ± 3.2	5.8 ± 1.4	0.05
<b>Insulin (mU/L)</b>	17.9 (10.1-26.5)	11.6 (7.4-18.3)	0.04
<b>HOMA</b>	5.4 (2.9-7.7)	2.9 (1.6-4.6)	0.003

**Table 7A. Gender differences in cardiometabolic risk factors in the whole cohort**

Data shown as mean ± SD or median (interquartile range). Comparisons were performed using *t* test or Wilcoxon test as appropriate. Significance was defined as  $P \leq 0.05$ .

Characteristics	Males	Females	<i>p</i> -value
<b>N</b>	11	44	
<b>Age (years)</b>	29 ± 7.5	32 ± 9.4	0.27
<b>BMI (kg.m<sup>-2</sup>)</b>	45.7 ± 6.5	42.9 ± 6.9	0.23
<b>SBP (mmHg)</b>	137.0 ± 11.4	122.0 ± 14.5	0.001
<b>DBP (mmHg)</b>	79.8 ± 15.7	70.4 ± 8.4	0.001
<b>Cholesterol (mmol/L)</b>	4.9 ± 0.8	4.6 ± 0.8	0.35
<b>LDL (mmol/L)</b>	2.9 ± 1.1	2.8 ± 0.7	0.66
<b>HDLC (mmol/L)</b>	1.1 ± 0.2	1.3 ± 0.3	0.07
<b>Triglyceride (mmol/L)</b>	1.4 (0.9-1.8)	1.0 (0.7-1.5)	0.11
<b>Interleukin-6 (pg/ml)</b>	3.3 (2.3-6.5)	3.7 (2.1-5.3)	0.76
<b>MCP1 (pg/ml)</b>	261.4 (135.4-308.8)	220.0 (183.0-295.5)	0.83
<b>Leptin (ng/ml)</b>	49.0 (38.6-81.1)	74.0 (52.7-96.8)	0.06
<b>Adiponectin (µg/ml)</b>	2.5 (2.4-5.3)	3.7 (2.4-5.0)	0.92
<b>Fasting Plasma Glucose (mmol/L)</b>	5.2 ± 0.6	5.1 ± 0.7	0.92
<b>Insulin (mU/L)</b>	16.9 (13.2-28.1)	11.2 (7.4-16.2)	0.01
<b>HOMA</b>	3.9 (3.0-6.5)	2.6 (1.5-3.8)	0.008

**Table 7B. Gender differences in cardiometabolic risk factors- matched for glycemia**

All glucose less than 6.1mmol/l. Data presented as mean ± SD or median (interquartile range). Comparisons were performed using *t* test or Wilcoxon test as appropriate. Significance was defined as  $P \leq 0.05$ .

Characteristics	MHO	PO	<i>p-value</i>
<b>N</b>	24	30	
<b>Age (years)</b>	32.8 ± 9.9	31.1 ± 8.6	0.50
<b>BMI (kg.m<sup>-2</sup>)</b>	42.5 ± 6.1	44.2 ± 7.5	0.38
<b>SBP (mmHg)</b>	123.8 ± 14.4	126.0 ± 15.8	0.61
<b>DBP (mmHg)</b>	70.2 ± 7.7	74.0 ± 12.6	0.17
<b>Cholesterol (mmol/L)</b>	4.6 ± 0.7	4.7 ± 0.9	0.83
<b>LDL (mmol/L)</b>	2.8 ± 0.7	2.9 ± 0.9	0.69
<b>HDLC (mmol/L)</b>	1.3 ± 0.3	1.2 ± 0.3	0.32
<b>Triglyceride (mmol/L)</b>	0.99 (0.75-1.3)	1.4 (0.87-1.8)	0.02
<b>Interleukin-6 (pg/ml)</b>	3.1 (1.78-5.0)	3.7 (2.6-6.0)	0.06
<b>MCP1 (pg/ml)</b>	198.0 (149.5-275.0)	250.2 (185.8-303.7)	0.16
<b>Leptin (ng/ml)</b>	80.9 (54.7-98.4)	54.0 (46.8-81.1)	0.04
<b>Adiponectin (µg/ml)</b>	3.8 (2.5-5)	2.8 (2.4-4.97)	0.83
<b>Plasma Glucose (mmol/L)</b>	4.8 ± 0.6	5.4 ± 0.7	0.001
<b>Insulin (mU/L)</b>	7.4 (6.5-10.0)	15.8 (13.5-27.2)	0.001
<b>HOMA</b>	1.6 (1.2-2.2)	4.0 (3.1-6.4)	0.001

**Table 8. Characteristics of Arab MHO and PO subjects**

All matched for glucose less than 6.1 mmol/L. Data presented as mean ± SD or median (interquartile range). Comparisons were performed using *t* test or Wilcoxon test as appropriate. Significance was defined as  $P \leq 0.05$ .

Characteristics	MHO	PO	<i>p-value</i>
<b>N</b>	22	22	
<b>Age (years)</b>	33.5 ± 10.1	31.1 ± 8.8	0.50
<b>BMI (kg.m<sup>-2</sup>)</b>	42.8 ± 6.2	43.0 ± 7.8	0.92
<b>SBP (mmHg)</b>	122.8 ± 14.5	121.0 ± 149.0	0.75
<b>DBP (mmHg)</b>	69.5 ± 7.6	71.4 ± 9.2	0.45
<b>Cholesterol (mmol/L)</b>	4.6 ± 0.7	4.6 ± 1.0	0.75
<b>LDL (mmol/L)</b>	2.8 ± 0.7	2.8 ± 0.8	0.90
<b>HDLC (mmol/L)</b>	1.3 ± 0.3	1.2 ± 0.4	0.54
<b>Triglyceride (mmol/L)</b>	1.0 (0.7-1.3)	1.5 (0.7-1.8)	0.03
<b>Interleukin-6 (pg/ml)</b>	3.7 (1.6-5.0)	3.7 (2.3-5.9)	0.20
<b>MCP1 (pg/ml)</b>	210.0 (165.0-288.0)	236.0 (183.6-299.0)	0.47
<b>Leptin (ng/ml)</b>	86.0 (68.0-99.0)	64.0 (49.4-81.5)	0.02
<b>Adiponectin (µg/ml)</b>	3.7 (2.2-5.5)	3.4 (2.3-4.8)	0.97
<b>Plasma Glucose (mmol/L)</b>	4.8 ± 0.6	5.4 ± 0.7	0.002
<b>Insulin (mU/L)</b>	7.4 (6.1-9.3)	16.0 (13.5-23.1)	0.001
<b>HOMA</b>	1.56 (1.16-2.1)	3.7 (3.0-5.7)	0.001

**Table 9. Characteristics of female Arab MHO and PO subjects**

All females and matched for glucose less than 6.1 mmol/L. Data presented as mean ± SD or median (interquartile range). Comparisons were performed using *t* test or Wilcoxon test as appropriate. Significance was defined as  $P \leq 0.05$ .

<b>Characteristics</b>	<b>Arabs</b>	<b>Caucasians</b>	<b><i>p-value</i></b>
<b>N</b>	<b>79</b>	<b>75</b>	
<b>Age (years)</b>	33.0 (9.2)	41.4 (10.6)	<0.001
<b>BMI (kg/m<sup>2</sup>)</b>	45.2 (12.5)	43.7 (9.3)	0.41
<b>Systolic BP (mmHg)</b>	124.0 (14.0)	129.0 (18.0)	0.15
<b>Diastolic BP(mmHg)</b>	74.0 (11.0)	76.0 (11.0)	0.14
<b>Plasma Glucose (mmol/L)</b>	5.9 (1.4)	5.3 (0.9)	0.001
<b>Insulin (mU/L)</b>	13.2 (7.5-20.2)	7.3 (5.2-12.7)	<0.001
<b>HOMA-1IR</b>	3.1 (2.0-5.9)	1.7 (1.2-2.9)	<0.001
<b>Betacell Function (%)</b>	111 (75-153)	89 (64-128)	0.04
<b>Insulin sensitivity (%)</b>	57 (37-104)	105 (63-147)	<0.001
<b>HOMA-2IR</b>	1.7 (1.0-2.7)	1.0 (0.7-1.6)	0.001
<b>Total-Chol (mmol/L)</b>	4.6 (1.1)	4.2 (1.1)	0.04
<b>LDL-Chol (mmol/L)</b>	2.9 (0.8)	2.5 (1.1)	0.02
<b>HDL-Chol (mmol/L)</b>	1.2 (0.3)	1.0 (0.3)	<0.001
<b>Triglycerides (mmol/L)</b>	1.3 (0.9-1.6)	1.4 (1.0-1.9)	0.02
<b>Interleukin-6 (pg/ml)</b>	3.8 (2.1-5.8)	2.3 (1.5-4.1)	0.001
<b>MCP-1 (pg/ml)</b>	220.6 (174.7-300.0)	132.7 (90.8-143.4)	<0.001
<b>Leptin (ng/mL)</b>	66.8 (49.8-90.8)	34.9 (21.4-67.9)	<0.001
<b>Adiponectin (µg/mL)</b>	2.9 (2.4-4.5)	4.3 (2.2-8.2)	0.06

**Table 10. Comparison of basic characteristics of the Arab and Caucasian cohorts**

Data are shown as mean ( $\pm$ SD) or median (interquartile range).

Insulin and TG significantly correlated in both cohorts ( $p=0.01$  for Arabs and  $p<0.01$  among Caucasians). There was a correlation between HOMA and TG in both cohorts: ( $p=0.01$  among Arabs and  $p<0.01$  in Caucasians).

In Arabs b-cell function correlated positively with FBG, insulin, HOMA-IR ( $p<0.01$ ) and leptin ( $p=0.03$ ), and negatively with age ( $p<0.01$ ).

Among the Caucasian cohort, %B negatively correlated with FBG ( $p<0.01$ ), %S ( $p<0.01$ ), HDLC ( $p=0.03$ ) and adiponectin ( $p<0.01$ ). While a positive correlation of %B was apparent with insulin, HOMA-IR, TG ( $p<0.01$ ) and MCP1 ( $p=0.01$ ).

Insulin sensitivity negatively correlated with FBG, insulin, %B, HOMA-IR and TG ( $p<0.01$ ) among Arabs and Caucasians while only Arabs showed negative correlation with DBP. The Caucasian cohort also revealed a correlation with Adiponectin ( $p<0.01$ ).

In only the Arabs HOMA-IR showed significant correlation with SBP ( $p=0.04$ ), DBP ( $p<0.01$ ) and IL-6 ( $p=0.07$ ).

Using either criteria of Metabolic Syndrome (MeS) (HOMA1-IR  $> 2.70$  and HOMA-2IR  $> 1.8$ ) the prevalence of MeS in Arabs was higher compared to Caucasians. Sixty two percent (62%) of the Arab study population ( $n=51$ ) exhibited MeS according to HOMA1-IR while 51% ( $n=42$ ) did so by HOMA-2IR. Twenty nine percent (29%) of the Caucasian patients ( $n=23$ ) had MeS by HOMA1-IR and 21% ( $n=17$ ) using HOMA-2IR. These data suggest a greater prevalence of MeS in the study population, which may precede the development of cardiovascular disease leading to an earlier age of onset in the Arab population (Table 11).

#### **3.7.4 Comparison of effects of surgical weight loss in MHO and PO groups**

Three months after surgery there was a significant reduction in BMI, as expected, and this was associated with reduction in insulin, HOMA and leptin (Figure 21 and Figure

22). There was no change in total-, LDL- and HDL-cholesterol, whereas triglycerides were reduced after the weight loss. The inflammatory biomarkers CRP and IL-6 were also unchanged (Figure 22).

	<b>Arabs MeS out of 82</b>		<b>Caucasians MeS out of 79</b>	
	<b>N</b>	<b>MeS (%)</b>	<b>N</b>	<b>MeS (%)</b>
<b>HOMA-1IR</b>	51	62.2	23	29.0
<b>HOMA-2IR</b>	42	51.2	17	21.5

**Table 11. MeS in Arabs and Caucasians**

Arabs had significantly higher MeS (%) using either meseasurements IR: HOMA-1IR or HOMA-2IR.



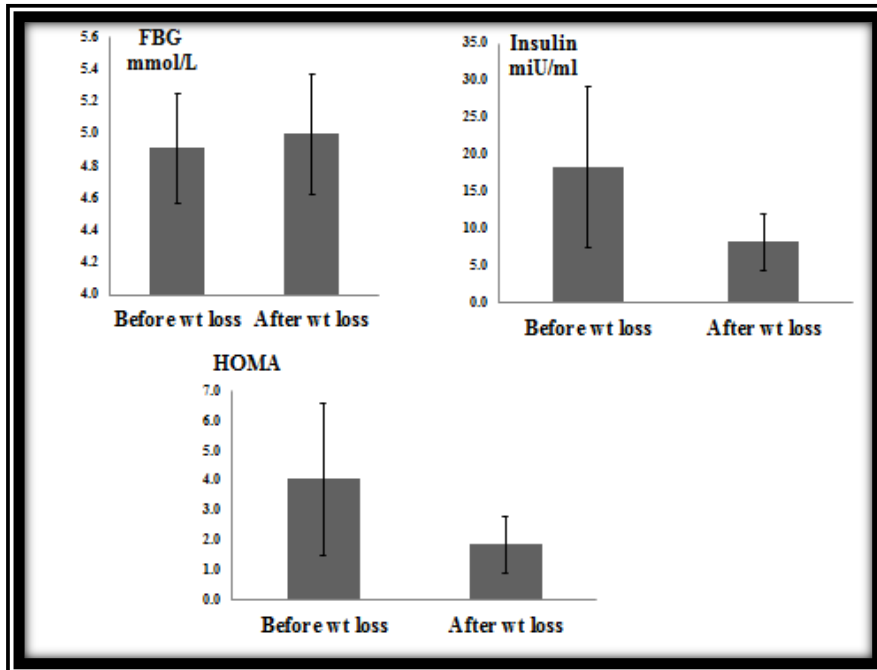


**Figure 24. Glucose and insulin parameters after weight loss**

Three months after surgery there was no change in fasting blood glucose (FBG), but significant reduction in insulin and HOMA.

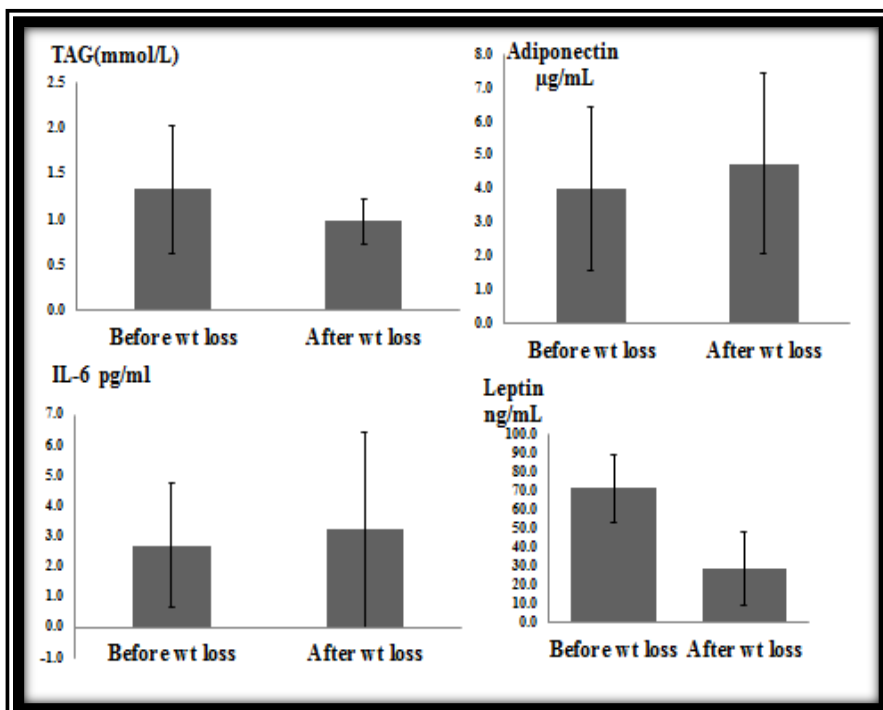


**Figure 25. Adipokines after weight loss**

Weight loss led to lower leptin but no change in plasma triacylglycerides (TAG), adiponectin or inflammatory biomarkers (IL-6).

### **3.8 Discussion**

**Effect of gender.** Morbidly obese Arab males had significantly higher systolic and diastolic higher blood pressure, compared to females. Furthermore they were also more hyperinsulinaemic and insulin resistant. As both the men and women in this population were relatively young a possible explanation for the greater BP and IR in the men may be attributed to greater levels of smoking and perhaps alcohol consumption. Only leptin, perhaps indicating greater fat mass, was higher in the females.

**Differences in insulin sensitivity.** MHO showed, as expected, lower levels of insulin and HOMA-IR, as well as triglycerides compared to PO. They also had lower fasting plasma glucose. In order to determine whether increased FPG may be driving these associations, analysis was repeated after matching for hyperglycemia, which confirmed prior observation of increased TG, insulin and HOMA-IR independent of FPG. Surprisingly the PO groups had lower leptin. Leptin may be a marker for hypertrophied adipocytes and in Caucasian populations this has been reported to be elevated in the PO (Makki et al, 2013). A possible explanation for low levels of leptin in the PO may be that these individuals have elevated SNS activation which directly inhibits adipose leptin production (Pinkney et al, 1998).

**Effect of Ethnicity.** In non-diabetic Arabs, compared to Caucasians, insulin resistance and inflammation appeared to be predominant lesions. Despite both populations being equally obese the Arabs had greater prevalence of risk factors for MeS, with fewer having a metabolically healthy phenotype. The young age at which Arab subjects were showing signs of MeS may be due to earlier onset of obesity, perhaps the reason for greater disease susceptibility, perhaps a consequence of sedentary life-style and

unhealthy diet.

**Effect of weight loss.** Three months after surgery, both MHO and PO subjects showed significant reduction in BMI, which was accompanied by lower systemic insulin, HOMA-IR and leptin.

These findings have driven the plan of the project to look at other factors, e.g. miRs, which may be important regulators of pathways leading to inflammation and insulin resistance. MiRs are remarkably stable, reproducible, and tissue specific among individuals. Several studies suggested the potential use of the blood miRs as biomarkers for the obesity, cardiovascular diseases, atherosclerosis, and T2DM.

Therefore, a better understanding of the function of miRs may provide new insights into the molecular basis of human pathologies, and act as novel biomarkers for disease diagnosis and therapy. In the next chapter samples generated in the MHO and PO patients were used to investigate circulating miR signatures as possible biomarkers and mediators of systemic diseases.

**Chapter 4**  
**Small RNA**  
**Signature for**  
**MHO**

## **4.1 Introduction**

The association between IR and inflammation is well documented (Lumeng, 2011), however the mediators of this association are still under investigation. A caveat to uncovering the nature of this association is that it is likely to be different depending on various factors, including age, gender, ethnicity and body composition. Thus, the mediators of this association may be specific for clinically defined groups of patients or even to individuals. This poses a challenge when trying to identify candidates that could underpin the association between IR and inflammation.

## **4.2 MiR in insulin responsive tissues**

The discovery of circulating miRs has highlighted their potential as both endocrine signalling molecules and disease markers. Several candidate miRs that are highly expressed in insulin responsive tissues and regulate pathways that lead to IR and inflammation have been reported. Some of these are discussed below.

In the liver, miR-122 is the most abundantly expressed miR and it appears to bind to the 3 untranslated region of PTP1B (PTPN1) mRNA, which has an important role in insulin resistance and in non-alcoholic fatty liver disease (NAFLD); (Elchebly, et al 1999). The role of miR-122 in lowering circulating cholesterol has been described by some studies (Elmen et al. 2008). Additionally in the liver miR-33a and miR-33b are SREBP gene regulators and control cholesterol and lipid homeostasis (Gerin et al. 2010).

In SMCs, miR-143 and miR-145 are expressed control blood pressure and vascular tone, and contribute to vascular remodelling. In addition in these cells miR-21 is induced after vascular injury and promotes proliferation and neointima formation. Also erythroid cell proliferation and differentiation is mediated by miR-451 (Eric et al. 2011).

In adipose tissue, several miRs appear to participate in the regulation of adipogenesis (Figure 23). For example, miR-27a inhibits adipocyte differentiation by suppressing

PPAR $\gamma$  expression. The down-regulation of miR-27a may also be associated with adipose tissue dysregulation in obesity, a strong risk factor for osteoarthritis (Kim et al.2010).

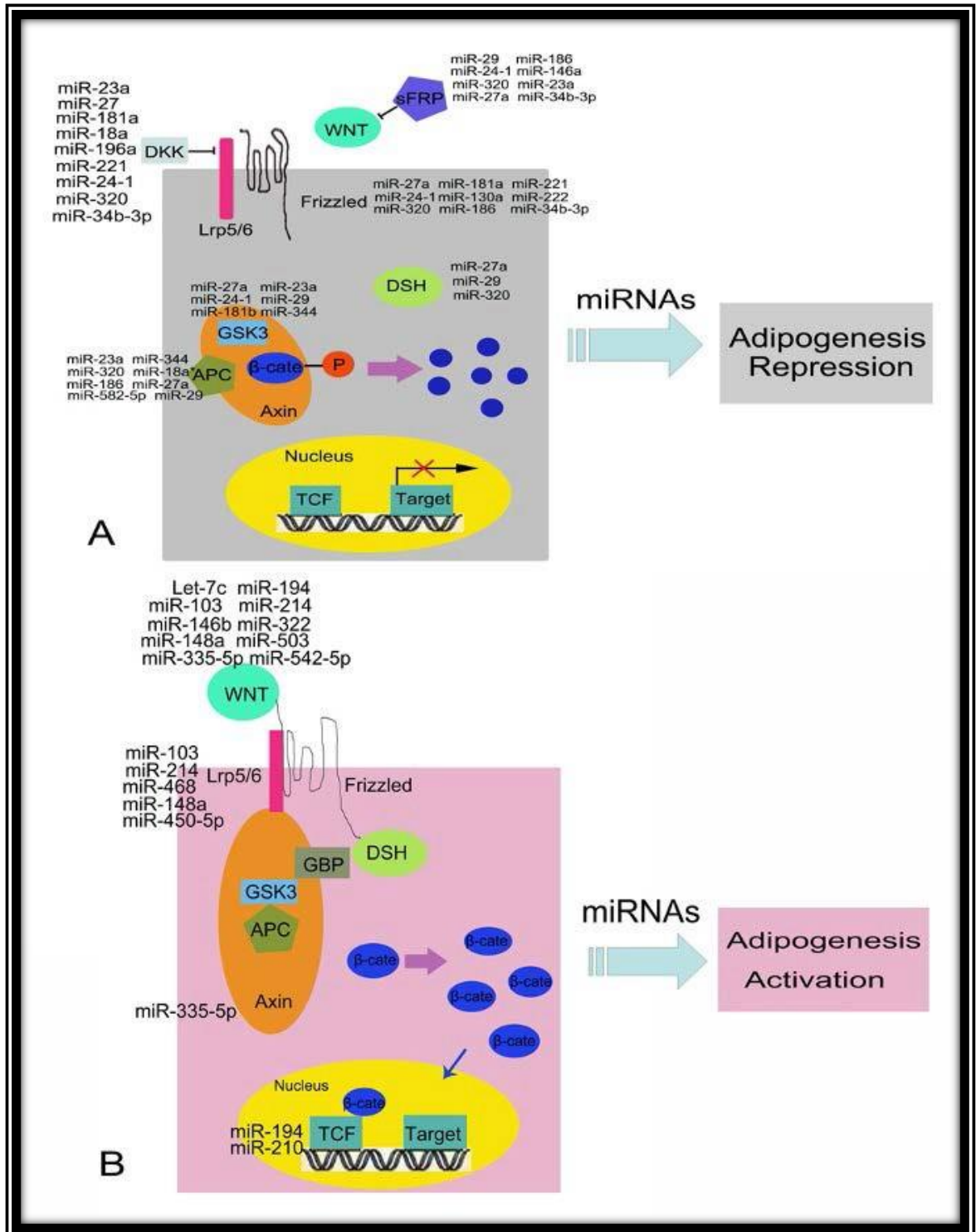


**Figure 26. The role of different miRs in adipogenesis**

A. Repression, B. Activation. (Moon et al, 2004).

More recently miRs in plasma have also been shown to be related to T2DM and IR. Zampetaki et al. reported lower plasma levels of miR-20b, miR-21, miR-24, miR-15a, miR-126, miR-191, miR-197, miR-223, miR-320, and miR-486 and an increase in miR-28-3p in samples from diabetic patients compared to non-diabetic subjects. Interestingly, the expression of miR-15a, miR-28-3p, miR-126, miR-223 and miR-320 was altered before the disease was manifested clinically. This was the first demonstration of a unique diabetic miR blood signature (Zampetaki et al, 2010).

Another miR, miR-29a, may target apoptosis through the regulation of several components of the mitochondrial outer membrane, including MCL1, PUMA and other members of the Bcl2 family of proteins (Gupta et al, 2014). The study also included the voltage-dependant anion channels 1 and 2 (VDAC1 and VDAC2) as targets of miR-29a during apoptosis. MiR-29 may also regulate fibrosis in cardiac tissue (Bargaje et al, 2012). However, reduction of miR29 expression in several myeloid cancers and its ability to cause AML in a mouse model suggests an anti-apoptotic role (Rabinowits et al. 2009). Reduced expression of miR-29a was also associated with cell death in neuronal cells (Kole et al. 2011).

The previous chapter recorded the clinical characteristics of patients with varying levels of IR, despite being age and BMI matched. It showed that inflammation and IR were the most likely mediators of any future development of T2DM and CVD. In view of the reported miRs in other tissues, and the samples generated previously, this chapter specifically explored a panel of inflammatory miRs and their relationship with biomarkers of IR and inflammation.

#### **4.3 Specific aims of the study**

1. Explore the differences in inflammatory miRs between the PO and MHO group using



- an inflammatory pathway specific panel in the blood and adipose tissue.
2. Validate the miRs identified by the arrays
  3. Validate the expression of miRs seen in the inflammatory pathway specific arrays using small RNA sequencing.
  4. Experimental validation of selected miR targets.
  5. Examine the effect of the weight loss on inflammatory miR expression.

#### **4.4 Methods**

Detailed methodologies have been provided in Chapter 2, sections 2.6, and 2.7.

**Samples used.** Blood, whole adipose tissue and collagenase digested tissue (SVF and adipocytes).

Thirty three patients were studied, 24 prior to weight loss and 9 after weight reduction surgery.

The pathway specific arrays were carried out in the blood samples of PO (n=14) and MHO (n=10). The effect of weight loss was investigated in PBCs of nine patients.

In addition SC and OM adipose tissues (n=5) were also used for these analysis. 14 RNA samples of whole adipose tissue SC and OM (2 MHO, 5 PO) were used to look at the variation between the groups in the level of collagen genes, which are miR-29 target genes, that was found to be significantly downregulated in the PO group compared to the MHO in blood and adipose tissue. Three PBCs samples were used for the small RNA sequencing (MHO=1, PO=1 and T2DM=1).

The inflammatory specific pathway array (Qiagen) used was able to assess the expression of 84 key miR genes.

**First method of data analysis (SA Biosciences):** Real-time PCR for Miscript Arrays was done (chapter 2 section 2.12) to analyze expression of genes in peripheral blood samples and adipose tissues (subcutaneous and omenta) from PO and MHO samples. Data were presented as fold change ( $2^{-\Delta\Delta CT}$ ) after normalization, using the Sabioscience Software online. These analyses were done at ADLQ.

**Second method of data analysis (QCRI):** In addition to the Sabioscience software analysis, the miR array data analysis was also performed using an R-based in-house tool. Raw data, Ct values, was normalized against the housekeeping genes to obtain  $\Delta Ct$  values, and the miR expression was calculated as  $2^{(-\Delta Ct)}$ . Differentially expressed microRNAs were selected by  $\Delta\Delta Ct$ . Fold Change  $\geq 2$  and their statistical significance was determined by Student's t-Test (p-Value  $\leq 0.05$ ). These analyses were done by Dr Michele Ceccarelli (QCRI; Qatar Computing Research Institute, Doha, Qatar) and Dr Fulvio d'Angelo (Biogem, Italy).

Ingenuity Pathways Analysis (IPA, <http://www.ingenuity.com/>) was used to perform gene enrichment analysis. Gene expression data was mapped into relevant pathways based on their functional annotation and known molecular interactions. Statistical significance was evaluated with Fisher's exact test adjusted for multiple comparisons by the Benjamini-Hochberg method.

#### **4.5 Results**

The inflammatory miR array was able to detect 84 different miR associated with targets that are in pathways that regulate inflammation. In all the samples at least 40% of the miRs in the panel were significantly detectable.

#### **4.5.1 Effect of IR on inflammatory miR expression in PBCs (analysed by SA Biosciences programme).**

The comparison of the differences in the expression of miRs between the PO group (n=14) to the control group MHO (n=10); showed the significant down regulation of 12 miRs (miR-142, miR-16, miR-185, miR-24, miR-15, miR-28, miR-29b, miR-19b, miR-374a, miR-195, miR-130a and miR-144; Figure 24).

##### **4.5.1.1 Correlation of miR expression and systemic cardiometabolic risk factors**

The correlation between the systemic biomarkers and the inflammatory miRs was examined. The heat map (Figure 25) showed that the majority of miRs in this array were increased in association with the classic inflammatory markers, MCP-1 and CRP. There was also a smaller cohort of the miRs that correlated positively with systemic insulin levels and HOMA, e.g: miR-122, miR-302a, miR-200c. Interestingly, miR-200c which is reported to enhance adipogenesis was upregulated in PO and correlated positively with insulin and negatively with leptin. MiR-200c, which decreased after weight loss, was related to lower levels of insulin.

Overall, the correlation studies indicated a unique inflammatory signature that may be functional. It was apparent that significant differences in expression of the miRs species occur along with changes in metabolic and inflammatory parameters in the two groups studied.

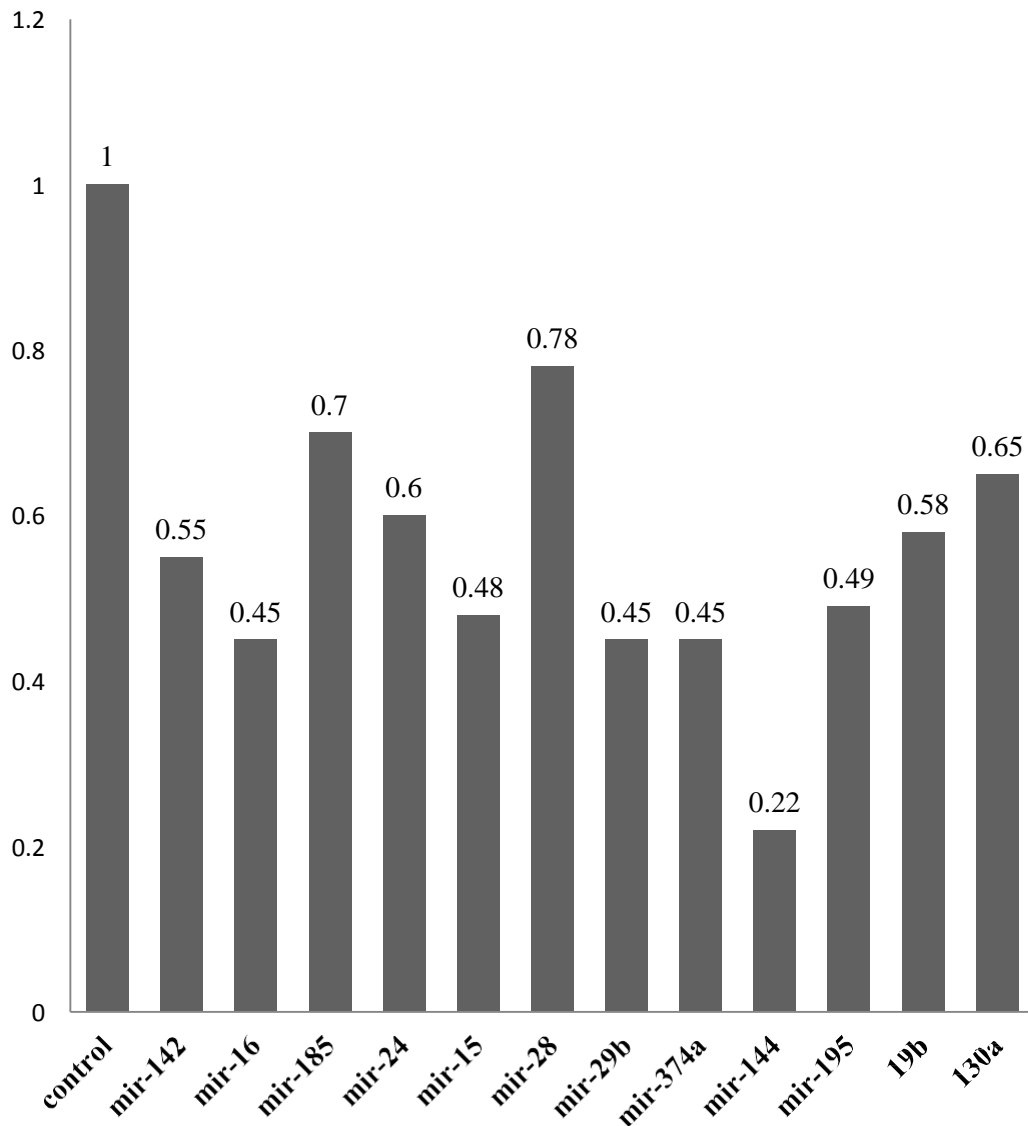


**Figure 27. Effect of insulin resistance on miRs expression (SA Biosciences)**

12 miRs were down regulated in the PO (n=14) compared to the control group (MHO, n= 10), normalised to 1. Downregulated miRs: miR-142, miR-16, miR-185, miR-24, miR-15, miR-28, miR-29b, miR-19b, miR-374a, miR-195, miR-130a and miR-144.

Data presented as fold change. ( $2^{-\Delta\Delta CT}$ ) after normalization using the Sabioscience Software.

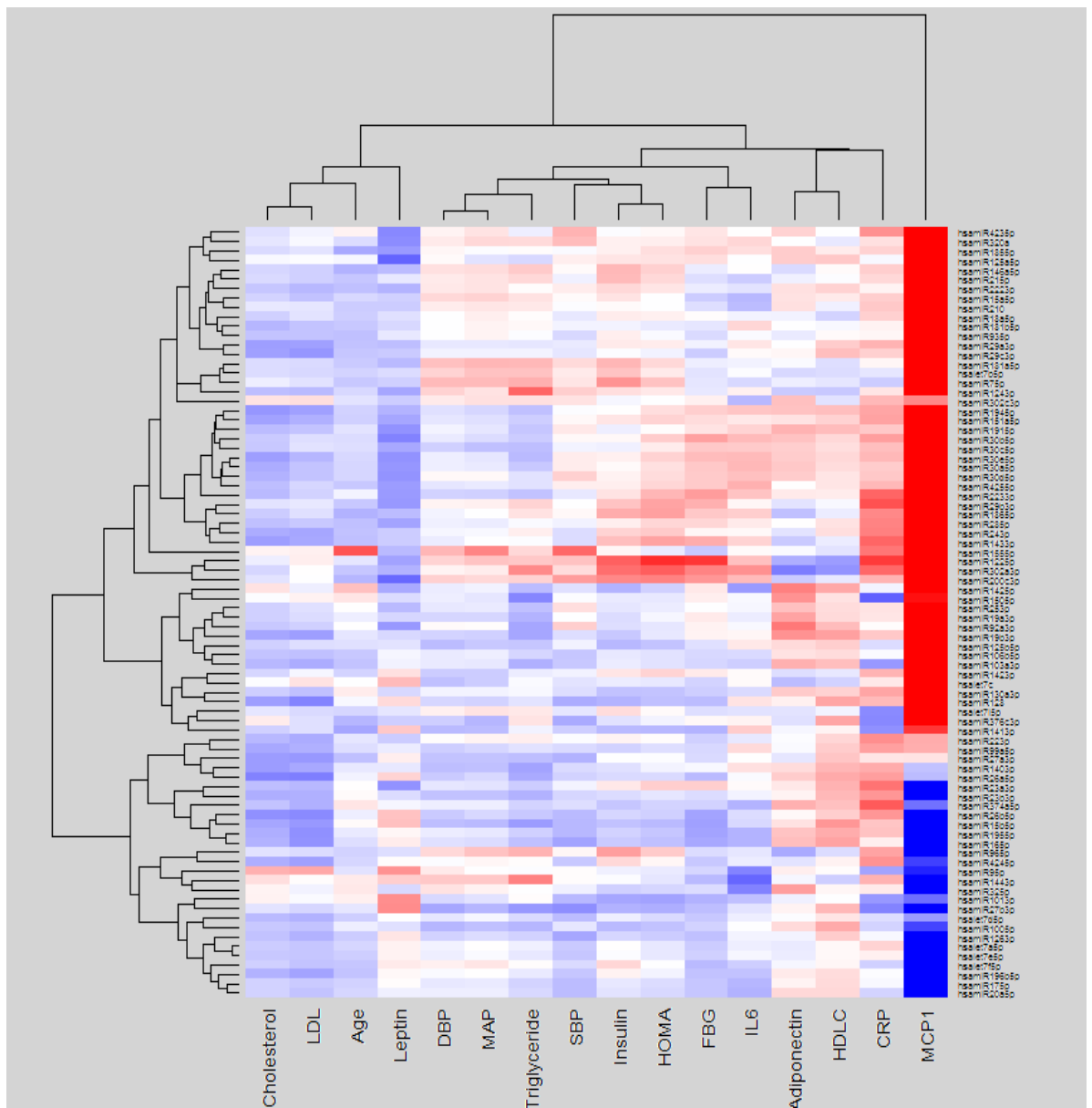


**Figure 28. Correlations between miRNAs and systemic biomarkers**

The positive correlations are in a red color while negative correlations are in blue. Three miRNAs (miR-122, miR-302a, and miR-200c) were positively correlated with insulin, glucose and HOMA.

#### 4.5.1.2 Inflammatory array data analysed by R-based in-house programme (QCRI)

The miR array data generated was analysed separately (QCRI) by a more stringent programme using a different algorithm to that of SA Biosciences programme.

This generated only 3 miRs that were significantly down regulated in the PO compared to MHO: miR-144, miR-29b and miR-374a (Figure 26). However, of note is that these three miRs were also present in the SABiosciences analysis.

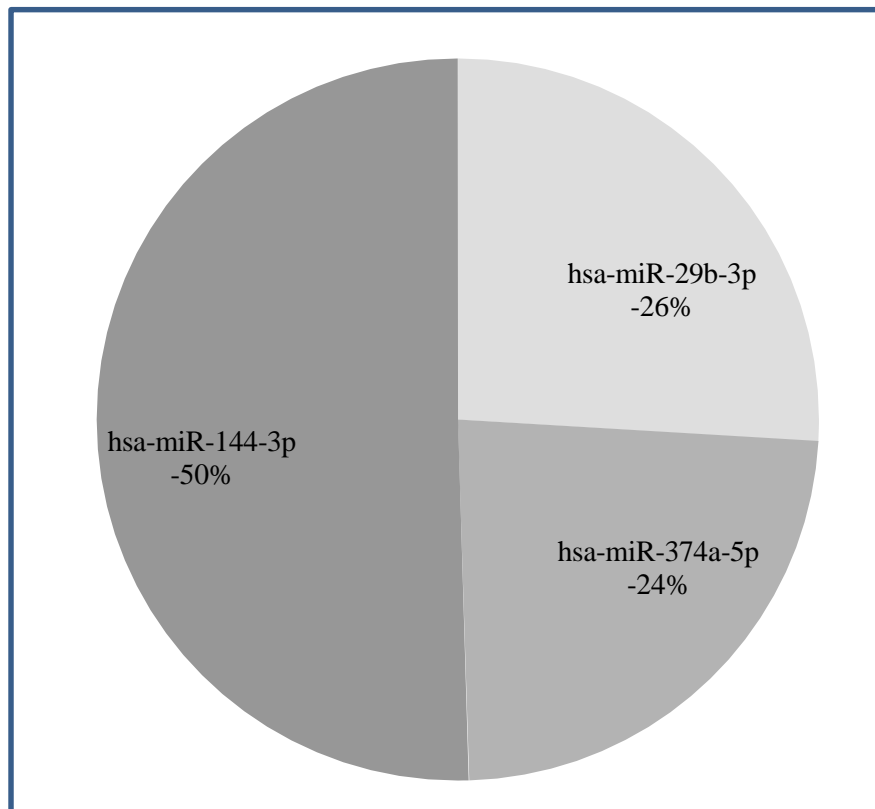


**Figure 29. Effect of insulin resistance on miRs expression (QCRI)**

3 miRs were down regulated in the PO (n=14) compared to the control group (MHO, n=10). Downregulated miRs: miR-29b, miR-374a and miR-144. The extent of the reduction in the PO samples compared to MHO is shown as a percent.

The miR array data from the abdominal SC and OM adipose tissue samples were then analysed using the QCRI programme.

#### 4.5.2 MiRs gene expression in OM adipose tissue (QCRI)

Comparison of the expression of miRs in OM adipose tissue of the PO compared to MHO samples showed down regulation, to varying degrees, of 7 miRs; miRs 101, 42, 15a, 376c, 424, 27a and 20a (Figure 27).

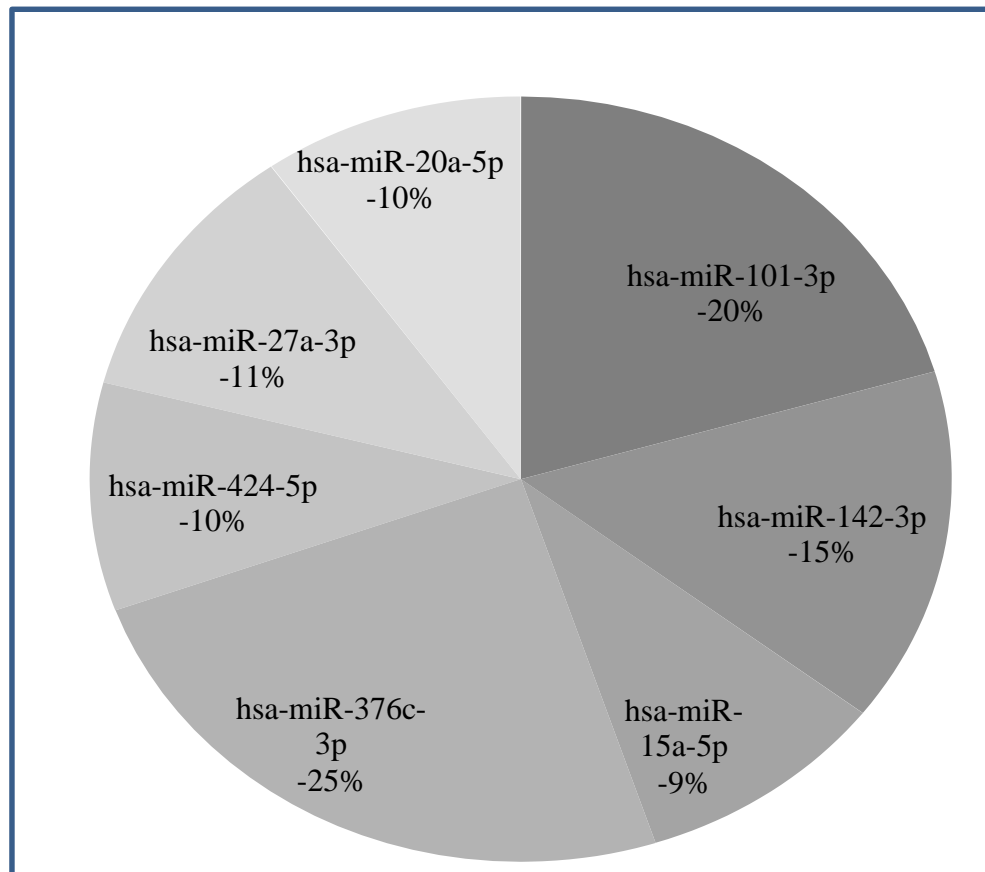


**Figure 30. Effect of IR on miR expression in the OM adipose tissue**

7miRs were reduced in the PO (n=4) compared to MHO (n=1) OM adipose tissue. The extent of the reduction in the PO samples compared to MHO is shown as a percent.

#### 4.5.3 MiRs gene expression in SC adipose tissue (QCRI)

Only two miRs were downregulated in the SC adipose tissue of the PO compared to the MHO, miR-29 and miR-142 (Figure 28).

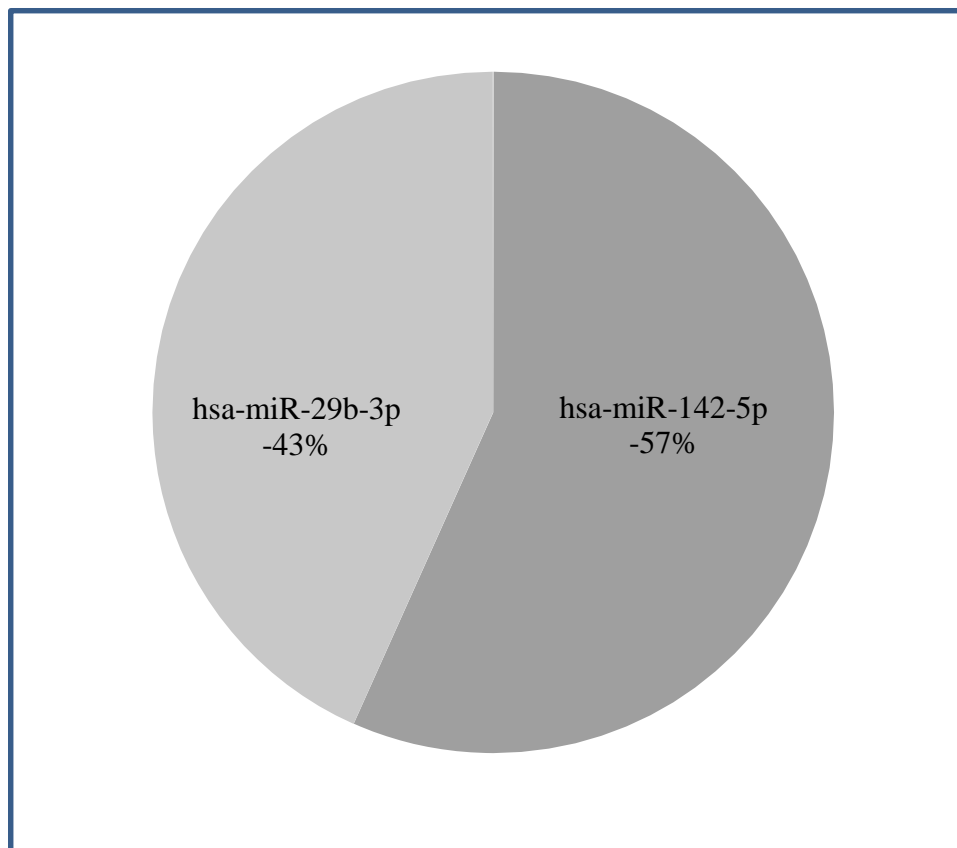


**Figure 31. Effect of IR on miR expression in the SC Adipose tissue**

2 miRs, 29b and 142, were reduced in the PO (n=4) compared to MHO (n=1) OM adipose tissue. The extent of the reduction in the PO samples compared to MHO is shown as a percent.



#### 4.5.4 MiRs gene expression in Adipocytes (QCRI)

Three miRs, 126, 194 and 376, were downregulated in adipocytes of PO compared to MHO (Figure 29). miR-376c was strongly expressed in these cells.

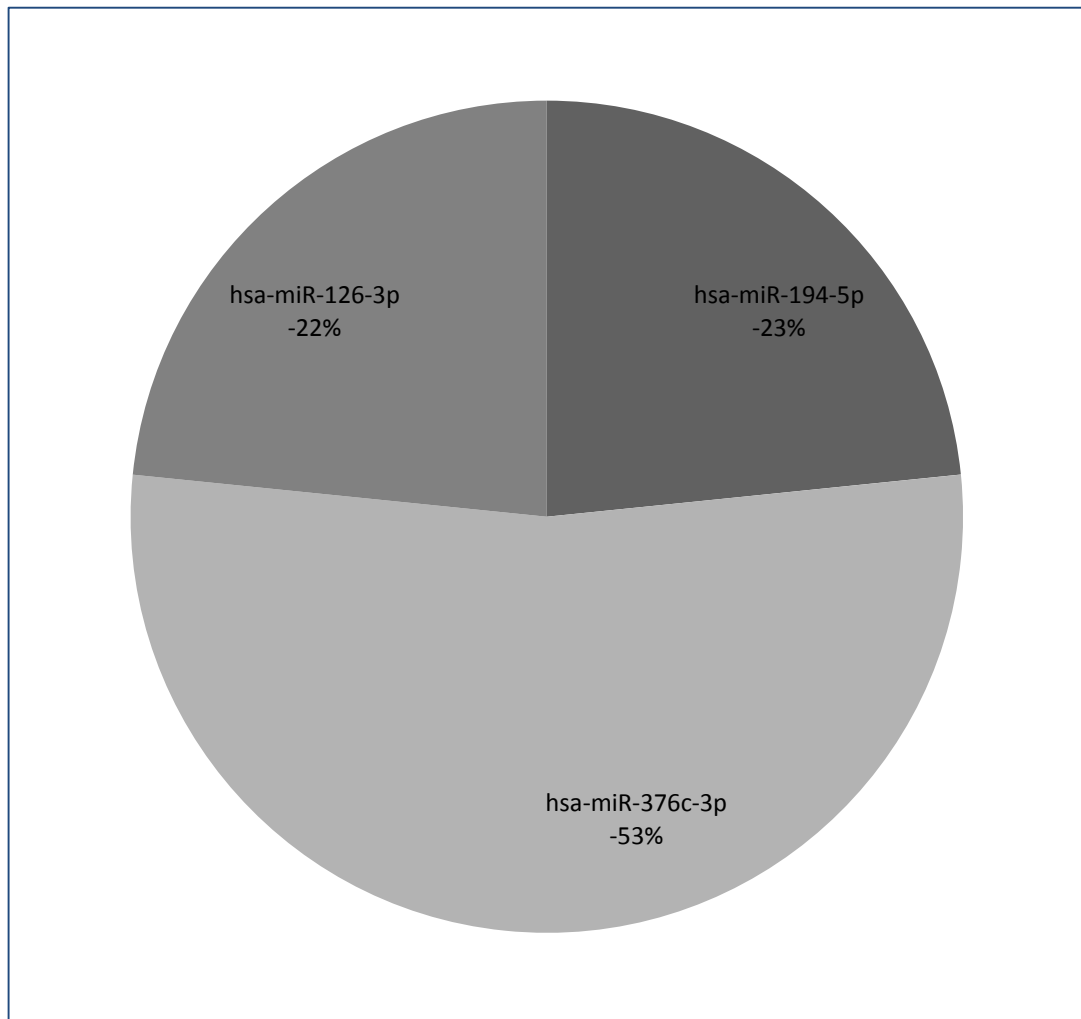


**Figure 32. Effect of IR on miR expression in the adipocytes**

3 miRs; 126, 376 and 194, were reduced in the PO compared to MHO adipocytes. The adipocytes from the OM and SC were analysed together. The extent of the reduction in the PO samples compared to MHO is shown as a percent.

#### **4.5.5 Validation of the inflammatory miR array**

MiR expression data from the array experiments must be validated because the oligonucleotide probes not only bind to the mature miR but also pre-miR, with only the mature miR being of biological relevance.

##### **4.5.5.1 Validation of circulating miRs**

Nine miRs were selected for validation in PBCs: miR-122, miR-29b, miR-124, miR-302a, miR-302b, miR-302c, miR-19a, miR-19b and miR-9. Housekeeping genes were included for normalization (e.g: SNORD-68, SNORD-96, and RUN-6). The expression of miRs were investigated in PO (n=10) and MHO (n=5).

All of the miRs were down-regulated (except for miR-124) in PO compared to MHO. Three key miRs that have been implicated in tissue fibrosis and angiogenesis showed difference in gene expression between MHO and PO, miR-29b, miR-122 and miR-19b. All were down regulated in PO.

The data confirmed the difference in the expression of selected miRs (miR-122, miR-29b, miR-124, miR-302a, miR-302b, miR-302c, miR-19a, miR-19b and miR-9) between MHO and PO.

MiR-302a (p=0.007) showed a significant downregulation that confirmed the differences between the two groups. MiR-29 was also downregulated and showed the difference clearly between the groups (p=0.06, Figure 30).

Therefore the qPCR data validated the differences in the expression of the selected miRs seen with the pathway specific array in the MHO and PO cross-sectional study.

##### **4.5.5.2 Validation of miRs in SVF samples**

Selected miRs were used for validation of the miR array data in SVF samples from SC

and OM adipose tissue (n=5 patients, 10 samples), specifically: (miR-122, miR-29b, miR-124, let7c, let7g, miR-302c, miR-19a, miR-19b and miR-9). There was a non-significant upregulation of miR-29 and downregulation of miR-122 and let7c

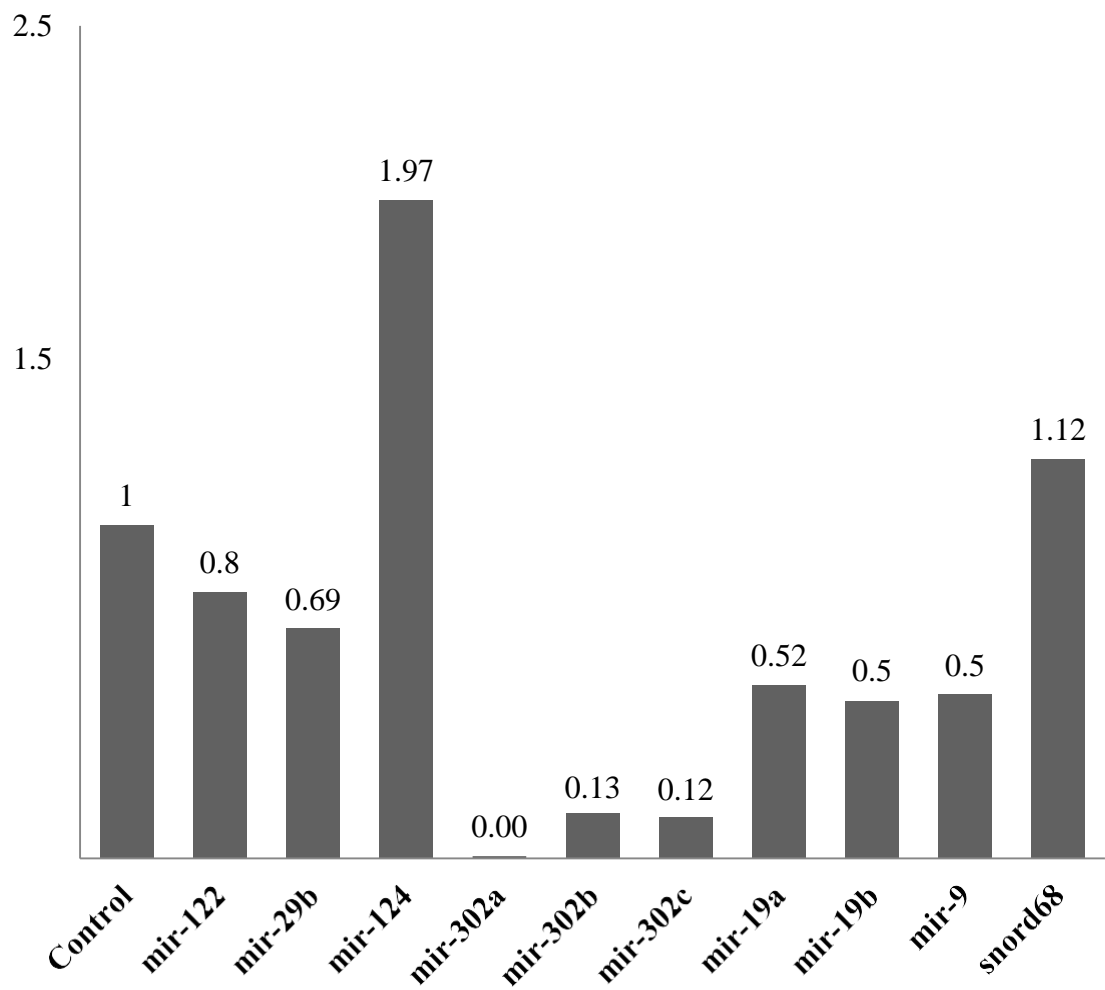


**Figure 33. Validation of the miR array data by q-PCR in PBCs**

MHO was the control and set at 1. All the selected miRNAs showed downward trends but only miR-302a reached statistical significance, while miR-124 was significantly upregulated.

#### **4.5.6 Small RNA sequencing of PBCs**

The main aim of sequencing miRs samples was to validate the findings and data outcome of the specific miRs found in the blood and the adipose tissue samples using the inflammatory pathway specific array. Further it could also help discover some other miRs which were not present in the arrays. One of the limitations of microarray expression profiling was the requirement of prior sequence information to be used for probe design. Until recently, this sequence information has been limited mostly to that found in public databases. In contrast, deep sequencing is not dependent on any prior sequence information. Instead it provides unbiased information about all RNA species in a given sample, thus allowing for discovery of novel miRs or other types of small RNAs. Next generation sequencing utilises massively parallel sequencing, generating millions of small RNA sequence reads from a sample.

Three samples were sequenced by PGM (chapter 2); one PO and one T2DM sample compared to an MHO sample as control. The results summary is shown in Figure 31 and 32.

The data from the T2DM patient was not further analysed as all other measurements were only available for the MHO and PO cohorts.

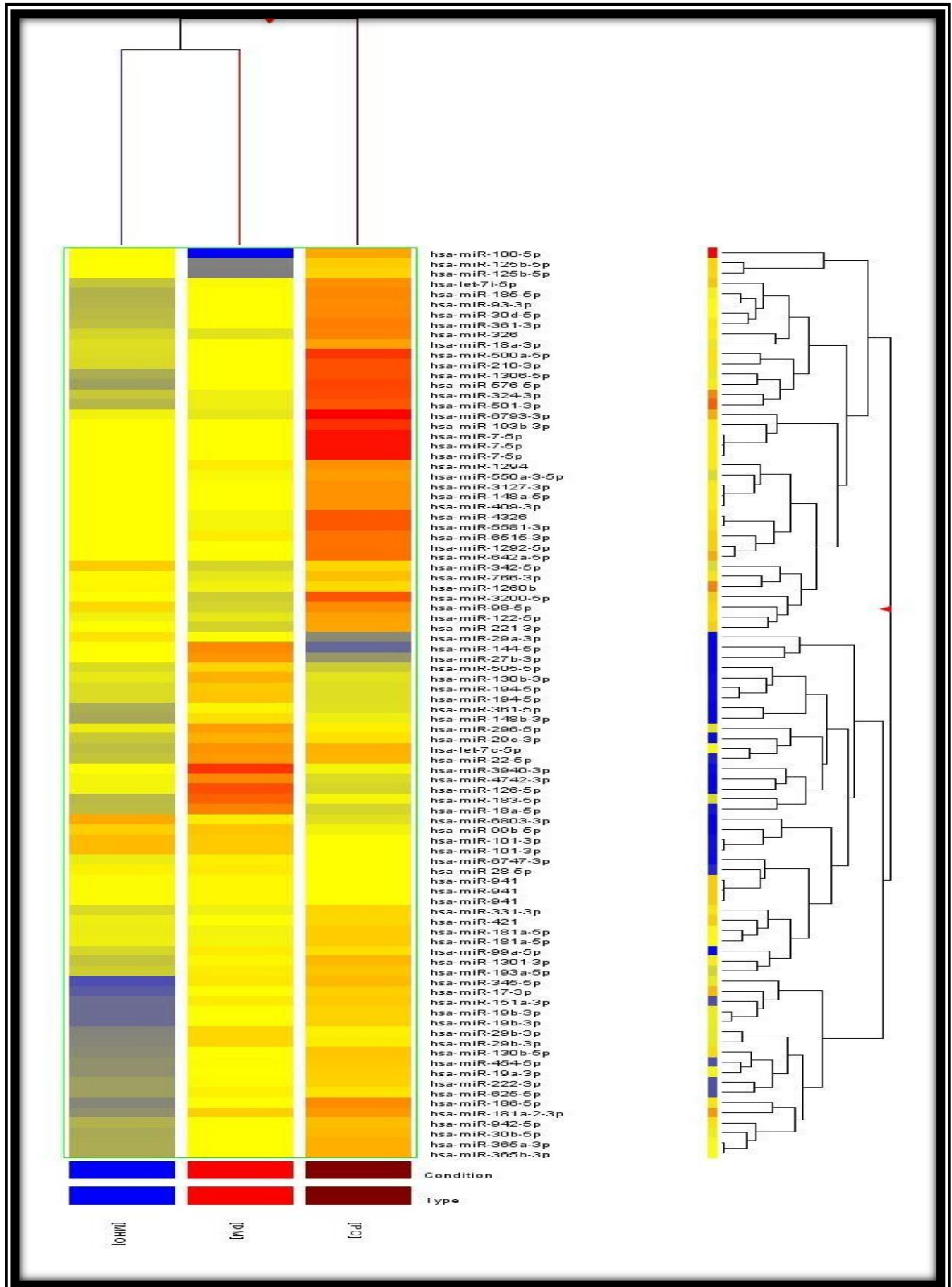
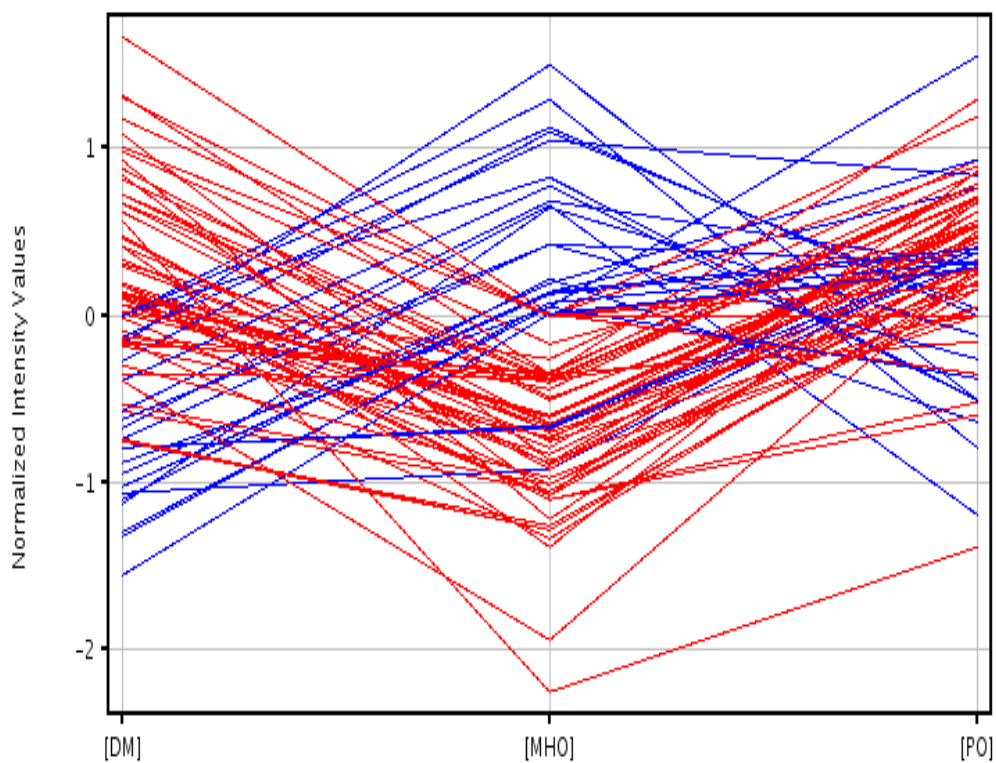


Figure 34. Summary of miR expression in MHO, PO and T2DM

A, showed the cluster map to illustrate the variation in gene expression between the samples used.



**Figure 35. Summary of miR expression in MHO, PO and T2DM**

B, showed trends in miR expression in PO and the T2DM compared to MHO. 66 miRs in the PO, and 67 miRs in the T2DM, blood samples, were upregulated compared to the MHO.

Also 9 miRs in the PO, and 6 miRs in the T2DM, blood samples, were downregulated compared to the MHO.

#### 4.5.6.1 The miRs expression profile in IR using NGS

Two runs were performed for the same samples PO (n=1) versus MHO (n=1) as explained in chapter 2.

Among these miRs, miR-27b miR-29a, miR-144 and miR-3607 were downregulated in the PO by NGS. miR-144 is a direct modulator of IRS1 and a potential therapeutic target of IR. MiR-29a targets Akt2 as well as components of the fibrotic pathway. A few novel miRs were found to be expressed highly, like miR-27b and miR-3607, which also targets IRS-1 (Figure 36).

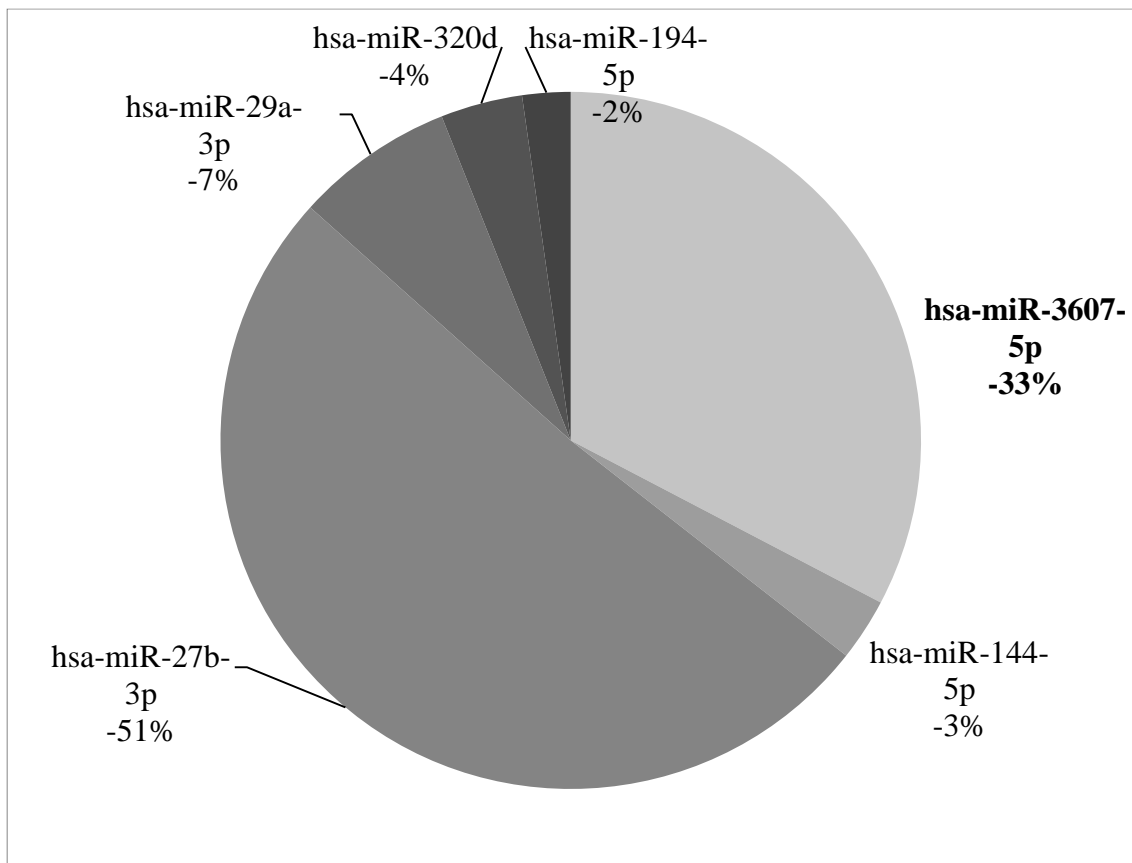


**Figure 36. Down regulation of miR by IR - identified by small RNA seq.**

Downregulation of miRs in PO compared to MHO (n=1 each). Shown as fold change. miR-144 and miR29 were previously identified in the inflammatory array.



The NGS data showed the upregulation of three main miRs, which were also highly expressed, in the PO: miR-181, miR-29b and miR-30e. Several other species were upregulated, but to a lesser extent (Figure 37).

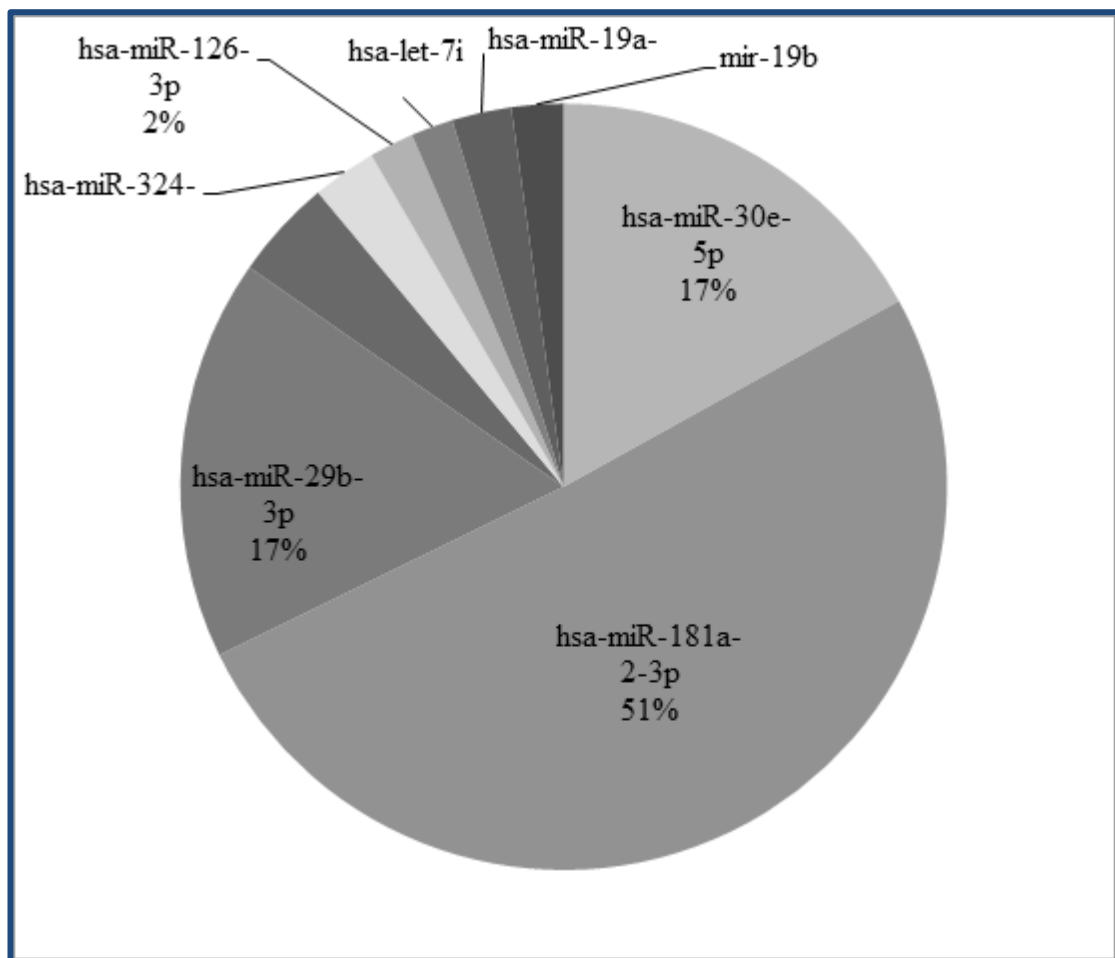


**Figure 37 Upregulation of miR by IR - identified by small RNA seq.**

PO (n=1) versus MHO (n=1). miR-181a, and to a lesser extent, miR 29b and miR 30e were upregulated in the PO sample.

#### 4.5.7 The predicted target genes of miRs

Using the data from the inflammatory pathway specific analysis, the qPCR validation and NGS the differentially expressed microRNAs, miR-29, miR-144 and miR-374a, were investigated further to find their experimentally validated target genes, using various databases: Ingenuity Knowledge Base (<http://www.ingenuity.com/>), miRecords (Xiao et al. 2009), TarBase (Vergoulis et al. 2012), and their predicted targets, using TargetScan (Lewis 2005). MiR expression and target gene expression results were integrated to verify if validated or predicted microRNA-targets were regulated coherently.

The data analysis of selected significant differentially expressed genes:

\* PO / MHO absolute log<sub>2</sub> Fold Change  $\geq$  1

\* corrected p-Value (FDR)  $\leq$  0.05

##### 4.5.7.1 The functional expression of miR-29 target genes

There were significant effects on the targets of miR-29.e.g: COL1A1, COL1A2 and COL3A1, which was highly expressed and control atherosclerosis signalling, and are mostly involved in the regulation of fibrosis (Figure 38). In addition other collagen genes have also been shown to be involved in hepatic fibrosis like COL6A6 COL5A6 and HSPG2. HSPG2 inhibits angiogenesis by TSP1 inhibition of matrix metalloproteases.

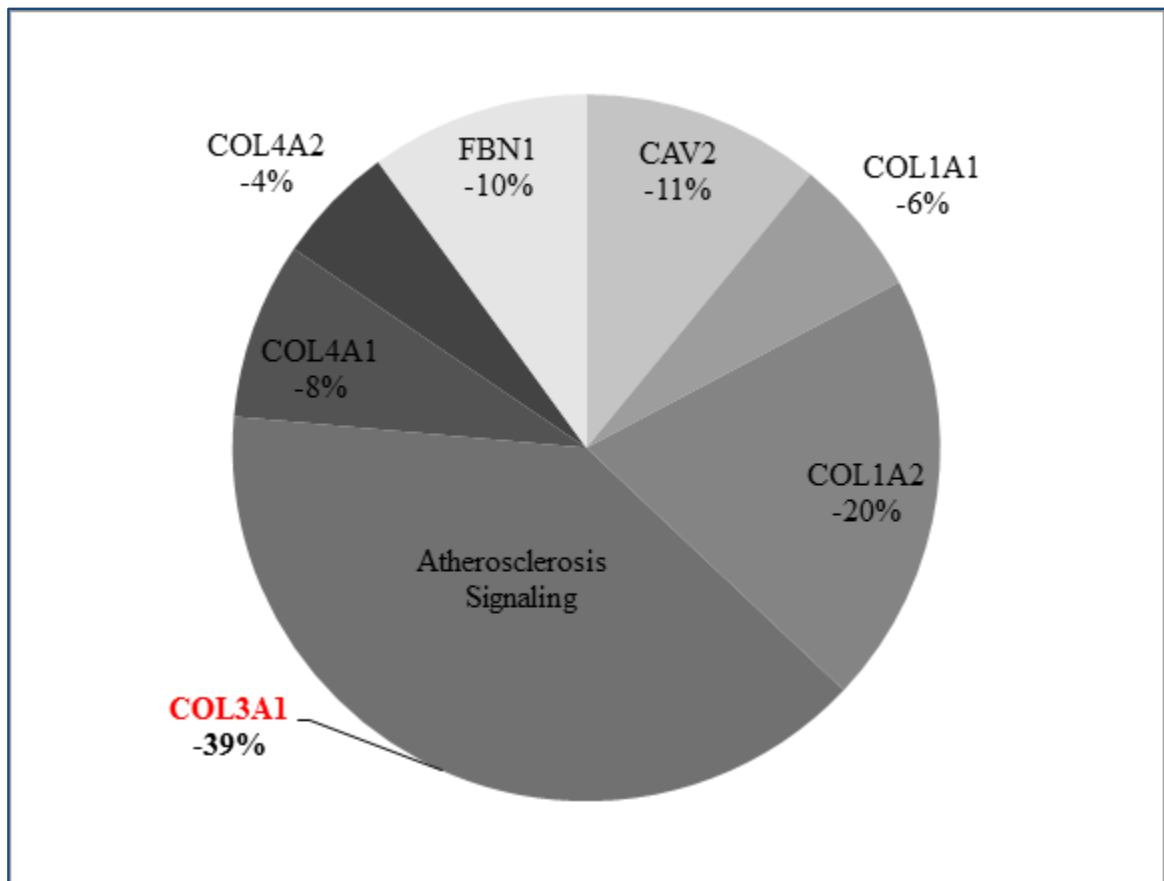


**Figure 38. The functional expression of miR-29 target genes**

Data showed significant effects on the targets of miR-29.e.g: COL1A1, COL1A2 and COL3A1. COL3A1 is highly expressed and regulates signalling during atherosclerosis; (Madrigal-Matute et al, 2013).

#### 4.5.7.2 The functional expression of miR-144 target genes

The functional targets for miR-144 also included genes regulating fibrosis such as FBN1, COL4A1 and PCDH18, as well as components of the insulin signalling pathway such as FZD4 and IGFBP5 (Figure 39).

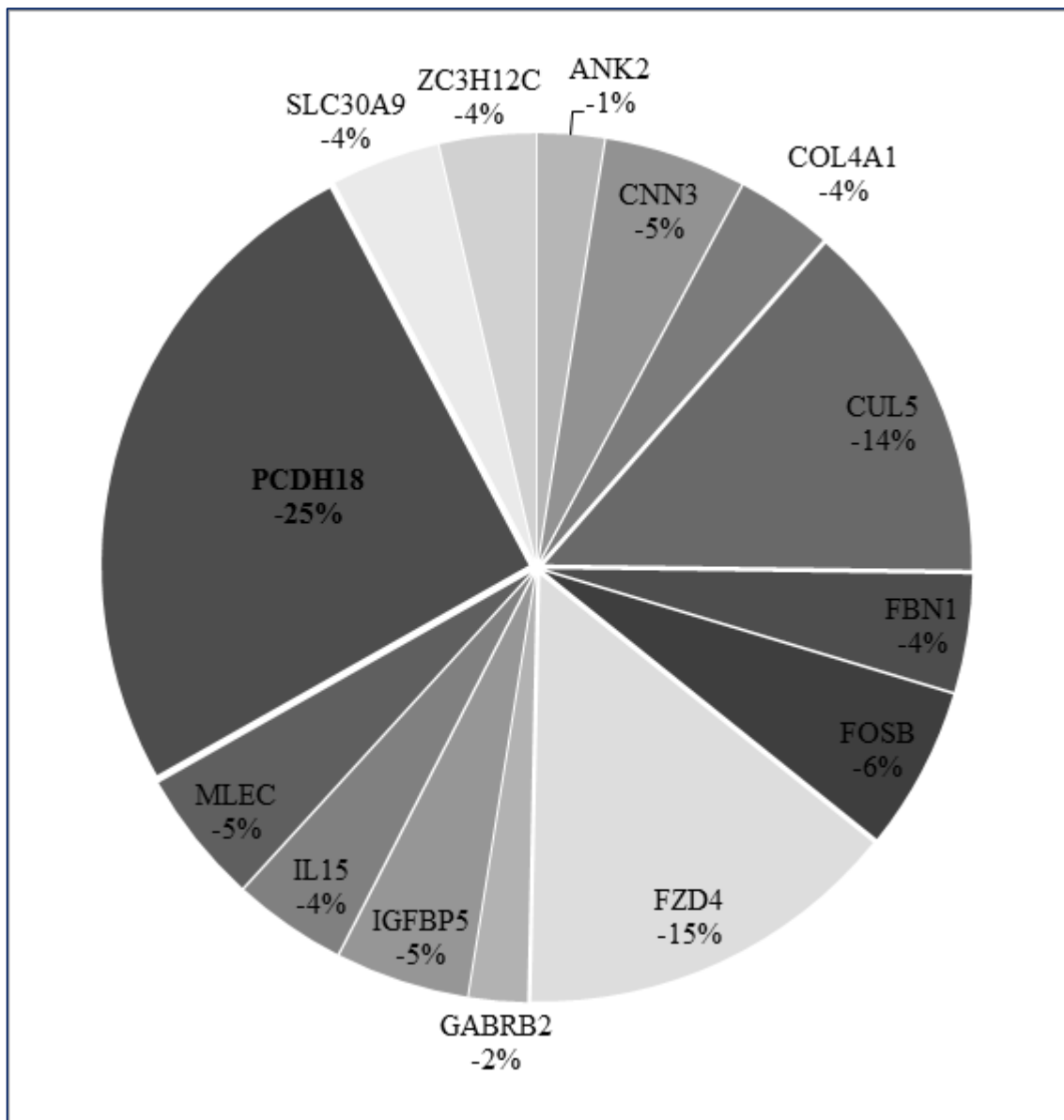


**Figure 39. The functional expression of miR-144 target genes**

All of the targets were significantly downregulated. PCDH18 (Protocadherin-18) is the most highly expressed gene, shown to play a role in the establishment and function of specific cell-cell connections in the brain (RefSeq, Jul 2008).

#### 4.5.7.3 The functional expression of miR-374a target genes

The functional targets for miR-374 included genes that are part of the TGF $\beta$  pathway which also regulates fibrosis such INHBB (Figure 40).

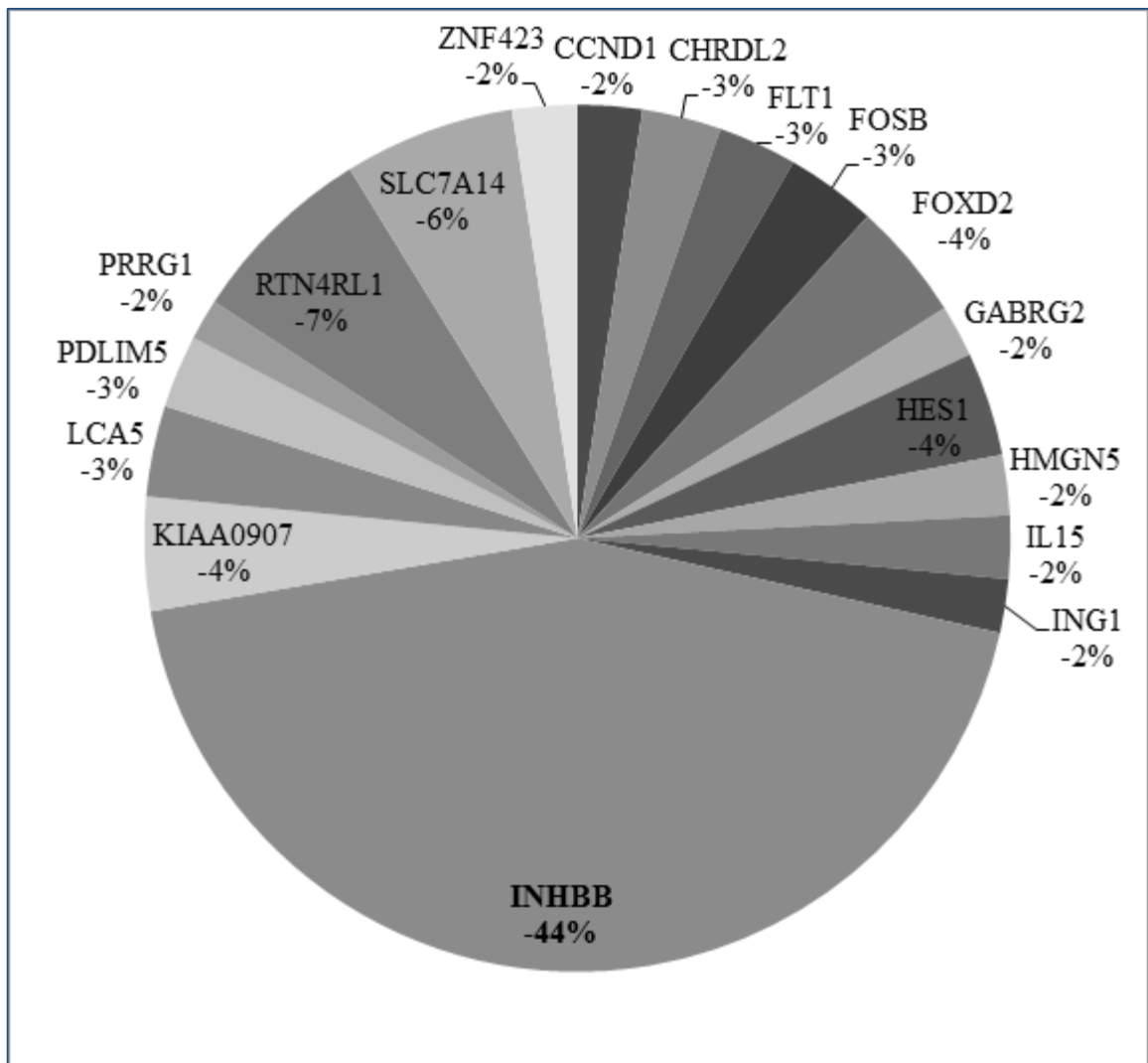


**Figure 40. The functional expression of miR-374a target genes**

Around 35 genes were downregulated. INHBB, which is involved in the TGF- $\beta$  signaling pathway, was the most abundant and downregulated target, with a fold change of 103 (P09529 - INHBB\_HUMAN).

#### **4.5.8 Experimental validation of miR-29 targets**

The results of the inflammatory miRs specific arrays, small RNA sequencing and also the predicted target data led to further experimental confirmation of targets of one of the miRs in the samples generated in this study.

MiR-29, was consistently shown to be downregulated in the presence of IR (i.e. the PO group). Therefore, three collagen genes, COL1A, COL3A and COL6A, which are its targets and also shown to be expressed ubiquitously were used for a further investigation of potential miR-29 function in the PBCs and SVF samples by qPCR (Tables 12 and 13).

	<b>Fold Change</b>	<b>95% CI</b>	<b>Comments</b>	<b>P value</b>
<b>COL1A</b>	0.54	( 0.00001, 2.63 )	OKAY	0.42
<b>COL3A</b>	0.32	( 0.00001, 1.42 )	B	0.89
<b>COL6A</b>	0.44	( 0.00001, 2.07 )	OKAY	0.52
$\beta$ -actin	1	( 1.00, 1.00 )	OKAY	0

**Table 12. Expression of collagen gene targets of miR-29b in PBCs by qPCR**

The results showed no differences in expression in PBCs between the PO and MHO.

<b>Symbol</b>	<b>Fold Change</b>	<b>95% CI</b>	<b>Comments</b>	<b>P value</b>
COL1A	0.68	( 0.00001, 1.97 )	OKAY	0.71
COL3A	0.75	( 0.00001, 1.65 )	OKAY	0.69
COL6A	2.07	( 0.00001, 11.03 )	A	0.60
$\beta$ -actin	1	( 1.00, 1.00 )	OKAY	0

**Table 13. Expression of collagen gene targets of miR-29b in SVF by qPCR**

The expression of OM SVF (n=5) was compared to SC SVF (n=5). COL6A was upregulated 2 fold in OM SVF compared to SC SVF but this did not reach significance.

The targets of miR-29 were also further investigated using specific target arrays. The miR-29 target array in the PBCs did not show any significant results.

Further analysis was carried out using SVF samples, where miR-29 targets may play a role in regulating fibrosis. Only two genes, SPARC 65 FC and SFPQ of 8 FC, were upregulated in the adipose tissue compared to the blood of the PO group. Interestingly MCL1 was downregulated when the SVF of OM depots were compared to SC.

The data showed a non-significant upregulation of the majority of miR-29 target genes when comparing the whole adipose tissues to their matched PBCs (2 PO blood and 2 matched tissues of OM and SC). The genes of interest, collagens, were upregulated with increased fold change but not significant.

The summary of the findings from the various analysis are shown in Tables 14 & 15.



Source	MiR
<b>Blood: Sabioscience</b>	miR-142, miR-16, miR-185, miR-24, miR-15, miR-28, miR-29b, miR-19b, miR-374a, miR-195, miR-130a and miR-144.
<b>Blood: QCRI</b>	miR-29b, miR-144, miR-374a
<b>Adipose tissue: OM</b>	MiR-27a, miR-376c, miR-142, miR-15 and miR-101, miR-424, miR-20a
<b>Adipose tissue: SC</b>	miR-29b, miR-142.
<b>Adipocytes</b>	miR-376c, miR-194, miR-126.
<b>Blood miR NGS:</b>	miR-27a, miR-29a, miR-144 and miR-3607

**Table 14. The summary of analysis of miR changes from different tissues.**

Targets	
<b>Predicted targets:</b>	miR-29: COL1A1, COL11A, COL3A1↓
	miR-144: PCDH18, IGFBP5, CUL5, FBN1, FZD4↓
	miR-374a: INHBB: TGFB-signalling.
	miR-142: IRS1.
<b>PCR arrays targets:</b>	
Adipose tissue versus blood	SPARC↑, SFPQ↑
OM (PO versus MHO)	MCL1↓

**Table 15. Summary of analysis of mRNAs (Targets of miRs) results from different tissues**

## 4.5.9 Inflammatory miR profile associated with weight-loss

### 4.5.9.1 Effect of weight loss on inflammatory miRs using pathway specific arrays

The inflammatory specific pathway in the blood was used to see the effect of the weight loss on these miRs. The profile of 84 miRs in 9 samples (3MHO and 6 PO) was investigated, after the weight loss (Figure 41).

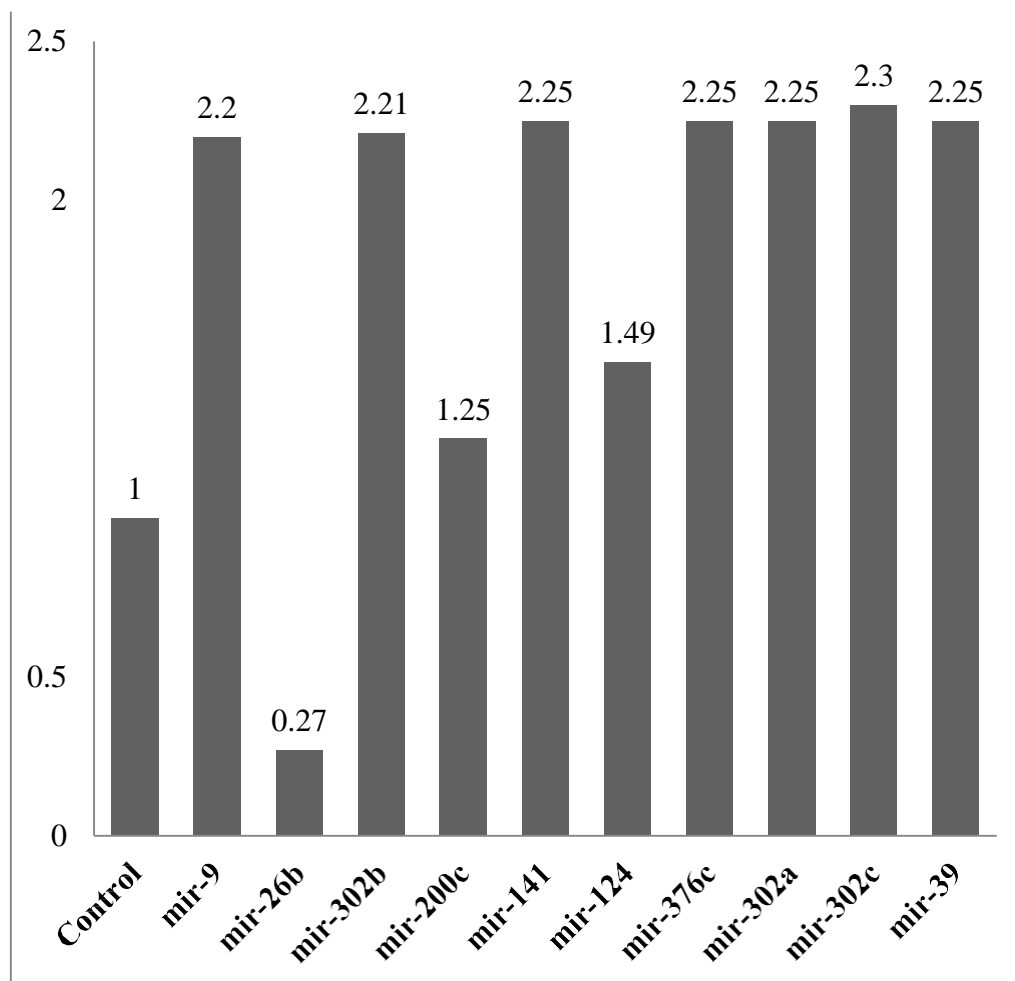


**Figure 41. Effect of weight loss on expression of systemic miRs**

The inflammatory array was used. Data were normalized to (1) and shown as expression before and after weight loss (in n=9 patients). The graph showed that the expression of 10 miRs: miR-9, miR-200c, miR-141, miR-124, miR-376c, miR-302 (a, b, c), and miR-39 were upregulated, and miR-26b was downregulated.

#### 4.5.9.2 The validation of selected miRs by qPCR after weight loss

The same profile of miR expression was seen in the samples obtained before and after weight loss. Thus, the results confirmed the upregulation of five miRs after the weight loss. These results matched the ones of the inflammatory arrays (Figure 42 and Table 16).

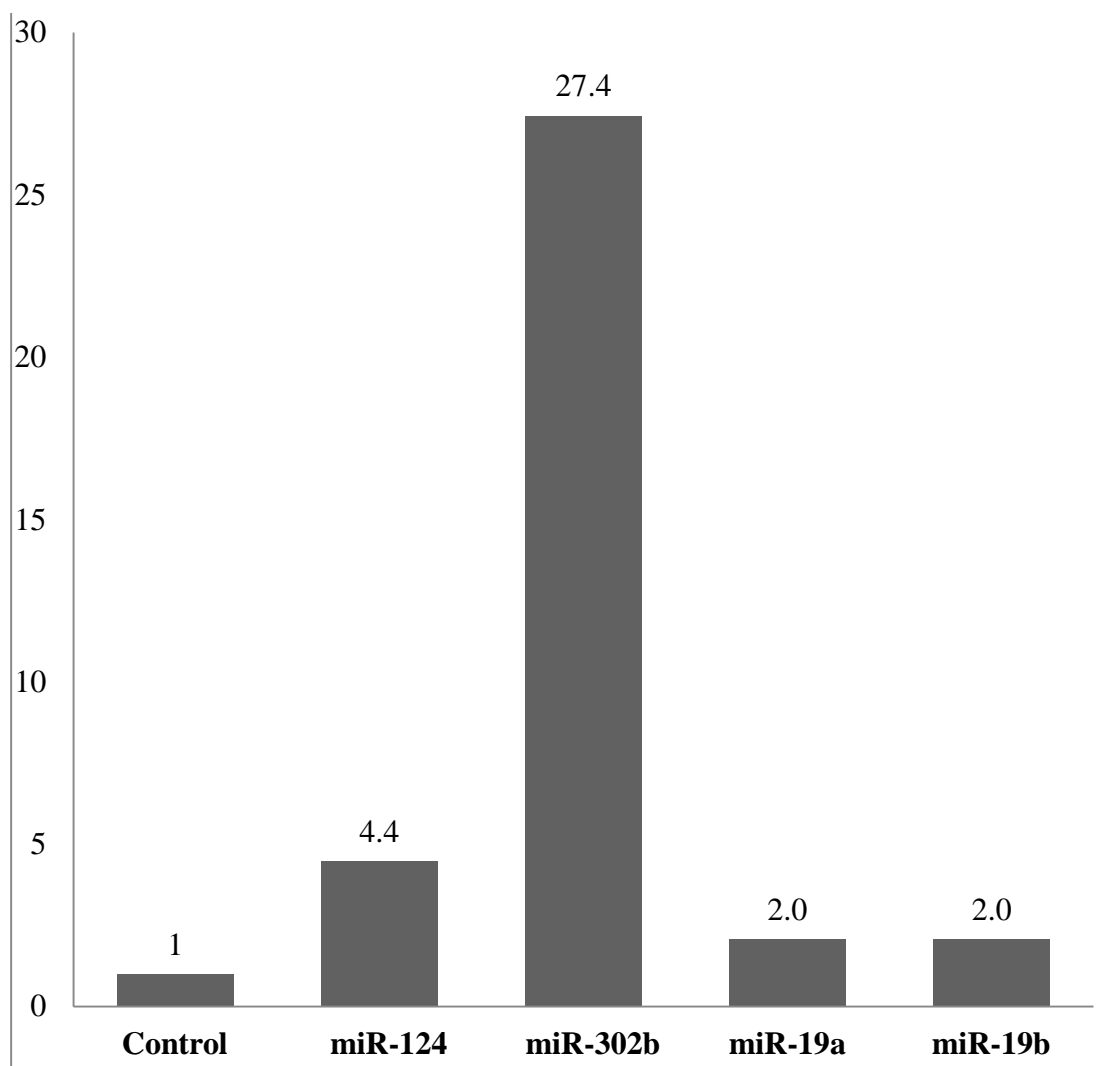


**Figure 42. The validation of the weight loss effects on miR expression by qPCR**

The expression of all the miRs were upregulated, but only miR-302b was statistically significant.

<b>Mature ID</b>	<b>Fold Change</b>	<b>95% CI</b>	<b>P value</b>
miR-124	4.5	( 0.00001, 11.27 )	0.006
miR-302b	27.4	( 0.00001, 243.86 )	0.005
miR-19a	2.1	( 0.00001, 5.43 )	0.03
miR-19b	2.1	( 0.00001, 5.53 )	0.03
miR-9	40861.9	( 0.00001, 339677.21 )	0.02

**Table 16. Validation of 5 miRs after weight loss**

Showed the fold change and p-value; miR-302b was highly and significantly expressed

## 4.6 Discussion

### 4.6.1 Downregulation of miR expression in PBCs of PO compared to MHO

In order to look at the differences in miR expression between PO (insulin resistant/hyperinsulinaemic) and MHO (insulin sensitive/normoinsulinaemic) subjects, two approaches were taken. Firstly, the use of PCR-based inflammatory pathway specific arrays in PBCs and adipose tissue components from these patients. These data were then analysed using two different software (SA Biosciences and QCRI). Secondly, by small RNA sequencing. While the arrays offer a sensitive method for identification of known miRNAs, the miRNA profiling via next-generation sequencing technologies can be used to identify both novel and known miRNAs.

The array data showed, in the PBCs, significant differences between MHO and PO in 12 miRs (miR-142, miR-16, miR-185, miR-24, miR-15, miR-28, miR-29b, miR-19b, miR-374a, miR-195, miR-130a and miR-144; SABiosciences). Three of these were confirmed by both softwares, miR-29b, miR-144 and miR-374a, which were all downregulated in PO, compared to MHO.

The expression of the majority of these inflammatory miRs was positively correlated with the systemic markers of inflammation (MCP-1 and CRP). In addition three miRs were also significantly associated with hyperinsulinaemia and HOMA index of IR, miR-122, miR-200 and miR-302.

Overall, miR-29 (either a or b) was the most consistent finding among these miRs and its targets were investigated using both predictive software and experimentally. The miR-29 family consists of three members expressed from two bicistronic miR clusters. MiR-29b-1 is coexpressed with miR-29a, whereas the second copy of miR-29b (miR-29b-2) is coexpressed with miR-29c. All family members share a conserved seed region and miR-29a and miR-29c differ by only one base from the miR-29b sequence.

Two important pathways that are regulated by miR-29 have a bearing on the pathological obesity scenario and may explain the greater susceptibility to disease in these subjects. Firstly, miR-29a has negative effects on some of the steps in the insulin-signaling pathway. This indicates that abnormal regulation of miR-29a could be part of the etiology of T2DM. Some miRs are tissue specific (Lagos-Quintana et al. 2002), however, miR-29 is present in many different tissues. He et al. were the first to report differences in miR-29 expression in the liver, skeletal muscle and adipose tissue of patients with T2DM, compared to tissues of non-diabetic subjects (He et al. 2007). Up-regulation of miR-29a, 29b and 29c were observed in adipose tissue and liver, but the difference was most profound in the skeletal muscle tissue (He et al. 2007; Figure 43).

Secondly, several of the collagens, which are miR-29 targets, were shown to be up-regulated in the PO samples (in whom miR-29 is down regulated), compared to the MHO, suggesting the involvement of fibrosis as part of the pathology. The effect of down regulation of miR-29b on fibrosis has been previously reported and appears to related to the overexpression of some of the collagen genes, eg COL1A, COL3A and FBN (Fibrilin). Therefore, downregulation of miR-29 would increase the gene expression of mRNAs of collagens and increase the fibrosis. Conversely upregulation of miR-29 is associated with decreased fibrosis.

Expression of miR-29 has been shown to play a major role in the regulation of cardiac fibrosis and may be used as a therapeutic target in the future. TGF- $\beta$ , a major regulator of cardiac fibrosis (Border et al. 1994), can repress miR-29 expression. Because of its role in fibrosis, there have been numerous efforts to therapeutically target TGF- $\beta$ , but the problem is that it is involved in mediating other functions, such as the immune response, and therefore likely to have major adverse consequences. In addition to miR-29 other miRs also regulate fibrogenetic events in various tissues, such as the liver, with

expression levels corresponding to those in the circulation (Figure 44).

In response to obesity-induced molecular and environmental signals, miRs in adipose tissue were strongly dysregulated, for example various miR-29 isoforms were induced in the tissue by hyperglycemia and hyperinsulinaemia (Herrera et al. 2010).

Interestingly, miR-29a and 29b both were lower in PO group and correlated positively with insulin (especially miR-29b) and other inflammatory miRs. Their targets were confirmed as being the collagen genes and MCL1.

miR-29 is one of the several miRs associated with inflammatory microvesicles. The up-regulation of miR-29a, b and c in non-obese diabetic mice caused pancreatic  $\beta$ -cell death via suppression of the myeloid cell leukemia-1 (MCL-1) gene, an essential member of the pro-survival BCL-2 family genes, and marked the first stage of type 1 DM (T1DM) (Roggli et al. 2012). Therefore, the miR-29-MCL-1 axis is a major contributor to pancreatic dysfunction in T1DM. Recent studies have highlighted the importance of MCL-1, where its deletion leads to cardiomyocyte disorganization, fibrosis, inflammation, and lethal heart failure (Wang et al. 2013; Thomas et al. 2013).

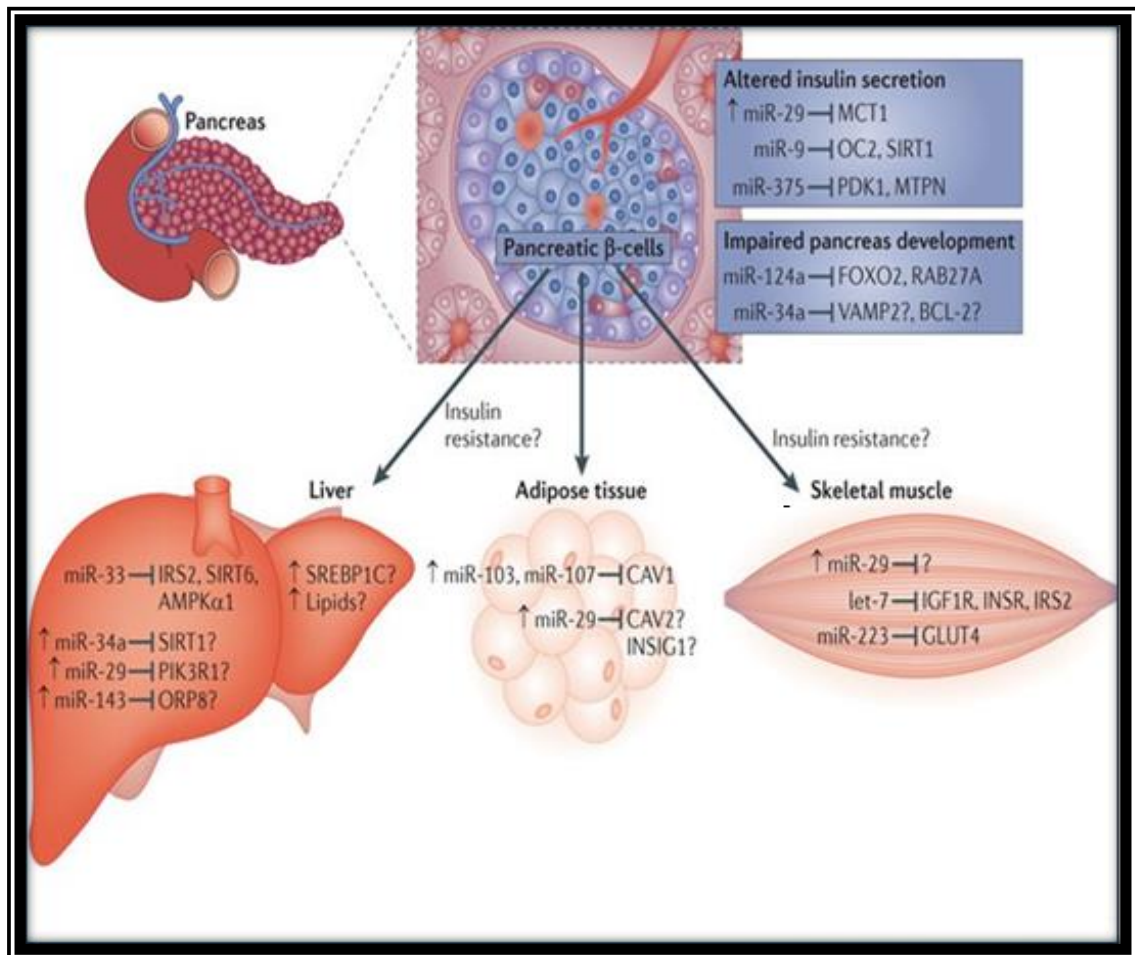


**Figure 43. The role of miR-29 in insulin responsive tissues**

Adipose tissue, liver and skeletal muscle mediate insulin signalling and glucose homeostasis (Rottlers et al, 2012).



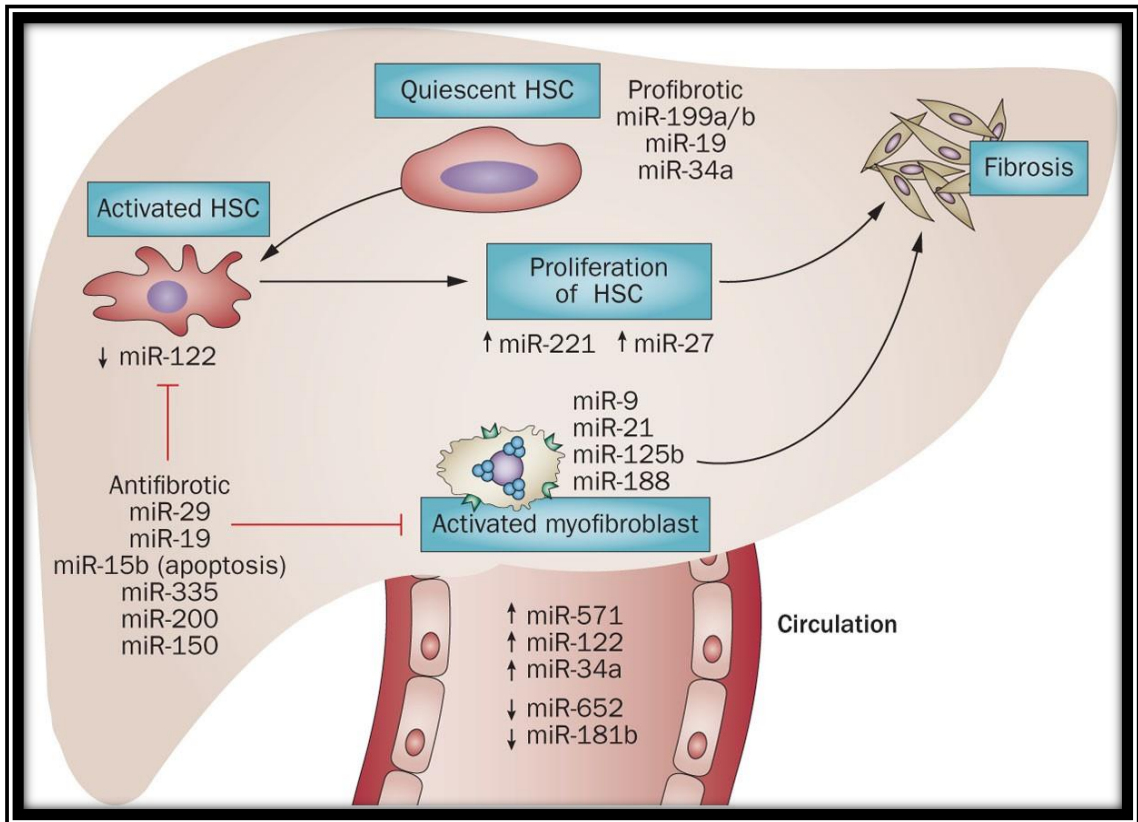


**Figure 44. Hepatic fibrosis associated with dysregulation of systemic miRNAs**

MiRs can be profibrotic (miR-199a/b, miR-19 or miR-34) and antifibrotic (such as miR-29, miR-19 and miR-150). (Szabo et al. 2013).

Another interesting finding was that of miR-374a downregulation in the PO, a miR that is known to target 35 genes. The Target Scan Software suggested that miR-374a was the most abundant gene and significantly downregulated, with a fold change of 103, INHBB, which is involved in the TGF- $\beta$  signaling pathway (Pan et al. 2006, 2013) and its downregulation could inhibit adipogenesis and differentiation in PO.

MiR-19b was another miR that was downregulated in the PO group. It is reported to play a major role in controlling inflammation and release of inflammatory cytokines, such as IL-5, IL-8, IL-10 and TNF- $\alpha$ , through its action on NF $\kappa$ B signalling (Gantier et al. 2012; Li et al. 2002). TNF- $\alpha$  release from adipocytes may impair pre-adipocyte differentiation in obese subjects and hence contribute to lipid deposition in liver and skeletal muscle (Gustafson et al. 2009). Release of inflammatory cytokines from adipose tissue also attracts macrophages to adipose tissue, while also increasing IR in other peripheral tissues (Rosen et al. 2006).

miR-122, and miR-144 are other miRs that were significantly associated with hyperinsulinaemia and down regulated in the PO respectively. They both may function through modulating IRS-1. IRS-1 is a protein downstream of insulin receptor that plays a significant role in insulin signaling and action, to mediate glucose uptake in fat cells. IRS1 is a direct target of miR-144. Thus, the control of miR-144 expression may be a potential therapeutic target for T2DM patients, deserving further studies (Karolina et al. 2011).

#### **4.6.2 miR expression in AT of PO compared to MHO**

Using the QCRI analytical tool, compared to MHO, the PO OM adipose tissue showed reduction in the expression of 7 miRs, but only miR-15 was also seen in PBCs. In the PO SC adipose tissue 2 miRs were down-regulated, miR-29a and miR-142.

The miR-29b was expressed and downregulated in the PO subcutaneous adipose tissue, compared to that of MHO, similar to the blood. However, it was not expressed in the omental. This depot specific difference in the expression of miR-29 may have a role in protecting the OM depots from fibrosis.

In SC adipose tissue both miR-29 and miR-142 were down regulated in PO compared to MHO, while in OM adipocytes other miRs (miR-101, miR-15a, miR376c, miR-424, miR-27, miR-20a) along with miR-142 were down regulated. Many of these miRs target adipogenesis as well as insulin secretion. This is linked to the fact that obesity is characterized of both hypertrophy (enlargement of the existing adipocytes) and hyperplasia (adipogenesis or adipocyte differentiation). It is also important to point out that miRs that were induced during adipogenesis, were repressed during obesity development (Xie et al, 2009; Figure 22). The miR-142-5p-regulated gene, BMP-4, is involved in adipogenesis regulation of the SC Adipocytes (Gimble et al, 1995).

The OM AD in PO has a lower expression of miR-27, miR-376c and miR-15. These results were consistent with a previous report showing that miR-27a is a negative regulator of adipocyte differentiation via suppressing PPAR $\gamma$  expression (Kim et al. 2010). Together, these results suggested that miR-27a could suppress adipocyte differentiation through targeting PPAR $\gamma$  (Kim et al. 2010). Interestingly, mature adipocytes of obese mice expressed less miR-27a, compared to lean mice, perhaps indicating that miR-27a downregulation may be necessary for adipocyte hypertrophy (Kim et al, 2010). Overexpression of miR-27b was found to suppress differentiation by targeting a predicted miR-27 binding site on PPAR $\gamma$  mRNA, inhibiting expression of PPAR $\gamma$  and downstream factor C/EBP $\alpha$  (Karbiener, et al).

miR-15a appeared to reduce pre-adipocyte size while promoting adipocyte proliferation. In preadipocytes miR-15a had been shown to target Delta homologue 1 (DLK1) at both

the mRNA and protein levels. Inhibition of miR-15a in pre-adipocytes resulted in a decrease in cell size along with an increase in cell number (Andersen et al. 2010). Differentiation and the concomitant reduction of lipid storage capacity may lead to ectopic fat deposition in the liver and skeletal muscle with detrimental side-effects, such as insulin resistance or steatosis (Rosen et al. 2006).

All miRs that were downregulated in the OM depots showed their effects on the target of genes required for the adipocyte differentiation (miR-27, miR-15), and insulin sensitivity (miR-142).

The validation in PBCs, using qPCR, of 9 selected miRs confirmed the down regulation of these miRs in the PO compared to the MHO before and after the weight loss. On the other hand the validation was not successful in adipose tissue which could be related to RNA degradation in the tissue, accounting for the poor results. The protocol has since been revised and improved, but patient numbers have to be boosted again in order to validate the findings to the tissue from both patient groups.

#### **4.6.3 miR NGS results**

The small RNA seq data showed changes in lots of miRs. However, it confirmed the downregulation of miR-27b, miR-29a, miR-144 and miR-3607 in the PO, implications of which have been discussed above. In addition it also showed upregulation of several miRs in the PO compared to the MHO, especially those of miR-181, miR-29b and miR-30e. miR-181b serves as a potent regulator of downstream NF- $\kappa$ B signaling in the vascular endothelium by targeting importin- $\alpha$ 3, a protein that is required for nuclear translocation of NF- $\kappa$ B (Sun et al. 2012). Overexpression of miR-181b inhibited importin- $\alpha$ 3 expression and an enriched in a set of NF- $\kappa$ B-responsive genes, such as adhesion molecules VCAM-1 and E-selectin in ECs in vitro and in vivo.

MiR-181a was first recognized as a contributor to hematopoietic lineage commitment and

differentiation (Chen et al. 2004). It appears to be an intrinsic modulator of T cell sensitivity and selection. Later studies revealed that increased miR-181a activity in primary embryonic lymphatic ECs resulted in substantially reduced levels of Prox1 mRNA and protein and, consequently, regulated vascular development and neo-lymphangiogenesis. Altered expression levels of both miR-181a and miR-181b have been detected in multiple tumors and leukemia/ lymphoma (Kazenwadel et al. 2008).

In IGF-1-stimulated PC12 cells it appears to function via CREB1 to inhibit dendritic growth of cultured hippocampal neurons (Figure 45).

Interestingly, Pohl et al. reported that upregulation of miR 29b in idiopathic pulmonary arterial hypertension (IPAH) might be responsible for the inhibited K<sup>+</sup> channel expression and function and may therefore provide a new therapeutic target to treat these patients. miR-29b expression was elevated in both the PO sample (hypertensive) and the patients with T2DM, compared to MHO.

The miR-30 family acts in an anti-inflammatory manner in ECs by regulating the expression of the cell-cell adhesion molecules E-selectin, VCAM1 and ICAM1 in an Ang2-dependent manner. The up-regulation of the miR-30 family members may contribute to the atheroprotective effects of shear stress (Demolli et al. 2013), as well as participating in the regulation of insulin signaling and as a useful marker of diabetes progression (Karolina et al, 2011).

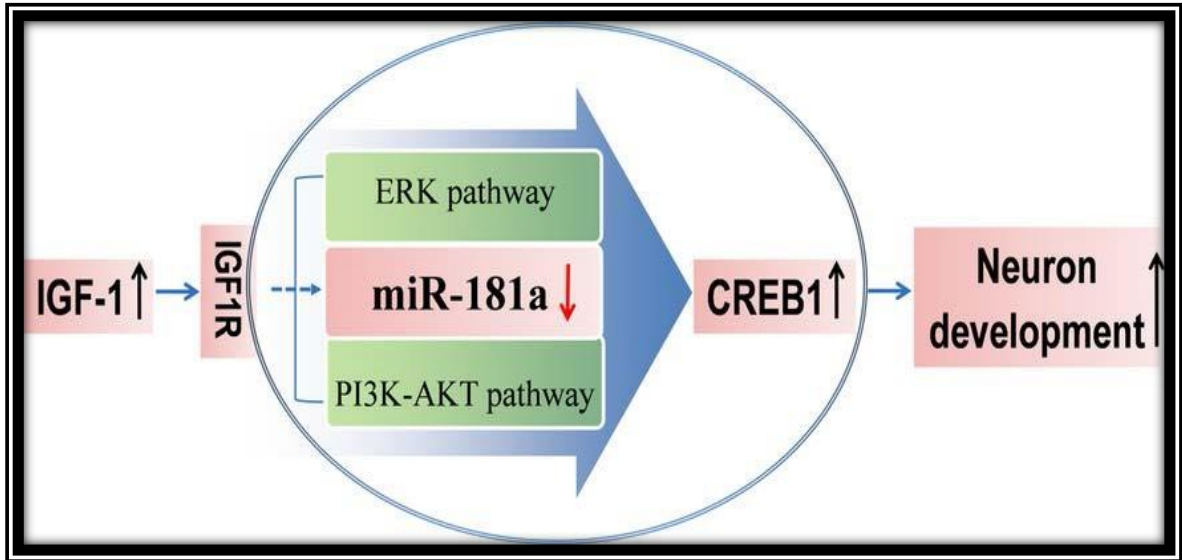


**Figure 45. The role of miR-181a in neural development**

miR-181a targets the mRNA of the IGF-1- regulated CREB1 expression.

#### **4.6.4 Changes in miR expression on weight loss**

Gastric bypass surgery is the most commonly performed bariatric surgical procedure and an effective approach for achieving sustained weight loss in obese patients, along with reducing insulin, leptin levels and other cardiovascular risk factors. The levels of many of these cardiovascular risk factors are determined by some of the miRs identified in this project. Thus, the miRs that were found to be down regulated in the PO, compared to the MHO might be attractive candidates for the study of the regulation of cell fate and obesity-related complications. Peripheral blood miRs are useful biomarkers for both the diagnosis and prognosis of systemic diseases. A significant modulation of nine circulating miRs was shown upon surgery-induced weight loss, as evidenced by the marked upregulation of miR-9, miR39, miR302b, miR200c, miR141, miR124, miR376c, miR302a, miR302c. Only one showed a down regulation, miR-26b. In the PO group, miR-122 especially was significantly downregulated, compared to the MHO and its expression was upregulated after weight loss. However, weight loss had no effect on the expression of miR-29, suggesting that the changes induced by the miR and its targets may be less reversible.

#### **4.6.5 Conclusions**

The relationship between obesity and diabetes was strongly related to glucose and lipid metabolism. miRs have been shown to regulate the activity of key cellular processes, including insulin release in pancreatic  $\beta$  cells and differentiation of adipocytes and are therefore thought to contribute to these pathologies. A consistent observation in obese patients and experimental models of obesity was that the miRs normally induced during adipogenesis were downregulated in the obese subjects. (Xie et al 2009). It was apparent that significant differences in expression of the miR species occurred along with changes in metabolic and inflammatory parameters between the groups studied. Elevated

production of collagens may be related to excess fibrosis, which caused a barrier around the adipocytes resulting in heterogeneity of adipocyte size and pockets where there is adipocyte hypertrophy, leading to higher production of leptin and inflammatory cytokines, as well as ROS production. This is a scenario that would lead to progression of IR, vascular dysfunction and inflammation.

There was a positive correlation between the inflammatory miRs and the inflammatory biomarkers, such as MCP-1 and CRP. These studies uncovered miR-29, miR-144 and miR-374 as important contenders for a pathological obesity (PO) miR signature, along with miR122, miR302, miR200, which were associated with hyperinsulinaemia and insulin resistance.

Nonetheless, further investigations using animal models as well as more human samples have to be carried out to validate these findings and to further elucidate the mechanisms of miR regulatory network. The changes that were found in the PO sample could have both diagnostic and therapeutic potential.

**Power calculation:** Data on the expression of certain miRs in the PBCs (using the statistical analysis provided by QCRI) showed significant down regulation, especially in mir-29b. The mean difference in its expression between PO compared to MHO was 0.44 (SD 0.22). With 10 MHO and 14 PO subjects the study is powered to detect difference at the 80% level. Therefore the study using PBCs is sufficiently powered. Despite miR-29 following a very similar pattern of expression in adipose tissue these studies had much lower numbers of samples from the two groups (i.e; MHO, n=1 and PO, n=4). In order to be sufficiently powered additional tissue (9 MHO and 6 PO) from both patient groups are currently being collected. Small RNA sequencing also needs to be powered adequately, currently 1 MHO and 1 PO have been sequenced.



**Chapter 5**

**The Whole**

**Transcriptome**

**Analysis**

## 5.1 Introduction

The simultaneous assessment of miRNA and mRNA expression profiles provides a powerful approach to identify groups of miRNAs whose expression levels are negatively coordinated with those of their target mRNAs. Microarrays have been used previously for jointly profiling and analysing miRNAs and mRNAs expression in brain cortex from Alzheimer's disease patients and age-matched controls (Nunez-Iglesias et al. 2010). These data allowed the study of the relationship between miRNA and mRNA expression in normal and affected tissue. The results showed a significant relationship between the levels of miRNAs and those of their targets in the brain. Co-expression analysis has also been reported elsewhere and recommended as a model for NGS procedures to help recognize true targets, confer functionality and identify miR signatures for diseases (Zhang et al.2011; Gennarino et al. 2012).

This approach has not been used previously when considering insulin resistance in obesity. Measurement of miRs and mRNA in PBCs and components of adipose tissue from normoinsulinaemic and hyperinsulinaemic obese, euglycaemic patients would allow for these targets to be elucidated in the different fat depots, as well as in their cellular constituents (SVF and adipocytes) and further to relate these to systemic cells (PBCs). A recent study reported omental and subcutaneous adipose tissue to have unique miR expression profiles (Klötting et al, 2009). Similarly studies reported differences in gene expression between subcutaneous and visceral/omental fat depots, accounting for increased production of inflammatory cytokines from omental depots (Rosen et al, 2006), which is also less adipogenic and more insulin resistant. Details of the miRs related to these various pathways and a limited study of their targets was done (chapter 4), specifically uncovering a signature that included miR-29, miR-144, miR-374, miR- 122, miR-302, miR-200. Their targets were then validated using NGS platforms.

## 5.2 Aims

1. Confirm, in the whole transcriptome, targets for the specific miRs.
2. Validate, in the whole transcriptome, targets for the specific miRs.
3. Compare expression of target genes in different depots (SVF and AD) and PBCs.
4. Using the data from whole transcriptome to assign functionality.

Methods were provided in Chapter 2.

### 5.3 NGS target genes in the blood

In order to confirm, in the whole transcriptome, targets for the specific miRs, mRNA expression was assessed by transcriptome analysis. For the majority of samples the Ion Proton platform was used for NGS. In a small subset of PBCs (n=4 patients) both microarrays and Ion Proton NGS was carried out.

#### 5.3.1 Sample selection and data analysis

Forty three samples (see Table 17) were sequenced using the Ion Proton. Details of the methods were described in Chapter 2.

	PBCs	OM SVF	OM Adips	SC SVF	SC Adips
MHO	7	2	2	2	2
PO	17	2	2	2	2
T2DM	3	-	-	-	-

**Table 17. Details of the samples used for sequencing studies** Two MHO and two PO patients had an entire complement of samples.

After filtering, dataset description (raw data, FASTQ) was used to analyse 6 MHO samples and 12 PO samples matched for age and sex, in addition to BMI. The T2DM data was not used for any further analyses.

To perform differential expression analysis, FASTQ files were processed following these steps:

1. Sequence quality check using FastQC
2. Two steps alignment of reads to human reference genome (GRCh37/hg19) using both TopHat2 and Bowtie2.
3. Counting of reads for each gene using count Overlaps function of Bioconductor package GenomicRanges

#### 4. Gene expression analysis using Bioconductor package edgeR.

In the step 1, quality control for some samples (n=4) resulted in very low coverage sequencing and they were excluded from the downstream analysis.

In the step 2, the short sequence reads contained in FASTQ file were mapped to the reference genome using the algorithm TopHat2: the reads were either aligned or un-aligned in this process. The un-aligned reads were then mapped with another algorithm *Bowtie2*. The output files (BAM format) from these two alignment processes were then merged to generate final aligned BAM for further downstream analysis.

The output produced in the step 3 is a count table with genes as rows and samples as columns, in which each cell is an integer that indicates how many reads in the sample overlap with the respective gene. These counts were then normalized for different library sizes and to account for sample-specific effects (using edgeR TMM method). The resulting normalized-count table was examined (RNAseq\_norm.counts.txt).

In the step 4, differential expression was determined using negative binomial exact test, and significant PO vs. MHO differentially expressed genes were selected:

Absolute  $\log_2$  (Fold Change)  $\geq 1$ , and corrected p-Value (FDR)  $\leq 0.05$

## 5.4 Results

### 5.4.1 NGS of PBCs using Ion Proton platform

Significant changes in 1448 mRNA were recorded, of which 133 were upregulated and 1315 down regulated in the PO compared to the MHO samples.

Keeping in mind the miR signature uncovered for the PO (miR-29, miR-144, miR-374, miR-122, miR-302, miR-200) these data were probed for their targets.

Specifically gene expression in PBCs from PO and MHO revealed significant disparity in components of the pathways leading to IR, inflammation and fibrosis (Table 18).

<b>Downregulation</b>	<b>miR target/ Functions</b>
Collagens COL26A1, COL3A1	miR-29 controlled by TGF- $\beta$ signalling pathway. Alteration of Col3A1 gene expression under hyperglycaemic and hyperinsulinaemic conditions, leads to fibrosis.
INHBB	MiR-374a plays a physiological role in energy balance or the insulin insensitivity associated with obesity. Controlled by TGF $\beta$
IGFBP5	IGFBP-5 is a direct or indirect target for Stat3 and its upregulation is essential to normal involution. It is targeted by miR-4731 (Adipose tissue)
<b>Upregulation</b>	<b>miR target/ Functions</b>
Notch	miR-200c blocks Notch signalling (Data showed positive correlation between insulin and miR200). Inhibition of Notch signaling ameliorates insulin resistance.(Kitamura et al 2007)
Akt2	miR-29 mediates TGF- $\beta$ 1-induced extracellular matrix synthesis through activation of PI3K-AKT pathway. It blocks the glucose and insulin signaling pathways.
DKK2 and DKK3	DKK1 is a direct target of miR-29a, leading to negative regulation of Wnt signalling. MiR-376c targets DKK2.
SMAD2	miR-29 is negatively regulated by TGF- $\beta$ /Smad signaling in fibrosis.
MCL1	miR-29 regulates MCL-1 protein expression and apoptosis.
SEC14L1	Reduce the Choline transport that has been shown to cause a fatty liver or muscle damage. Fischer et al 2007.
CARD8	Proinflammatory, Dysregulation is associated with a susceptibility to rheumatoid arthritis.

**Table 18. PBCs target gene expression, miRs and affected function in PO**

#### 5.4.2 The dysregulation of the target genes in whole adipose tissues

In the PO adipose tissue the modulated targets, along with their function and the regulatory miR species is shown, compared to MHO (Table 19).

Similar to results from the PBCs the collagen genes, IRS genes and INHBB were downregulated. In addition, upregulation of NOTCH and SMAD, involved in fibrosis and vascular dysfunction and IR, were also evident.

<b>Downregulation</b>	<b>miR target/ Functions</b>
Collagens (COL1,COL4,COL5, COL6,COL12	MiR-29 controlled by TGF- $\beta$ signalling pathway. Alteration of Collagen gene expression under hyperglycaemic and hyperinsulinaemic conditions, leads to fibrosis.
IRS1and IRS2.	IR.
PCDH18	The target of miR-144 plays a role in the establishment and function of specific cell-cell connections in the brain. (RefSeq, Jul 2008).
INHBB	The target of miR-374a, controlled by TGF- $\beta$
<b>Upregulation</b>	<b>miR target/ Functions</b>
NOTCH signalling: NOTCH2, NOTCH2NL	miR-200c blocks Notch signalling (Data showed positive correlation between insulin and miR-200). Inhibition of Notch signaling ameliorates insulin resistance.
Smad1, smad 6, and smad 7	miR-29 is negatively regulated by TGF- $\beta$ /Smad signalling in fibrosis.

**Table 19. NGS target genes in the AD of PO compared to MHO**

#### 5.4.3 The dysregulation of the target genes in the SVF and Adipocytes of PO

In addition to the miRs found previously using the pathway specific approach other miR species were found in the SVF and AD, and their main reported targets in the different depots (SC and OM; Table 20).

<b>Downregulation of genes in the SVF of PO SC versus OM</b>	COL3A1, ASS1P1, ASS1P7 and ASS1P11 (Arginine), miR-1245A, miR-663B (it has a role in Myocardial infarction, Peng et al 2014)
<b>Downregulation of genes in the AD of PO SC versus OM</b>	COL3A1, ASS1P1, ASS1P7 and ASS1P11 (Arginine) MiR-4731.

**Table 20. Depot specific downregulated genes in PO, SVF and AD**

Further analysis was carried out to look at the blood, AD and SVF from PO samples, as well as comparing differences in mRNA expression in SVF of PO compared to MHO (Table 21).

<b>Diff Expr AD versus blood in PO:</b>	Upregulation: LCP2 target of miR-142. Downregulation: COL12A1, FBN1, PPAR $\gamma$ .
<b>Diff Expr SVF versus blood in PO</b>	Downregulation: COL12A1, FBN1, PPAR $\gamma$ .
<b>Diff Expr SVF PO versus MHO</b>	Downregulation: SLCO5A1; NOTCH2, COL11A2, INTS4 (integrator complex subunit 4), DKK2, WNT7A, and PPRG.

**Table 21. mRNA target in the adipose tissue components compared to PBCs**

AD and SVF was compared to PBCs. Also in the SVF, the PO were compared to MHO.



## 5.5 Validation of the NGS samples using the SurePrint G3 Human gene expression

### Microarrays

Microarrays expression was used to compare between two sets of samples PO (n=2) and MHO (n=2), in duplicate. Overall, the results showed that 1567 target genes were downregulated and 922 genes were upregulated, in the PO compared to MHO (Figure 46 and Table 22).

Samples hybridize	Replicates	Analysis Plan	<u>Summary of Differentially Regulated Genes PO/MHO (n=4, 2 per group)</u>	
			Up	Down
MHO-102	Technical replicates	Control	922	1567
MHO-102_R				
MHO-128	Technical replicates			
MHO-128_R				
PO-122	Technical replicates	Treated	922	1567
PO-122_R				
PO-48	Technical replicates			
PO-48_R				

**Table 22. The summary of differentially regulated genes in PO compared to MHO**

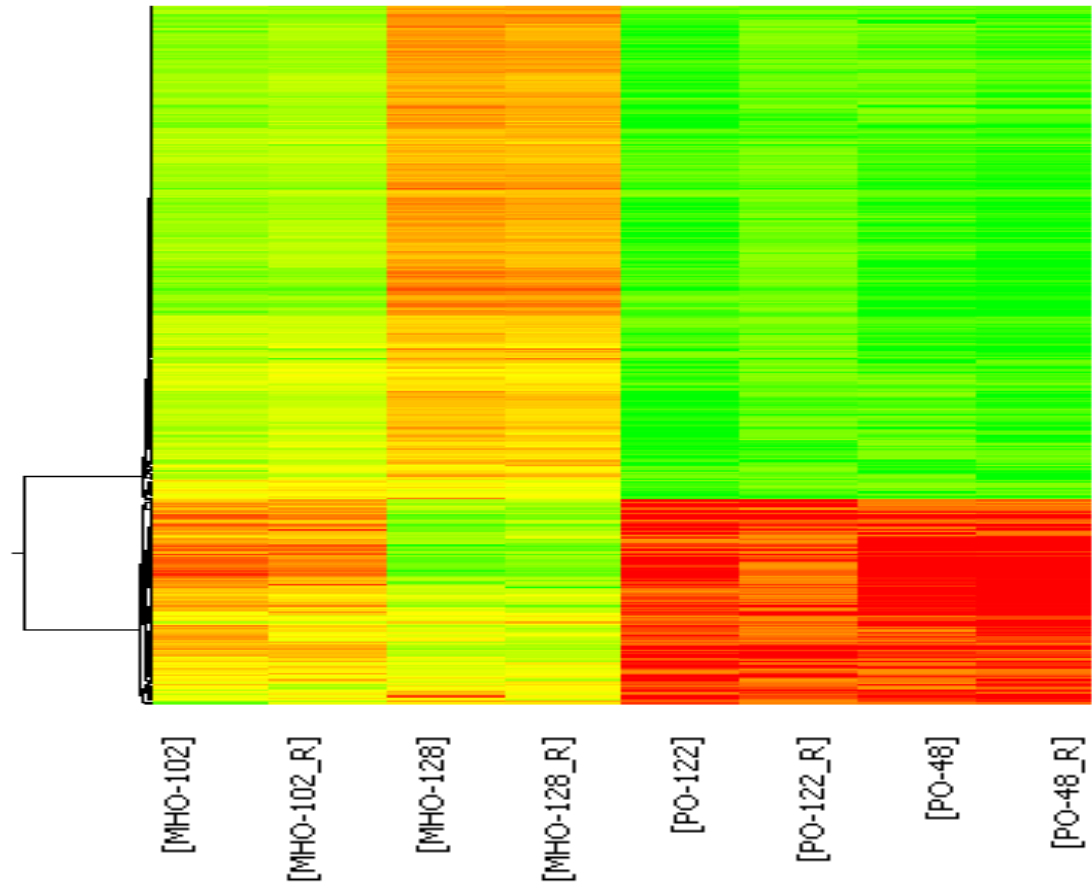


**Figure 46. The cluster map showing variability in gene expression.** Samples included PO (n=2) and MHO (n=2). The replication was done as a test of technical reproducibility. From the cluster map it is apparent that there was greater heterogeneity in the gene expression pattern in the MHO (control) samples compared to the PO.

### 5.5.1 The upregulation of pathways in PO

The Pie chart reveals the participation of the various gene changes in pathways upregulated in PO compared to MHO in the blood and their possible contribution to elevation in insulin signalling and inflammation, hence reflecting IR of PO phenotypes (Figure 47).

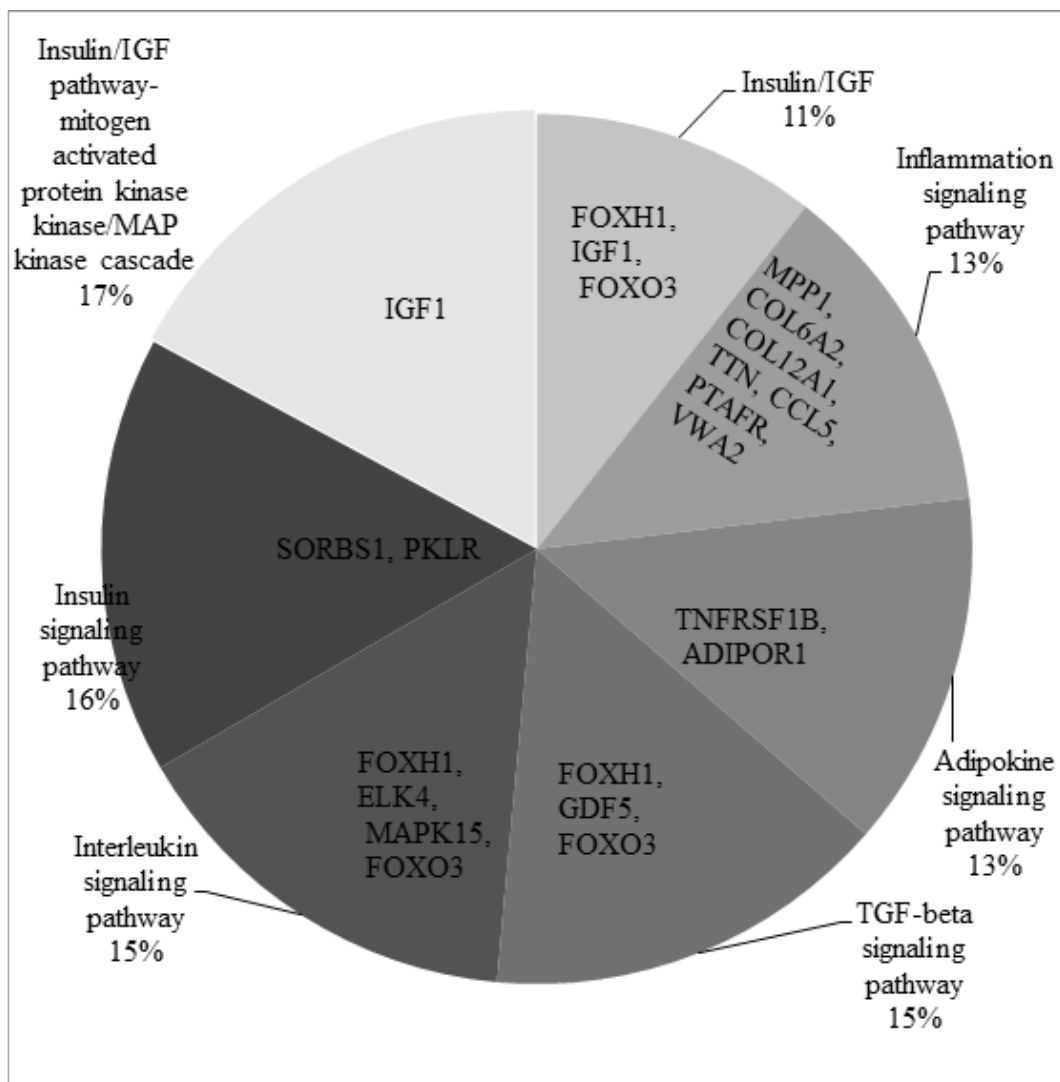


**Figure 47.** The results showed the up-regulation in PO (n=2) versus MHO (n=2)

Many pathways were involved in different diseases. The pie chart suggested upregulation of insulin signalling and inflammation.

### 5.5.2 The upregulated mRNA in specific tissues

Further analyses were carried out to look at the contribution of the mRNA in different tissues. COL12A1, a target of miR-29 is apparent (Figure 48).

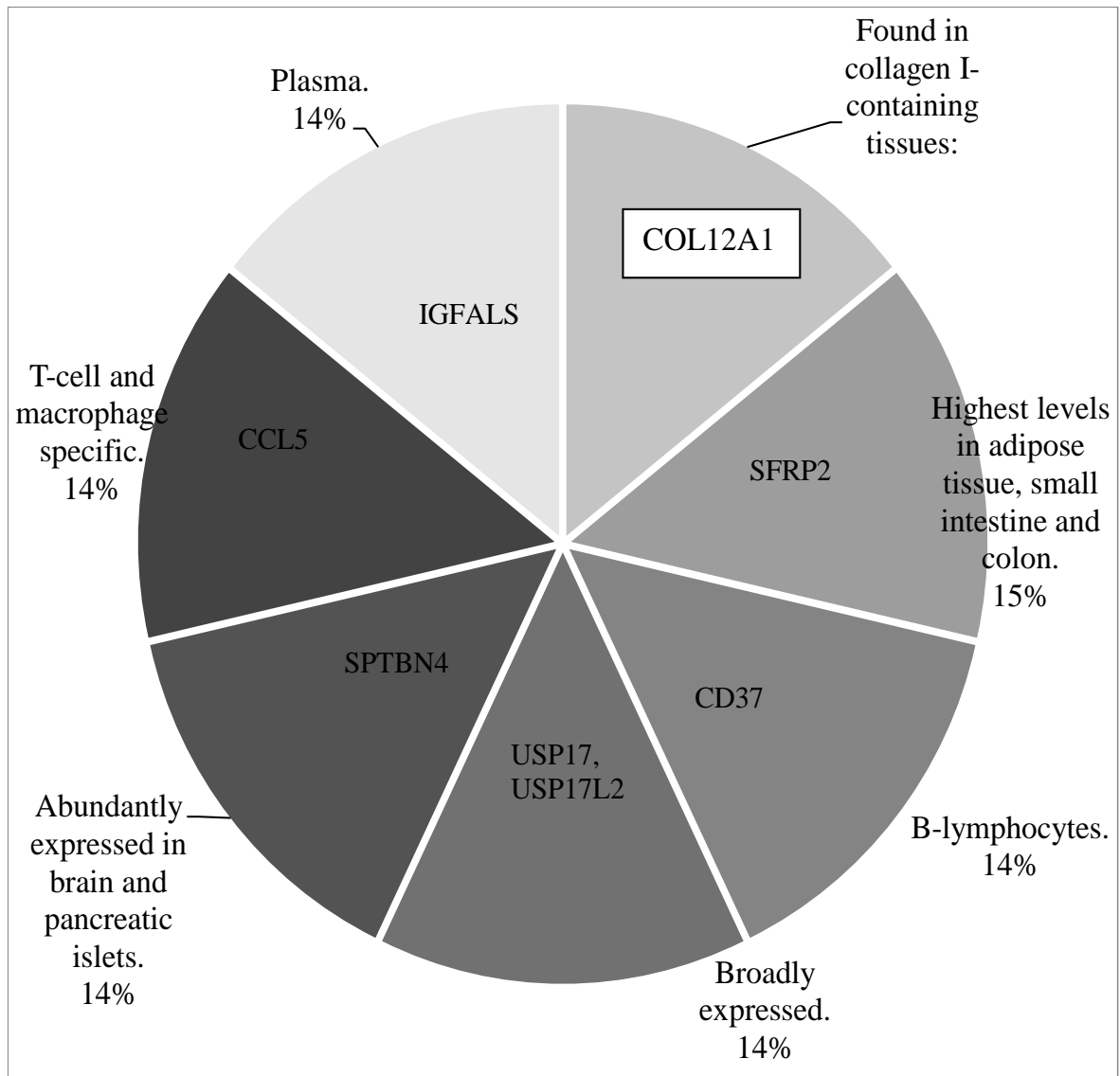


**Figure 48. Up-regulation of mRNAs implicated in insulin signaling and inflammation**

### 5.5.3 The role of certain target genes in signalling pathways

The implication of these gene changes in modulating key signalling pathways was also investigated.

### 5.5.4. The down regulation of pathways in PO

These pathways, especially those of Wnt, PPAR and TGF $\beta$ , all point to inflammation and insulin resistance being important lesions in the PO compared to MHO (Figure 49).

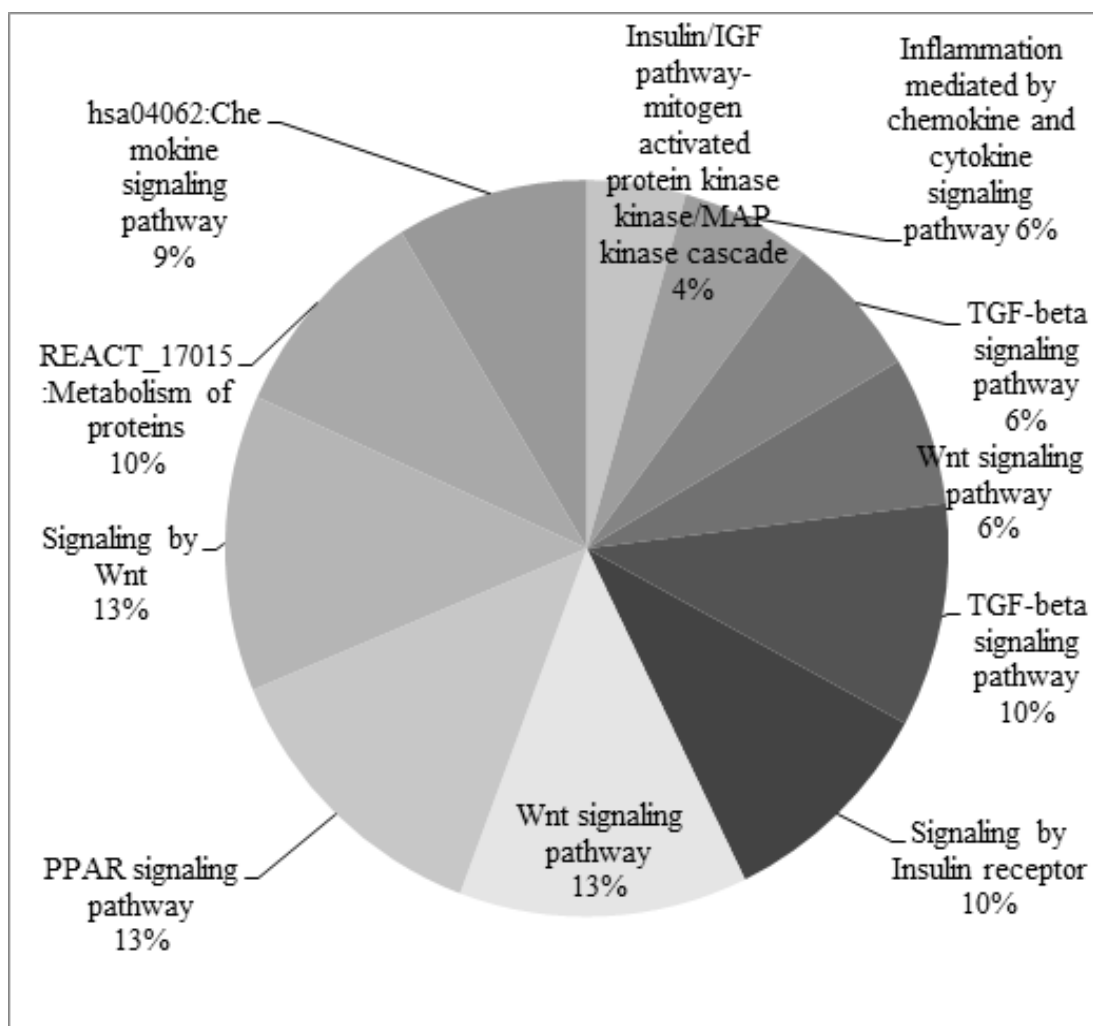


Figure 49. Down-regulation of key pathways of IR and inflammation

Several of the specific genes in these pathways are shown in Table 23.

<b>Term</b>	<b>P Value</b>	<b>Genes</b>
hsa04620:Toll-like receptor signaling pathway	0.109	IRAK4, MAP2K4, TLR1, TLR4, TRAF6, TLR6, TAB2, TLR7, CHUK, TLR8, SPP1
hsa04920:Adipokine signaling pathway	0.25	CD36, SOCS3, PRKAB2, JAK2, PRKAA1, CHUK, PTPN11
P00032:Insulin/IGF pathway-mitogen activated protein kinase kinase/MAP kinase cascade	0.34	RPS6KA3, SOS2, MAP2K4, RPS6KB1, MYO19
P00031:Inflammation mediated by chemokine and cytokine signaling pathway	0.44	ROCK1, PTGS2, SOCS3, CAMK2G, PRKCI, RHOQ, SOCS4, AKAP9, RGS18, ITGA4, ARPC5, ITPR1, PRKCB, PLA2G4A, ITGA6, CCR3, GNG10, SOS2, CCR2, NFAT5, JAK2
hsa04350:TGF-beta signaling pathway	0.48	EP300, ROCK1, ZFYVE16, RPS6KB1, SMAD1, MYC, ACVR1
hsa04310:Wnt signaling pathway	0.50	EP300, ROCK1, CAMK2G, NFAT5, PPP3CB, FRAT1, FZD1, FRAT2, MYC, PRKCB, CTNNB1
P00052:TGF-beta signaling pathway	0.75	EP300, RAB28, DCP1A, FOXN2, FKBP1A, SMAD1, FOXJ3, RAB10, ACVR1
REACT_498:Signaling by Insulin receptor	0.76	EIF4E, PDE3B, RPS6KB1
P00057:Wnt signaling pathway	0.991	SMARCAD1, PRKCI, FZD1, TLE4, SMAD1, ITPR1, PRKCB, CTNNB1, EP300, GNG10, PPP3CB, MYC, ACVR1
hsa03320:PPAR signaling pathway	1	CD36
REACT_11045:Signaling by Wnt	1	CTNNB1

**Table 23. The specific genes involved in diferent downregulated pathways**

### 5.5.5. The down regulation of genes in specific tissues

From the data analyses specific genes that were highly expressed in important insulin responsive tissues were revealed (Figure 50).

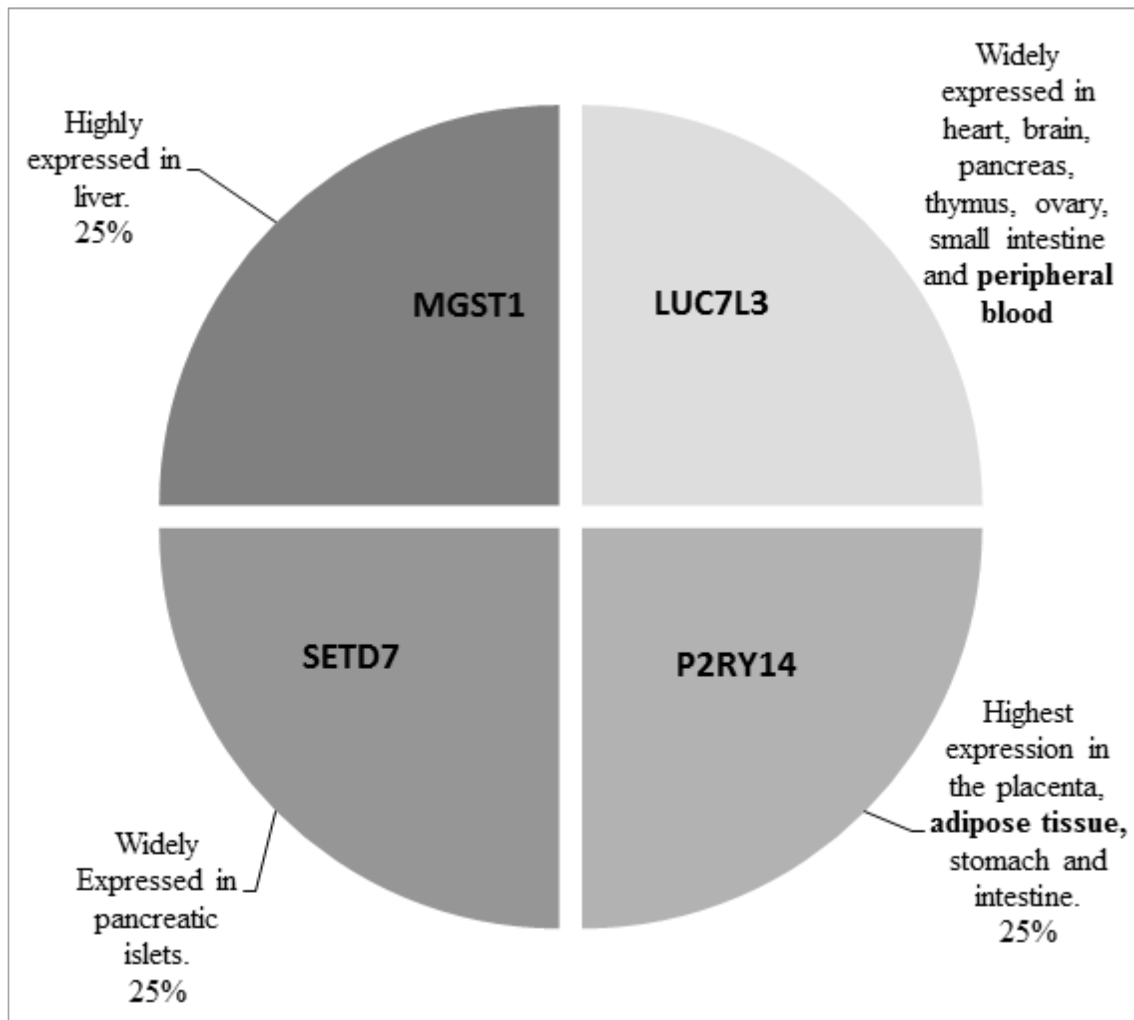


**Figure 50. Tissue specific downregulation of genes**

Many mRNAs were downregulated in different tissues.

## 5.6 Discussion

### 5.6.1 mRNA seq using the Ion Proton platform

NGS using the Ion Proton platform revealed dysregulation in specific genes like IRS, IGF, collagens, MCL1, SMAD and Notch. Notch acts as a major player in angiogenesis, whereas collagens (Col3A) MCL1 and SMAD were all involved in fibrosis. In addition to IGF and Akt2, IRS1, 2 and IRS4 were all involved in the insulin signaling pathway. Similar results were shown when validated by microarrays.

The miR-29 family targets a cadre of mRNAs that encode proteins involved in fibrosis, including multiple collagens, fibrillins, and elastin. Thus, down-regulation of miR-29 would be predicted to depress the expression of these mRNAs and enhance the fibrotic response. Indeed, downregulation of miR-29 with anti-miRs *in vitro* and *in vivo* induced the expression of collagens, whereas over-expression of miR-29 in fibroblasts reduces collagen expression. Furthermore, miR-29-MCL-1 axis is a major contributor to pancreatic dysfunction and T1DM. Recent studies have highlighted the importance of MCL-1 where the deletion of MCL-1 gene leads to cardiomyocyte disorganization, fibrosis, inflammation, and lethal heart failure (Wang et al and Thomas et al, 2013).

The results here also point to miR-29 as a regulator of fibrosis and a potential therapeutic target for tissue fibrosis in general.

The sequencing results showed a significant mediation of several of the targets of the components of the PO miR signature uncovered.

### 5.6.2 The validation of Ion Proton mRNA seq by microarrays

Validation of the NGS by microarrays using four peripheral blood samples, in duplicate, showed the difference between the two groups in the gene expression of the mRNAs that were down regulated in many pathways. Our focus here was on specific pathways that



were involved in the insulin and IGF pathway. IGF1 was initially considered purely as a circulating growth factor produced by the liver and mediating the effect of growth hormone on body growth. Several studies identified a number of miRs affecting IGF-1. Among them, miR-29 was shown to target 3' UTR of IGF-1 mRNA to suppress IGF-1 expression. (Kwiecinski et al,2012). Our study showed that in addition to Insulin/IGF pathway-protein kinase B signaling cascade, IGF-1 was involved in many pathways including hypertrophic cardiomyopathy (HCM), Diabetes pathway and cancers. Another gene that found downregulated was IRS1. It was reported that, insulin binding to IR activates phosphatidylinositol 3-kinase (PI3K)-protein kinase (Akt) pathway and disruption of which can lead to diabetes (Bouzakri et al; 2003).

The data showed that many of the genes that were the targets of the identified miRs (Chapter 4) involved in the metabolic pathway leading insulin resistance, inflammation and fibrosis were disrupted in the PO. All these processes have a major role in developing the pathological disorder in the PO which leads to greater susceptibility to T2DM and CVD.

Power calculations:

Targets of mir-29 done by the NGS: The power calculation used the differences in the expression of Col3A, based on data from the pilot study using next generation sequencing (n=6). In order to reach 80% CI, 4 more MHO samples and 2 more PO samples are required. The data analysis was done for 12 POs compared to 6 MHOs in PBCS. However, the number of samples from adipose tissues was too small for sufficient statistical power (n-2 PO compared to n-2 MHO). Although it was predictive for significant expression of the collagen genes this still needs to be confirmed in larger number of adipose tissue samples and then expression patterns compared to those in blood.

# **Chapter 6**

# **Discussion**

## **6.1 Introduction**

There is a significant global increase in the prevalence of obesity. Obesity and its associated co-morbidities have substantial healthcare and social costs. Prevention, especially of the obesity associated pathologies, comes from a better understanding of the different mechanisms involved, but it will also be important to help develop strategies to treat those already affected. Even relatively modest weight loss of 5-10% has been shown to reverse many of the comorbidities associated with obesity and to result in significant health gains, both in terms of risk factors and also in the amelioration of disease. However, in the face of the global epidemic of this disease, a clear ability to stratify obesity groups depending on varying disease risk would help to design and target therapy effectively.

## **6.2 Clinical Parameters**

Differences in gender, IR, ethnicity and weight loss were considered in an obese Arab (Qatari) population to help further group them by disease risk using clinical and systemic markers.

### **6.2.1 Comparison of cardiometabolic risk factors by gender**

Data showed that when subjects were stratified into two groups based on their gender (Chapter 3), as expected and already reported in other studies; females had higher leptin and adiponectin levels, probably associated with sex hormones in this relatively young cohort, compared to males. Arab men were more hyperinsulinaemic, were IR to a degree and had greater elevation in blood pressure, predisposing them to an increased risk for developing T2DM and CVD. As the population was young and the prevalence of obesity in males and females was not significantly different a factor that could underlie this difference may be associated to lifestyle. Smoking, and perhaps alcohol consumption, is

more prevalent in males in this population. No further analysis in terms of differences in miR signatures by gender was possible because of small numbers of males in the study.

### 6.2.2 Clinical parameters between MHO and PO groups

The PO group had higher insulin and HOMA-IR, lower adiponectin and, interestingly, lower leptin, compared to MHO (Chapter 3). The lower leptin in the PO, despite no difference in obesity, may suggest greater SNS activation directly inhibiting adipose leptin production. This points to perhaps a stress mediated phenomenon underlying the PO phenotype. This may be a consequence of the rapid changes in lifestyle in this population (Figure 51). In the PO there was also upregulation of the collagen genes, and possibly, generalised tissue fibrosis as a result. Furthermore the vascular dysfunction was increased pointing to the high blood pressure (Figure 51). SNS mediated decrease in leptin may also predispose them to hyperphagia and therefore obesity.

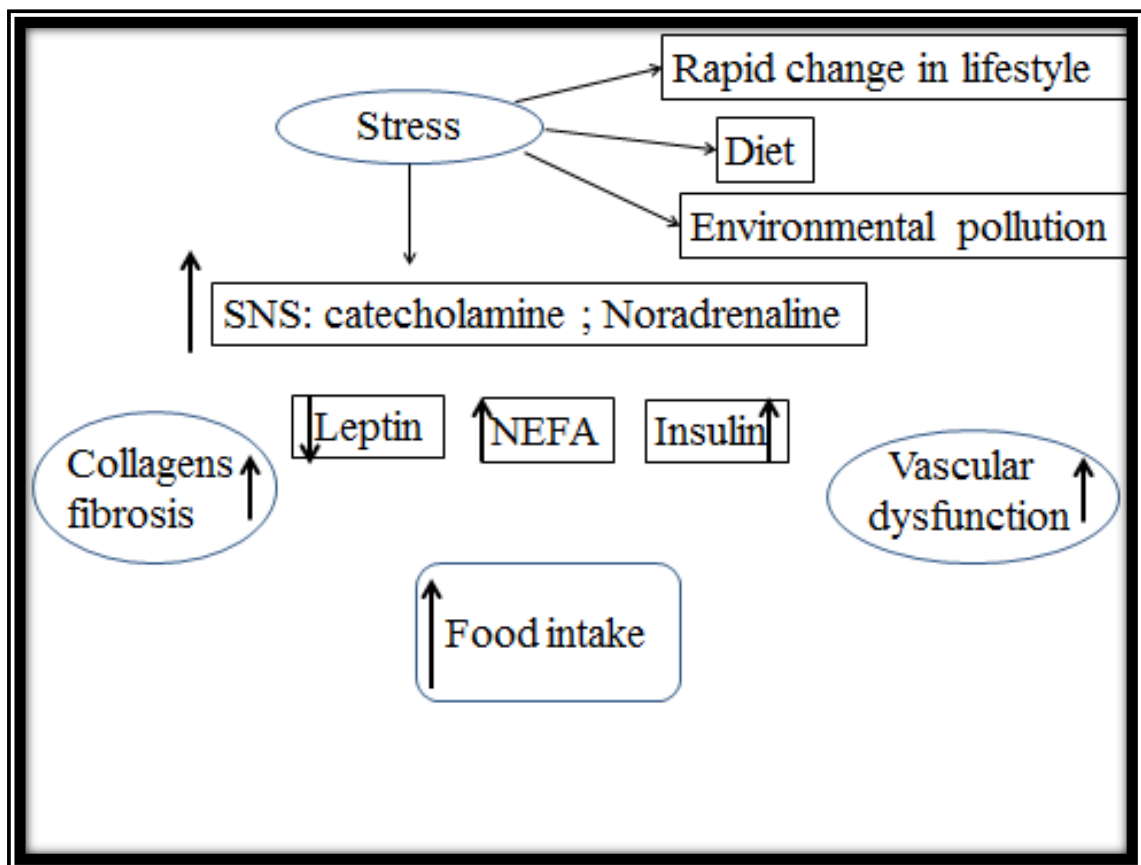


Figure 51. Effects of stress in developing IR, Fibrosis and Vascular dysfunction

The clinical differences between the two groups based on IR, the MHO and PO, have been highlighted in chapter 3. Further comparison of these phenotypes between two different ethnicities was then carried out. In the Arabs, despite being younger, hyperinsulinaemia/insulin resistance and inflammation were higher. The longer exposure to high levels of insulin in the presence of chronic inflammation, perhaps due to early/adolescent onset obesity may account for the greater prevalence of the associated diseases, such as T2DM and hypertension, in this population.

The outcome of the comparison between the two populations showed that MHO Caucasians had lower BP (SBP, DBP and MAP) and triglyceride in addition to insulin and HOMA compared to PO Caucasians. On the other hand, MHO Arabs had lower FBG, insulin and HOMA, in addition to the triglycerides, than PO Arabs. On the other hand Arab MHO had a higher systemic leptin level than PO group.

Obesity in Arab subjects was accompanied by greater degree of hyperinsulinaemia and hyperleptinaemia compared to Caucasians, suggesting elevated fat mass contribution to the BMI in Arabs. The lower prevalence of MHO in Arabs also reflects the largely insulin resistant phenotype of the population. In Caucasians the PO subjects were hypertensive and hypertriglyceridaemic compared to the MHO, while these differences were not apparent (only TAG showed to be higher in PO) in the Arab MHO and PO groups because they were younger. The greater incidence and younger age of onset of obesity may warrant more aggressive treatment for obesity amongst the Arab. Therefore the prevention of obesity has to start in the younger age groups, and should focus on simple measures such as encouraging adoption of a healthy diet and promoting a non-sedentary lifestyle, particularly by encouraging physical activity within schools and outdoors activities.

### **6.2.3 Effect of weight loss on the clinical parameters**

Three months after surgery, both the PO and MHO groups showed significant reduction in BMI associated with reduction in insulin, HOMA and leptin, but no significant changes in lipids. After weight loss there was only a slight elevation in systemic adiponectin. The difference between the MHO and PO after weight loss was not significant suggesting that weight reduction surgery benefits both cohorts equally in this population.

### 6.3 MiR Signature in obesity

MicroRNA added a further level of regulation. The potential use of blood miRs as biomarkers for the obesity, cardiovascular diseases, atherosclerosis, and T2DM, was discussed by multiple reports. miRs play a major role as regulators of the different pathways like the insulin signalling, TGF- $\beta$  and the inflammatory signalling pathways. The inflammatory pathway has been regulated through different immune cells including the B-cells, T-cells and their secreted cytokines. The best example is miR-181 which plays a major role in specific developmental stages of T-cell differentiation.(Chen et al,2004), Since macrophages and hypertrophied adipocytes are the main sources of AT inflammation, the miR mediated interactions (adipocytes-macrophages and larger adipocytes-smaller adipocytes) may be novel mechanisms for miRs contributing to regulation of AT inflammation (Lumeng et al,2011).

MiR expression patterns in OM and SC adipose tissue suggest a common developmental origin of both fat depots. Differences in miR expression might contribute to differences in adipose tissue biology between OM and SC depots. A subset of miRs could be packaged into adipocyte-derived microvesicles and delivered into blood or neighboring cells, mediating intercellular communication.

There was a positive correlation between the majority of the inflammatory miRs and the biomarkers like MCP-1 and CRP involved in inflammation. Additionally miR-200c, miR-302a and miR-122 were correlated positively with high insulin, glucose and HOMA. The data of the inflammatory pathways arrays and miR NGS showed the role of some inflammatory circulating miRs likes: miR-142, miR-16, miR-185, miR-24, miR-15, miR-28, miR-29b, miR-19b, miR-374a, miR-195, miR-130a and miR-144, which were all downregulated in the PO, compared to MHO.

miR-29b, which was down regulated in the PBCs and SC of the PO, has a major role in



fibrosis and acts as a regulator of the collagen genes through the TGF- $\beta$  signalling pathway or through controlling MCL1 that lead to apoptosis, IL-6 and P13K/Akt signalling (discussed in chapter 4). MCL1 was upregulated in the PBCs of the PO group which could explain the effect of apoptosis during obesity related to hypoxia and inflammation. The TGF- $\beta$  pathway, which plays an important role in obesity, and stress, both share MAPKK to activate the same transcription factors. This could explain the effect of stress and TGF- $\beta$  pathway to dysregulate the same genes, perhaps resulting in the development of the similar disorders.

Another miR, miR-142, was involved in IR which targets the IRS1 as shown by NGS (Chapter 5). In addition to miR-374a, which targets INHBB, regulated by the TGF- $\beta$  pathway, was shown to be inhibited in PBCs of the PO group.

NOTCH, targeted by miR-200c, was another key player that mediates hypoxia/angiogenesis -vascular function. Notch signalling pathway was higher in the PO group compared to the MHO.

Some miRs that were downregulated in the OM depots showed their effects on the targets of genes required for the adipocyte differentiation (miR-27 targets PPAR $\gamma$  pathway, miR-15 targets BCL2 for adipocyte differentiation). Interestingly, INHBB down regulation was inhibits adipogenesis and insulin secretion. DLK1 was highly upregulated in the PBCs of PO compared to MHO. DLK1 activity was another important gene involved in adipocyte differentiation.

#### **6.4 Effect of weight loss on the miR gene expression**

Interestingly there was a differential effect of weight loss on the expression of some of the miRs. All were increased after the weight loss, except one that was downregulated (miR-26b). When the insulin level was reduced after the weight loss, the inflammatory miRs were upregulated except miR-29b, which did not change after the weight loss,

perhaps suggesting that the effect of this miR on fibrosis was irreversible.

Surgical weight loss improved metabolic profiles of both cohorts. MiR expression in the PO compared to the MHO before weight loss showed significant down regulation of those associated with inflammation (miR-19b, miR-9), IR (miR-142, miR-144, miR-122), fibrosis (miR-29) and adipogenesis (miR-15, miR-130a, miR-374a). Weight loss lead to upregulation of miR expression (miR-302a, b, c, miR-9, miR-200c, miR-141, miR-124, miR-376c, and miR-39).

Therefore some, but not all, of the metabolic and inflammatory lesions that accompany obesity and IR are ameliorated by weight loss, along with up-regulation of miRs mediating IR and inflammation, but not fibrosis.

## 6.5 The whole transcriptome analysis

The main aim of this project was to investigate by various approaches (clinical, miR and transcriptome) the importance of IR and inflammation as the major difference between MHO and PO and the involvement of fibrosis and vascular function in these. The transcriptome analysis was used to investigate the miR target genes and also discover further involvement of the effected pathways suggested by the studies on the miR.

Whole transcriptome analysis of mRNA in the blood and adipose tissue samples revealed downregulation/upregulation of several genes in the metabolic, inflammatory and insulin pathways in the PO compared to MHO. Also genes leading to increased fibrosis were identified in the PO.

The data showed a dysregulation in certain target genes by NGS of the PBCS which were further validated by HTA. Specifically looking at the targets of the PBCS miRs, which have been explored by the inflammatory specific pathway arrays and small RNA sequencing like:

- ↓IRS1 (↓miR-142) controlling the insulin signaling pathway, IGF, Akt2, IRS1, 2 and IRS4 all were involved in insulin signaling pathway
- ↓Col3A (↓miR-29b), ↑MCL-1 (↓miR-29b), ↑SMAD (↓miR-29b), three of them were involved in the dysregulation of TGF-β signaling pathway and lead to fibrosis;
- ↑Notch (miR-200c) affected the vascular pathway. Notch acts as a major player in angiogenesis, ASS1B11 was another interesting finding controls the Arginine and NOS that are involved in the vascular dysfunction through the regulation of TGF-β.
- ↓INHBB (↓miR-374a, in addition to miR-27 and miR-15) inhibited adipogenesis.
- Data of NGS showed a new miR, miR-4731 in adipose tissue which targeted

IGFBP-5 that acts as a direct or indirect target for Stat3.

### **6.5.1 Two different technologies were used - RNAseq versus HTA**

The NGS data was used for the discovery of the related miR targets that were found using the microarray pathways and look at their effects on different pathways. Two approaches – one PCR based known as Human Transcriptome array (HTA) and NGS by IonProton was done for better understanding and reproducibility. It was very interesting to look at the targets of the miRs in the blood samples of the MHO and PO groups from different techniques and compare results and data from RNAseq to HTA microarrays. The data showed a dysregulation in certain target genes by NGS of the whole transcriptome analysis which were confirmed by HTA microarrays of these specific targets. The effects and roles of the four main pathways, IR, fibrosis, pathological angiogenesis and inflammation, were all involved in distinguishing between MHO and PO (Figure 52).

It was very useful to run two different techniques (NGS and HTA for mRNA) in parallel where we gained the same information about mRNAs targets and their pathways. The whole transcriptome was done by the NGS which can be used as a discovery platform for the novel targets whereas the HTA can be used for the expansion of samples (increasing numbers /reproducibility of the targets).

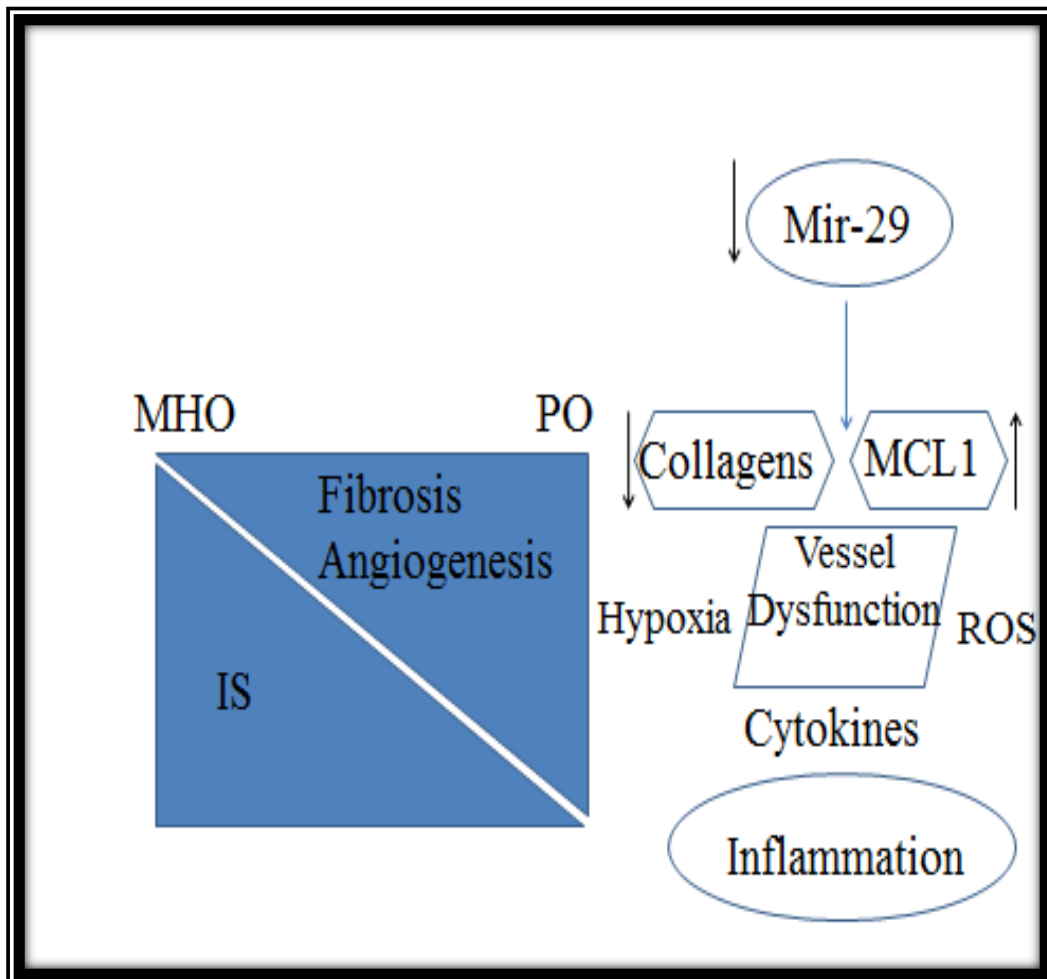


**Figure 52. miR-29 mediated changes in IR and inflammation**

The possible mechanisms and dysregulation involved in developing fibrosis, pathological angiogenesis, insulin resistance and inflammation in the MHO and PO.

## 6.6 Conclusions

The current study dichotomised a morbidly obese Arab population into those that were euglycemic and normoinsulinaemic (MHO) and the majority that were euglycemic and hyperinsulinaemic (PO). The hyperinsulinaemia of pathological obesity was accompanied by adipocyte hypertrophy and hyperleptinaemia, along with higher levels of adipokines (MCP-1 and CRP), inflammatory miRs and fibrosis. In this group surgical weight loss led to a decrease in the systemic insulin levels, HOMA and the proinflammatory biomarkers, as well as the expression of specific miR species. Therefore the surgical weight loss could be useful in the treatment of obesity and its related metabolic disorders in the PO. All results collected from various sources including clinical, miR specific inflammatory pathways/small mRNA sequencing and transcriptome were support the importance of IR and inflammation as the major difference between MHO and PO and the involvement of fibrosis and vascular function in these.

The cross talk between three main pathways insulin/metabolic pathway, TGF- $\beta$  signalling, and inflammation could help to understand the mechanisms where higher insulin level interacts with higher level of FFAs and adipokines in the presence of the inflammatory miRs (miR-29, miR-144, miR-374a) and their targets to end up with the accumulation of more collagens and increase the fibrosis that along with ROS leading to CVD and vascular dysfunction in addition to T2DM (Figure 50).

Therefore, a better understanding of the function of miRs to distinguish between MHO and PO is providing new insights into the molecular basis of human pathologies, as well as acting as new biomarkers for disease.

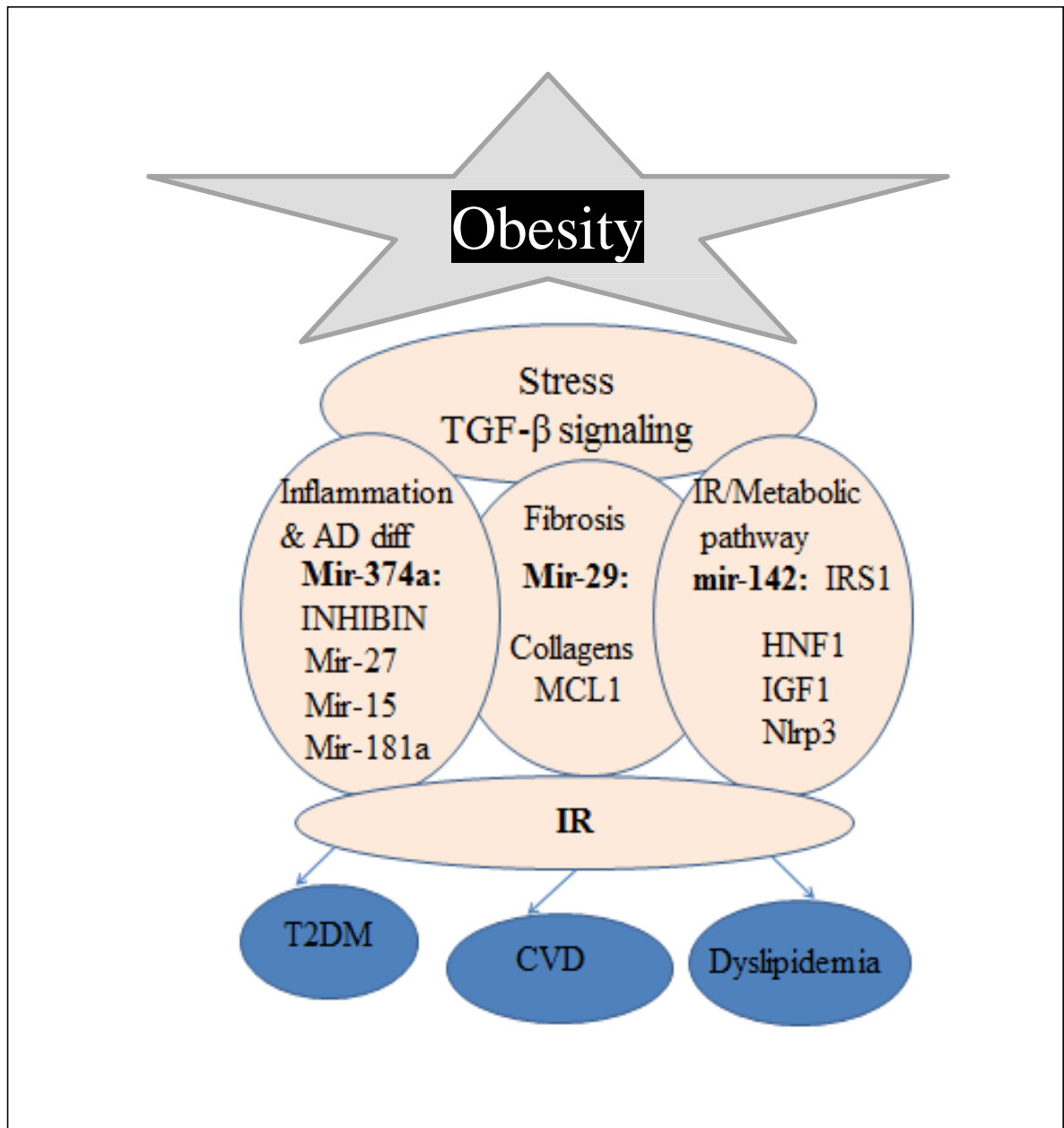


**Figure 53. Schemma of pathways involved in development of disorders in PO**

Three major pathways involved in the progress of the IR and the development of T2DM, CVD, and MeS related to the Obesity comorbidities.

## **6.7 Limitations of the study**

Obviously, the number of subjects was relatively small, RNA degradation in both PBCs and adipose tissues on storage was a major culprit, and the described associations between anthropometric and metabolic parameters and miR expression for the blood samples, and their follow up after weight loss, will require confirmation in larger cohorts. To date there is no study on the relationship of microRNA expression in human SC and OM adipose tissue and therefore, we believe it was necessary to report our findings that may be verified by studies in larger cohorts. In addition, there are some difficulties in the interpretation of miR expression data. For example, to investigate biological functions of miRs, it is critical to identify miR-directed target genes. Currently available computational methods (e.g, miRanda, PicTar, and TargetScan) predict numerous target genes that contain many false positives for miR. Also, experimental verification of miR-target relationship was complicated by the potential outcome of such an interaction being either translational repression or degradation. Furthermore, miRs can target multiple genes, and thereby the biological function of a single miR can be diverse. Hence, not only to achieve a higher degree of specificity of the prediction, but also to comprehensively understand the function of miR, large-scale prediction of targets across a whole genome would be required.

## **6.8 Long term future direction**

The project was planned to find markers or mediators of the MHO/PO phenotypes in morbid obesity. The differences were seen in the peripheral blood cells which was possible that the miR were borne in the systemic circulation to affect other insulin-sensitive organs and initiated the development of comorbidities associated with insulin resistance, such as liver and skeletal muscle dysfunction through adipocyte dysregulation and vascular dysfunction.



Depending on the results the specific miRs that were found to change uniquely in either MHO or PO alone would be further investigated and assigned a function(s) from any available data in the literature or through experimental means. Some interesting miRs like miR-29b, would be followed by more detailed functionality studies, perhaps involving silencing of some miR in whole adipose tissue. It is worth looking at the effects of glucose or insulin as well as the SNS stimulation on the level of miR-29 gene expression in adipose tissue, liver and skeletal muscle in vivo and in vitro. This could help understand the cross talk occurs between these different organs to explain the main pathways involved between these different organs.

miR profiling studies had identified miRs involved in adipogenesis and associated with obesity, but the challenge remained to determine how these miRs were regulated in adipose tissue. Therefore, it would be worthwhile to investigate if there are parallel changes in miR transcription, biogenesis and degradation which can explain the dysregulated miRs observed in obesity. Furthermore, the role of other extracellular stresses and nutrient availability regulating obesity associated miRs remained unknown. From a clinical point of view, with the recent discovery of miRs being secreted into extracellular fluids, it allows for the establishment of a circulating miR profile that can distinguish healthy obese and pathologic obese subjects. Potentially circulating miR profiles could be used by clinicians for obesity management and to track the efficacy of miR based therapeutics. Finally, further identification and characterization of miRs associated with adipogenesis and obesity could provide a new generation of therapeutic targets which will help facilitate the development of new anti-obesity treatments.

## **6.9 Future studies**

1. Further comparison between the Caucasian and the Arab population need to be carried to distinguish the effect of the ethnicity over the gene expression of miR and their

targets in the blood and adipose tissue.

2. Functional studies including the protein expression and gene silencing. The best example for the gene silencing is the miR-29. We plan to treat the adipose tissue with anti-miR-29 to see its effects on the collagen genes that are involved in the regulation of fibrosis, in addition to MCL1 which has a major role in the apoptosis. miR silencing in vivo suggest that anti-miRs are useful tools for validating disease-associated miR targets in animal disease models.

A previous study (Van Rooij et al, 2008) showed the knockout of the miR-29b in vivo using cholesterol- modified oligonucleotides. They reported the inhibition of miR-29b gene expression in all examined tissues after three days of infusion that induced fibrosis.

3. In order to understand the difference between the obese groups related to the stress. The future plan is to look at the effect of catecholamines, insulin, glucose and other inflammatory mediators on miR-29 gene expression and fibrosis in different tissues (e.g: AT, cardiac cell lines, muscle and liver). This could be done in vitro and in vivo.

# Appendix

## Appendix 1

Extra work was done along with sample collection which needs further completion and data analysis for future studies. 50 adipose tissue samples (SC, OM) from Al-Emadi hospital were excised and incubated for a day to see the effects of the secretory capacity and the cellular make up of the AT.

### **Adipose organ culture: Secretory capacity of the adipose tissue**

Subcutaneous and omental adipose tissue explants were excised ranging from 0.049g to 0.052g in size and incubated for 24 hours at 37°C and 5% CO<sub>2</sub> in CellGro Complete Medium (Mediatech, USA) + 1% Penicillin/Streptomycin solution (Invitrogen, Paisley UK) to assess secreted adipokine levels.

### **Histology samples: to investigate cellular makeup of the AT.**

0.2-0.3g sample from subcutaneous and omental adipose tissue was excised for histological purposes and incubated in neutral buffered formalin (VWR International, USA) for 24 hours and then transferred to 50% Ethanol and stored at 4°C.

## Appendix 2

Gene list of miR-29 targets:

Position	Symbol	Description	Gene Name
A01	ACVR2A	Activin A receptor, type IIA	ACTRII, ACVR2
A02	ADAM12	ADAM metallopeptidase domain 12	ADAM12-OT1, CAR10, MCMP, MCMPM <sup>tna</sup> , MLTN, MLTNA
A03	ADAMTS9	ADAM metallopeptidase with thrombospondin type 1 motif, 9	-
A04	AK3	Adenylate kinase 3	AK3L1, AK6, AKL3L, AKL3L1, FIX

A05	BACE1	Beta-site APP-cleaving enzyme 1	ASP2, BACE, HSPC104
A06	BAK1	BCL2-antagonist/killer 1	BAK, BAK-LIKE, BCL2L7, CDN1
A07	BBC3	BCL2 binding component 3	JFY-1, JFY1, PUMA
A08	BCL2	B-cell CLL/lymphoma 2	Bcl-2, PPP1R50
A09	BCL2L11	BCL2-like 11 (apoptosis facilitator)	BAM, BIM, BOD
A10	BMF	Bcl2 modifying factor	-

A11	NREP	Chromosome 5 open reading frame 13	C5orf13, D4S114, P311, PRO1873, PTZ17, SEZ17
A12	CD276	CD276 molecule	4Ig-B7-H3, B7-H3, B7H3, B7RP-2
B01	CDC42	Cell division cycle 42 (GTP binding protein, 25kDa)	CDC42Hs, G25K
B02	CDK6	Cyclin-dependent kinase 6	PLSTIRE
B03	COL15A1	Collagen, type XV, alpha 1	-
B04	COL1A1	Collagen, type I, alpha 1	OI4
B05	COL1A2	Collagen, type I, alpha 2	OI4
B06	COL21A1	Collagen, type XXI, alpha 1	COLA1L, dJ682J15.1, dJ708F5.1
B07	COL2A1	Collagen, type II, alpha 1	ANFH, AOM, COL11A3, SEDC, STL1
B08	COL3A1	Collagen, type III, alpha 1	EDS4A
B09	COL4A1	Collagen, type IV, alpha 1	HANAC, ICH, POREN1, arresten
B10	COL4A2	Collagen, type IV, alpha 2	ICH, POREN2
B11	COL5A2	Collagen, type V, alpha 2	-
B12	COL5A3	Collagen, type V, alpha 3	-
C01	COL7A1	Collagen, type VII, alpha 1	EBD1, EBDCT, EBR1
C02	CTNNBIP1	Catenin, beta interacting protein 1	ICAT
C03	DGKD	Diacylglycerol kinase, delta 130kDa	DGKdelta, dgkd-2
C04	DICER1	Dicer 1, ribonuclease type III	DCR1, Dicer, HERNA, MNG1, RMSE2
C05	DNAJB11	DnaJ (Hsp40) homolog, subfamily B, member 11	ABBP-2, ABBP2, DJ9, Dj-9, EDJ, ERdj3, ERj3, ERj3p, PRO1080, UNQ537, hDj-9
C06	DNMT1	DNA (cytosine-5-)-methyltransferase 1	ADCADN, AIM, CXXC9, DNMT, HSN1E, MCMT
C07	DNMT3A	DNA (cytosine-5-)-methyltransferase 3 alpha	DNMT3A2, M.HsaIIIA
C08	DNMT3B	DNA (cytosine-5-)-methyltransferase 3 beta	ICF, ICF1, M.HsaIIIB
C09	DUSP2	Dual specificity phosphatase 2	PAC-1, PAC1
C10	ELF2	E74-like factor 2 (ets domain transcription factor)	EU32, NERF, NERF-1A, NERF-1B, NERF-1a,b, NERF-2
C11	ELN	Elastin	SVAS, WBS, WS
C12	EOMES	Eomesodermin	TBR2
D01	FBN1	Fibrillin 1	ACMICD, ECTOL1, FBN, GPHYSD2, MASS, MFS1, OCTD, SGS, SSKS, WMS, WMS2
D02	FEM1B	Fem-1 homolog b (C. elegans)	F1A-ALPHA, F1AA, FEM1-beta

D03	FGA	Fibrinogen alpha chain	Fib2
D04	FGB	Fibrinogen beta chain	HEL-S-78p
D05	FGG	Fibrinogen gamma chain	-
D06	FOXJ2	Forkhead box J2	FHX
D07	GLUL	Glutamate-ammonia ligase	GLNS, GS, PIG43, PIG59
D08	GRN	Granulin	CLN11, GEP, GP88, PCDGF, PEPI, PGRN
D09	HDAC4	Histone deacetylase 4	AHO3, BDMR, HA6116, HD4, HDAC-4, HDAC-A, HDACA
D10	HRK	Harakiri, BCL2 interacting protein (contains only BH3 domain)	DP5, HARAKIRI
D11	IFI30	Interferon, gamma-inducible protein 30	GILT, IFI-30, IP30
D12	IREB2	Iron-responsive element binding protein 2	ACO3, IRP2, IRP2AD
E01	ITGA11	Integrin, alpha 11	HsT18964, RP11-709B3.2
E02	LAMC1	Laminin, gamma 1 (formerly LAMB2)	LAMB2
E03	LPL	Lipoprotein lipase	HDLCQ11, LIPD
E04	MBTD1	Mbt domain containing 1	SA49P01
E05	MCL1	Myeloid cell leukemia sequence 1 (BCL2-related)	BCL2L3, EAT, MCL1-ES, MCL1L, MCL1S, Mcl-1, TM, bcl2-L-3, mcl1, EAT
E06	MMP15	Matrix metalloproteinase 15 (membrane-inserted)	MT2-MMP, MTMMP2, SMCP-2
E07	MMP24	Matrix metalloproteinase 24 (membrane-inserted)	MMP-24, MMP25, MT-MMP 5, MT-MMP5, MT5-MMP, MT5MMP, MTMMP5
E08	MYCN	V-myc myelocytomatosis viral related oncogene, neuroblastoma derived (avian)	MODED, MYCNOT, N-myc, NMYC, ODED, bHLHe37
E09	NAV3	Neuron navigator 3	POMFIL1, STEERIN3, unc53H3
E10	NID1	Nidogen 1	NID
E11	PCDHA12	Protocadherin alpha 12	PCDH-ALPHA12
E12	PIK3R1	Phosphoinositide-3-kinase, regulatory subunit 1 (alpha)	AGM7, GRB1, p85, p85-ALPHA
F01	PMP22	Peripheral myelin protein 22	CMT1A, CMT1E, DSS, GAS-3, HMSNIA, HNPP, Sp110
F02	PPM1D	Protein phosphatase, Mg <sup>2+</sup> /Mn <sup>2+</sup> dependent, 1D	PP2C-DELTA, WIP1
F03	PPP1R13B	Protein phosphatase 1, regulatory (inhibitor) subunit 13B	ASPP1, p53BP2-like, p85

F04	PTEN	Phosphatase and tensin homolog	10q23del, BZS, CWS1, DEC, GLM2, MHAM, MMAC1, PTEN1, TEP1
F05	PXDN	Peroxidase homolog (Drosophila)	D2S448, D2S448E, MG50, PRG2, PXN, VPO
F06	RLF	Rearranged L-myc fusion	ZN-15L, ZNF292L
F07	S100B	S100 calcium binding protein B	NEF, S100, S100-B, S100beta
F08	SERPINB9	Serpin peptidase inhibitor, clade B (ovalbumin), member 9	CAP-3, CAP3, PI-9, PI9
F09	SESTD1	SEC14 and spectrin domains 1	SOLO
F10	SFPQ	Splicing factor proline/glutamine-rich	POMP100, PSF
F11	SP1	Sp1 transcription factor	-
F12	SPARC	Secreted protein, acidic, cysteine-rich (osteonectin)	ON
G01	SPRY1	Sprouty homolog 1, antagonist of FGF signaling (Drosophila)	hSPRY1
G02	SRSF10	Serine/arginine-rich splicing factor 10	FUSIP1, FUSIP2, NSSR, SFRS13, SFRS13A, SRp38, SRp40, TASR, TASR1, TASR2
G03	TBX21	T-box 21	T-PET, T-bet, TBET, TBLYM
G04	TCL1A	T-cell leukemia/lymphoma 1A	TCL1
G05	TDG	Thymine-DNA glycosylase	hTDG
G06	TET1	Tet oncogene 1	CXXC6, LCX, ba119F7.1
G07	TFAP2C	Transcription factor AP-2 gamma (activating enhancer binding protein 2 gamma)	AP2-GAMMA, ERF1, TFAP2G, hAP-2g
G08	TGFB3	Transforming growth factor, beta 3	ARVD, ARVD1, RNHF, TGF-beta3
G09	TNFAIP3	Tumor necrosis factor, alpha-induced protein 3	A20, OTUD7C, TNFAIP2
G10	VEGFA	Vascular endothelial growth factor A	MVCD1, VEGF, VPF
G11	ZFP36	Zinc finger protein 36, C3H type, homolog (mouse)	GOS24, GOS24, NUP475, RNF162A, TIS11, TTP, zfp-36
G12	ZFP36L1	Zinc finger protein 36, C3H type-like 1	BRF1, Berg36, ERF-1, ERF1, RNF162B, TIS11B, cMG1
H01	ACTB	Actin, beta	BRWS1, PS1TP5BP1
H02	B2M	Beta-2-microglobulin	-
H03	GAPDH	Glyceraldehyde-3-phosphate dehydrogenase	G3PD, GAPD
H04	HPRT1	Hypoxanthine phosphoribosyltransferase 1	HGPRT, HPRT
H05	RPLP0	Ribosomal protein, large, P0	L10E, LP0, P0, PRLP0, RPP0



H06	HGDC	Human Genomic DNA Contamination	HIGX1A
H07	RTC	Reverse Transcription Control	RTC
H08	RTC	Reverse Transcription Control	RTC
H09	RTC	Reverse Transcription Control	RTC
H10	PPC	Positive PCR Control	PPC
H11	PPC	Positive PCR Control	PPC
H12	PPC	Positive PCR Control	PPC

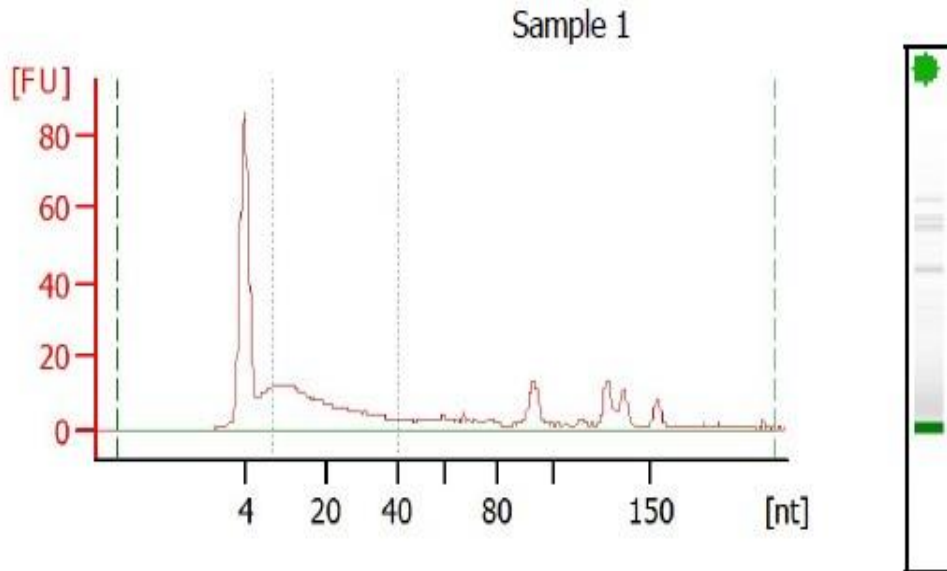
### **Appendix 3**

Different concentrations of the enriched miRNA were shown in the figures (App 3.1, 3.2 and 3.3) for sample 1,2,and 3, the concentration of miRs was between 10-40nt. The average size was used in pg/ $\mu$ l. All of them were used in the library preparation for the miRNA NGS.

### **Appendix 4**

Different summary reports of the various runs on the Ion Torrent are shown in the figures App.4.1, 4.2 and 4.3.

App.3.1



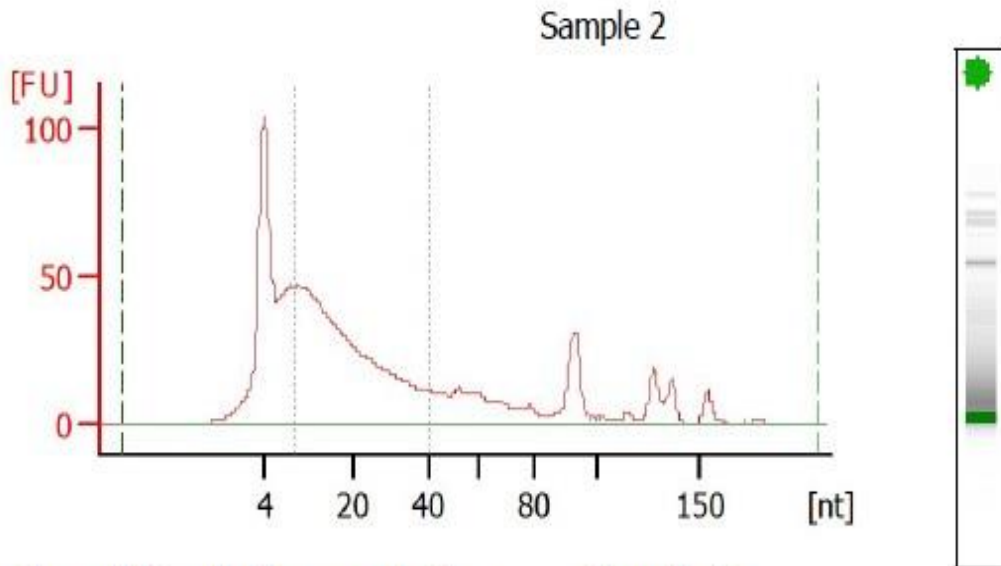
**Overall Results for sample 1 :**      **Sample 1**

Small RNA Concentration [pg/μl]:      1,363.0  
 miRNA Concentration [pg/μl]:      950.5  
 miRNA / Small RNA Ratio [%]:      70  
 Result Flagging Color:        
 Result Flagging Label:      70 % miRNA; Concentration: 950.50 pg/μl

**Region table for sample 1 :**      **Sample 1**

Name	From [nt]	To [nt]	Average Size [nt]	Size distribution in CV [%]	Conc. [pg/μl]	% of Total	Color
Small RNA	0	214	43	100.0	1,363.0	100	<span style="background-color: red; display: inline-block; width: 15px; height: 10px;"></span>
miRNA	10	40	20	41.4	950.5	70	<span style="background-color: green; display: inline-block; width: 15px; height: 10px;"></span>

App.3.2



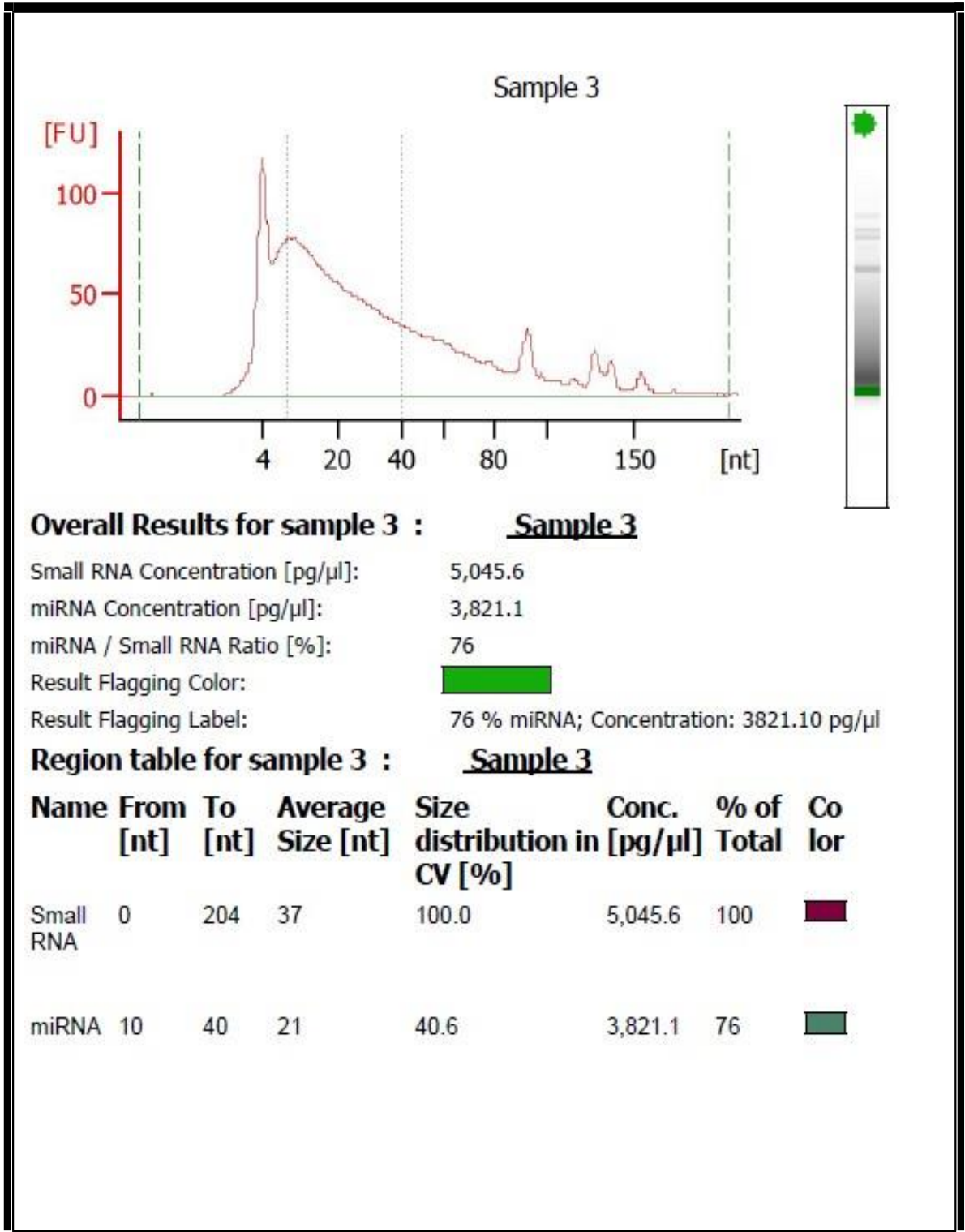
**Overall Results for sample 2 :**      **Sample 2**

Small RNA Concentration [pg/μl]:      2,913.7  
 miRNA Concentration [pg/μl]:      2,208.3  
 miRNA / Small RNA Ratio [%]:      76  
 Result Flagging Color:        
 Result Flagging Label:      76 % miRNA; Concentration: 2208.30 pg/μl

**Region table for sample 2 :**      **Sample 2**

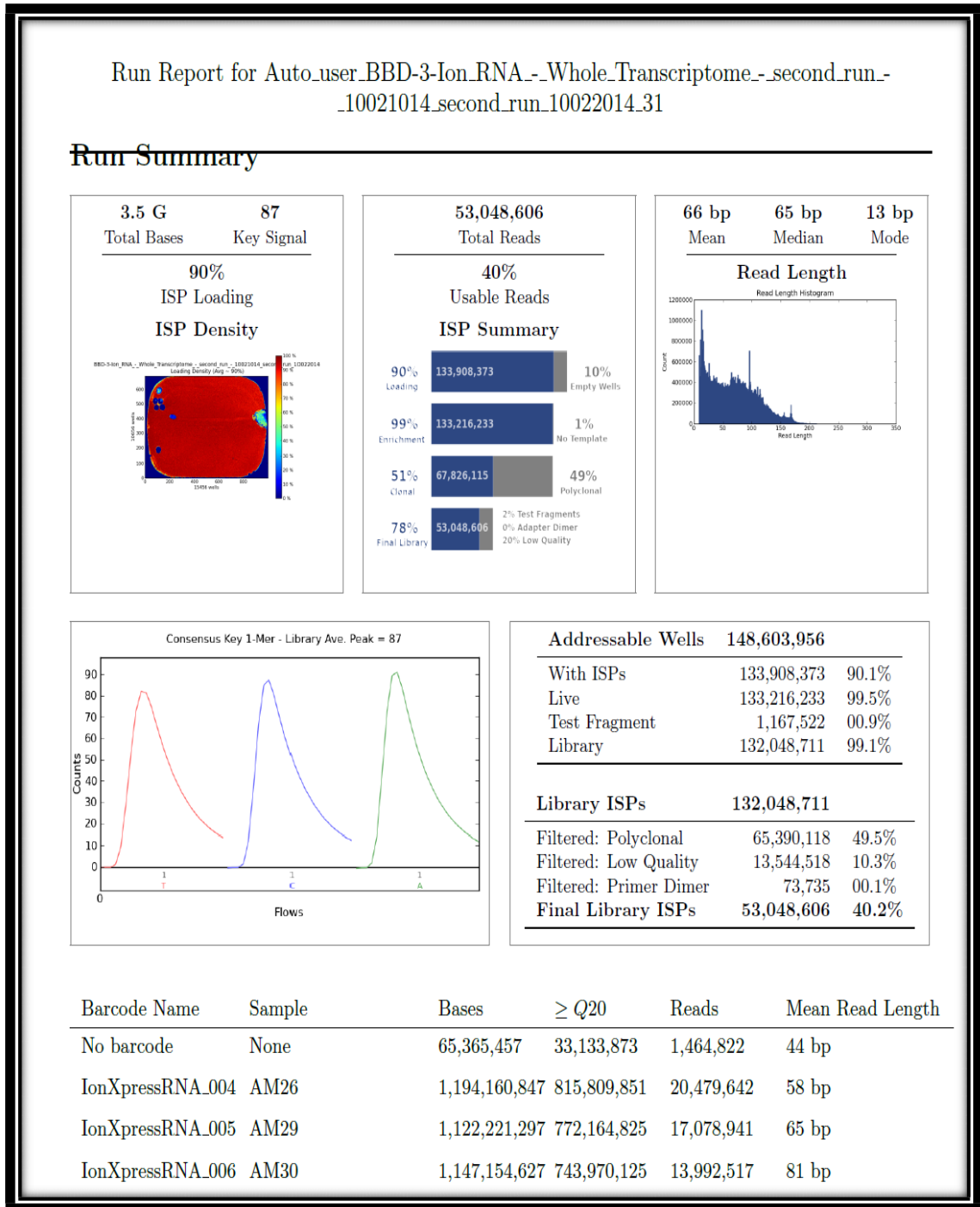
Name	From [nt]	To [nt]	Average Size [nt]	Size distribution in CV [%]	Conc. [pg/μl]	% of Total	Color
Small RNA	0	207	33	100.0	2,913.7	100	<span style="background-color: purple; display: inline-block; width: 15px; height: 10px;"></span>
miRNA	10	40	20	41.2	2,208.3	76	<span style="background-color: green; display: inline-block; width: 15px; height: 10px;"></span>

App.3.3

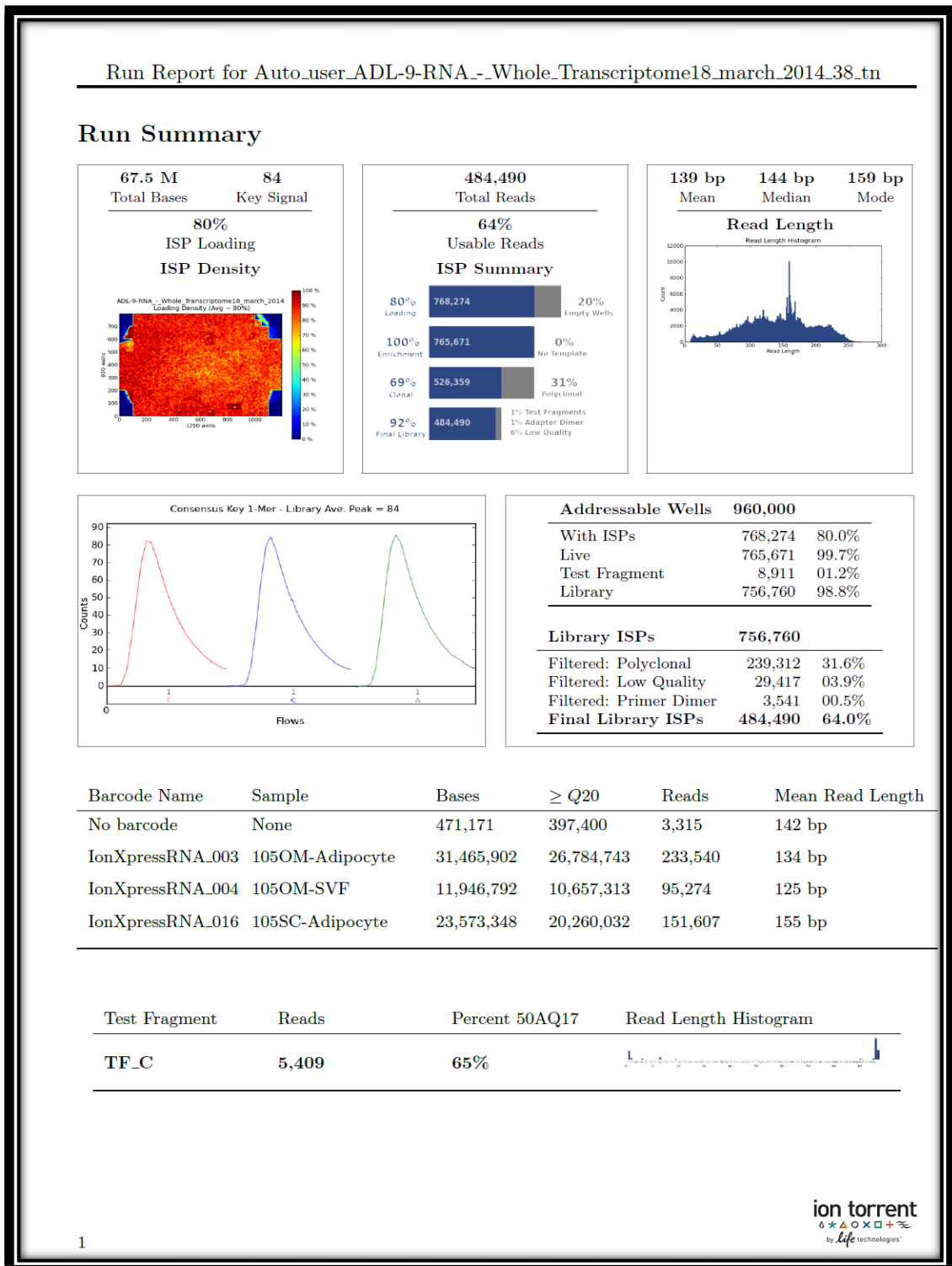


### App.4.1 The summary report of three different blood samples.

They show the differences of ISP loading, final ISP library % and the number of reads.

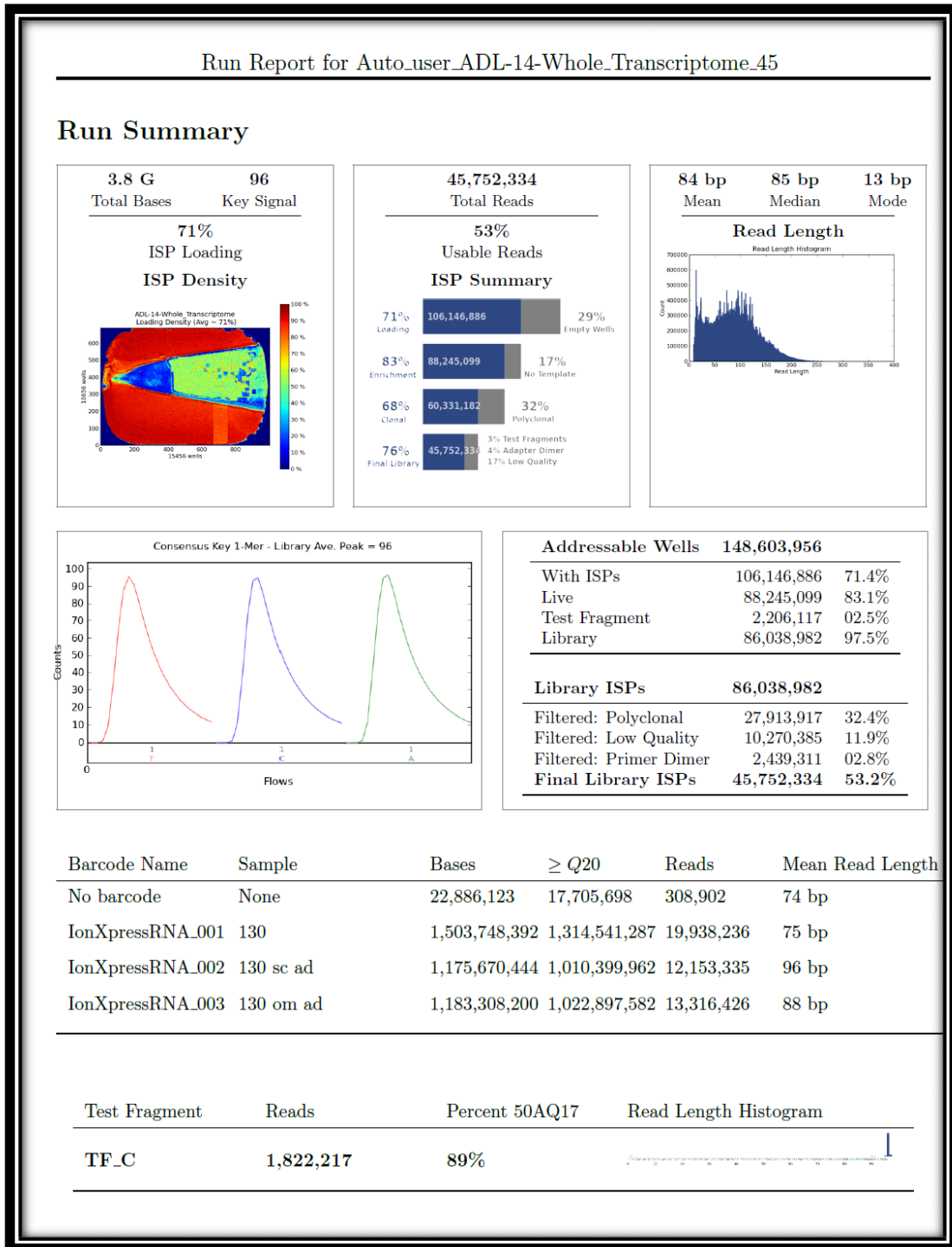


**App.4.2 The run summary report of three adipose tissue samples (AD and SVF).  
Showed the difference of ISP loading, final ISP library % and the reads.**



### App.4.3 The run summary report for the blood sample and matched adipocytes of SC and OM.

Showed the difference of ISP Loading, final ISP library % and the reads.



# **Chapter 7**

## **References**



Abdul-Ghani MA, DeFronzo RA. Pathogenesis of insulin resistance in skeletal muscle. *J Biomed Biotechnol*,2010. 2010:476279.

Adams TD, Gress RE, Smith SC, Halverson RC, Simper SC, Rosamond WD, Lamonte MJ, Stroup AM, Hunt SC. Long-term mortality after gastric bypass surgery. *N Engl J Med*, 2007. 357:753-61.

Adiels M, Olofsson SO, Taskinen MR, Borén J. Overproduction of very low- density lipoproteins is the hallmark of the dyslipidemia in the metabolic syndrome. *Arterioscler Thromb Vasc Biol*. 2008.28:1225-36.

Ambros V, Lee RC, Feinbaum RL. The *C. elegans* heterochronic gene *lin-4* encodes small RNAs with antisense complementarity to *lin-14*. *Cell*. 1993. 75:843–854.

Anders S, Huber W. Differential expression analysis for sequence count data. *Genome Biol*, 2010.11:R106.

Arita Y, Kihara S, Ouchi N, Takahashi M, Maeda K, Miyagawa J, Hotta K, Shimomura I, Nakamura T, Miyaoka K, Kuriyama H, Nishida M, Yamashita S, Okubo K, Matsubara K, Muraguchi M, Ohmoto Y, Funahashi T, Matsuzawa Y. Paradoxical decrease of an adipose-specific protein, adiponectin, in obesity. *Biochem Biophys Res Commun*, 1999. 257:79–83.

Bang JO, Dyberg J. Fish oil consumption and mortality from coronary heart disease. *N Engl J Med*, 1985. 313:822-823.

Bargaje R, Gupta S, Sarkeshik A, Park R, Xu T, Sarkar M, Halimani M, Roy SS, Yates J, Pillai B. Identification of novel targets for miR-29a using miRNA proteomics. *PLoS One*, 2012. 7:e43243.

Benjamin P Lewis, Christopher B Burge, David P Bartel. Conserved Seed Pairing, Often Flanked by Adenosines, Indicates that Thousands of Human Genes are MicroRNA Targets. *Cell*, 2005.120:15-20.

Blüher M, Rudich A, Klötting N, Golan R, Henkin Y, Rubin E, Schwarzfuchs D, Gepner Y, Stampfer MJ, Fiedler M, Thiery J, Stumvoll M, Shai I. Two patterns of adipokine and other biomarker dynamics in a long-term weight loss intervention. *Diabetes Care*, 2012.35:342-9.

Border WA, Noble NA. Transforming growth factor beta in tissue fibrosis. *N Engl J Med*, 1994. 331:1286-92.

Boström, P., Wu, J., Jedrychowski, M. P., Korde, A., Ye, L., Lo, J. C., Rasbach, K. A., Boström, E. A., Choi, J. H., Long, J. Z. et al. A PGC1- $\alpha$ -dependent myokine that drives brown-fat-like development of white fat and thermogenesis. *Nature*.2012. 481, 463-468.

Brevig K, Esquela-Kerscher A: The complexities of microRNA regulation: mirandering around the rules. *Int J Biochem Cell Biol* 2010, 42:1316-1329.

Brunzell JD, Hokanson JE. Low-density and high-density lipoprotein subspecies and risk for premature coronary artery disease. *Am J Med*. 1999.107:16S-18S.

Buchwald H, Estok R, Fahrbach K, Banel D, Jensen MD, Pories WJ, Bantle JP, Sledge I. Weight and type 2 diabetes after bariatric surgery: systematic review and meta-analysis. *Am J Med*, 2009. 122:248-256.

Burge SW, Daub J, Eberhardt R, Tate J, Barquist L, Nawrocki EP, Eddy SR, Gardner PP, Bateman A. Rfam 11.0: 10 years of RNA families. *Nucleic Acids Res*, 2013. 41:D226-32.

Caby MP, Lankar D, Vincendeau-Scherrer C, Raposo G, Bonnerot C. Exosomal-like vesicles are present in human blood plasma. *Int Immunol*, 2005. 17:879-87.

Cannon, B., Nedergaard, J., Lundberg, J. M., Hökfelt, T., Terenius, L. and Goldstein, M. 'Neuropeptide tyrosine' (NPY) is co-stored with noradrenaline in vascular but not in parenchymal sympathetic nerves of brown adipose tissue. *Exp. Cell Res.* (1986).164, 546-550.

Carruth LL, Reisert I, Arnold AP: Sex chromosome genes directly affect brain sexual

differentiation. *Nat Neurosci* 2002, 5:933–934.

Chan SY, Loscalzo J. MicroRNA-210: a unique and pleiotropic hypoxamir. *Cell Cycle* 9: 2010.

Chan SY, Zhang YY, Hemann C, Mahoney CE, Zweier JL, Loscalzo J. MicroRNA-210 controls mitochondrial metabolism during hypoxia by repressing the iron-sulfur cluster assembly proteins ISCU1/2. *Cell Metab.*10: 273–284, 2009.

Chen C, Ridzon DA, Broomer AJ, Zhou Z, Lee DH, Nguyen JT, Barbisin M, Xu NL, Mahuvakar VR, Andersen MR, Lao KQ, Livak KJ, Guegler KJ. Real-time quantification of microRNAs by stem-loop RT-PCR. *Nucleic Acids Res*, 2005. 33:e179- 9.

Chen CZ, Li L, Lodish HF, and Bartel DP. MicroRNAs modulate hematopoietic lineage differentiation. *Science*, 2004. 303: 83–86.

Chen XL, Hausman DB, Dean RG, Hausman GJ. Hormonal regulation of leptin mRNA expression and preadipocyte recruitment and differentiation in porcine primary cultures of S-V cells. *Obes Res*, 1998. 6:164-72.

Chen Y, Stallings RL. 2007. Differential patterns of microRNA expression in neuroblastoma are correlated with prognosis, differentiation, and apoptosis. *Cancer Res* 67: 976–983.

Chobanian AV, Alexander RW. Exacerbation of atherosclerosis by hypertension. Potential mechanisms and clinical implications. *Arch Intern Med*, 1996.156:1952–1956.

Cinti, S. (2009a). Reversible physiological transdifferentiation in the adipose organ. *Proc. Nutr. Soc.* 68, 340-349.

Clarke DK, Mohamed-Ali V. Adipokines and Insulin Resistance. In *Insulin Resistance: Insulin Action and its Disturbances in Disease*. Eds. Stephen O’Rahilly and Sudesh Kumar, John Wiley & Sons. 2004.

Cornier MA, Dabelea D, Hernandez TL, Lindstrom RC, Steig AJ, Stob NR, Van Pelt RE, Wang H, Eckel RH. The metabolic syndrome. *Endocr Rev.* 2008.29:777-822.

Cummings DE, Bloom SR, Rubino F. At the heart of the benefits of bariatric surgery. *Nature medicine*, 2012. 18:358-9.

DeFronzo RA. Insulin resistance, lipotoxicity, type 2 diabetes and atherosclerosis. *Diabetologia*, 2010. 53:1270–1287

DeFronzo RA, Ferrannini E. Insulin resistance. A multifaceted syndrome responsible for NIDDM, obesity, hypertension, dyslipidemia, and atherosclerotic cardiovascular disease. *Diabetes Care*, 1991:173-94.

DeFronzo RA, Tripathy D. Skeletal muscle insulin resistance is the primary defect in type 2 diabetes. *Diabetes care*, 2009. 32:S157-63.

De Luis DA, Aller R, Izaola O, Conde R, Gonzalez Sagrado M. The ratio of adiponectin to HOMA as an index of metabolic syndrome in obese women. *Annals of nutrition & metabolism*, 2011. 58:301-6.

Demolli S, Doebele C, Kaluza D, Dimmeler S, Boon R A. MicroRNA-30 Mediates Shear Stress-Induced Anti-Inflammatory Properties of Endothelial Cells via Angiopoietin-2. *Circulation*, 2013. 128: A14742.

Dent M, Chrisopoulos S, Mulhall C, Ridler C. *Bariatric surgery for obesity*. Oxford: National Obesity Observatory, 2010.

Dobbins RL, Chester MW, Daniels MB, McGarry JD, Stein DT. Circulating fatty acids are essential for efficient glucose-stimulated insulin secretion after prolonged fasting in humans. *Diabetes*, 1998. 47:1613–1618.

Dobbs R, Sawers C, Thompson F, Manyika J, Woetzel J, Child P, McKenna S, Spatharou A. *Overcoming obesity: An initial economic analysis*. Mckinesy Global Institute. November 2014.

Drummond, M.J.Glynn, E.L.; Fry, C.S.Dhanani, S.; Volpi, E.; Rasmussen, B.B. Essential aminoacidsincreasemicroRNA-499,-208b, and-23a and down-regulate myostatin and myocyte enhancer factor2C mRNAexpressionin human skeletal muscle. *J. Nutr.* 2009, 139:2279–2284.

Elchebly M, Payette P, Michaliszyn E, Cromlish W, Collins S, Loy AL, Normandin D, Cheng A, Himms-Hagen J, Chan CC, Ramachandran C, Gresser MJ, Tremblay ML, Kennedy BP. Increased insulin sensitivity and obesity resistance in mice lacking the protein tyrosine phosphatase-1B gene. *Science.* 1999; 283:1544-8.

Elmen J, Lindow M, Schutz S, Lawrence M, Petri A, Obad S, Lindholm M, Hedtjarn M, Hansen HF, Berger U, Gullans S, Kearney P, Sarnow P, Straarup EM, Kauppinen S. LNA-mediated microRNA silencing in nonhuman primates. *Nature,* 2008. 452:896-899.

Esau C, Kang X, Peralta E, Hanson E, Marcusson EG, Ravichandran LV, Sun Y, Koo S, Perera RJ, Jain R, Dean NM, Freier SM, Bennett CF, Lollo B, Griffey R. MicroRNA- 143 regulates adipocyte differentiation. *J Biol Chem,* 2004. 279:52361-5.

Fain JN, Bahouth SW. Regulation of leptin release by mammalian adipose tissue. *Biochemical & Biophysical Research Communications,* 2000. 274:571-5.

Favaro E, Ramachandran A, McCormick R, Gee H, Blancher C, Crosby M, Devlin C, Blick C, Buffa F, Li JL, Vojnovic B, Pires das Gupta, R. K., Mepani, R. J., Kleiner, S., Lo, J. C., Khandekar, M. J., Cohen, P., Frontini, A., Bhowmick, D. C., Ye, L., Cinti, S. et al. (2012). Zfp423 expression identifies committed preadipocytes and localizes to adipose endothelial and perivascular cells. *Cell Metab.* 15, 230-239.

Ferrannini E, Camastra S, Coppack SW, Fliser D, Golay A, Mitrakou A. Insulin action and non-esterified fatty acids. The European Group for the Study of Insulin Resistance (EGIR), *Proc Nutr Soc.* 1997.56:753-61.

Fischer LM, daCosta KA, Kwock L, Stewart PW, Lu TS, Stabler SP, Alen RH, Zeisel SH. Sex and menopausal status influence human dietary requirements for the nutrient choline. *Am J Clin Nutr,* 2007.85:1275-85.

Furukawa S, Fujita T, Shimabukuro M, Iwaki M, Yamada Y, Nakajima Y, Nakayama O, Makishima M, Matsuda M, Shimomura I. Increased oxidative stress in obesity and its impact on metabolic syndrome, *J Clin Invest*, 2004.114:1752-61.

Gantier MP, Stunden HJ, McCoy CE, Behlke MA, Wang D, Kaparakis-Liaskos M, Sarvestani ST, Yang YH, Xu D, Corr SC, Morand EF, Williams BR. miR-19 regulon that controls NF- $\kappa$ B signaling. *Nucleic Acids Res*, 2012.40:8048-58.

Gennarino VA, D'Angelo G, Dharmalingam G, Fernandez S, Russolillo G, Sanges R, Mutarelli M, Belcastro V, Ballabio A, Verde P, Sardiello M, Banfi S. Identification of microRNA-regulated gene networks by expression analysis of target genes. *Genome Res*. 2012; 22:1163–1172.

Gerin I, Clerbaux LA, Haumont O, Lanthier N, Das AK, Burant CF, Leclercq IA, MacDougald OA, Bommer GT. Expression of miR-33 from an SREBP2 intron inhibits cholesterol export and fatty acid oxidation. *J Biol Chem*. 2010. 285:33652-61.

Gesta Stephane, Tseng Yu-Hua, and Ronald Kahn C. Developmental Origin of Fat: Tracking Obesity to Its Source Cell. 2007.131: 242-255.

Gómez-Ambrosi J, Catalán V, Díez-Caballero A, Martínez-Cruz LA, Gil MJ, García-Foncillas J, Cienfuegos JA, Salvador J, Mato JM, Frühbeck G. Gene expression profile of omental adipose tissue in human obesity. *FASEB J*. 2004.18:215-7.

Gong Y, Renigunta V, Himmerkus N, Zhang J, Renigunta A, Bleich M, Hou J. Claudin-14 regulates renal  $\text{Ca}^{2+}$  transport in response to CaSR signaling via a novel microRNA pathway. *EMBO J*. 2012. 31:1999-2012.

Groop L C, Bonadonna R C, DelPrato S. Glucose and free fatty acid metabolism in non-insulin-dependent diabetes mellitus. Evidence for multiple sites of insulin resistance. *The Journal of Clinical Investigation*, 1989.84:205–213.

Grundy SM, Hansen B, Smith SC Jr, Cleeman JI, Kahn RA. Clinical management of metabolic syndrome. American Heart Association; National Heart, Lung, and Blood

Institute; American Diabetes Association. *Circulation*, 2004. 109:551-6.

Guo KY, Halo P, Leibel RL, Zhang Y. Effects of obesity on the relationship of leptin mRNA TG, Uysal T, expression and adipocyte size in anatomically distinct fat depots in mice. *Am J Physiol Regul Integr Comp Physiol*, 2004. 287:R112–R119.

Gupta P, Cairns MJ, Saksena NK. Regulation of gene expression by microRNA in HCV infection and HCV–mediated hepatocellular carcinoma. *Virology Journal*, 2014.11:64.

Gustafson B, Gogg S, Hedjazifar S, Jenndahl L, Hammarstedt A, Smith U. Inflammation and impaired adipogenesis in hypertrophic obesity in man. *Am J Physiol Endocrinol Metab*, 2009.297:E999-E1003.

Gustafson B, Hammarstedt A, Andersson CX, Smith U. Inflamed adipose tissue: a culprit underlying the metabolic syndrome and atherosclerosis. *Arterioscler Thromb Vasc Biol*, 2007.27:2276-83.

Gustafson B, Smith U. Cytokines promote Wnt signaling and inflammation and impair the normal differentiation and lipid accumulation in 3T3-L1 preadipocytes. *J Biol Chem*, 2006. 7; 281:9507-16.

Hah N, Danko CG, Core L, Waterfall JJ, Siepel A, Lis JT, Kraus WL: A Rapid, Extensive, and Transient Transcriptional Response to Estrogen Signaling in Breast Cancer Cells. *Cell* 2011, 145:622–634.

Halberg N, Khan T, Trujillo ME, Wernstedt-Asterholm I, Attie AD, Sherwani S, Wang ZV, Landskroner-Eiger S, Dineen S, Magalang UJ, Brekken RA, Scherer PE. Hypoxia-inducible factor 1alpha induces fibrosis and insulin resistance in white adipose tissue. *Mol Cell Biol*, 2009.29:4467-83.

Hamilton BS, Paglia D, Kwan AY, Deitel M. Increased obese mRNA expression in omental fat cells from massively obese humans. *Nat Med*, 1995. 1:953-6.

Hansen D, Dendale P, Beelen M, Jonkers RA, Mullens A, Corluy L, Meeusen R, van Loon

LJ. Plasma adipokine and inflammatory marker concentrations are altered in obese, as opposed to non-obese, type 2 diabetes patients. *Eur J Appl Physiol*, 2010.109:397- 404.

Hardy OT, Czech MP, Corvera S. What causes the insulin resistance underlying obesity? *Current opinion in endocrinology, diabetes, and obesity*, 2012. 19:81-7.

Hardy OT, Perugini RA, Nicoloso SM, Gallagher-Dorval K, Puri V, Straubhaar J, Czech MP. Body mass index-independent inflammation in omental adipose tissue associated with insulin resistance in morbid obesity. *Surg Obes Relat Dis*, 2011. 7:60–67.

He A, Zhu L, Gupta N, Chang Y, Fang F. Overexpression of Micro Ribonucleic Acid 29, Highly Up-Regulated in Diabetic Rats, Leads to insulin Resistance in 3T3-L1 Adipocytes. *Mol Endocrinol*, 2007. 21:2785-2794.

Hedtjarn M, Hansen JB, Hansen HF, Straarup EM, McCullagh K, Kearney P, Kauppinen S. Antagonism of microRNA-122 in mice by systemically administered LNA-antimiR leads to up-regulation of a large set of predicted target mRNAs in the liver. *Nucleic Acids Res*, 2008. 36:1153-1162.

Heneghan H M, Miller N, Kerin M J, Role of microRNAs in obesity and the metabolic syndrome, *Obesity Reviews*, 2010. 11: 354–361.

Herrera BM, Lockstone HE, Taylor JM, Ria M, Barrett A, Collins S, Kaisaki P, Argoud K, Fernandez C, Travers ME, Grew JP, Randall JC, Gloyn AL, Gauguier D, McCarthy MI, Lindgren CM. Global microRNA expression profiles in insulin target tissues in a spontaneous rat model of type 2 diabetes. *Diabetologia*, 2010. 53:1099-109.

Himms-Hagen, J. et al. Multilocular fat cells in WAT of CL-316243-treated rats derive directly from white adipocytes. *Am. J. Physiol. Cell Physiol.* 279, C670–C681 (2000).

Hivert MF, Sullivan LM, Fox CS, Nathan DM, D'Agostino RB Sr, Wilson PW, Meigs JB. Associations of adiponectin, resistin, and tumor necrosis factor-alpha with insulin resistance. *J Clin Endocrinol Metab.* 2008.93:3165-72. 20.



Hotamisligil GS. Inflammation and metabolic disorders. *Nature*, 2006. 444:860–67.

[http://www.iaso.org/site\\_media/uploads/Global\\_prevalence\\_of\\_adult\\_obesity\\_Ranking\\_by\\_country\\_2012.pdf](http://www.iaso.org/site_media/uploads/Global_prevalence_of_adult_obesity_Ranking_by_country_2012.pdf).

<https://www.safefood.eu/SafeFood/media/SafeFoodLibrary/Documents/Professional/All-island%20Obesity%20Action%20Forum/obesity-taskforce.pdf>.

<http://www.who.int/mediacentre/factsheets/fs311/en/>. Overweight and obesity, Fact sheet N311. May 2012.

Hulsmans M, Holvoet P. MicroRNAs as early biomarkers in obesity and related metabolic and cardiovascular diseases. *Curr Pharm Des*, 2013.19:5704-17.

Isakov O, Ronen R, Kovarsky J, Gabay A, GanI, Modai S, Shomron N. Novel Insight into the Non-Coding Repertoire Through Deep Sequencing Analysis. *Nucl. Acids Res*, 2012. 40:e86.

Isakson P, Hammarstedt A, Gustafson B, Smith U. Impaired preadipocyte differentiation in human abdominal obesity: role of Wnt, tumor necrosis factor- $\alpha$ , and inflammation. *Diabetes*, 2009. 58:1550-7.

Ishibashi, J. and Seale, P. (2010). Medicine. Beige can be slimming. *Science* 328, 1113-1114.

Jernås M, Palming J, Sjöholm K, Jennische E, Svensson PA, Gabrielsson BG, Levin M, Sjögren A, Rudemo M, Lystig TC, Carlsson B, Carlsson LM, Lönn M. Separation of human adipocytes by size: hypertrophic fat cells display distinct gene expression. *FASEB J*, 2006. 20:1540-2.

Jespersen, N.Z. et al. A classical brown adipose tissue mRNA signature partly overlaps with brite in the supraclavicular region of adult humans. *Cell Metab*. 17, 798–805 (2013).

Jin, W., M. Dodson, S. Moore, J. Basarab, and L. L. Guan. 2010. Characterization of

microRNA expression in bovine adipose tissues: A potential regulatory mechanism of subcutaneous adipose tissue development. *BMC Mol. Biol.* 11:29.

Kadowaki T, Yamauchi T. Adiponectin and adiponectin receptors. *Endocr Revs*, 2005. 26:439-51.

Kahn SE, Haffner SM, Heise MA, Herman WH, Holman RR, Jones NP, Kravitz BG, Lachin JM, O'Neill MC, Zinman B, Viberti G; ADOPT Study Group. Glycemic durability of rosiglitazone, metformin, or glyburide monotherapy. *N Engl J Med*, 2006. 355:2427-43.

Kahn SE, Hull RL, Utzschneider KM. Mechanisms linking obesity to insulin resistance and T2DM. *Nature*, 2006. 444:840-6.

Kannel WB, McGee DL. Diabetes and cardiovascular disease. The Framingham study. *JAMA*, 1979. 241:2035–2038.

Kantartzis K, Machann J, Schick F, Rittig K, Machicao F, Fritsche a, et al. Effects of a lifestyle intervention in metabolically benign and malignant obesity. *Diabetologia*, 2011.54:864–8.

Kapoun AM, Gaspar NJ, Wang Y, Damm D, Liu YW, O'young G, Quon D, Lam A, Munson K, Tran TT, Ma JY, Murphy A, Dugar S, Chakravarty S, Protter AA, Wen FQ, Liu X, Rennard SI, Higgins LS. Transforming growth factor-beta receptor type 1 (TGFbetaRI) kinase activity but not p38 activation is required for TGFbetaRI-induced myofibroblast differentiation and profibrotic gene expression. *Mol Pharmacol*, 2006.70:518-31.

Kapoun AM, Liang F, O'Young G, Damm DL, Quon D, White RT, Munson K, Lam A, Schreiner GF, Protter AA. B-type natriuretic peptide exerts broad functional opposition to transforming growth factor-beta in primary human cardiac fibroblasts: fibrosis, myofibroblast conversion, proliferation, and inflammation. *Circ Res*, 2004.94:453-61.

Karastergiou K, Mohamed-Ali V. The autocrine and paracrine roles of adipokines, *Mol Cell Endocrinol*, 2010. 318:69-78.

Karbiener M, Fischer C, Nowitsch S, Opriessnig P, Papak C, Ailhaud G, Dani C, Amri EZ, Scheideler M. miR-27b impairs human adipocyte differentiation and targets PPARgamma. *Biochem Biophys Res Commun*, 2009. 390:247-51.

Karelis AD. Metabolically healthy but obese individuals. *Lancet*, 2008.372:1281–3.

Karolina DS, Armugam A, Tavintharan S, Wong MT, Lim SC, Sum CF, Jeyaseelan K. MicroRNA 144 impairs insulin signaling by inhibiting the expression of insulin receptor substrate 1 in type 2 diabetes mellitus. *PLoS One*, 2011

Keaney JF Jr, Larson MG, Vasani RS, Wilson PW, Lipinska I, Corey D, Massaro JM, Sutherland P, Vita JA, Benjamin EJ. Obesity and systemic oxidative stress: clinical correlates of oxidative stress in the Framingham Study. *Arterioscler Thromb. Vasc Biol*, 2003. 23:434-9.

Khaodhjar L, Ling PR, Blackburn GL, Bistrian BR. Serum levels of interleukin-6 and C-reactive protein correlate with body mass index across the broad range of obesity. *J Parenteral Enteral Nut*, 2004. 28: 410-415.

Kim D, Pertea G, Trapnell C, Pimentel H, Kelley R, Salzberg SL. TopHat2: accurate alignment of transcriptomes in the presence of insertions, deletions and gene fusions. *Genome Biology*, 2013. 14:R36.

Kim SY, Kim AY, Lee HW, Son YH, Lee GY, Lee JW, Lee YS, Kim JB. miR-27a is a negative regulator of adipocyte differentiation via suppressing PPARgamma expression. *Biochem Biophys Res Commun*, 2010.392:323-8.

Kirchgessner TG, Wiesbrock SM, Marino MW, Hotamisligil G. Tumor necrosis factor – alpha contributes to obesity related hyperleptinemia by regulating leptin release from adipocytes. *J Clin Invest*, 1997. 100: 2777-2782.

Kitamura T, Kitamura YI, Funahashi Y, Shawber CJ, Castrillon DH, Kollipara R, DePinho RA, Kitajewski J, Accili D. A Foxo/Notch pathway controls myogenic

differentiation and fiber type specification. *J Clin Invest.*, 2007.117:2477-85.

Klötting N, Berthold S, Kovacs P, Schön MR, Fasshauer M, Ruschke K, Stumvoll M, Blüher M. MicroRNA expression in human omental and subcutaneous adipose tissue. *PLoS One.* 2009.4:e4699.

Kole AJ, Swahari V, Hammond SM, Deshmukh M. miR-29b is activated during neuronal maturation and targets BH3-only genes to restrict apoptosis. *Genes Dev.* 2011. 25: 125–130

Kosaka N, Iguchi H, Yoshioka Y, Takeshita F, Matsuki Y, Ochiya T. Secretory Mechanisms and Intercellular Transfer of MicroRNAs in Living Cells. *J Biol Chem.* 2010. 285: 17442–17452.

Kovsan J, Blüher M, Tarnowski T, Klötting N, Kirshtein B, Madar L, Shai I, Golan R, Harman-Boehm I, Schön MR, Greenberg AS, Elazar Z, Bashan N, Rudich A. Altered autophagy in human adipose tissues in obesity. *J Clin Endocrinol Metab.* 2011.96:E268-77.

Kozomara A, Griffiths-Jones S. miRBase: integrating microRNA annotation and deep-sequencing data. *Nucleic Acids Res.* 2011. 39:D152–7.

Kursawe R, Eszlinger M, Narayan D, Liu T, Bazuine M, Cali AM, D'Adamo E, Shaw M, Pierpont B, Shulman GI, Cushman SW, Sherman A, Caprio S. Cellularity and adipogenic profile of the abdominal subcutaneous adipose tissue from obese adolescents: association with insulin resistance and hepatic steatosis. *Diabetes.* 2010.59:2288-96.

Lagos-Quintana M, Rauhut R, Yalcin A, Meyer J, Lendeckel W, Tuschl T. Identification of tissue-specific microRNAs from mouse. *Curr Biol.* 2002. 12:735-9.

Langmead B, Salzberg S. Fast gapped-read alignment with Bowtie 2. *Nature Methods.* 2012. 9:357-359.

Laterza OF, Lim L, Garrett-Engele PW, Vlasakova K, Muniappa N, Tanaka WK, Johnson JM, Sina JF, Fare TL, Sistare FD, Glaab WE. Plasma MicroRNAs as sensitive and

specific biomarkers of tissue injury. *Clin Chem*, 2009.55:1977-83.

Lee, Y.H., Petkova, A.P., Mottillo, E.P. & Granneman, J.G. In vivo identification of bipotential adipocyte progenitors recruited by  $\beta$ 3-adrenoceptor activation and high-fat feeding. *Cell Metab.* 15, 480–491 (2012).

Li H. and Durbin R. Fast and accurate short read alignment with Burrows-Wheeler Transform. *Bioinformatics*, 2009. 25:1754-60.

Livak KJ, Schmittgen TD. Analysis of relative gene expression data using real-time quantitative PCR and the 2(-Delta Delta C (T)) Method. *Methods*. 2001. 25:402-8.

Li QJ, Chau J, Ebert PJ, Sylvester G, Min H, Liu G, Braich R, Manoharan M, Soutschek J, Skare P, Klein LO, Davis MM, Chen CZ. miR-181a is an intrinsic modulator of T cell sensitivity and selection. *Cell*, 2007. 129:147-61.

Li Q. Verma I.M. NF-kB regulation in the immune system. *Nat. Rev. Immunol*, 2002. 2:331-367.

Li S, Shin HJ, Ding EL, van Dam RM. Adiponectin levels and risk of type 2 diabetes: a systematic review and meta-analysis. *Journal of the American Medical Association*, 2009. 302: 179-188.

Li Z, Hassan MQ, Jafferji M, Aqeilan RI, Garzon R, Croce CM, van Wijnen AJ, Stein JL, Stein GS, Lian JB. Biological functions of miR-29b contribute to positive regulation of osteoblast differentiation. *J Biol Chem*, 2009. 284:15676-84.

Lodish HF, Zhou B, Liu G, Chen C. Micromanagement of the immune system by microRNAs. *Nat Rev Immunol*, 2008. 8:120–30.

Loffreda S, Yang SQ, Lin HZ, Karp CL, Brengman ML, Wang DJ, Klein AS, Bulkley GB, Bao C, Noble PW, Lane MD, Diehl AM 1998. Leptin regulates proinflammatory immune responses. *FASEB J*, 1998. 12:57–65.

Loscalzo J. The cellular response to hypoxia: tuning the system with microRNAs. *J Clin Invest* 120: 3815–3817, 2010.

Lu J, Getz G, Miska EA, Alvarez-Saavedra E, Lamb J, Peck D, Sweet-Cordero A, Ebert BL, Mak RH, Ferrando AA, et al. 2005. Micro-RNA expression profiles classify human cancers. *Nature* 435: 834– 838.

Lumeng CN and Saltiel A R. Inflammatory links between obesity and metabolic disease. *J Clin Invest*, 2011. 121:2111–2117.

Lundgren M, Svensson M, Lindmark S, Renstrom F, Ruge T, Eriksson JW. Fat cell enlargement is an independent marker of insulin resistance and ‘hyperleptinaemia’. *Diabetologia*, 2007.50:625-633.

Madani R, Ogston NC, Mohamed-Ali-V. In *Peptides in Energy Balance and Obesity*. Cabi, 2009. Pp.195-228. Adipokines in the immune-stress response. Frühbeck, G. (Eds).

Madrigal-Matute J, Rotllan N, Aranda JF, Fernández-Hernando C. MicroRNAs and atherosclerosis. *Curr Atheroscler Rep*, 2013.15:322.

Makki K, Froguel P, Wolowczuk I. Adipose tissue in obesity-related inflammation and insulin resistance: cells, cytokines, and chemokines, *ISRN Inflamm*. 2013:139239.

Matsuoka T, Kajimoto Y, Watada H, Kaneto H, Kishimoto M, Umayahara Y, Fujitani Y, Kamada T, Kawamori R, Yamasaki Y. Glycation-dependent, reactive oxygen species-mediated suppression of the insulin gene promoter activity in HIT cells. *J Clin Invest*, 1997.99:144-50.

McCarthy MM, Wright CL, Schwarz JM: New tricks by an old dogma: Mechanisms of the Organizational / Activational Hypothesis of steroid-mediated sexual differentiation of brain and behavior. *Horm Behav* 2009, 55:655–665.

McDonald RA, Hata A, MacLean M, Morrell NW, Baker AH. MicroRNA and vascular remodelling in acute vascular injury and pulmonary vascular remodelling. *Cardiovasc Res*,

2012. 93:594–604.

McGregor RA, Choi MS. MicroRNAs in the regulation of adipogenesis and obesity. *Curr Mol Med*, 2011. 11:304-16.

McKeigue PM. Metabolic consequences of obesity and body fat pattern: lessons from migrant studies. Wiley, Chichester, UK, 1996. 201: 54–67.

McLaughlin T, Deng A, Yee G, Lamendola C, Reaven G, Tsao PS, Cushman SW, Sherman A. Inflammation in subcutaneous adipose tissue: relationship to adipose cell size. *Diabetologia*, 2010.53:369-77.

McLaughlin T, Sherman A, Tsao P, Gonzalez O, Yee G, Lamendola C, Reaven GM, Cushman SW. Enhanced proportion of small adipose cells in insulin-resistant vs insulin-sensitive obese individuals implicates impaired adipogenesis. *Diabetologia*. 2007, 50:1707-15.

Meale S. J, Romao J. M, He M. L, Chaves A. V, McAllister and Guan L. L. Tissues Effect of diet on microRNA expression in ovine subcutaneous and visceral adipose. *J ANIM SCI* 2014, 92:3328-3337.

Meigs JB, Wilson PW, Fox CS, Vasan RS, Nathan DM, Sullivan LM, D'Agostino RB. Body mass index, metabolic syndrome, and risk of type 2 diabetes or cardiovascular disease. *J Clin Endocrinol Metab*, 2006. 91:2906–2912.

Michael A, Bajracharya SD, Yuen PS, Zhou H, Star RA, Illei GG, Alevizos I. Exosomes from human saliva as a source of microRNA biomarkers. *Oral Dis*. 2010 .16:34-8.

Miko E, Czimmerer Z, Csányi E, Boros G, Buslig J, Dezso B, Scholtz B. Differentially expressed microRNAs in small cell lung cancer. *Exp Lung Res*, 2009.35:646-64.

Mohamed-Ali V, Goodrick S, Rawesh A, Katz DR, Miles JM, Yudkin JS, Klein S, Coppack SW. Subcutaneous adipose tissue releases interleukin-6, but not tumor necrosis factor- $\alpha$ , in vivo. *J Clin Endocrinol Metab*, 1997. 82:4196-200.

Mohamed-Ali V, Pinkney JH & Coppack SW. Adipose tissue as an endocrine and paracrine organ. *International Journal of Obesity*.1998. 22,1145-1158.

Moon RT, Kohn AD, De Ferrari GV, Kaykas A: WNT and beta-catenin signalling: diseases and therapies. *Nat Rev Genet*, 2004. 5:691-701.

Neschen S, Morino K, Dong J, Wang-Fischer Y, Cline GW, Romanelli AJ, Rossbacher JC, Moore IK, Regittnig W, Munoz DS, Kim JH, Shulman GI: n-3 Fatty acids preserve insulin sensitivity in vivo in a peroxisome proliferator-activated receptor-alpha- dependent manner. *Diabetes*, 2007. 56:1034-1041.

Neves R, Glazer P, Iborra F, Ivan M, Ragoussis J, Harris AL. MicroRNA-210 regulates mitochondrial free radical response to hypoxia and krebs cycle in cancer cells by targeting iron sulfur cluster protein ISCU. *PLoS One* 5: e10345

Novina CD, Sharp PA. The RNAi revolution. *Nature*. 2004.430:161-4.

Nunez-Iglesias J, Liu CC, Morgan TE, Finch CE, Zhou XJ. Joint genome-wide profiling of miRNA and mRNA expression in Alzheimer's disease cortex reveals altered miRNA regulation. *PLoS One*. 2010;5:e8898. doi: 10.1371/journal.pone.0008898.

Ober C, Loisel DA, Gilad Y: Sex-specific genetic architecture of human disease. *Nature reviews. Genetics* 2008, 9:911-922.

O'Connell J, Lynch L, Cawood TJ, Kwasnik A, Nolan N, Geoghegan J, McCormick A, O'Farrelly C, O'Shea D. The relationship of omental and subcutaneous adipocyte size to metabolic disease in severe obesity. *PLoS One*, 2010.5:e9997.

O'Connell J, Lynch L, Hogan A, Cawood TJ, O'Shea D. Preadipocyte factor-1 is associated with metabolic profile in severe obesity. *J Clin Endocrinol Metab*, 2011.96:E680-4.

Ohlson LO, Larsson B, Sva helmsen L, Björdsudd K, Welin L, Eriksson H, Wil'ntorp P,



Tibblin G. The influence of body fat distribution on the incidence of diabetes mellitus—13.5 years of follow-up of the participants in the study of men born in 1913. *Diabetes*, 34:1055–1058. *Am J Physiol*, 1997. 273:E425-32.

Ohno, H., Shinoda, K., Spiegelman, B.M. & Kajimura, S. PPAR $\gamma$  agonists induce a white-to-brown fat conversion through stabilization of PRDM16 protein. *Cell Metab.* 15, 395–404 (2012).

Olga T. Hardy, Michael P. Czech, and Silvia Corvera. What causes the insulin resistance underlying obesity? *Curr Opin Endo Diab Obes*, 2012. 19: 81–87.

Olivieri F, Antonicelli R, Capogrossi MC, Procopio AD. Circulating microRNAs for diagnosing acute myocardial infarction: an exciting challenge. *Int J Cardiol*, 2013. 167:3028–3029.

Ortega FJ, Moreno-Navarrete JM, Pardo G, Sabater M, Hummel M, Ferrer A, Rodriguez-Hermosa JI, Ruiz B, Ricart W, Peral B, Fernandez-Real JM. MiR Expression Profile of Human Subcutaneous Adipose and during Adipocyte Differentiation. *PLoS One*. 2010. 5:e9022.

Ozen M, Creighton CJ, Ozdemir M, Ittmann M. 2008. Widespread deregulation of microRNA expression in human prostate cancer. *Oncogene* 27: 1788–1793.

Pan S, Zheng Y, Zhao R, Yang X: miR-374 regulates dexamethasone-induced differentiation of primary cultures of porcine adipocytes. *Horm Metab Res*, 2013. 45:518–525.

Pan S, Zheng Y, Zhao R, Yang X. MicroRNA-130b and microRNA-374b mediate the effect of maternal dietary protein on offspring lipid metabolism in Meishan pigs. *Br J Nutr*. 2013, 109: 1731-1738.

Pasarica M A, Sereda OR, Redman LM, Albarado DC, Hymel DT, Roan LE, Rood JC, Burk DH, Smith SR. Reduced adipose tissue oxygenation in human obesity: evidence for rarefaction, macrophage chemotaxis, and inflammation without an angiogenic response.

Diabetes, 2009.58:718-25.

Petrovic, N. et al. Chronic peroxisome proliferator-activated receptor  $\gamma$  (PPAR $\gamma$ ) activation of epididymally derived white adipocyte cultures reveals a population of thermogenically competent, UCP1-containing adipocytes molecularly distinct from classic brown adipocytes. *J. Biol. Chem.* 285, 7153–7164 (2010).

Phillips DIW, Caddy S, Ilic V, Fielding BA, Frayn KN, Borthwick AC, Taylor R. Intramuscular triglyceride and muscle insulin sensitivity: evidence for a relationship in non-diabetic subjects. *Metabolism*, 1996.45:947–950.

Pinkney JH, Coppack SW, Mohamed-Ali V. Effect of isoprenaline on plasma leptin and lipolysis in humans. *Clin Endocrinol (Oxf)*, 1998. 4:407-11.

Pohl N M, Yamamura A, Yamamura H, Makino A, Yuan J. microRNA 29b is upregulated in pulmonary artery smooth muscle cells from patients with idiopathic pulmonary arterial hypertension and inhibits K<sup>+</sup> channel expression and function. *The FASEB Journal*, 2012.26:884.10.

Ponomarev ED, Veremeyko T, Barteneva N, Krichevsky AM, Weiner HL. MicroRNA-124 promotes microglia quiescence and suppresses EAE by deactivating macrophages via the C/EBP- $\alpha$ -PU.1 pathway. *Nat Med* 17: 64–70, 2011.

Poy MN, Hausser J, Trajkovski M, Braun M, Collins S, Rorsman P, Zavolan M, Stoffel M. miR-375 maintains normal pancreatic alpha- and beta-cell mass. *Proc Natl Acad Sci U S A*, 2009. 7: 106:5813-8.

Prentki M, Nolan CJ. Islet  $\beta$  cell failure in type 2 diabetes. *J Clin Invest*, 2006. 116: 1802–1812.

Primeau V, Coderre L, Karelis AD, Brochu M, Lavoie ME, Messier V, Sladek R, Rabasa-Lhoret R. Characterizing the profile of obese patients who are metabolically healthy. *Int J Obes (Lond)*, 2011.35:971-81.

Rabinowits G, Gercel-Taylor C, Day JM, Taylor DD, Kloecker GH. Exosomal microRNA: a diagnostic marker for lung cancer. *Clin Lung Cancer*, 2009.10: 42–46.

Radom-Aizik S, Zaldivar FP Jr, Haddad F, Cooper DM. Impact of brief exercise on circulating monocyte gene and microRNA expression: implications for atherosclerotic vascular disease. *Brain Behav Immun*, 2014 39: 121–129.

Radom-Aizik S, Zaldivar F Jr, Oliver S, Galassetti P, Cooper DM. Evidence for microRNA involvement in exercise-associated neutrophil gene expression changes. *J Appl Physiol*, 2010. 109: 252–261.

Rawlings-Goss RA, Campbell MC, Tishkoff SA. Global population-specific variation in miRNA associated with cancer risk and clinical biomarkers. *BMC Medical Genomics*. 2014, 7:53.

Rink C, Khanna S. MicroRNA in ischemic stroke etiology and pathology. *Physiol Genomics*, 2010,

Robinson MD, McCarthy DJ Smyth GK. Edge R: a Bioconductor package for differential expression analysis of digital gene expression data. *Bioinformatics*, 2010. 26:139-40.

Roggli E, Gattesco S, Caille D, Briet C, Boitard C, Meda P, Regazzi R. Changes in microRNA expression contribute to pancreatic b-cell dysfunction in prediabetic NOD mice. *Diabetes*, 2012. 61: 1742–1745.

Roldo C, Missiaglia E, Hagan JP, Falconi M, Capelli P, Bersani S, Calin GA, Volinia S, Liu CG, Scarpa A, Croce CM. MicroRNA expression abnormalities in pancreatic endocrine and acinar tumors are associated with distinctive pathologic features and clinical behavior. *J Clin Oncol*, 2006.24:4677-84.

Romao, J. M., W. Jin, H. Maolong, T. A. McAllister, and L. L. Guan. 2012. Altered microRNA expression in bovine subcutaneous and visceral adipose tissues from cattle under different diets. *PLoS One* 7:e40605.

Rosen ED, MacDougald OA. Adipocyte differentiation from the inside out. *Nat Rev Mol Cell Biol*, 2006. 7:885-96.

Rossi D, Zlotnik A. The biology of chemokines and their receptors. *Annu Rev Immunol*. 2000; 18:217-42.

Rot A, von Andrian UH. Chemokines in innate and adaptive host defense: basic chemokine grammar for immune cells. *Annu. Rev. Immunol*, 2004. 22: 891–928.

Rottiers V, Näär AM. MicroRNAs in metabolism and metabolic disorders. *Nat Rev Mol Cell Biol*, 2012. 13:239-50.

Roy S, Sen CK. miRNA in innate immune responses: novel players in wound inflammation. *Physiol Genomics*, 2010.

Rudich A, Tirosh A, Potashnik R, Hemi R, Kanety H, Bashan N. Prolonged oxidative stress impairs insulin-induced GLUT4 translocation in 3T3-L1 adipocytes. *Diabetes*, 1998.47:1562-9.

Ryan M. O'Connell, Aadel A. Chaudhuria, Dinesh S. Raoab, William S. J. Gibsona, Alejandro B. Balazsa, and David Baltimorea, MicroRNAs enriched in hematopoietic stem cells differentially regulate long-term hematopoietic output. *PNAS*, 2010. 32: 14235–14240.

Sabina S, Pulignani S, Rizzo M, Cresci M, Vecoli C, Foffa I, Ait-Ali L, Pitto L, Andreassi MG. Germline hereditary, somatic mutations and microRNAs targeting-SNPs in congenital heart defects. *J Mol Cell Cardiol*. 2013 Jul; 60:84-9.

Salans Lester B, Knittle Jerome L, and Hirsch Jules . The Role of Adipose Cell Size and Adipose Tissue Insulin Sensitivity in the Carbohydrate Intolerance of Human Obesity. *J Clin Invest*, 1968. 47:153-165.

Saltiel AR, Kahn CR. Insulin signaling and the regulation of glucose and lipid metabolism. *Nature*, 2001.414:799-806.

Sanchez-Gurmaches, J. et al. PTEN loss in the Myf5 lineage redistributes body fat and reveals subsets of white adipocytes that arise from Myf5 precursors. *Cell Metab.* 16, 348–362 (2012).

Seale, P. et al. PRDM16 controls a brown fat/skeletal muscle switch. *Nature* 454, 961–967 (2008).

Semenza GL. Surviving ischemia: adaptive responses mediated by hypoxia-inducible factor 1, 2000. *106*:809–812.

Sen CK, Gordillo GM, Khanna S, Roy S. Micromanaging vascular biology: tiny microRNAs play big band. *J Vasc Res* 46: 527–540, 2009.

Sengupta S, den Boon JA, Chen IH, Newton MA, Stanhope SA, Cheng YJ, Chen CJ, Hildesheim A, Sugden B, Ahlquist P. MicroRNA 29c is down-regulated in nasopharyngeal carcinomas, up-regulating mRNAs encoding extracellular matrix protein. *Proc Natl Acad Sci U.S.A.*, 2008. 105:5874-8.

Sesti G, Folli F, Perego L, Hribal ML, Pontiroli AE. Effects of weight loss in metabolically healthy obese subjects after laparoscopic adjustable gastric banding and hypocaloric diet. *PLoS One*, 2011.6:e17737.

Shantikumar S, Caporali A, Emanuelli C. Role of microRNAs in diabetes and its cardiovascular complications. *Cardiovasc Res*, 2012. 93:583–593.

Sharp, L.Z. et al. Human BAT possesses molecular signatures that resemble beige/brite cells. *PLoS ONE* 7, e49452 (2012).

Sims EA, Danforth E. Expenditure and Storage of Energy in Man. *J Clin Invest.* 1987. 79:1019-1025.

Skurk T, Alberti-Huber C, Herder C, Hauner H. Relationship between adipocyte size and adipokine expression and secretion. *J Clin Endocrinol Metab*, 2007. 92:1023-33.

Small EM, Olson EN. Pervasive roles of microRNAs in cardiovascular biology. *Nature*, 2011. 469:336-42.

Stefan N, Kantartzis K, Machann J, Schick F, Thamer C, Rittig K, Balletshofer B, Machicao F, Fritsche A, Häring HU. Identification and characterization of metabolically benign obesity in humans. *Arch Intern Med*, 2008.168:1609-16.

Strum JC, Johnson JH, Ward J, Xie H, Feild J, Hester A, Alford A, Waters KM. MicroRNA 132 regulates nutritional stress-induced chemokine production through repression of SirT1. *Mol Endocrinol*, 2009.23:1876-84.

Sun X, Icli B, Wara AK, Belkin N, He S, Kobzik L, Hunninghake GM, Vera MP; MICU Registry, Blackwell TS, Baron RM, Feinberg MW. MicroRNA-181b regulates NF- $\kappa$ B-mediated vascular inflammation. *J Clin Invest*, 122:1973-90.

Svedberg J, Björntorp P, Smith U, Lönnroth P. Free-fatty acid, inhibition of insulin binding, degradation, and action in isolated rat adipocytes. *Br Med J, Diabetes*, 1990.39:570–574.

Szabo G, Bala S. MicroRNAs in liver disease. *Nat Rev Gastroenterol Hepatol*. Epub, 2013. 10:542-52.

Timmons, J.A. et al. Myogenic gene expression signature establishes that brown and white adipocytes originate from distinct cell lineages. *Proc. Natl. Acad. Sci. USA* 104, 4401–4406 (2007).

Toledo FG, Watkins S, Kelley DE. Changes induced by physical activity and weight loss in the morphology of intermyofibrillar mitochondria in obese men and women. *J Clin Endocrinol Metab*, 2006.91:3224-7.

Tonevitsky AG, Maltseva DV, Abbasi A, Samatov TR, Sakharov DA, Shkurnikov MU, Lebedev AE, Galatenko VV, Grigoriev AI, Northoff. H. Dynamically regulated miRNA-mRNA networks revealed by exercise. *BMC Physiol* 13: 9, 2013.

Trajkovski, M., Ahmed, K., Esau, C.C. & Stoffel, M. MyomiR-133 regulates brown fat differentiation through Prdm16. *Nat. Cell Biol.* 14, 1330–1335 (2012).

Tran, K. V., Gealekman, O., Frontini, A., Zingaretti, M. C., Morroni, M., Giordano, A., Smorlesi, A., Perugini, J., De Matteis, R., Sbarbati, A. et al. (2012). The vascular endothelium of the adipose tissue gives rise to both white and brown fat cells. *Cell Metab.* 2010.15, 222-229.

Trayhurn P, Duncan JS, Hoggard N & Rayner DV. Regulation of leptin production: a dominant role for the sympathetic nervous system? *Proceedings of the Nutrition Society*, 1998.57:413–419.

Trujillo ME, Scherer PE. Adiponectin-journey from an adipocyte secretory protein to biomarker of the metabolic syndrome. *J Intern Med*, 2005.257:167-75.

Tsuchiya S, Fujiwara T, Sato F, Shimada Y, Tanaka E, Sakai Y, Shimizu K, Tsujimoto G. MicroRNA-210 regulates cancer cell proliferation through targeting fibroblast growth factor receptor-like 1 (FGFRL1). *J Biol Chem* 286: 420–428, 2011.

Turer E, Scherer PE. Adiponectin: mechanistic insights and clinical implications. *Diabetologia*, 2012.55:2319–2326.

Vandanmagsar B, Youm YH, Ravussin A, Galgani JE, Stadler K, Mynatt RL, Ravussin E, Stephens JM, Dixit VD. The NLRP3 inflammasome instigates obesity induced inflammation and insulin resistance. *Nat Med*, 2011. 17:179–188.

Van Gaal LF, Mertens IL, De Block CE. Mechanisms linking obesity with cardiovascular disease. *Nature*, 2006. 444: 875-880.

Van Mil A, Grundmann S, Goumans MJ, Lei Z, Oerlemans MI, Jaksani S, Doevendans PA, Sluijter JP. MicroRNA-214 inhibits angiogenesis by targeting Quaking and reducing angiogenic growth factor release. *Cardiovasc Res.* 2012.93:655-65.

Van Rooij, Lillian B. Sutherland, Jeffrey E. Thatcher, J. Michael DiMaio, R. Haris Naseem,

William S. Marshall, Joseph A. Hill, and Eric N. Olson. Dysregulation of microRNAs after myocardial infarction reveals a role of miR-29 in cardiac fibrosis. *PNAS*, 2008.35:1303.

Vergoulis T, Vlachos IS, Alexiou P, Georgakilas G, Maragkakis M, Reczko M, Gerangelos S, Koziris N, Dalamagas T, Hatzigeorgiou AG. Tarbase 6.0: Capturing the Exponential Growth of miR Targets with Experimental Support. *Nucl. Acids Res*, 2012. 40: D222-D229.

Vitali, A. et al. The adipose organ of obesity-prone C57BL/6J mice is composed of mixed white and brown adipocytes. *J. Lipid Res.* 53, 619–629 (2012).

Voskuhl R: Sex differences in autoimmune diseases. *Biol Sex Differ* 2011.

Vojarova B, Weyer C, Hanson K, Tataranni PA, Bogardus C, Pratley RE. Circulating interleukin-6 in relation to adiposity, insulin action, and insulin secretion. *Obes Res*, 2001.9:414-7.

Wajchenberg BL. Subcutaneous and visceral adipose tissue: their relation to the metabolic syndrome. *Endocr Rev*, 2000. 21:697-738.

Wajchenberg BL, Malerbi DA, Rocha MS, Lerario AC, Santomauro AT. Syndrome X: a syndrome of insulin resistance. Epidemiological and clinical evidence. *Diabetes Metab Rev.* 1994.10:19-29.

Weyer C, Foley JE, Bogardus C, Tataranni PA, Pratley PE. Enlarged subcutaneous abdominal adipocyte size, but not obesity itself, predicts type II diabetes independent of insulin resistance. *Diabetologia*, 2000. 43:1498-1506.

Weyer C, Funahashi T, Tanaka S, Hotta K, Matsuzawa Y, Pratley RE, Tataranni PA. Hypoadiponectinemia in obesity and type 2 diabetes: close association with insulin resistance and hyperinsulinemia. *J Clin Endocrinol Metab*, 2001. 86:1930–1935.

Wildman RP, Muntner P, Reynolds K. The obese without cardiometabolic risk factor clustering and the normal weight with cardiometabolic risk factor clustering — prevalence



and correlates of 2 phenotypes among the US population (NHANES 1999– 2004) Arch. Intern. Med, 2008.168:1617–1624

Wu, J. et al. Beige adipocytes are a distinct type of thermogenic fat cell in mouse and human. Cell 150, 366–376 (2012).

Wu, J., Cohen, P. & Spiegelman, B.M. Adaptive thermogenesis in adipocytes: is beige the new brown? Genes Dev. 27, 234–250 (2013).

Xiao F, Zuo Z, Cai G, Kang S, Gao X, Li T: miRecords: an integrated resource for microRNA-target interactions. Nucleic Acids Res, 2009. 37: D105-D110.

Xie H, Lim B, Lodish HF. MicroRNAs induced during adipogenesis that accelerate fat cell development are downregulated in obesity. Diabetes, 2009. 58:1050–1057.

Yamagata K, Fujiyama S, Ito S, Ueda T, Murata T, Naitou M, Takeyama K-I, Minami Y, Malley BWO, Kato S: Maturation of MicroRNA Is Hormonally Regulated by a Nuclear Receptor. Molecular Cell 2009, 36:340–347.

Yang and Wang. Regulation of microRNA expression and function by nuclear receptor signaling. Cell & Bioscience 2011, 1:31.

Yeh S-H, Chen P-J: Gender Disparity of Hepatocellular Carcinoma: The Roles of Sex Hormones. Oncology 2010, 78:172–179.

Zampetaki A, Kiechl S, Drozdov I, Willeit P, Mayr U, Prokopi M, Mayr A, Weger S, Oberhollenzer F, Bonora E, Shah A, Willeit J, Mayr M. Plasma microRNA profiling reveals loss of endothelial miR-126 and other microRNAs in Type 2 diabetes. Circ Res. 2010; 107:810–7.

Zeng Y, Cullen BR. Structural requirements for pre-microRNA binding and nuclear export by Exportin 5. Nucleic Acids Res, 2004.32:4776-85.

Zhang J, Liu B, He J, Ma L, Li J. Inferring functional miRNA-mRNA regulatory modules

in epithelial-mesenchymal transition with a probabilistic topic model. *Comput Biol Med.* 2012; 42:428–437.

Zhu N, Pankow JS, Ballantyne CM, Couper D, Hoogeveen RC, Pereira M, Duncan BB, Schmidt MI. High-molecular-weight adiponectin and the risk of type 2 diabetes in the ARIC study. *J Clin Endocrinol Metab*, 2010. 95:5097-104.